THE American Journal of ANATOMY

MANAGING EDITOR

DONALD DUNCAN

THE UNIVERSITY OF TEXAS
MEDICAL BRANCH
GALVESTON, TEXAS

VOLUME 114

JANUARY, MARCH, MAY 1964

PUBLISHED BY

THE WISTAR INSTITUTE OF ANATOMY AND BIOLOGY
PHILADELPHIA, PA

CONTENTS

No 1 JANUARY 1964

No. 2 MARCH 1964

Female animals were classed as sexually active if they (1) were pregnant (2) were lactating (3) had an enlarged uterus (4) had recent placental scars (5) had enlarged mammae or (6) had perforate vaginas. Sexual activity in the male was determined from the size of the testes size of the seminal vesicles and appearance of the tubules of the epididymis.

Differences in compared values were considered to be statistically significant when P was ≤ 0.05

OBSERVATIONS

Adrenal glands Average adrenal size fluctuated from month to month; but there was no seasonal pattern in variations in size of glands from the reproductive and age classes of either sex, despite the fact that there was considerable variation in the percentage of reproductively active adults (table 1) This may be explained in part by the fact that in neither sex did mean adrenal weight of reproductively active animals differ significantly from that of non-active adults (fig 1) There was no significant difference in adrenal size of the various reproductive classes of females. Adrenals of sexually active females were significantly larger than those of adult males Adrenals of juvenile animals averaged larger than those of adults, but the difference was significant only between non-active adult and juvenile females

Animals were grouped by 2.5-gm body weight classes and adrenal size of the vari

TABLE 1

Monthly reproductive status and relative abundance of Peromyscus maniculatus

Month	Per cent of adults reproductively active		Average number embryos per female	Average number placental scars per female	Catch per 100 trap-nights
	Males	Females			
January	0.0 (23)	0.0 (16)	—	—	9.3
February	7.4 ± 5.0 (27)	8.7 ± 5.9 (23)	—	—	6.1
March	52.0 ± 7.0 (52)	84.6 ± 7.1 (26)	4.0 (7)	4.8 (8)	3.7
April	73.0 ± 5.8 (60)	70.8 ± 6.6 (48)	4.2 (14)	3.6 (5)	3.8
May	97.5 ± 2.5 (40)	94.9 ± 3.5 (39)	4.6 (14)	4.5 (6)	3.0
June	90.1 ± 4.6 (43)	96.9 ± 3.1 (32)	4.8 (13)	4.3 (21)	1.8
July	86.2 ± 6.4 (29)	91.7 ± 5.8 (24)	4.0 (5)	6.7 (9)	2.3
August	51.0 ± 7.1 (49)	76.9 ± 8.3 (26)	4.5 (8)	4.4 (13)	2.2
September	32.2 ± 8.4 (31)	54.2 ± 10.2 (4)	4.5 (3)	6.2 (10)	3.2
October	22.5 ± 8.0 (37)	48.1 ± 9.6 (27)	4.6 (5)	4.3 (6)	1.4
November	38.1 ± 10.6 (31)	30.0 ± 14.5 (10)	4.5 (2)	7.0 (1)	1.8
December	14.3 ± 13.2 (7)	80.0 ± 12.7 (10)	4.0 (1)	3.8 (5)	3.5
Average	53.6	67.8	4.4 (71)	4.9 (82)	

Figures in parentheses equal sample size ± values equal one standard error

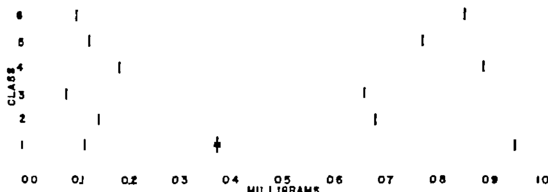


Fig. 1 Adrenal weight, in milligrams per gram body weight, for *Peromyscus maniculatus* which were classified according to sex, age and reproductive condition. The classes, and sample size of each, were as follows class 1 sexually active males, 193; class 2, non-active adult males, 154; class 3 juvenile males, 101; class 4, sexually active females, 174; class 5, non-active adult females, 83; class 6, juvenile females, 101. Median vertical line represents the mean, the horizontal bar represents ± two standard errors, and the horizontal line represents the extremes.

ous groups compared (fig 2) Adrenals from males of the 2.6–5 0-gm class were significantly smaller than those of animals in other weight classes. In both active and non-active males, adrenals of animals in the 15.1–17.5-gm class were smaller than those of the 12.6–15 0-gm class; in non-active animals they were also smaller than those of the 10 1–12.5-gm class. Glands of sexually active animals did not differ significantly from those of non-active animals of the same weight class.

Adrenals from females in the 2.6–5 0-gm class were significantly smaller than those of animals of any other weight group except the 5.1–7.5 gm class. There was no significant difference in adrenal size among other body weight classes of active and non-active females or between active and non-active animals of the same weight class.

Individuals of the same age or reproductive class exhibited a 6- to 9-fold variation in relative adrenal size. Individuals of the same weight class showed a 3- to 9-fold variation in adrenal size. Such variations require that each class be represented by a large sample a condition not fulfilled for some weight classes.

Adrenals of reproductively active and non-active animals of both sexes were examined histologically Width of each of the three cortical zones was measured and the width of each zone expressed as a percentage of the total width of the cortex (fig. 3) There was no significant difference in width of the zona glomerulosa of the four classes. The zona fasciculata and zona reticularis were approximately equal in relative width in males, and there was no appreciable difference in the width of either zone in active and non-active males. In females the fasciculata was approximately the same width in both active and non-active animals as was the reticularis, but the fasciculata was much wider than the reticularis in both classes. Furthermore in females the fasciculata was significantly wider and the reticularis significantly narrower than the corresponding zone in male glands.

Adrenals of adult animals had a thin connective tissue capsule, usually only one or two cells thick, with extremely flattened nuclei. The zona glomerulosa was well defined and consisted of ovoid cells elongated parallel to the radius of the gland. Cells were not arranged in a definite pattern. Nuclei of glomerular cells were one-half to two-thirds as large as those of the fasciculata. Fascicular cells were cuboidal or columnar with the long axis parallel to the radius of the gland. The cells were arranged in single radial columns. Fascicular cells of females, particularly sexually active animals were more elongated

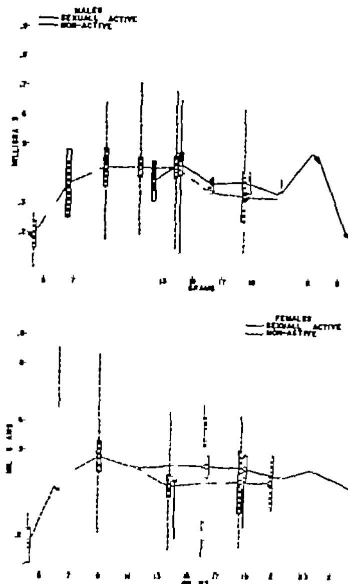


Fig. 2 Adrenal weight, in milligrams per gram body weight, plotted against body weight in grams, for Peromyscus maniculatus. Points represent the mean for each 2.5-gm interval of body weight. The enclosed area represents ± two standard errors, and the vertical line represents the extremes.

than those of males (figs. 11 and 12) In some specimens of both sexes as many as one-half the fascicular cells had greatly enlarged nuclei. Some of the enlarged nuclei stained intensely throughout, while others contained from one to four vacuoles (fig. 15) similar to those found in the platypus *Ornithorynchus* by Chester Jones ('57)

The reticularis was a distinct zone well differentiated from the fasciculata and medulla in all classes In females the reticularis was more vascular than that males (figs. 13 and 14) The reticularis sexually active females was [illegible] vascular and contained many cells pyknotic nuclei In some animals reticularis consisted of a narrow band connective tissue.

Adrenals from animals 2 to 4 days old were surrounded by a heavy cellular capsule Cortical tissue could be

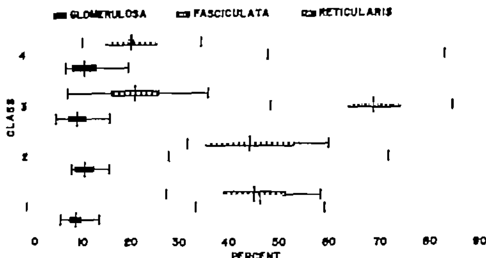


Fig. 3 Relative width of the three zones of the adrenal cortex, expressed as percentage of the total width of the cortex, for 4 classes of *Peromyscus maniculatus*. The classes, and sample size of each, were as follows class 1 sexually active males, 12; class 2, non-active males, 9; class 3 sexually active females, 16; class 4 non-active females 13. The median vertical line represents the mean, the shaded area represents ± two standard errors, and the horizontal line represents the extremes.

guished from medullary tissue, but cortical zones were not differentiated (fig. 16)

Comparison of annual average adrenal weights of all specimens for the four-year period revealed that there was a significant increase in gland size from '58 to '59 ($P < 0.001$) and from '60 to '61 ($P < 0.05$). Average gland size was greater in '60 than in '59 but the difference was not significant (fig. 4) During the four year period, there was a significant decrease in population size in both forest types from '58 to '59 and from '59 to '60 This was followed by an increase in the population in both forest types to a level significantly greater than that of '58. Thus adrenal size increased while population size decreased in '59 remained the same while population size decreased during '60 and increased while population size increased in '61 However adrenal size increased only slightly from '60 to '61 while population size more than doubled in the fir type and increased by 44% in the pine type.

During the four year period there was no consistent correlation between population size and either the per cent of juveniles in the population, the per cent of sexually active adults or the number of embryos per pregnant female (table 2) Although the number of embryos per female decreased in '59 and '60 and increased in '61 the differences among years were not significant.

Monthly changes in the per cent of reproductively active adults were not correlated, either positively or negatively with population density (table 1) Mice were more abundant in January and February when reproductive activity was at a minimum; but during the remainder of the year the population was relatively stable while the percentage of sexually active adults fluctuated from 14–97%

Annual body weights of sexually active and non-active adults and juveniles of both sexes fluctuated during the four years (fig 5) but differences within a given class were significant only for active females in '59 and '60 Decline in the average weights of juveniles in '61 was caused by an increase in the number of captures of animals which weighed less than 7.5 gm.

Seasonal changes in food habits of mice reflected abundance and availability of the food items, but there was no apparent relationship between seasonal reproductive activity and seasonal food habits. Annual variations in foods were slight, except that

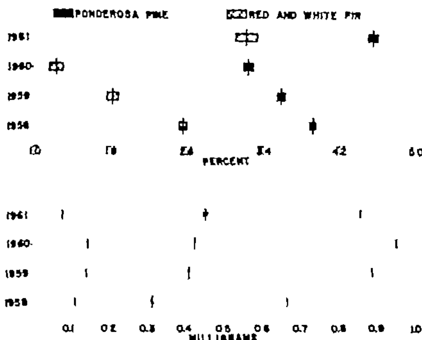


Fig. 4 Population size expressed as per cent trap success (upper figure) compared with adrenal size, expressed in milligrams per gram body weight (lower figure) for *Peromyscus maniculatus* during four consecutive years. Sample size of adrenal weights for each year was '58 240; '59 167; '60, 135; and '61 264. The median vertical line represents the mean, the shaded area represents ± two standard errors and the horizontal line represents the extremes.

TABLE 2

Reproductive state of Peromyscus maniculatus in northeastern California from 1958–61

Year	Number of adults	Number of juveniles	Per cent juveniles	Per cent sexually active males	Per cent sexually active females	Number of embryos per female
1958	238	63	20.9 ± 2.3	44.7	54.8	4.8 ± 0.23 (13)
1959	134	55	29.1 ± 3.2	37.7	77.2	4.7 ± 0.33 (15)
1960	139	25	15.2 ± 2.8	75.3	82.0	4.2 ± 0.26 (20)
1961	192	45	18.8 ± 2.5	63.9	68.7	4.3 ± 0.26 (23)

Numbers in parentheses equal sample size; ± values equal one standard error

much seed was eaten in '58 when there was a large crop of pine seed. However there were no differences in food habits that would account for changes in adrenal size or population fluctuations.

Pituitary gland. Relative weights of the pituitary gland of six classes of animals were compared (fig. 6). Pituitaries of sexually active males were significantly larger than glands of non-active adults; they were also larger than the pituitaries of juvenile males but the difference was not significant. Pituitaries of sexually active females were significantly larger than those of any other class. In contrast to males, pituitaries of non-active adult females averaged larger than those of juvenile females but the difference was not significant. Pitui

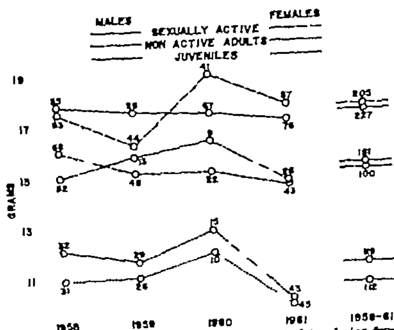


Fig. 5 Body weights of six classes of *Peromyscus maniculatus* during four consecutive years. Figures at each point represent sample size.

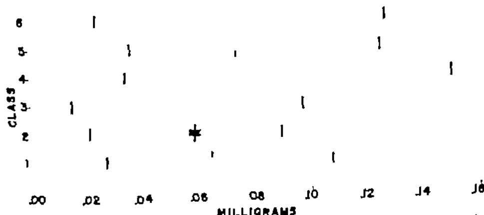


Fig. 6 Pituitary weights, in milligrams per gram body weight, for *Peromyscus maniculatus* classified according to sex, age and reproductive condition. The classes, and sample size of each were as follows class 1 sexually active males, 154; class 2, non-active adult males, 96; class 3 juvenile males, 71; class 4 sexually active females, 125; class 5, non-active adult females, 45; class 6, juvenile females, 71 The median vertical line represents the mean, the shaded area represents ± two standard errors, and the horizontal line represents the extremes.

taries of both active and non-active adult females were larger than those of males but glands of juvenile females did not differ from those of any class of males.

Among six classes of reproductively active females, the pituitary was smallest in pregnant animals and largest in those that were lactating (fig. 7) The difference in pituitary size between these two classes was significant, but neither class differed from the other four classes.

Weights of pituitary glands from animals grouped by 2.5-gm body weight classes were compared for reproductively

ity probably accounts for the larger size of the pituitary in reproductively active animals of both sexes.

Greater size of the pituitary of lactating animals, compared with those of pregnant animals probably was associated with increased production of prolactin by pituitaries of lactating individuals

SUMMARY

In natural populations of *Peromyscus maniculatus* adrenal gland size in milligrams per gram body weight showed no pattern of seasonal change, and no change in size related to reproductive activity Adrenals of females were larger and had a wider fasciculata and narrower reticularis than those of males Adrenals of 2.6–5.0-gm animals were smaller than those from animals of any other weight class. Adrenal size showed no consistent correlation with changes in population density per cent of reproductively active adults body weight, or food habits. However the average annual adrenal weight increased throughout the study period.

The thyroid gland was largest in 2.6–5.0- m animals The gland decreased in size as … of m … animals in… …re sed … al variatio… thyroid …

Th… of adult males w… … uall… … pit… … an not … …

In cont… the 5 1–… cells the lu… enlarged and the prop… cell mass greatly increa… adult animals the height o… cells was further reduced, a… the lumina and proportion creased over that of jun… (fig 18)

Bendell, J F 1959 Food as a control of population of white-footed mice *Peromyscus leucopus noveboracensis* (Fischer) Can. Zool., 37 173–209

Chester Jones, I. 1957 *The adrenal cort…* Cambridge Univ Press Cambridge, pp. 9–1… 104; 209

Christian, J J 1952 The relation of adren… weight to body weight in mammals. N… Med. Res. Ins. Memo. Rep., 52–7 941–946.

——— 1953 Effect of population size on t… adrenal glands and reproductive organs of ma… mice in populations of fixed size. J Physio… 182 292–300

——— 1959 The role of endocrine and beha… ioral factors in the growth of mammali… populations. In Gorbman, A. (Ed.) Compar… tive Endocrinology John Wiley and Son… New York, pp. 71–93.

——— 1961 Phenomena associated with pop… lation density Proc. N t. Acad. Sci., 47 42… 449.

Eleftheriou B. E., and M. X. Zarrow 1961 … comparison of body weight and thyroid gla… in two subspecies of Peromyscus maniculat… as affected by age and season. Anat. Re… 139 224

Falconer I R., and H. A. Robertson 19… Changes in thyroid activity during growth … the sheep. J Endocrin. (London) 22: 23–3…

Hall P F 1959 The Function of the Endocri… Glands. W B S unders Company Philade… phia pp. 34–44

Hoffman, R. A., and C. M. Kirkpatrick 19… Seasonal changes in thyroid gland morpholo… f male gray squirrels. J Wildl. Mgt., 2… 421–435.

Hormay A. L., and M. W Talbot 1961 R… rotation grazing … a new management sy… tem for perennial bunchgrass ranges. U.S.D… For Serv Prod. Res. Rep., 51 iii + 43 pp.

McKeever S. 1959 Effects of reproductive … tivity on the weight of adrenal glands in M… rotus montanus. Anat. Rec 135 1–5

… us, N C E. Gould and R. K. Chipman 19… … of the rice rat, Oryzomys palustr… …ton Island, Gulf of Mexic… … of the social stress theor… Zool., 8 95–123 … he Physiology and Patholo… …tress. Acta Endocrinologic… 81

… 10 Some ffect of artifici… reproduction in the whit… …eromyscus leucopus noveboracensis… Zool., 41 33–60.

PLATE

PLATE 1

EXPLAN TION OF FIGURES

Peromyscus maniculatus

11 Adrenal gland of sexually active female howing elongated cells of the zona fasciculata, compared with those of the adult male in figure 12. Pasini. × 300.

12 Adrenal gland of an adult male showing cell of the zona fasciculata. H & E. × 300.

13 Adrenal gland f a sexually active female showing the inner reticularis with a row of medullary cell on the extreme right The inner reticularis is highly vascular and many pyknotic nuclei are present. Pasini. × 300.

Adrenal gla id of an adult male showing lack of vascularity in the in ner icularl compared with the dult female gland. The right the photograph is of medullary tissue H & E. × 300

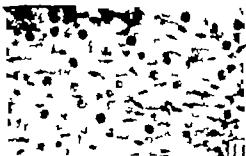
po na fasciculata of an adult non-active female al nuclei and an enlarged nucleu containing H E. × 750

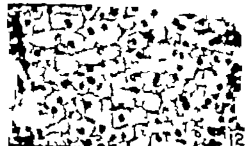
urenile howing lack of zonation in the cells are present along the right border

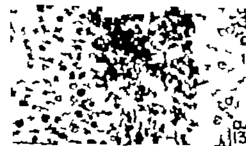
howing very small lumen in follicles. lial cell Pasini. × 300.

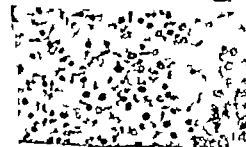
showing enlarged lumina nd more ure 10. P sini. × 300

n le showing the greatly enlarged Pasini. × 300

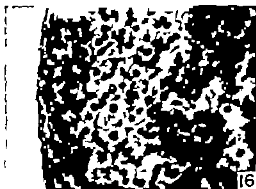

11

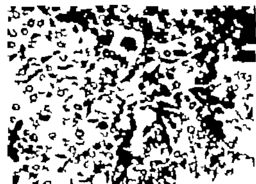

12

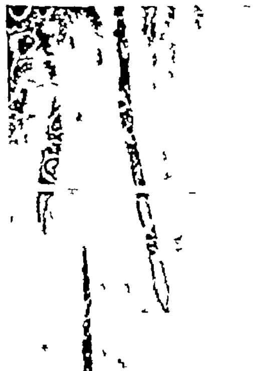

13


14




16





lateral borders the cytoplasm had short thick footlets while on the side facing the articular surface footlets were scarce. Pinocytotic vesicles were numerous Free RNA granules were present the ER was granular abundant and formed large cisterns. Mitochondria and Golgi structures were conspicuous (figs 6 7)

Midzone The chondrocytes were lying singly or in pairs their nuclei were small and electron-dense some had bilobed or double nuclei. Cytoplasmic footlets were elongated and evenly distributed over the cell surfaces Short strands of delicate fibrillar material was superimposed on the intact plasmalemma. These filaments ran parallel to the cell surface or extended at an angle into the matrix. The ER widened into large cisterns. The deeper in the tissue the cells were situated the more abundant were the Golgi structures often forming juxtanuclear aggregates of vesicles vacuoles and lamellae Glycogen was deposited in small peripheral foci or amassed in large lakes about which many long mitochondria were scattered Pinocytotic vesicles were numerous as were multivesicular bodies Some of the latter were apposed to the plasmalemma. The bodies [illegible] re w[illegible]lled off by a limiting membrane [illegible]ich [illegible] frequently showed openings [illegible] rou[illegible]h the interior of the body [illegible] d with the ground plasma of [illegible] 8)

D[illegible] th[illegible] zone of calcification [illegible] reached their largest dim[illegible] ER and Go[illegible] of the [illegible] filled [illegible] [illegible]

calcified matrix At no time were capillaries seen in the vicinity of intact hypertrophic chondrocytes

Mice 6 to 8 months old:
14 femurs

Surface layer Small "blisters filled with amorphous material caused slight irregularities of the surface The underlying matrix showed foci of loosening The typical oblong cells were larger and their cytoplasmic footlets were longer and more tortuous than those of young animals The ER was devoid of cisterns and free RNA granules were scarce Golgi apparatus and mitochondria had remained essentially unchanged Some chondrocytes showed indistinct or homogenized organelles others resembled those of the midzone

Midzone and deep layer The uppermost cells had hardly changed from their appearance towards the end of the growth period. The amount of ER and Golgi material was further increased but it varied with individual cells Mitochondria were numerous and large and sometimes degenerating In the deep cells the ER lamellae were tortuous. Many mitochondria showed concentric constriction in addition to regressive changes others had thickened outer membranes and were transformed into large vacuoles with mere spurs of cristae left There were many osmiophilic droplets and some small dense cytoplasmic bodies resembling lysosomes Glycogen was abundant Intermingled with these cells were chondrocytes of hypertrophic type The latter contained less glycogen were less hydrated than their counterparts of earlier ages and they were too few to form a distinct separate layer

Mice 11 to 12 months old
16 femurs

Surface layer Bundles of fibers protruded into the articular space cystic vacuoles within the matrix and "blisters opening on the surface were numerous and larger than earlier in life Fibers were [illegible] led by scant ground substance the [illegible] be[illegible] haphazardly oriented Cal[illegible] [illegible] extended upward in an irregular [illegible] stopped short of the surface [illegible] lular foci composed of inter[illegible]

twined thick fibers had outlines conforming to those of chondrocytes. Some oblong cells contained bilobed or double nuclei and many multivesicular bodies. Osmiophilic globules were dispersed throughout the cytoplasm, and glycogen was present in moderate amounts. Superimposed on the plasmalemma were delicate fibrils; some were lying free in the pericellular ground substance especially in the scalloped bays formed by the cytoplasmic footlets. This electron-lucent matrix was sharply delimited from the remainder of the matrix. A few cells showed signs of degeneration; other cells resembled those of the midzone (figs. 10–13).

Midzone and deep layer. There were fewer cell layers than in younger animals and the delineation of the remaining layers was indistinct. The cells were lying singly or in pairs; some had long footlets and abundant cytoplasm. The organelles were well defined, and varying amounts of glycogen were present. The cells situated in the deepest layer were distended, but smaller and more haphazardly oriented than the hypertrophic chondrocytes of the growing animal. Their most distinctive feature was the large number of densely packed mitochondria (figs. 14, 15).

Mice 20 to 27 months old. 22 femurs

Surface layer. Some surfaces were more irregular than before owing to the increased coarseness of protruding fiber bundles. "Blisters" were numerous; vacuoles in the matrix began to coalesce and there were fibrillar microscars (figs. 16, 17). Calcium was deposited in irregular patches, but spared the uppermost layer of the cartilage. The cells varied considerably in shape and structure. Some showed small nuclei and scanty organelles, others had large nuclei with pores, a well-developed ER and Golgi apparatus, pinocytotic vesicles and multivesicular bodies. Mitochondria were slender and short, or large and degenerating with disoriented and [illegible] grating cristae. Electron-opaque [illegible] and small deposits of glycogen were occasionally seen in the cytoplasm. The electron-dense pericellular matrix was [illegible] that seen at earlier ages. It [illegible] short closely packed [illegible] indistinct [illegible] was set off sharply from the remainder of the matrix. Degenerating cells and cells of unusual type were also seen (figs. 18, 19).

Midzone and deep layer. Some chondrocytes were paired; others were surrounded by dense matrix found also in the surface cells. The ER was irregularly clustered; large Golgi vacuoles and oddly-shaped large degenerated mitochondria aggregated about glycogen. Pinocytotic vesicles and multivesicular bodies were scarce. A few dumb-bell-shaped cells showing partial homogenization and breakdown of organelles were surrounded by electron-lucent material resembling ground plasm.

DISCUSSION

The present observations extend and supplement our previous findings concerning the ultrastructure of articular cartilage. In young mice the joint surfaces were slightly roughened owing to protrusion of fiber bundles. With advancing age this condition became accentuated while the matrix underwent vacuolation. The main orientation of fibers was parallel to the surface; in old age the fibers did not assume a vertical direction as described for the aging human hip joint (Little, Pimm and Trueta, '58).

The cellular changes occurring during life may be interpreted in te[illegible]. During the ascending phase [illegible] the cytoplasm disclos[illegible] an [illegible] complex state of orga[illegible] indicated by the appe[illegible] elongated foot[illegible] of ER and Gol[illegible] cytosis [illegible] chondr[illegible] large [illegible] ently [illegible] ander [illegible] 61 [illegible] prob[illegible] the [illegible] pe[illegible] chondr[illegible] the [illegible] incre[illegible] el[illegible] [illegible] Golg[illegible]

came less conspicuous and were finally homogenized. Mitochondria became first numerous but broke down in the end. During the last stage of the cycle hydration and swelling of the cytoplasm caused rupture of the plasmalemma and discharge of cytoplasmic contents into the pericellular matrix. Swelling and hydration of cells were most pronounced in the young animal. After cessation of growth differences *between cell types in the various layers* were less definite than before although there was still a gradient in cell organization from the surface to the deep layers.

Not all events taking place in the articular cartilage during life are cyclic. Cells die at all ages; their disintegration must be rapid since cell fragments were only rarely found. Sloughing of dead cells from the articular surface supposed to result from "wear and tear" was not observed in our mice just as it failed to occur in adult rabbits (Davies et al '62) However the tissue pattern of the cartilage was occasionally interrupted by foci of interlacing bundles of collagen fibers These areas are interpreted as microscars replacing sintegrated cartilage cells. By early obrvers fading or dying chondrocytes have been thought to contribute to interstitial growth of cartilage (Silberberg and Silberberg 1) Dying cells are uncommon in grow' c rtilage and therefore could not
c erially to an increase of
hey become frequent after
th and may therefore
maintenance of the con
aged cartilage In the
de enzymes or cal
l berated which
f fibers A com-
ved in
of der
esence

In he
ter t
all ng
the
al c
If
c lls
er
r

cells. There was no evidence in support of a perichondral or synovial origin of these atypical chondrocytes. On the other hand these surface cells may have persisted from early youth and thus represent the oldest chondrocytes of the joint. This explanation is consistent with the appearance of their mitochondria which resemble those seen in aged cells of other tissues (Rouillier '60 Novikoff '61; André '62)

Correlation of cell structure and function

Both uptake and discharge of materials by cells are facilitated by development of cytoplasmic footlets which may play a role similar to that of microvilli in glandular secretions (Dempsey '58) Since youthful surface cells possess only few footlets the exchange of metabolic products between them and the matrix must be slow Furthermore the limited development of ER and the scarcity of free RNA granules noted in these cells point to low grade activity as regards the synthesis of proteins probably including collagen. Production of proteins and other materials required for cell growth and formation of matrix seems most active in the midzonal cells in which the organelles are highly developed Multivesicular bodies serving intracellular transport were only rarely seen to open onto the surface as described for embryonal epiphyseal cartilage (Godman and Porter '60) This finding is consistent with a slower rate of growth of articular as compared to epiphyseal cartilage but it may also denote a retardation of discharge of synthesized material with advancing age Moreover from static pictures alone it is impossible to decide which way intracellular transport is moving and whether the open membranes of these bodies indicate incomplete formation or rupture Conceivably these bodies may serve the transport *of ingested material as well as that of* secretions The structural findings suggest that in aged cartilage some of the functions of young midzonal cells are taken over by hondrocytes lying close to the su f

Th I ased number of mitochondria In d T artilage cells of aging an-
ma ir ecent of similar observations
in r during hibernation (Poche

'59 Moreland, '62) or in oncocytes of the salivary glands and parathyroids (Roth, Olen and Hansen, '62 Munger and Roth, '63) The condition may reflect storage of enzymes owing to decreased requirements or it may indicate a past increased demand for mitochondrial enzymes or exhaustion of individual mitochondria followed by compensatory newformation of others.

The aged surface cells seem to be atypical in function as well as in structure as suggested by the appearance of the peri cellular matrix. Aged chondrocytes show increased uptake of S^{35} (Collins and McElligott, '60) indicative of newformation of sulfated mucopolysaccharides. On the other hand, aged matrix differs from youthful matrix inasmuch as total hexosamine decreases, while keratosulfate increases (Kaplan and Meyer '59 Lash and Whitehouse '60) Moreover cartilage matrices of different ages may differ in hydration or polymerization (Collins and McElligott, '60 Silberberg and Silberberg, '61a) While thus the ability of the aging chondrocytes to produce ground substance appears altered, it still retains the power to produce primitive fibrillar material. Whether the atypical appearance of peri cellular fibrils is due to changes in the composition of the ground substance or alterations in cellular function will be determined by further studies.

SUMMARY

The ultrastructural changes taking place during life in the chondrocytes of femoral heads of the mouse may be expressed in terms of cycles. During the ascending phase of the curve there was progressive organization of the cytoplasmic organelles the descending grade of the cycle was characterized by a temporary increase of mitochondria and subsequent degeneration of organelles by appearance of larg amounts of cytoplasmic glycogen and lipid and by swelling and breakdown cell Both length and amplitude of the cycle varied during different perio e th amplitude reaching a peak ng the height of ossification. Cel k a fol lowed by ossification or t by fibrillar scars. Erosion ... hyper trophic chondrocytes by capillaries was not observed. With advancing age, cartilage cells of the surface layer assumed charac teristics of midzonal cells of earlier ages. In old age, superficial chondrocytes showed evidence of growth and production of dense matrix containing short broken off fibrils a condition not seen at any other period of life. The matrix underwent in creasing vacuolation and blisterformation at the surface while nearby chondrocytes were intact. The structural changes are discussed in relation to cell function.

LITERATURE CITED

André J 1962 Contributions à la connaissance du chondriome. J Ultrastruct. Research, Suppl. 5. 1–185.

Collins, D. H., and T F McElligott 1960 Sulphated ($^{35}SO_4$) uptake by chondrocytes in relation to histological changes in osteoarthritic human articular cartilage. Ann. Rheumat. Dis., 19 318–330.

Davies, D V C. H. Barnett, W Cochrane and A. J Palfrey 1962 Electron microscopy of articular cartilage in the young rabbit. Ann. Rheumat. Dis., 21 11–22.

Dempsey E. W 1958 Current concept of cellular structure. In Frontiers in Cytology Ed. S L. Palay Yale University Press, New Haven, 9–18.

Godman, G C., and K. C. Porter 1960 Chondrogenesis, studied with the electron [illegible]roscope. J Biophys. and Biochem. Cytol., 8 [illegible]–760.

Kaplan, D., and K. Meyer 1959 A [illegible] human cartilage N [illegible] 183. 126[illegible]

Keech, M. K. 1961 The f[illegible] from collagen solution. [illegible] polysaccharides and m[illegible] microscopic study Cell [illegible]

Lash, J W and M W Wh[illegible] tions in the pol[illegible] tilage with [illegible] 90 159–160.

Little, K L [illegible] Osteo[illegible] micro[illegible] 402

[illegible]

PLATE 2

EXPLANATION OF FIGURES

2 Newborn mouse surface There is loose network of fibers, some cut lengthwise some cut acros ; both l yers run parallel t the surface There is tangential cut of superficial cell (C) Uranylacetate × 22,000.

3 Newborn mouse Deep cell embedde l in loose matrix with delic t fibrils. The nucleus shows infolding, the cytoplasm contains ER lamellae lined by RNA granules. The mitochondria (m) are larger the footlet longer than in the surface cell (fig. 1) Golgi material (g) and multivesicular bodies (b) are present. Uranylacetate 22,000


c
2

PLATE 3

EXPLANATION OF FIGURES

4 Newborn mouse deep cell in divisior The line of cleavage is incomplete; in some areas, there is sepa tion of the cells, while in the center they are still onnected. Cister (C) are seen. Uranylacetate. 22,000.

5 Close-up of line f cleavage (arro) in dividing cell shown in figure 4 The dividing line can be llowed from the lower end of the newly formed intercellular spa (I) The plasmalemma are incomplete and dove-tailed into eac other Between the upper and the lower pairs of arrows re areas n which the line of clear ge is fully visible ER e) Ura lacetate × 63,000.



PLATE 5

EXPLANATION O FIGURE

7 Five week-old mouse urface cell ER is well developed ( ) pinocytotic vesicles (p) nd numerou mitochondria (m) are seen which are larger than in the newborn mouse Compare with figure 1 The nuclear envelope bow pores (rrow) Footlets (F) re numerous and long Uranylacetate × 32,000


B
F
7

PLATE 6

EXPLANATION FIGURE

8 Five-week-old mouse Fully developed midzonal cell with long cytoplasmic footlets. Advanced organiz tion ER lamellae ( ) lined by RNA granules; abundant Golgi material (G) large mitochondria (m) and large multivesicular bodies (b partly with incomplete membranes and pinocytotic vesicles (p) pposed to the cytoplasmic membrane Uranylacetate. × 32,000


B
G
G
D
D
8

PLATE 7

EXPLANATION OF FIGURE

9 Six-week-old mouse Hypertrophic artilage cell of deep l yer near zone f ossification. Compressed ER) Golgi material near nucleus multivesicular body (b) and some glycogen in upper and large glycogen lake (g) in lower part of he cell. Uranylacetate × 16,000.

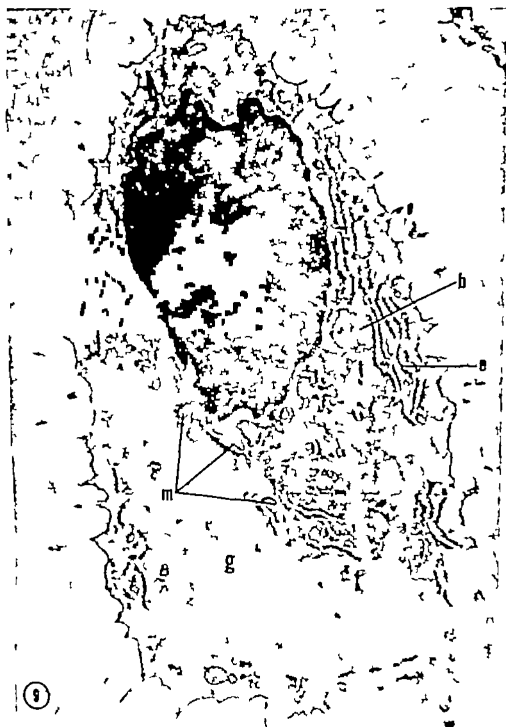

b
e
m
g
9

PLATE 9

EXPLANATION O FIGURES

12 One-year-old mouse Midronal cell bowing double nuclei separated by ER. Uranylacetate × 22,000.

13 Eleven-month-old mouse Delic te fibrils or brush-lik deposits of fibrillar material near the cell membrane are indicated by arrows. Uranylacetate 44,000.



PLATE 10

EXPLAN TION O FIGURE

14 One yea -old mouse Cell of deep la er close t calcification front (C) The cell h many long footlet densely packed ER and many mitochondria. Much Golgi material some glycogen (g) and a few multi esicular bodies (b) are seen Tangential section through nu- leus (N Ura)lacetate × 22,000


11

The Ultrastructure of Human Gingival Epithelium[1]

MAX A. LISTGARTEN[2]
Harvard School of Dental Medicine Boston, Massachusetts

In the last decade many investigators have helped to expand our knowledge of the morphology of epithelial tissues through the use of electron microscopy By far the most popular epithelial tissue studied has been skin and its appendages. The first electron microscopic study dealing with the epithelial lining of the oral cavity was published in '58 by Sognnaes and Albright. They studied the intermediate and superficial epithelial layers of the cheek and gingival mucosa in weanling mice, in an attempt to clarify the nature of the normal process of cornification and desquamation occurring in the mouth Since that time several papers have been published dealing with oral epithelium both in animal and human material (Sognnaes and Albright, '58 Albright, '60; Fasske and Themann, '59 Zelickson and Hartmann, '62 Stern '62; Gibbins '62; Kurahashi and Takuma, '62) In man, the lining of the oral cavity is normally not cornified. Certain portions of this lining, however frequently show a distinct stratum corneum. This is usually observed in epithelium lining the masticatory surfaces, namely the attached gingiva and palatal mucosa and in the specialized epithelium of the dorsum of the tongue. The present study was undertaken to investigate the fine structure of clinically healthy human gingival epithelium The results will serve as a baseline for further studies of gingival disease.

MATERIALS AND METHOD

Clinically healthy gingival specimens were obtained from donors of both sexes ranging in age from 9 to 42 years. Anesthesia was achieved through nerve block. In every case the sample was ob ained from the marginal gingiva (fig 1) in an area as far removed as possible from the site of injection of the anesth etic

The tissue was secured with a minimum of handling and immediately immersed in ice cold 2% osmic acid fixative buffered to pH 7 4 with veronalacetate buffer and osmotically balanced by the addition of 8% w/v sucrose to the fixative (Caulfield, '57) While immersed in the fixative the samples were subdivided into smaller blocks (fig. 1 B and C) After 30 to 60 minutes fixation each block of tissue was further subdivided into small slices measuring approximately 0 5 mm in thickness (fig. 1-C and D) These were left in the osmic acid solution for a total fixation time of two hours.

After removal from the fixative the blocks were dehydrated by passage through graded concentrations of ethanol, infiltrated with propylene oxide for one hour and embedded in epon according to the method described by Luft, 61) Sections measuring 0 1 to 0 2 μ in thickness were cut in a Porter Blum microtome collected on carbon reinforced formvar coated grids and stained for one hour in a recently filtered saturated solution of uranyl acetate in 60% ethano e grids were washed in 60% ethanol d ied and examined in an RCA mode EM 3B elec tron microscope For orientation purpo s thicker sections from eac l ck v collected or a glass slide a l st ned light microscop with toluid e i e.

OBSERVATIONS

No morphol cal differ nces hic could be elated to either age or i en apparent i the mate ial studie Th observations w follow are there for e cable o gingival epithelium o pers both sexes within the age ran ind previo sly

[1] [illegible]
[2] [illegible]

dermis. J Biophys. Biochem. Cytol., 4 529–538.

——— 1960 A submicroscopic granular component in human epidermis. J Invest. Derm 34 11–15.

Robertson J D 1959 The ultrastructure of cell membranes and their derivatives. Biochem. Soc Sympos., 16 3–43.

Rogers G. E., and B. K. Filshie 1962 Electron staining and fine structure of keratins. Proc. Fifth International Congress of Electron Microscopy Vol. II Academic Press, New York. Abstract.

Sognnaes, R. F and J T Albright 1956 Preliminary observations on the fine structure of oral mucosa. Anat. Rec., 126 225–239

——— 1958 Electron microscopy of the epithelial lining of the human oral mucosa. Oral Surg., 11 662–673

Stern, I. B 1962 Study of the ultrastructure of rat gingival epithelium. I.A.D.R., 40: 78 Abstract.

Weiss, P., and W. Ferris 1954 Electronmicrographs of larval amphibian epidermis. Exp Cell Res., 6 546–549

Wolf J 1960 Die Oberflache der Verhornten Zelle der Epidermis im Reliefbild. Proc. Fourth International Conference on Electron Microscopy Vol. II Springer Verlag, Berlin. Abstract.

Zelickson, A. S and J F Hartmann 1962 An electron microscope study of normal human non-keratinizing oral mucosa. J Invest. Derm., 38 99–108

PLATE 1

EXPLANATION OF FIGURES

2 Epithelium — connective tissue junction. Note amorphous basement membrane (BM) separating epithelial cells (EP) from underlying lamina propria (LP) × 35,000 Insert — Higher magnification of basement membrane area EP Epithelial cell; d, modified desmosome BM, Basement membrane Col gen fibrils. 60,000.

3 Basal cell. Note distribution of mitochondria (M) around nucleus (N) tf Tonofilaments. × 35,000


EP
BM
LPA
BM
2
N
M
M
3

PLATE 3

EXPLAN TION O FIGURES

5 Cell in stratum spinosum. Note large number of desmosomes (D) × 5,800

6 Cell in tratum pinosum. Note fibrill r nature of cytopl m. N Nucleu f Tonofilament ; D Desmosomes cut in different planes; ics Intercellular space × 26,000


5
6

PLATE 5

EXPLANATION OF FIGURES

10 Flattened cell of uperficial l yers. SC Stratum corneum; CC Cells undergoing cornification; N Nucleu of cell from stratum granu-los m. 6,500 Insert — Magnific tion f outlined are illustrating large granules in peripheral cytopl sm of stratum granulosum cells. 10,500.

11 Keratohy lin gra ule (arrow) in trat m gr losum. Note cyto-pl smic depletion in the vicinity f the granul 46 000.

10



PLATE 5

EXPLANATION OF FIGURES

10 Flattened cells of superficial layers SC Stratum corneum; CC Cell undergoing cornific tion; N Nu leus of cell from tratum granulosum 6,500 Insert — Magnific tion of outlined area illustrating large g anules in peripheral cytopl sm of tratum granulosum cells. 16,500

11 Kera oh alin granule (arrow) in tratum granulosum Note cytopl sm depletion in the vicinity the granule × 46,000

Electron Microscopic Alterations in the Rat Hypophysis after Scalding[1]

EDWARD G. RENNELS
Department of Anatomy University of Texas Medical Branch, Galveston Texas

Previous studies in our laboratory have shown that within 12 hours after subjecting rats to a standardized scald there is a loss of more than one-half of the pituitary store of ACTH (adrenocorticotrophic hormone) (Timmer '60) Since the cellular locus of ACTH production and storage has remained an unresolved facet of pituitary cytophysiology it was of interest to study the pituitary glands of burned animals with the electron microscope. It was reasoned that some electron microscopic changes might be found which could be related to the stress-induced outpouring of ACTH or to the heightened synthesis of this hormone which follows the initial discharge In previous studies on this problem with the light microscope (Rennels '60) we reported the following changes in cells of the anterior pituitary (1) a marked but transient increase in the number of glandular cells in mitosis (2) a general reduction in the size of all parenchymal cells which becomes most marked at 12 hours after stress and (3) an increase at 12 and 24 hours after stress in cytoplasmic basophilia of the acidophiles. In preliminary reports (Rennels '60 '61) we have described certain electron microscopic changes in the pituitary of the rat after thermal stress. The present report extends and documents these earlier findings.

MATERIAL AND METHODS

Animals and experimental procedures

The pituitary material was ob-ained from young male Holtzman rats weighing 150–200 gm. All animals received an intraperitoneal injection of sodium pentobarbital (Nembutal, 4 5 mg/100 gm) 30 minutes prior to sacrifice or prior to scalding The standardiz-d scald w- e fected by immersion of the animal (ex-ept for the head) in water at 70 C for five seconds Material was obtained from unstressed controls and from animals killed by decapitation at the following time periods after scalding 30 minutes, 1 3 12 and 24 hours. Several series of animals have been used in these studies although this report is based on pituitary material from only two series consisting of 26 and 19 animals.

Preparation of material for electron microscopy

After decapitation, the pituitary gland was quickly exposed by cutting away the dorsum of the skull and lifting up the brain The gland was freed from the dura with fine jewelry forceps and transferred to a moistened piece of paper towel The posterior lobe was removed with forceps and discarded. Two slices of about 1 mm width were cut from the remaining anterior lobe one from the medial region of the gland and the other from the lateral tip. These two specimens were fixed and processed separately for microscopy Consequently all observations were limited to these two regions of the gland (In a few cases samples of the intermediate and posterior lobe were also processed and studied.)

The pituitary material was fixed in cold osmium tetr-xide-sucrose mixture (Caulfield '57) for periods of 20–30 minut-- Follo-ing fixation the tissues were d-drated in increasing concentrations c ethanol and sta-ed for ten min 0 1% phospho- -ta- acid in ethanol Infiltr- [illegible]

[1] Supported by contract N[illegible] [illegible] University of [illegible] available through [illegible]

Electron Microscopic Alterations in the Rat Hypophysis after Scalding[1]

EDWARD G. RENNELS
Department of Anatomy U iversity f Texas Medical Branch Galveston Texas

Previous studies in our laboratory have shown that within 12 hours after subject ing rats to a standardized scald there is a loss of more than one-half of the pituitary store of ACTH (adrenocorticotrophic hor mone) (Timmer '60) Since the cellular locus of ACTH production and storage has remained an unresolved facet of pituitary cytophysiology it was of interest to study the pituitary glands of burned animals with the electron microscope It was rea soned that some electron microscopic changes might be found which could be related to the stress-induced outpouring of ACTH or to the heightened synthesis of this hormone which follows the initial dis charge In previous studies on this prob lem with the light microscope (Rennels, '60) we reported the following changes in cells of the anterior pituitary: (1) a marked but transient increase in the number of glandular cells in mitosis (2) a general reduction in the size of all parenchymal cells which becomes most marked at 12 hours after stress and (3) an increase at 12 and 24 hours after stress in cytoplasmic basophilia of the acidophiles In prelimi nary reports (Rennels '60 '61) we have described certain electron microscopic changes in the pituitary of the rat after thermal stress. The present report extends and documents these earlier findings

MATERIAL AND METHODS

Animals and experimental procedures

The pituitary material was ob ined from young, male, Holtzman rats weighing 150–200 gm. All animals received an intraperitoneal injection of sodium pentobarbital (Nembutal, 4 5 mg/100 gm) 30 minutes prior to sacrifice or prior to scalding. The standardiz d scald w e fected by immersion of the animal (ex pt for the head) in water at 70 C for five seconds. Material was obtained from unstressed controls and from animals killed by decapitation at the following time peri ods after scalding 30 minutes 1 3 12 and 24 hours Several series of animals have been used in these studies although this report is based on pituitary material from only two series consisting of 26 and 19 animals.

Preparation of material for electron microscopy

After decapitation the pituitary gland was quickly exposed by cutting away the dorsum of the skull and lifting up the brain. The gland was freed from the dura with fine jewelry forceps and transferred to a moistened piece of paper towel. The posterior lobe was removed with forceps and discarded Two slices of about 1 mm width were cut from the remaining ante rior lobe one from the medial region of the gland and the other from the lateral tip. These two specimens were fixed and processed separately for microscopy Consequently all observations were limited to these two regions of the gland. (In a few cases samples of the intermediate and posterior lobe were also processed and studied)

The pituitary material was fixed in cold osmium tetr xide-sucrose mixture (Caul field '57) for periods of 20–30 minutes Follo ing fixation the tissues were d drate in increasing concentrations c ethanol and sta ed r ten min 0 1% phospho ic acid in ethanol. Infiltr... [illegible]

[1] Supported by contract N the Office of Na al Research, ... and th University of ... [illegible]

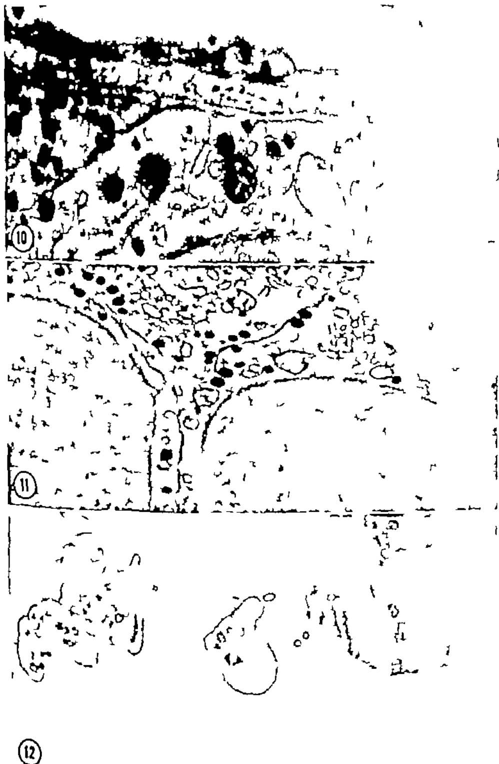
PLATE 6

EXPLAN TION OF FIGURES

10 Capill ry w ll showing lumen bos containing portion of rythrocyt t upper right corner Several secretory granules ha bee truded from the somatotroph and be either between djacent cell membranes (1) or in the extracellular pace bordering the basement membrane (2) Thi material w removed one hour after scalding (× 23,500)

11 Portions of three somatotroph f om a gl nd removed 30 min tes fter sc lding Note the accumulation of secretory gr nules near the ll membranes (× 9,500)

12 Pituitary capillary from gland removed 30 minutes fter scaldi g showing platelet (P) and retic locyte (R) within lumen both oc curred in increased mbers i he pituit ry essel of scalded ani mal (10 000)


10
11
12

was observed undergoing phagocytosis in the cortical pits occupied by macrophages. Ingestion of nuclear debris by these macrophages accounted for nearly all the DNA which we observed Preparations treated with desoxyribonuclease prior to staining with methyl green or the Feulgen method lost their affinity for these stains.

Ribonucleic acid. In normal rats ribonucleic acid was histochemically discernible following application of the Kurnick ('55) method in medium and large lymphocytes and in the reticular cells of the thymus. It was located principally in the cytoplasm (fig. 1) though in large nuclei it could be seen in the nucleolus as well. It was occasionally visible in some of the small lymphocytes Incubation in a medium which contained ribonuclease before staining with pyronin Y abolished the stain and established its specificity for RNA.

Following the administration of ACTH cortisone hydrocortisone or DOC the formation of RNA positive cytoplasmic blebs or bubbles preceded shedding or loss of RNA (fig 2) In certain instances elongated droplets were noted prior to complete pinching off which may be indicative of an orderly and functional departure of the cytoplasmic RNA Free particles of RNA were occasionally observed in the medulla as well as the cortex. The fate of such RNA particles was somewhat more obscure than that of the DNA but some of them were probably phagocytized by reticular cells or became associated with Hassall's corpuscles while others may have passed into the circulation

The administration of DOC did not result in the pycnosis of cortical lymphocytes but it did appear to result in a decreased amount of histochemically stainable RNA. The nuclei of cells which exhibited bleb formation were normal and discrete with no evidence of pycnosis

Glycogen and PAS positive material Glycogen and in some cases PAS positive material increased following single or series of injections of cortisone hydrocortisone and ACTH No comparable increase was observed following the administration of either single or a series of injections of DOC The cells containing glycogen or PAS positive material were located at the cortico-medullary border and appeared to be reticular cells though the nuclei in some of them were smaller and more dense than those generally observed in these cells.

Intracellular glycogen or PAS positive material was not observed at sites other than the cortico-medullary border This is of particular interest since clusters of alkaline phosphatase reactive cells occurred in this same location. The PAS method sharply outlined vascular walls perivascular lymphatics and to some extent the connective tissue stroma of the thymus.

Alkaline phosphatase In normal rats as well as in those treated with cortical steroids alkaline phosphatase was observed at the cortico-medullary border sub-capsularly at the periphery of the cortex perivascularly throughout the thymus, and in scattered individual cells particularly in the cortex. By employing either the Gomori or the Burstone technique and 10 or 20 minute periods of incubation respectively a discrete pattern of cellular activity was revealed which indicated that various cell types or morphological variants of similar cells were reactive In addition a degree of organization was revealed within individual cells particularly with the Gomori technique which was not otherwise evident (fig 3)

Single injections of cortisone hydrocortisone DOC and ACTH led to an increase in alkaline phosphatase within 6 hours This increase was accompanied in certain instances by a disorganized intracellular disposition of the enzyme (fig 4). In adrenal-ectomized rats a decrease in alkaline phosphatase was evident by the sixth day and the enzyme appeared to be more granular and dispersed than in normal animals or following cortical steroid administration (fig 5)

These observations led to a comparative study in which alkaline phosphatase activity was evaluated following single injections of 6 mg of cortisone 6 mg of hydrocortisone 3 mg of DOC and 4 mg of ACTH Phosphatase activity was also observed following seven consecutive days of two equal d ily injections totaling 1 mg per day of cortisone hydrocortisone and DOC A similar series of injections of

ACTH were administered for four days. Daily injections of ACTH, and each of the cortical steroids employed increased intracellular alkaline phosphatase activity as had single injections of these hormones.

Material stained by both the Gomori and Burstone methods indicated a definite pattern of alkaline phosphatase activity which appeared to be directly related to the hormonal preparation utilized the dosage employed, and the duration of treatment. Both the number and size of the clusters of reactive cells varied depending on the experimental situation (tables 2 and 3)

A single injection of hydrocortisone or DOC resulted in substantial increases in the number of alkaline phosphatase reactive cells in clusters while multiple injections of hydrocortisone resulted in the largest clusters of phosphatase reactive cells observed following a series of daily injections (tables 2 and 3) The number of phosphatase staining cells in a cluster following a series of daily hydrocortisone injections increased to 188 from a control value of 30 while similar treatment with cortisone increased the number to 144 (table 2) Multiple DOC injections increased phosphatase reactive cells to 100 from a control value of 29 while ACTH was followed by an increase from 70 to 160 per cluster Hormone treatment, notwithstanding the various dosages employed or the number of injections ad

TABLE 2

Effects of cortisone and hydrocortisone on quantitative and qualitative values of alkaline phosphatase activity

Treatment	R	S	C	A
Single 6 mg injections six hours before sacrifice				
Control	1.4	2.3	15	23
Cortisone	1.6	2.9	27	38
Hydrocortisone	1.6	2.6	40	34
Series of daily 1 mg injections for seven days. Dosage equally divided between A.M. and P.M.				
Control	1.0	3.0	30	30
Cortisone	3.3	9.0	114	56
Hydrocortisone	4.2	7.2	188	85

R — average of rating (0 to 5) made with scanning lens.
S — average of number of reactive sites in the most reactive section of tissue from each experimental animal (scanning lens).
C — average number of alkaline phosphatase positive cells in the largest cluster (low power).
A — average number of reactive cells in an area 250 square (high power).

TABLE 3

Effects of ACTH and DOC on quantitative and qualitative values of alkaline phosphatase activity

Treatment	R	S	C	A
Single injection of 3 mg of DOC, or 4 mg of ACTH six hours before sacrifice				
Control	1.5	3.3	28	38
DOC	3.3	5.1	62	39
Control	2.0	6.3	75	64
ACTH	3.4	8.6	107	70
Series of daily 1 mg injections of DOC for seven days, or ACTH for four days				
Control	1.0	3.3	29	16
DOC	3.0	9.2	100	66
Control	3.0	6.3	79	35
ACTH	4.0	5.7	160	78

R — average of rating (0 to 5) made with scanning lens.
S — average number of reactive sites in the most reactive section of tissue from each experimental animal (scanning lens).
C — average number of alkaline phosphatase positive cell in the largest cluster (low power).
A — average number of reactive cells in an area 250 square (high power).

ministered resulted in larger clusters of alkaline phosphatase reactive cells in each case

The observation that DOC generally reported not to cause involution of the thymus noticeably increased alkaline phosphatase activity is of particular interest. A single injection of DOC (3 mg) resulted in a greater number of clusters of alkaline phosphatase reactive cells than did either a single injection of 6 mg of cortisone or of hydrocortisone (tables 2 and 3). In some of these cases the sites of alkaline phosphatase activity also appeared to be more intense and more highly reactive following the administration of DOC. The regulation of alkaline phosphatase activity was shared by the glucocorticoids cortisone and hydrocortisone and by the mineralocorticoid DOC while pycnosis karyorrhexis and the phagocytosis of small lymphocytes was brought about only by the former

Examination of cells stained by the Gomori method and showing alkaline phosphatase activity indicated that the cellular activity was discrete and that it may be both cytoplasmic and nuclear. The enzymatic activity appeared to be cytoplasmic because of its generally peripheral distribution within the cells. However cells in similar sites stained by other techniques indicated basophilia as well as Feulgen positive and methyl green staining in the same intracellular areas of cells which were alkaline phosphatase positive. The possibility that nuclear enzyme activity also occurs must be considered as a result of these observations

Histochemical visualization of alkaline phosphatase following staining by Burstone's method and counterstained with methyl green (fig. 6) did not appear so discrete under high magnification as that following utilization of Gomori's method possibly because of the high refractive index of the polyvinyl pyrrolidone mounting medium employed (Pearse '60)

Acid phosphatase Acid phosphatase is a normal constituent of the thymus. It was most prevalent in cells along the cortico-medullary border and stained with increasing intensity following the administration of ACTH and the cortical steroids employed. [illegible] fore cells [illegible] the cortex appeared to contain acid than alkaline phosphatase which may account for the somewhat diffuse staining sometimes observed in the thymus. Histochemically acid phosphatase has generally been considered to be more labile in terms of preservation and accurate localization than alkaline phosphatase. This is particularly true following acetone fixation and staining by the Gomori technique (Pearse '60)

DISCUSSION

This study places further emphasis on the importance of making observations almost immediately following endocrine manipulations. The six hour interval appeared to be an ideal time to examine and quantitate histological and histochemical events following hormone administration since maximal histological changes had been observed at this time by Dougherty and White ('45) and Lee ('58 '62). Cowan and Sorenson ('63) utilizing the electron microscope reported a rearrangement of chromatin in small lymphocytes of the mouse thymus within 4 to 8 hours after hydrocortisone injection. The utilization of a six hour period after treatment as well as one of several days prior to examination enabled us to make a comparative study of the early enzymatic changes at the cellular level not previously reported. Prolonged treatment generally enhanced modifications noted following single injections. Further observations on the sequence of histochemical changes at various time intervals greater as well as less than six hours would be of considerable interest.

Morphologically similar cells particularly the small lymphocytes appeared to have varying degrees of sensitivity to cortical steroids. The apparent resistance of large and medium lymphocytes to the involutionary effects of ACTH cortisone and hydrocortisone may indicate a lack of the necessary enzyme systems or a cellular impermeability to cortical steroids (Dougherty '60). It could also be accounted for by the capacity of the less mature cells to inactivate the lymphocytolytic effect of hydrocortisone as discussed by Dougherty ('62)

The reduction in number of small lymphocytes and the increase in the num

ber of reticular cells observed in our experiments confirms the report of Udall ('55) in which similar observations were made following the administration of cortisone in suckling rats. Our observations also substantiate the work of Santisteban ('59) who observed that the adrenal cortex may have stimulatory as well as inhibitory effects on the thymus. Evidence of a supporting nature is also provided for the Stem Cell Renewal Theory of St. Marie and Leblond ('58a, b).

Any change in activity or in number of the reticular cells is of interest since these cells are implicated in phagocytosis as well as in the proliferation of lymphocytes. Gregoire (43) implicated perivascular phagocytic or epithelial cells such as those located at the cortico-medullary border as participating, at least to some extent, in the renewal of thymus cells.

Our observations on RNA bleb formation following the administration of ACTH and cortical steroids confirm the observations on cytoplasmic bubbling reported by Dougherty and White (45) and Schneebell and Dougherty ('55). The latter postulated that RNA may be released into the blood stream or pass into the medulla to be incorporated in the cytoplasm of reticular cells. This hypothesis would seem to require additional cytological evidence. The observations on cytoplasmic RNA blebs or bubbles is of interest since the application of a histochemical technique in our study confirmed this effect which had previously been best demonstrated by the application of histological or *in vitro* studies.

Our observations help to establish the adrenal cortical regulation of alkaline phosphatase activity in the thymus and confirm previous reports which implicated the adrenal cortex in the regulation of this enzyme. Herlant and Timiras ('50) reported an increase of alkaline phosphatase in the rat thymus following cold stress while Moog ('53) observed a precocious appearance of this enzyme in the duodenum of the mouse following cortisone administration. Verzar ('53) reported a decrease in alkaline phosphatase in the intestine of the rat following adrenalectomy.

In our study the Gomori and Burstone methods confirmed one another with respect to alkaline phosphatase staining. Our observations indicate that considerable resolution may be obtained by using prolonged cold acetone fixation, paraffin embedding, shorter incubation periods and Yokoyama's modification of the Gomori method. From a technical aspect these *procedures are highly desirable and may* be readily followed since the equipment usually found in any microanatomical laboratory is sufficient. Tissues can be more readily processed than in situations where frozen preparations are employed. Moreover, our observations indicated that prolonged periods of acetone fixation ranging from 48 hours to seven days provided better preservation of cytological details. Excellent preservation of the enzyme without inactivation or diffusion was obtained under these conditions.

Quantitative estimates on alkaline phosphatase activity utilizing histochemical means to evaluate the activity of a number of hormones, have provided a method whereby the effects on this enzyme may be determined in tissue sections. The advantages include a degree of quantitation on the histochemical level, localization of activity in intact tissues and the possible examination of certain cytological aspects of its disposition.

The employment of short incubation periods for Gomori and Burstone stained material made quantitation possible. Brief periods of incubation permitted histochemical visualization of discrete reactive sites and made possible the rating of a given tissue as well as the counting of individual reactive cells. While shorter incubation periods have now been employed for some time, periods ranging from 1 to 4 hours, and sometimes in excess of ten hours, particularly with the Gomori alkaline phosphatase technique have frequently been employed. Sulur (61) utilizing the Gomori technique with a two hour incubation period, reported alkaline phosphatase activity in the thymus of the mouse. While relatively long incubation can be both necessary valid, prolonged incubation is permit diffusion or in enzyme which may result in

and false negative staining The accuracy of alkaline phosphatase localization following long incubation periods is thus reduced and renders any hope of quantitation or accurate cytological observation as achieved by our method less likely

The observation that DOC increases alkaline phosphatase is of considerable interest and provides indirect histochemical evidence which substantiates the *in vitro* studies of Jedeiken and White ('58) in which DOC as well as cortisone and hydrocortisone were found to inhibit endogenous respiration, oxygen consumption, and the oxidation of glucose to CO_2 in rat lymphoid tissue. They observed that the administration of DOC resulted in the greatest inhibition of the three parameters measured Blecher and White ('60) found that cortisol inhibited the anaerobic glycolysis of glucose but not that of glucose-6-phosphate or fructose-6-phosphate while DOC inhibited the utilization of all substrates and stimulated the hydrolysis of labile phosphate esters. This may account for the lack of glycogen deposition following the administration of DOC as well as the increased intensity in the alkaline phosphatase reaction. Dougherty ('62) noted that compounds unsubstituted at the C-11 position on the steroid nucleus of which DOC is an example are not lymphocytolytic

The increased intracellular alkaline phosphatase activity observed in our experiments appears in some instances to involve both the nucleus and the cytoplasm and may be indicative of a phosphate transfer between them Ehrich and Seift r ('53) implicated purines and pyrimidi es as breakdown products of nucleo- id , which may conceivably be important n al lite of lymphocytolysis and could be oci l with phosphate transfer earse ('6(reported that efforts to establish he u/polyholic hyrroi nce of alkaline phat, employed (Pearse d if this en- is sphatase Acid phosphate trans- constituent of the thymphosphate / prevalent in cells alon essarily dullary border and stained w since g intensity following th admi ob- of ACTH and the cortical steroid der td fore cell l the cortex ap- d e

alkaline phosphatase activity was greatly enhanced following the administration of DOC without a concomitant pycnosis of lymphocytes leads to the conclusion that this enzyme may be an intergral part of a stimulatory mechanism of cell proliferation in the thymus under adrenal cortical control.

The identity of the specific cell or cell types revealing alkaline phosphatase activity requires further investigation. From a morphological aspect more than one cell type appears to be reactive though we may be concerned with one cell type during its different morphological stages. It is possible that the reactive cells are lymphocytes monocytes or granular leucocytes particularly eosinophils which are known to be sequestered in the thymus spleen and lymph nodes following the administration of various cortical steroids Clark ('63) reported numerous eosinophils near blood vessels in an electron microscope study of the mouse thymus. Gordon ('54) described various degenerative stages in eosinophilic nuclei which morphologically appear to be identical with many of the reactive cells we have observed However Schreck (48) reported degenerative stages in lymphocytes of the thymus which following x-irradiation underwent nuclear vacuolization and ultimate pycnosis which are also morphologically similar to our reactive cell types.

The administration of DOC resulted in a cortical thickening hence the increased alkaline phosphatase could be associated with the development of macrophages (or reticular cells) from monocytes as reported by Rabinowitz and Schreck ('6?) Previous observations have been made on the differentiation of perivascular phagocytes or reticular cells into thymus lymphocytes (Gregoire 43) The electron microscope studies of the mouse thymus by Clark (63) and Weiss ('63) both emphasize the importance of the epithelial reticular cell in the vascular barrier between the cortex and medulla. These reticular or epithelial cells might in some instances be the alkaline phosphatase positive cells undergoing transformation. An increase in alkaline phosphatase following cortisone administration was reported by Moog ('53) in the duodenum of the suck

ling mouse and by Goldsmith and Ross ('56) in the developing incisor of the fetal rat. We may be observing hormonal augmentation of a series of normal cellular transformations (tissue fibroblast — reticular cell — large, medium small lymphocyte) in the thymus with DOC stimulating cytodifferentiation while cortisone and hydrocortisone stimulate both cytodifferentiation of reticular stem cells and karyorrhexis of small lymphocytes, liberating DNA for reutilization as proposed by Trowell ('58) Bailiff ('49) who investigated thymic regeneration, reported cords of hyperplastic epithelial cells in the medulla which sometimes extended into the cortex. He concluded that these epithelial cells gave rise to thymocytes by transformation since mitotic figures were rarely seen.

The morphology of many of our reactive cells is identical with that reported by Smith ('61) who concluded that under some circumstances lymphocytes reveal alkaline phosphatase activity She made no mention of eosinophils or neutrophils despite the fact that the May-Grunwald Giemsa stain was employed. Further histochemical and cytological studies employing the cryostat and touch impression techniques are currently underway and should provide additional information regarding the identity of the reactive cell or cell types as well as the ultimate nuclear or cytoplasmic disposition of the alkaline phosphatase.

The data, particularly in the case of alkaline phosphatase indicate the possibilities of a further development of techniques for the histochemical investigation of tissue enzyme kinetics as proposed by Benditt and Arase ('58) The importance of enzyme systems in hormone action may account for the observation of Schreck ('49) that cortisone was cytotoxic at 37 C but not at 27 C or 45 C which may be indicative of a temperature retardation or inhibition of enzyme systems. The importance of these systems in the hormonal control of lymphocyte de lopment is further emphasized by Dougherty Berliner and Berliner ('62) in a review of their observations on the capacity of thymic lymphocytes to metabolize adrenal cortical steroids by enzymes present in these cells In addition the relationship between hormones and the response of specific target cells discussed by Stetten ('59) is of considerable interest particularly since the various cell types present in the thymus exhibit singular reactions following hormone treatment.

Our observations on the increased staining activity of alkaline and acid phosphatase as well as glycogen or PAS positive material at the cortico-medullary border following the administration of hormonal agents is of special interest This well vascularized area has been noted to be the location of large histochemically active cells. Barka Schaffner and Popper ('61) reported acid phosphatase in reticular cells of the rat thymus particularly in those located at the cortico-medullary border while Kahri Hannuksela and Karaharju ('63) reported succinate tetrazolium reductase activity in large cells at the cortico-medullary border of rat thymus tissue.

SUMMARY

1 Histological and histochemical modifications were observed in the rat thymus six hours following single injections of ACTH (4 mg) cortisone (6 mg) hydrocortisone (6 mg) or DOC (3 mg) Similar changes followed daily injections of 1 mg of cortisone hydrocortisone or DOC for seven days and ACTH (1 mg) for four days.

2. Injections of ACTH cortisone and hydrocortisone were followed by pycnosis of small lymphocytes [illegible] marked increase in alkaline phosphatase activity vascular congestion and hemorrhage and an increase in glycogen [illegible] tion and acid phosphatase staining [illegible] of cytoplasmic RNA and [illegible] DNA positive nuclear debris we[illegible] noted

3. Multiple injections of DOC [illegible] renalectomy [illegible] ing. Sing[illegible] technique [illegible] of [illegible] were foll[illegible] period reported [illegible] phatase [illegible] activity in the thym[illegible] duced. While relatively long [illegible] DOC [illegible] tion can be both necess[illegible] [illegible] prolonged incubation is [illegible] [illegible] diffusion or inactivation [illegible] enzyme which [illegible] result in [illegible]

dle phalanges of the second to fifth toes and of all distal phalanges.

The findings on development of appendicular ossification centers have been summarized in two bar-graphs for the upper extremity (fig. 11) and the lower extremity (fig 12)

Sex differences in ossification

The report on postnatal ossification (van Wagenen and Asling, '58) described an appreciable advancement in the new-born female when compared with the male This judgment was based on roentgenograms of 21 males and 37 females. It was of interest to attempt to determine the time at which this difference developed in fetal life

The earliest comparable plates were those of a 70-day-old female fetus and a 72-day-old male The male showed slightly less ossification in that the proximal phalangeal ossification centers in the hand were not seen and the fibular shadow was very faint.

In an earlier age-pair, consisting of 54-day male and 58-day female fetus, the faint shadows of beginning appendicular ossification were seen only in the female. In view of the age difference and the difficulty of visualizing early ossification roentgenographically it cannot be suggested that this is significant sex difference

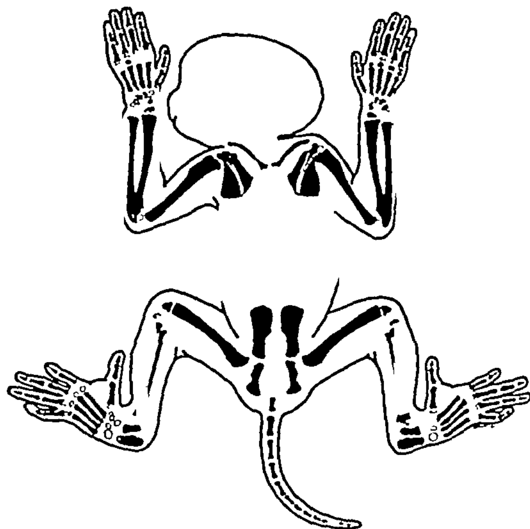


Fig. 8 Ossification in the monkey fetus at 132 days on left; on right at 136 days See description of figure 3

At 100 days two females and eight males could be compared. In the males the ossification center of the talus, the maturity indicator for this age was almost invariably smaller than, and at most only equal to the center in the less well developed of the two females.

At 125 days a male was slightly *more* advanced than a female in that traces were seen of epiphyses for the distal end of the radius and the third and fourth metacarpals. The male was 25% heavier than the female although both had the same sitting height.

Of two animals at 132 days, in which the male exceeded the female in weight by 32% and in sitting height by 13% the female was more advanced. She showed ossification centers in the proximal and distal tibial epiphyses and the centers for the recently established distal femoral and distal ulnar epiphyses were larger than those in the male.

Two females at 150 days were more advanced than two slightly older males (154 and 158 days) showing centers for the head greater tuberosity and distal epiphysis of the humerus and for the proxi-

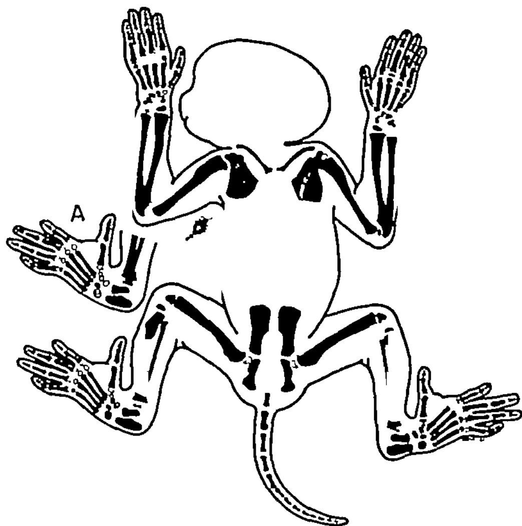


Fig. 9 Ossification in the monkey fetus on left, t 140 days (with inset A, ankle and foot at 139 days) on right, at 145 days See description of figure 3.

mal end of the femur Both females showed seven tarsal and five carpal centers whereas the males showed only four tarsal and three carpal centers.

Although differences were not of a magnitude which could exclude individual variation it appears that bony development in the female exceeded that in the male almost from the beginning of ossification

Maturity indicators in the vertebral column

Although the developing vertebral column did not show age indicators as definitive as those in the appendicular skeleton useful evidence could be gained from its inspection.

At 50 to 56 days along with beginning ossification of the cranial base a series of small shadows was found sharpest in the thoracic and upper lumbar regions. They represented centra. The shadows were faint and difficult to count especially at the extremes of the series where calcification was scanty and the shadows blended with those of adjacent tissues.

At 70 days the vertebral column showed a series of shadows of vertebral centra and separate arches complete from the cervical to the sacral region. By day 74 the centra

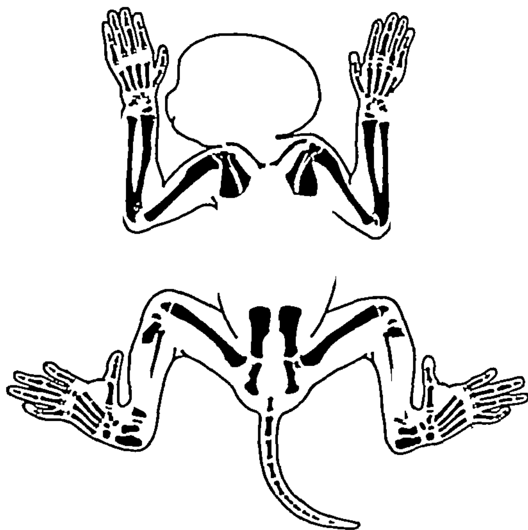


Fig. 10 Ossification in the monkey fetus at 156 d ys on left on right, t 171 d ys See description of figure 3

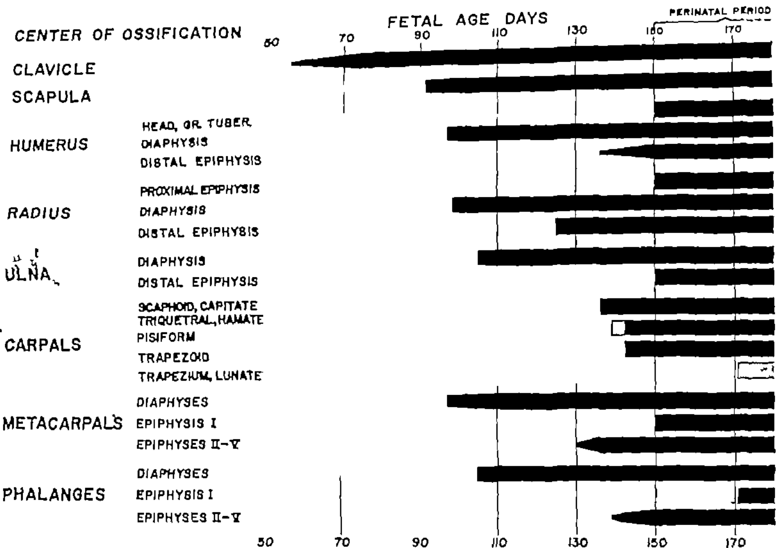


Fig. 11 Bar-graph summarizing ossification in the upper extremity of the monkey fetus. Expanding portions of solid bars indicate period during which the bone is attaining its definitive (neonatal) proportion. Stippled bars indicate variability in presence of the ossification center

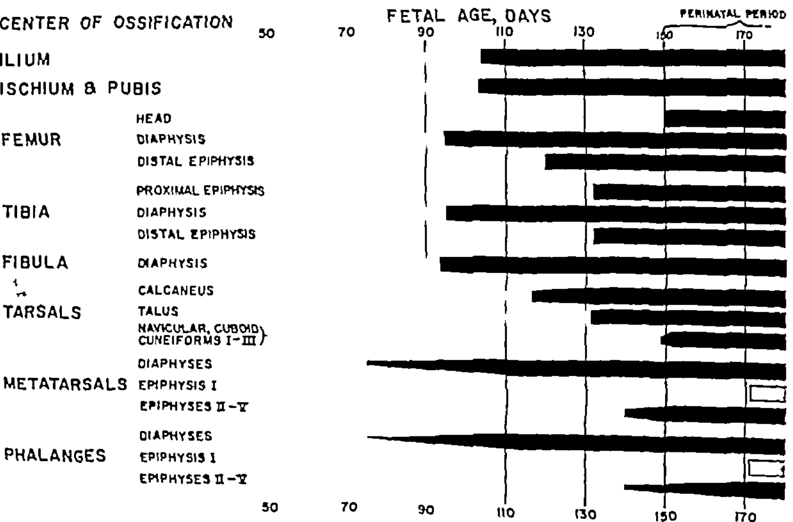


Fig. 12 Bar graph summarizing ossification in the lower extremity of the monkey fetus, with symbols in figure 11

were growing rapidly especially in the lumbar region. During this age-period, shadows of the primary centers of caudal vertebrae appeared rapidly. Using the ossification center in the ischium as a reference level, ten such centers were seen on day 75 (fig. 4) although none had been seen on day 70 (fig. 3). Gradation in the intensity of the shadows (fainter distally) indicated that they were formed in sequence. Subsequent centers were established more slowly.

By day 90 the shadows of the lumbar centra came to overlie those cast by the arches. In the ensuing days this overlapping extended into the thoracic vertebrae (mid-thoracic by day 97 and upper thoracic by day 105). Extension caudally into the sacral region was complete by day 110. Throughout this time oblique views showed that the separation of centra and arches persisted at all levels. In the tail, the definitive number of caudal vertebrae (13) was always seen by days 100 to 110 (figs. 5 and 6).

On day 100 the ala sacri were first seen; they extended almost to the ilium by day 125.

Between days 125 and 132, the shadows of the cervical centra overlapped those of their arches. The sacral centra remained discrete until birth, although angulation could cause the shadows of these segments to overlap and give false impressions of fusion into a unit.

Estimation of fetal age in utero

As mentioned earlier favorable fetal positions and roentgenographic contrast are not always obtained in roentgenograms with the fetus *in utero*. In particular small or newly developing centers may be missed because of their scanty calcification or their masking by shadows of larger bones. This is especially true in the smaller bones of wrist and hand, and ankle and foot, since these parts are commonly flexed. Nevertheless it is possible to divide pregnancy into major time periods on the basis of fetal bone shadows and often a favorable view of a specific region allows rather accurate estimation of fetal age.

First period. During the first 60 days of gestation, bone shadows are not found.[5]

Second period. From 60 to 75 days the shadows of the cranium and axial skeleton are seen and the primary ossification centers in the girdle bones and main long bones of the extremities. In figure 13 the faint bony images visible in the roentgenogram could not be reproduced photographically but the characteristic position and size of the uterus are well-shown. The inset is a drawing of the roentgenogram.

Third period. From 75 to 125 days the shadows of metacarpals, metatarsals, phalanges and caudal vertebrae appear. Earlier in this period, hand shadows are better defined than foot shadows. Later the calcaneus and subsequently the talus may be demonstrated. Figure 14 at the middle of this age-period illustrates most of the features which can be recognized in roentgenograms.

Fourth period. From 125 to 150 days skeletal development is marked by the appearance of the carpal and tarsal bones, and epiphyseal ossification centers of the long bones (including metacarpals, metatarsals and phalanges). In figure 15 a number of these ossification centers can be recognized even in photographic reproduction.

Fifth period. From 150 days, the beginning of the age of viability, favorable roentgenograms such as that reproduced in figure 16 may allow demonstration of the remaining epiphyseal centers of the larger long bones. In particular one may look earlier in this period for the proximal femoral and distal ulnar epiphyses, and later for the greater tuberosity of the humerus and proximal radial epiphyses.

---

[5] As described above in roentgenograms of fetuses obtained by hysterotomy faint shadows of the skull and vertebral column may be recognized by 50 days conception [illegible], and shadows of major long bones by 60 days. The authors believe that it is difficult to identify these shadows dependably in roentgenograms of fetuses in utero before 60 days. Factors which interfere with development of adequate contrast include scanty bone mineralization and the absorption and scattering of roentgen rays passing through the additional soft tissue layers of maternal uterine and body walls.

With plates which show the fetal extremities in hyperflexion or otherwise overlapping markedly, it is well to select the extremities which lie closer to the x-ray film (i.e., show sharper outlines or greater radiopacity) and follow them proximo-distally in orderly sequence to detect epiphyseal centers. It is also helpful to note, where the presence of [illegible] center is suspected but masked by overlapping shadows, that [illegible] end of the diaphysis often indicates the [illegible] epiphyseal center, whereas [illegible] usually terminate with [illegible] shadow.

Although the possibility should not be overlooked of erring on the low side in age estimates if the fetus is male major errors are unlikely The sex differences mentioned above are for the most part, based on the time of appearance and initial size and density of small centers. Their early appearance is difficult to recognize roentgenographically *in utero*.

Unusual obstetrical events

Of the various findings regarding the fetus which may be obtained by roentgenography two unusual events in which the skeletal shadows were especially interest ing are described here namely twinning and fetal death

Twinning On the occasion of an early diagnosis of a twin pregnancy in the colony the opportunity was taken to fol low development of the fetuses roentgenographically (A separate report dealing with obstetrical phenomena of major interest encountered in over 500 pregnancies in the colony will analyze the incidence of twinning in the rhesus monkey raw data suggest that its occurrence is of approximately the same frequency as that in man) In the set of diagrams in figure 17 all are tracings from roentgenograms in the same twin pregnancy They were selected from a series of 14 taken for the most part at weekly intervals during the period between the seventy third and the one hundred and sixty-seventh day of gestation. On day 167 hysterotomy resulted in the delivery of viable twins Not only is progressive fetal development and uterine enlargement demonstrated in the illustration but also the degree of fetal activity is vividly conveyed in the changing postures and positions It is apparent that such pregnancies in monkeys offer an opportunity for study of twin relationships which could not be undertaken in human beings because of the radiation hazard in volved in obtaining the necessary sequence of plates

Fetal death Two cases are presented in which roentgenography provided useful findings in fetal death In the first case the course of pregnancy was apparently uneventful until the one hundred and fortieth day of gestation. At that time palpation of the abdomen gave the impression that the uterus had retrogressed in size rather than continuing to enlarge. A roentgenogram obtained on day 146 confirmed this finding. Figure 18 shows the smaller globular uterus which should be compared with the normal appearance at this time of the uterus of another monkey (fig 15 148 days) Moreover Spalding's sign (22) of fetal death consisting of overlapping of cranial bones is visible at the vertex of the skull shadow This dead fetus was retained *in utero* three days past the average length of pregnancy 168 days. Figure 19 illustrates the appearance of the skeleton of this fetus at birth (171 days conception age) The sutural overlapping had increased markedly The ground glass appearance of the bones results from the demineralization and loss of tra becular structure By examination of the shadows of ossification centers it was possible to assign a skeletal age to this fetus and, presumably to establish the age at death The maturity indicators present coincided precisely with those seen in a normal fetus of the same sex (male) of 132 days conception age The insets in figure 19 from the normal fetus show this correspondence Shadows of small ossifi cation centers are seen in the epiphyses of the distal end of the radius and of the sec ond to fourth metacarpals of both fetuses but the shadows to be expected at approxi mately 135 days or after (four carpals fifth metacarpal epiphysis and distal hu meral epiphysis) are not present In the lower extremity a tiny shadow of the distal femoral epiphysis is seen but not those of the proximal and distal tibial epiphyses which would follow immediately there after

Snow and Nadel (44) in their analysis of the use of roentgenography in human pregnancy have reported that they were able to observe Spalding's sign as soon as four days after cessation of the fetal heart beat In the present case although uterine palpation gave the first intimation of fetal death sutural overlapping proved a very early and sensitive confirmatory observa tion The markedly curved and contracted fetal position which was associated with the change in uterine size and shape should also be noted (fig 18) Snow and Nadel reported that somewhat after the

time of appearance of Spalding's sign the spine may become abnormally curved.

In another case (not illustrated) roentgenograms of the mother at 81 116 and 140 days of gestation showed the uterus to be normal in size and the fetus to have appropriate bony development moreover at the 140-day interval the fetus reacted to uterine palpation by moving At 151 days the fetus was unresponsive and flaccid on palpation and Spalding's sign was observed in a roentgenogram. The cranial overlap was more pronounced in a 175 day roentgenogram, and on day 179 of gestation the dead fetus was delivered spontaneously after rupture of the membranes. Again, thus, the early sensitivity of Spalding's sign was demonstrated.

DISCUSSION

Comparisons with other species. In the previous study on postnatal ossification in the *Maccaca mulatta* (van Wagenen and Asling, '58) it was shown that the sequence of *fusion* of the various epiphyses to their diaphyses corresponded to that which Washburn ('43) Schultz ('56) and others have suggested is a general primate pattern, namely earliest at the elbow and followed in succession by fusions at hip ankle, knee, wrist and shoulder In the present study no corresponding sequence of *appearance* of ossification centers could be found. Indeed, Nissen and Riesen ('49) have noted appreciable differences in the rank-order of appearance of ossification centers in man and the chimpanzee, and have attributed them to functional differences in the regions concerned. Furthermore when studies on man have included sufficiently large samples, variability in the rank-order of appearance is of a degree such that it would be difficult to establish a definitive sequence (Sawtell. '29 Francis et al., '39; Flecker '42 Pyle and Sontag, '43 Elgenmark, '46) Similar variability was encountered among various breeds of dogs (Hare, '61)

Although differences in the rank-order of ossification among the various species and the lack of a large statistical sample in the present study prevent establishment of precise age equivalences in skeletal development, there is some basis for making useful approximations. It has been noted that there is a wide range in the number of ossification centers present in the newborn of the various species studied. The *Macaca mulatta* is remarkable for the advanced stage of development of the skeleton at birth. Almost all of the ossification centers for the epiphyses and for the small bones of the wrist and ankle are present. In other animals (including man) many and often the majority appear after birth. When comparisons are limited to ossification centers developed during the fetal period, discrepancies in the order of appearance of these centers become less marked. On this basis, the newborn great apes (chimpanzee Nissen and Riesen, '49 and Schultz, '56 orang and gorilla, Schultz, '56) show an ossification approximating that of the mulatta macaque fetus at 130 to 140 days and the human newborn (Menees and Holly '32 Hill, '39 Flecker '42) like that of the 120-day macaque fetus. In newborn puppies (Hare '61) and rats (Walker and Wirtschafter '57) only diaphyseal and some girdle-bone ossification centers are found, corresponding to the 75-day macaque fetus. Furthermore one may estimate that the ossification in the newborn *Macaca mulatta* resembles that of the 15 to 18 month old chimpanzee (Nissen and Riesen, '49) or the 5 to 8 year old child (Noback, '54 and others cited) Puppies achieve comparable ossification at approximately six weeks and rats (in spite of their much-compressed developmental period) at 7 to 8 weeks.

Sex differences In primates it has been well-established that ossification in newborn females is more advanced than in males (man Menees and Holly '32 Francis et al., '39 Pyle and Sontag, '43 chimpanzee Nissen and Riesen, '49 *Macaca mulatta*, van Wagenen and Asling, '58) Sex differences in earlier stages of skeletal development, such as have been proposed in the present study are less well-documented. Smith ('56), studying twin and triplet sheep fetuses found that if the sibling pairs being compared were of the same size (within 10 mm crown-rump length) the females were more advanced. However if they were of different lengths

---

¹ Hare ('61) did not find any in newborn puppies.

A slight increase in complexity is illustrated in the next example (fig 3b) In this case the right nerve grew across the wound zone in two branches both of which reached the distal stump The left nerve sent one branch across the wound zone to the distal stump another branch how ever grew dorsally and failed to reach either the distal stump or any lateral-line organs.

Another case (fig. 3c) shows similar branching on the right and left sides in the wound zone One branch from the right proximal nerve stump and one from the left grew across to the distal stumps as shown Another branch from each nerve grew dorsally On the left side this branch reached and innervated a cluster of displaced *lateral-line organs on the right side* the similar branch innervated nothing

This case afforded an opportunity for an additional experiment to see whether or not the two dorsal branches one functional and one non functional would be reproduced if the right and left nerves were recut farther anteriorly The operation was performed and the result showed that both branches were reoccupied after a suitable time by regenerating nerve fibers. Interestingly enough, however myelin segments developed only on the functional branch which innervated the organs.

In the next figure (fig 4) are given three examples of complex regenerative patterns. Multiple branches arose from the proximal stumps in each of these A feature of interest in the first of these (fig. 4a) is that two branches from the right proximal stump crossed the midline and innervated the left distal stump The right and left proximal stumps were recut farther anteriorly to see how completely the plexus pat terns would be reproduced with the second set of regenerating fibers All but three of the paths of the plexus were reoccupied by the ensuing regenerating nerve fibers.

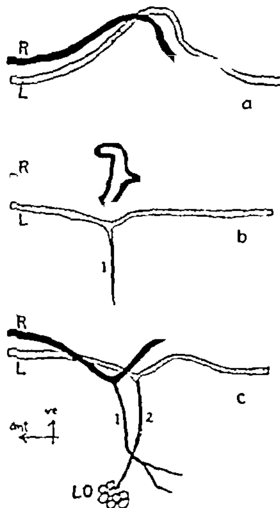


Figure 3

Fig 3 Right lateral views of simple regeneration patterns of the dorsal lateral line nerves on the right and left sides which have grown across the wound zone In each case the nerve on the right side is shown in solid black, that on the left in stipple The direction of nerve regeneration was from left to right a Tadpole no. 2850. Proximal stump fibers of the right nerve (R) grew in a gentle curve across the wound zone as a single nerve and innervated the right distal stump Proximal stump fibers of the left nerve (L) similarly innervated the left distal stump b Tadpole no 2890 The proximal stump of the right nerve grew into the wound zone in two branches which recombined to innervate the right distal stump The proximal stump of the left nerve (L) also gave rise to two branches one of these grew across the wound to the left distal stump the other (1) grew dorsally toward the edge of the fin as an aberrant branch c Tadpole no 2634 The proximal stump of the right nerve gave rise to one branch that crossed the wound to innervate the right distal stump and to a smaller aberrant branch (1) The proximal stump of the left nerve exhibited a similar regenerative pattern, except that one branch (2) found and innervated a cluster of displaced lateral line organs (LO) The dorsal lateral line nerves were recut farther anteriorly after six months. The pattern was repeated. Myelin however did not reappear on the aberrant branch (1) though it did on all the others.

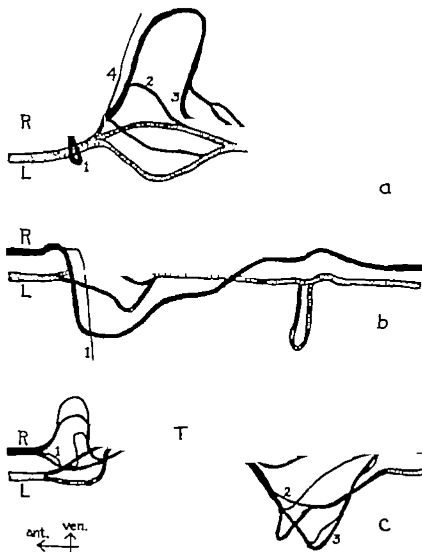


Fig. 4 Right lateral views of complex patterns of regeneration. a, Tadpole no. 2891. The proximal stumps of the right and left nerves gave rise to several branches which formed plexus in the wound zone. One of these (4) from the left dorsal lateral line nerve was aberrant. The others reached and innervated the distal stumps t the right of the figure. Note that the right nerve contributed to both right and left distal stumps. Three branches (1 2, 3) were not duplicated on recutting the nerves farther anteriorly; all others were duplicated. b Tadpole no. 2861. The proximal stump of the right nerve gave rise to two branches, one of which was aberrant (1); the other innervated the right distal stump. The proximal stump of the left nerve gave rise to three branches which recombined; also side loop was formed farther along in the wound zone. All of its fibers innervated the left distal stump. On recutting, the entire pattern was duplicated, including the aberrant branch (1) c, Tadpole no. 2863 Proximal stump fibers of the right and left nerves formed plexuses from which emerged single common trunk (T) in the wound zone. This gave rise to several branches near the distal edge of the wound. Some of these found the right distal stump, some the left, as shown. The right and left dorsal lateral-line nerves were recut farther anteriorly. Almost the entire plexus pattern was duplicated; branches 1 2, and 3 were the only ones not reoccupied by regenerating fibers.

A slight increase in complexity is illustrated in the next example (fig. 3b) In this case the right nerve grew across the wound zone in two branches both of which reached the distal stump The left nerve sent one branch across the wound zone to the distal stump another branch, however grew dorsally and failed to reach either the distal stump or any lateral-line organs

Another case (fig. 3c) shows similar branching on the right and left sides in the wound zone. One branch from the right proximal nerve stump and one from the left grew across to the distal stumps as shown Another branch from each nerve grew dorsally On the left side this branch reached and *innervated a cluster of displaced lateral-line organs* on the right side the similar branch innervated nothing.

This case afforded an opportunity for an additional experiment to see whether or not the two dorsal branches one functional and one non-functional would be reproduced if the right and left nerves were recut farther anteriorly The operation was performed and the result showed that both branches were reoccupied after a suitable time by regenerating nerve fibers. Interestingly enough, however myelin segments developed only on the functional branch which innervated the organs.

In the next figure (fig. 4) are given three examples of complex regenerative patterns. *Multiple* branches arose from the proximal stumps in each of these. A feature of interest in the first of these (fig. 4a) is that two branches from the right proximal stump crossed the midline and innervated the left distal stump The right and left proximal stumps were recut farther anteriorly to see how completely the plexus patterns would be reproduced with the second set of regenerating fibers. All but three of the paths of the plexus were reoccupied by the ensuing regenerating nerve fibers.

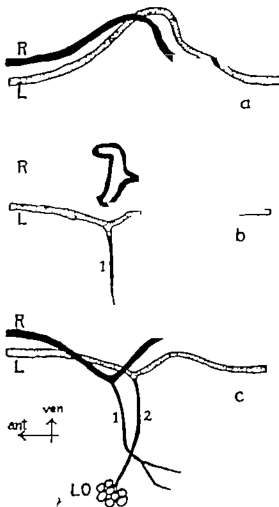


Figure 3

Fig. 3 Right lateral views of simple regeneration p tterns f the dorsal lateral-line nerves on the right and left sides which have grown across the wound zone. In each case the nerve on the right side is shown in solid black, that on the left in stipple. The direction of nerve regeneration was from left to right. a, Tadpole no. 2880 Proximal stump fibers of the right nerve (R) grew in gentle curve across the wound zone as single nerve and innervated the right distal stump Proximal stump fibers of the left nerve (L) similarly innervated the left distal stump b, Tadpole no. 2890. The proximal stump of the right *nerve grew into the wound zone in two branches* which recombined to innervate the right distal stump The proximal stump of the left nerve (L) also gave rise to two branches; one of these grew across the wound to the left distal stump the other (1) grew dorsally toward the edge of the fin as an aberrant branch. c, Tadpole no 2894 The proximal stump of the right nerve gave rise to one branch that crossed the wound to innervate the right distal stump and to a smaller aberrant branch (1) The proximal stump of the left nerve exhibited a similar regenerative pattern, except that one branch (2) found and *innervated* cluster of displaced lateral-line organs (LO) The dorsal lateral-line nerves were recut farther anteriorly after six months. The pattern was repeated. Myelin however did not reappear on the berrant branch (1) though it did on all the others.

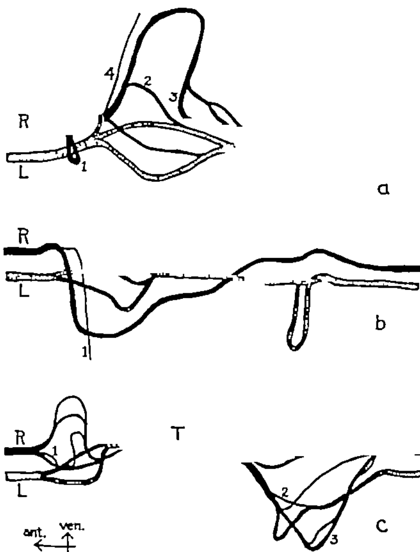


Fig. 4 Right lateral views of complex patterns of regeneration. Tadpole no. 2091 The proximal stumps of the right and left nerves gave rise to several branches which formed plexus in the wound zone. One of these (4) from the left dorsal lateral line nerve was berrant. The others reached and innervated the distal stumps at the right of the figure. Note that the right nerve contributed to both right and left distal stumps. Three branches (1, 2, 3) were not duplicated on recutting the nerves farther anteriorly; all others were duplicated. b, Tadpole no. 2861. The proximal stump of the right nerve gave rise to two branches, one of which was aberrant (1); the other innervated the right distal stump. The proximal stump of the left nerve gave rise to three branches which recombined; also a side loop was formed farther along in the wound zone. All of its fibers innervated the left distal stump On recutting, the entire pattern was duplicated, including the berrant branch (1) c, Tadpole no. 2863. Proximal stump fibers f the right and left nerves formed plexuses from which emerged single common trunk (T) in the wound zone. This gave rise to several branches near the distal edge of the wound. Some of these found the right distal stump, some the left shown. The right and left dorsal lateral-line nerves were recut farther anteriorly Almost the entire plexus pattern was duplicated; branches 1 2, and 3 were the only ones not reoccupied by regenerating fibers.

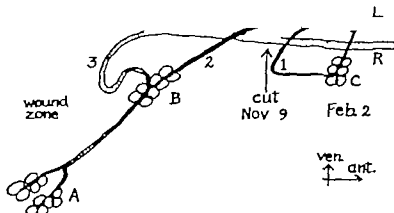


Fig. 6 Left lateral view of innervation of lateral-line organs in and near the wound zone by blocked lateral-line nerves that failed to reach distal stumps. Tadpole no. 2870. The proximal edge of gap cut on November ninth is indicated by the arrow; the sketch shows the regenerative status on February second, nearly three months after the operation. Both left (L) and right (R) proximal stumps failed to grow across the wound zone. Instead they grew as indicated by branches 2 and 3 and supplied clusters of lateral-line organs at A and B on the left side, which developed from displaced organ material that had been carried into the wound zone. An additional branch (1) t the proximal edge of the wound curved back to supply accessory innervation for cluster of organs (C) which was also supplied by another branch.

crossed the wound zone to the distal stump The lateral-line organs of the cluster nearest the proximal edge of the wound were also deflected dorsally along the regenerating nerve fibers. As the individual nerve fibers grew and became myelinated there occurred marked increase in the number of associated organs. These became arranged in a much elongated cluster or clusters along the deflected nerve. On April eighteenth the number of organs had increased to 27 on May second to 36 on May twentieth to 44 and on May thirtieth (and June seventh) to 48 In contrast to this large number the nearest three clusters proximally consisted respectively of 8 7 and 7 organs. Twelve myelinated fibers furnished the nerve supply for the 48 organs.

On the opposite side in this tadpole, the right proximal stump fibers crossed the wound zone and entered the distal stump. There was no similar extraordinary multiplication of organs like that on the left. Thus in this case as in the preceding one blocked regenerating lateral-line nerves induced compensatory organ multiplication in the last cluster they innervated. A suitable balance was thus attained between the number of nerve fibers and the number of organs.

The next example (fig 7) illustrates another complex regenerative pattern with some additional noteworthy features. Several branches deserve special attention One of these grew across the wound zone and innervated a cluster of two organs at the distal edge It did not reach either distal stump. A second branch arose from the right proximal stump grew nearly to the edge of the dorsal fin, then looped back to join a branch from the left proximal stump. It became myelinated and remained so an indication that it successfully innervated a lateral-line organ. A third branch from the right proximal stump grew across the midline and innervated a cluster of organs on the left side, a cluster which was already innervated by a branch from the left proximal stump A total of 11 organs developed in this cluster This large number which was greater than the average was probably ascribable to the rich nerve supply

The next case history is presented in two sketches (fig 8) During the early regenerative period after the first operation some sense organs were carried into the repair zone From these arose a cluster of ten organs. The organs were innervated by three separate nerves of the plexus in the

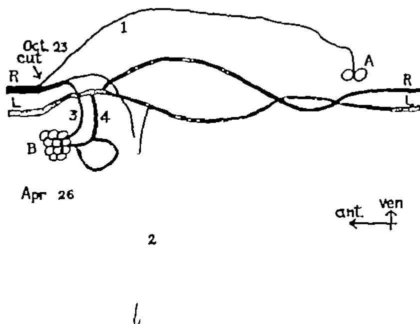


Fig. 7 Right lateral view of a regenerative pattern featured by a very long loop formation. Tadpole no. 2066. The conditions are shown on April twenty-sixth six months after a cut on October twenty-third From the proximal stump of the right nerve three branches arose. One branch (2) grew dorsally almost to the edge of the fin and then looped back to join branch f the left nerve, distance of about 2.5 mm. Branch 1 reached a pair of lateral-line organs (A) at the distal edge of wound zone. Branch 3 innervated some of a cluster of lateral-line organs (B) at the proximal edge of wound zone on the left side opposite. The chief innervation for this cluster of lateral-line organs (B) came from branch 4 of the left side.

repair zone. A second operation caused temporary denervation only Regenerating nerve fibers once again occupied the various pathways of the plexus including the three that led to the cluster of organs.

Another cluster presented an interesting history This cluster of four organs at the distal edge of the wound zone was provided with two innervating branches after the first operation. One of these was lost before the second operation the other was duplicated after the second operation.

The three sketches of the next case history (fig. 9) illustrate a repair zone pattern at different times over an eight-month period. Three subsidiary paths were eliminated. Thus an aberrant branch which joined a spinal nerve failed to innervate a lateral-line sense organ. Being functionless it ultimately degenerated and disappeared. Two other minor paths were also eliminated by the second operation. They were not reoccupied by any of the second set of regenerating fibers, though all of the main paths in the repair zone were One of the eliminated branches was featured by its sharp change in direction as it doubled back on itself to rejoin the nerve from which it originated.

The next case history (fig 10) shows successively the first regenerative pattern in the wound zone the second regenerative pattern, and then the pattern of degeneration resulting from transection of the left proximal stump nerve only A comparison of the first two sketches shows how the main paths were occupied by the second set of regenerating fibers. Subsidiary pathways, however were permanently lost. Transection of the left proximal stump nerve was followed by degeneration of this nerve and its branches in the wound zone. The degenerating fibers were readily identifiable under the microscope These fibers were distributed to both right and le distal stumps as indicated in the thi sketch.

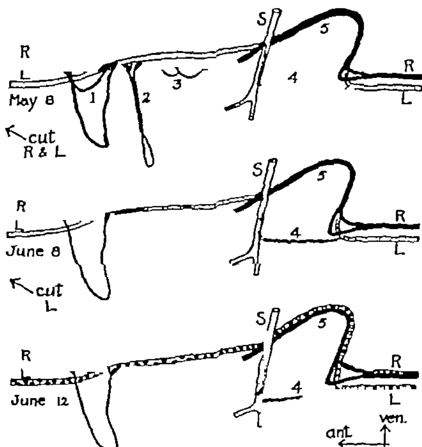


Fig. 10 Elimination of subsidiary paths and duplication of main pattern on recutting; also demonstration of mixed nerve distribution to distal stumps. Tadpole no. 2882. Lateral view from right side (upper sketch) showing regenerative pattern on May eighth six months after initial cut on November ninth. On May eighth second cut through both nerves (R, L) anteriorly was made, as indicated by the arrow. By June eighth as shown in the second sketch, the main pattern was duplicated, including branch 4 which followed spinal nerve (S) for short distance then left it to join the left distal stump. Branches 1, 2, and 3 were not duplicated. On June eighth the left lateral-line nerve was cut again anteriorly; the right one was left intact. On June twelfth, wallerian degeneration, as indicated by the circles, was conspicuous, involving some fibers of the common trunk 5 and of both right and left distal stumps. Branch 4 likewise degenerated.

Spinal nerve fibers in lateral-line distal stumps

Several cases have already been described in which aberrant lateral-line fibers joined spinal nerves. Some cases have also been seen in which aberrant spinal nerve fibers grew into the distal stumps of lateral line nerves. Two cases are illustrated.

In the first of these (fig. 13) the distal stump of a cut lateral-line nerve was entered only by regenerating spinal nerve fibers. These fibers grew past two clusters of lateral-line organs but failed to send any branches whatever toward the organs. It was apparent that there was no particular affinity between spinal nerve fibers and lateral-line organs corresponding to that between lateral-line nerve fibers and organs. In sharp contrast, on the opposite side of the fin in this same tadpole (not illustrated) the cut distal stump of the lateral-line nerve was reoccupied by regenerating lateral-line nerve fibers. These readily innervated all clusters of organs along the path.

In the second of these cases (fig. 14) the distal stump of a lateral-line nerve was oc-

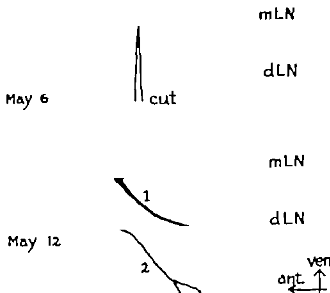


Fig. 11 Occupation of a distal stump of dorsal lateral-line nerve by branch from the main lateral-line nerve following cut. *Pseudacris* tadpole no. 1668, lateral view from right side showing deep cut on May sixth through dorsal fin severing dorsal lateral-line nerve (dLN) and reaching the main lateral-line nerve (mLN) Regeneration quickly followed. By May twelfth new branch (1) had grown out from the main lateral-line nerve dorsally and into the distal stump of the dorsal lateral-line nerve. A regenerating aberrant branch (2) of the dorsal lateral-line nerve was also visible growing along the edge of the wound rms dorsally

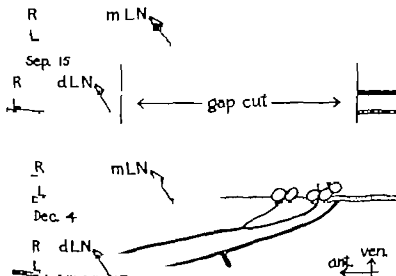


Fig. 12 Innervation of main lateral-line nerve and organs by aberrant proximal stump branches of dorsal lateral-line nerves. Tadpole no. 3009 Lateral view from right side showing long gap cut in dorsal fin on September fifteenth severing both dorsal lateral-line nerves (dLN). Both proximal stumps regenerated along an obliquely ventral course and missed innervating their distal stumps. By December fourth the right dorsal lateral-line nerve (RdLN) had innervated some lateral-line organs on the right associated with the main lateral-line (mLN) as shown. The left dorsal lateral-line nerve had joined the left main lateral-line nerve.



Fig. 13 Occupation of distal stump of dorsal lateral-line nerve by spinal nerve fiber with failure of this to innervate associated lateral-line organs. Tadpole no. 2655. Lateral view from right side showing spinal nerve (S) near right dorsal lateral-line nerve (dLN) A gap was cut in dorsal fin on January first (upper sketch) severing the dorsal lateral-line nerve anteriorly as indicated by the arrow N regenerating fibers from the proximal stump reached the distal stump. From February second on, this stump was occupied by fibers of new branch from the nearby spinal nerve. By February eighteenth (lower sketch) the spinal nerve fibers, one myelinated, had grown past the two clusters of lateral-line organs (A B) shown, a distance of more than 3 mm. There were no branches given off to the organs.

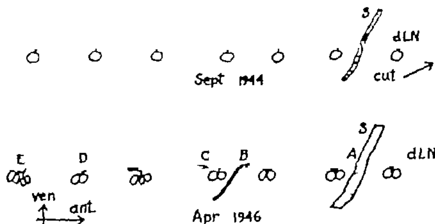


Fig. 14 Neurotization of distal lateral-line nerve stump by both lateral-line and spinal nerve fibers, with innervation of lateral-line organs by lateral-line nerve fibers only Tadpole no. 3002. Lateral view from left side showing site of gap cut in dorsal lateral-line nerve (dLN) as indicated by the arrow September 1944 A spinal nerve (S) and seven single lateral-line organs, indicated by the circles are shown. A single lateral-line nerve fiber grew across the wound zone and entered the distal tump innervating the lateral-line organs. The condition is shown for April 1946. A spinal nerve fiber also joined the distal stump and grew along it for about 2 mm (A to B) Although it passed two lateral-line organ clusters, it gave no branches to them. At C the l teral-line nerve fiber divided into two branches; one of these innervated two clusters of organs ending at D the other innervated the terminal cluster t E

cupied by both a lateral-line nerve fiber and a spinal nerve fiber. The former innervated the organs along the path, the latter did not. Again it was apparent that there was no affinity between spinal nerve fibers and lateral-line organs even though by chance these were placed in close juxtaposition.

Successive shifts from side to side in the reinnervation of the distal stumps of the dorsal lateral-line nerves and their associated sense organs

The accompanying case history (fig. 15) showed that *either* the right or left proximal stump of the dorsal lateral-line nerve could furnish the reinnervating fibers for both of the distal stumps and their associated sense organs.

In this animal as a result of several previous operations both proximal stumps supplied nerve fibers to both distal stumps, as shown in the sketch of February tenth. This condition afforded a favorable anatomical basis for subsequent operations to induce side-to-side shifts in innervation. First the left proximal stump was transected, leaving the right proximal stump as the sole source of reinnervating fibers. Next the right proximal stump was sectioned, leaving the left proximal stump as the sole source of reinnervating fibers. Resectioning the left proximal stump once more after an appropriate time interval again brought about sole reinnervation by right proximal stump fibers (April first). Then, after resectioning the right proximal stump another shift to the left followed (April fourteenth). At the end of the experiment (May twenty ninth) both proximal stumps supplied reinnervating fibers to both distal stumps.

Throughout this case history time enough was allowed between cuts for the reinnervating fibers to become myelinated and to innervate the clusters of sense organs. It is interesting to note that, despite the many operations, the number of sense organs increased markedly on both sides. Furthermore the repeated nerve transections in this case did not prevent the regenerating fibers from growing all the way to the ends of the distal stumps.

Experiments affecting polarity of reinnervation

The next four case histories provided regenerative patterns which involved a *change in the polarity of reinnervation* featured by growth of fibers in distal stumps in *reverse* direction that is toward the root of the tail instead of toward the tip. In the first of these, (fig. 16) three preliminary *gaps* were *cut in the dorsal fin* in October. On the right side regenerating fibers failed to cross the most caudal gap. On the left side regenerating fibers crossed this gap grew to the end of the left distal stump then crossed by way of a loop to the tip of the right distal stump and grew proximally to the edge of the gap. Thus the ten distal clusters of sense organs on the right became reinnervated by nerve fibers growing in reverse direction (December eleventh). This reverse growth covered a distance of 5.8 mm.

Next an extensive gap was cut severing the nerves of both sides. It was thought that such an operation might induce fibers from the right proximal stump to cross the wound zone and take over the innervation of the right distal stump. This did not occur however. Instead regenerating fibers from both proximal stumps crossed the gap and innervated the left distal stump only (February fourth). The left nerve was then recut twice leaving regenerating fibers from the right proximal stump as the sole source of reinnervation of the left distal stump and the associated sense organs. Only six of the nine clusters became innervated (February twenty-fifth). A final transection of the proximal stump nerve on the right side was followed by innervation of the same part of the left distal stump and of the same six clusters of sense organs (March eighth).

The following features were of particular interest in this case: (1) Ten clusters of sense organs received their innervation in reverse order from nerve fibers of the opposite side, (2) there was marked over growth by way of a *terminal* loop of regenerating fibers of one side, apparently to compensate for the nerve deficit of the other side, (3) proximal stump fi[illegible] finally blocked in regeneration by [illegible] sue on one side were able after

assembled and directed to arrive at and neurotize the distal stump (cf. figs. 4c 5a, c, 8 9 10)

We have never seen regenerating lateral-line fibers from the proximal edge of the gap grow across the repair zone and into the old terrain of the tail fin outside of the distal stumps. This is probably to be accounted for by the efficiency of the sheath cell lines in directing the regenerating nerve fibers to the distal stump. Many *long-range case histories* of outwandering neurilemma cells from degenerating lateral-line nerve stumps have been recorded following both single and multiple gap operations. These will be reported separately (Speidel, in preparation)

If *multiple* gaps are cut in the dorsal fin the more distal zones of repair are flanked by nerveless lateral-line stumps at both proximal and distal edges. As a result sheath cell outgrowths then occur at *both* edges before nerve sprouts arrive. Such outgrowths may form connecting links between proximal and distal stumps of the same or opposite sides, or between two proximal stumps or between two distal stumps. They likewise may serve to direct the course of regenerating nerve tips that arrive later

At caudal end of distal stump Another interesting outgrowth may be mentioned at this point though this occurs far from the gap zone. At the caudal ends of distal stumps of the right and left dorsal lateral-line nerves, sheath cells may migrate into the normal surrounding mesenchymal tissues. Outgrowths of this sort may make contact with one another thus bringing about a terminal connection between the nerves of right and left sides. Later regenerating fibers on one side may then grow around the loop and into the nerve of the other side.

Variations in reneurotization of plexus patterns and distal stumps

In repair zones After a plexus has become well established in a repair zone and myelination has taken place on some of its component fibers, as in most of our cases it was noted that a second transection of the lateral-line nerves farther anteriorly did not destroy the main plexus pattern. The sheath cells were still left in place and maintained the pattern. Later regenerating fibers on reaching the repair zone merely followed the lines of the sheath cells as was to be expected.

A few minor deviations were noted. There was a tendency toward elimination of aberrant and subsidiary lines including those which doubled back sharply on themselves (cf. figs. 4a, c 5b c, 8 9 10) No extra nerve lines were formed.

In distal stump zones The distal stump of a dorsal lateral-line nerve may be completely or partially occupied by regenerating fibers. In some cases it may remain entirely devoid of fibers in a few instances regenerating fibers may grow past the original caudal terminus of the stump. Thus, all gradations of reneurotization may occur

The *source* of fibers that reneurotized a distal stump of the dorsal lateral-line nerve was variable. The distal stump might be occupied by fibers from (1) the proximal stump of the same or opposite side (2) the proximal stump of the opposite side growing in reverse direction, and (3) the main lateral-line nerve. Furthermore, experimental shifts from one source to another were possible. Lateral-line nerve fibers from any source apparently furnished adequate reinnervation of the dorsal lateral-line nerves and associated sense organs.

When the distal stump was occupied by spinal fibers however there was no reinnervation of the associated sense organs by such fibers. Or when the distal stump was occupied by both lateral-line and spinal fibers only the former reinnervated the associated sense organs Conversely when lateral-line fibers entered distal stumps of spinal nerves or when they took other aberrant paths they failed to establish any functional peripheral connections and ultimately displayed regressive changes.

Adjustments associated with oversupply and undersupply of nerves to sense organs or of sense organs to nerves

Dorsal lateral-line nerve adjustments Scores of examples of the normal amount of regeneration of dorsal lateral-line nerves have been recorded After a simple nerve transection the regenerating fibers grow

into the distal stump and extend exactly to the end. They innervate the associated sense organs just as before the transection. The later history of nerve fibers and sense organs in the reinnervated zones was essentially normal.

Cases of nerve underregeneration have also been observed frequently. In such cases the regenerating fibers enter the distal stump but fail to grow all the way to the end (cf fig. 16 also Speidel 48). Results of this kind are likely to follow multiple transections done simultaneously or successively. They sometimes follow a single operation in which an extensive gap is cut in the dorsal fin.

The most distal sense organs, being left without nerve supply ultimately degenerate. Those which receive a relatively meager nerve supply undergo slow adjustments. The final condition demonstrates that there is a less than normal total number of sense organs and a less than normal average number of sense organs in a cluster.

Examples of nerve overregeneration have also been observed, particularly following operations done at strategic sites. The best example of overregeneration has been illustrated (fig. 17). In this interesting case the left doral lateral-line nerve regenerated past its original terminus, crossed to the other side and grew in reverse direction up the right distal stump for a distance of 5 8 mm supplying ten extra clusters of sense organs which it had previously not supplied.

Another case (fig 15) also illustrates overgrowth of the same type though to a less degree. The overgrowth in both of these cases seemed clearly correlated with and perhaps stimulated by the presence nearby of an uninnervated distal stump with its associated clusters of nerveless sense organs.

These observations suggest that there is inherent in nerve cells a reserve potential or capacity for growth. Such reserve potential is probably greater in a young animal such as a tadpole than in an adult. In cases of simple nerve transection this is sufficient ordinarily to bring about complete restoration of normal nerve supply to the denervated zones in unusual cases it may bring about an overregeneration to supply more than the original terrain; in cases of sizable gap-cutting operations, or of multiple nerve transections, the reserve capacity may become so exhausted or diminished that underregeneration results. It is intersting to note in this connection the results of Duncan and Jarvis (43) who repeatedly destroyed motor branches of the facial nerve in cats by sectioning (as well as by crushing and by treatment with benzyl alcohol). They report good nerve regeneration with complete functional recovery after five successive nerve sections. The number of fibers, peripheral to the cuts however was greatly reduced.

In addition, many histories of regenerative deviations of dorsal lateral-line nerves have been recorded. In such cases the regenerating fibers fail to reach a distal stump or any lateral-line organs. They end blindly in the zone of repair without terminal functional connections. Ultimately such fibers degenerate as far proximally as the last cluster of sense organs which they innervate.

Sense organ adjustments Irregularities in sense organ arrangements following wound infliction are also of special interest when correlated with their innervation. In a few cases a cluster of organs at the proximal edge of a repair zone receives an oversupply of nerve fibers, as a result of failure of nerve regeneration across a wide zone of repair. Multiplication of the organs in the cluster takes place. Apparently the regenerative urge of the blocked fibers is expended chiefly on the organs of the last cluster innervated with the result that these organs are stimulated to divide and multiply. This seems to be an adjustment that compensates in a way for the many organs left uninnervated along the distal stump.

Sometimes organs, or dedifferentiated organ cells, move into a repair zone and become supplied with more than the ordinary number of nerve fibers. Such a relationship as in the case above leads to increase in number of organs until a proper balance obtains.

Conversely a cluster of organs that for a long time is left innervated by a single nerve fiber or by a deficient number of fibers undergoes regressive change. Reduction in the number of organs co[illegible]

ing the cluster takes place. This adjustment also appears to be a compensatory one that results in a suitable nerve-organ balance.

Trophic influences

A final comment may be made on the nature of reciprocal trophic relations that are suggested by the case histories of this study. It seems clear that lateral-line nerves exert a definite trophic influence on lateral-line sense organs and that the sense organs exert a trophic influence on the nerves. The immediate mechanism(s) by which such reciprocal effects are accomplished is unknown.

We regard trophic mechanisms as one aspect of the larger problem of how *form regulation* and *physiological adjustment* are accomplished. Suitable adjustments in structure and in function occur progressively throughout the developmental history of an animal. Similar adjustments, though they are less perfect, take place during the progress of regeneration. Our experiments disturb the closely-knit structural and functional unit of the lateral-line system. The ensuing regenerative phenomena represent an attempt to restore the previous normal condition as perfectly as possible. Doubtless the hereditary material is involved basically. That leaves unanswered the more immediate steps of the mechanism by which the structures involved influence one another to help in bringing about an approximation of the normal condition.

Related experiments

Results from a few related experiments may now be cited briefly. Many years ago we pointed out (Speidel '33) that cutaneous nerves in tadpoles were stimulated to send out new sprouts and branches to innervate an adjacent denervated region of the skin. More recently Weddell, L. Guttman, and E. Guttman ('41) also reported that in rabbits there was a local extension of new nerve fiber collaterals into denervated areas of skin. A denervated sensory zone therefore appears to act as a stimulus to elicit collateral branches from nearby sensory nerves.

On the motor side Edds ('50) has demonstrated clearly that partial denervation of a muscle in the rat stimulates the formation of collateral branches on neighboring residual intramuscular axons. A similar result has been reported by Hoffman ('50). The collateral branches invade the sheaths of adjacent interrupted nerve fibers and reneurotize denervated end plates. Edds ('53) has also presented a good comprehensive review of results obtained by many investigators, together with associated problems and theories.

The influence of terminal connections on nerve fiber diameters has also been investigated. Weiss, Edds, and Cavanaugh ('45) compared regenerating nerve fibers that were allowed to make successful end connections with those that were prevented from doing so. The former attained large diameter size, ultimately approaching that of the normal; this size greatly exceeded the diameter size attained by the latter. Furthermore the reduced diameter size of the latter extended proximally beyond the level of the original nerve transection. Similarly Simpson and Young ('45) and Young ('50) concluded from their experiments that the diameter reached by regenerating fibers from similar-sized nerve cells depended upon their effecting connection with their end organs.

Sperry's interesting investigations may also be mentioned. An important series of his experiments (Sperry, '48, '51) involved surgical rotation of the eye in amphibians. Visuomotor effects were noted in animals after recovery. Thus, information was obtained on reflex circuits that involved sensory, associative and motor units. Sperry concluded that peripheral connections influenced the associative patterns in the central nervous system. A sensory end organ and its nerve exerted a trans-synaptic effect on central nerve cells. Likewise a muscle and its motor nerve exerted a trans-synaptic effect on central nerve cells. Conversely, the central nervous system pattern exerted an effect on the peripheral structures. In his excellent comprehensive review Sperry ('51) discusses mechanisms of neural maturation including problems of differentiation, specificity, chemo-affinity, trophism, and patterning of integrative circuits.

Thus the evidence from investigations of other workers as cited above, together with

our own results, leads us to conclude that (1) suitable peripheral sensory connections affect the structure of the sensory nerves involved and *vice versa*, (2) suitable peripheral motor connections affect the structure of the motor nerves involved and *vice versa*, and (3) suitable peripheral sensory and motor connections of a reflex arc unit affect the patterning of the related associative nerve cells in the central nervous system and *vice versa*.

SUMMARY

1 Patterns of vagus nerve regeneration were observed *in vivo* in frog tadpoles following single and mutiple operations. The operations involved transections and the cutting of gaps in the dorsal tail fin which severed the dorsal lateral-line nerves. The fibers in these nerves were processes of vagus ganglion cells they transmitted special afferent impulses from the special sense organs of the lateral-line. Spinal nerve fibers were also severed in these operations they transmitted general afferent impulses from the skin.

2. After simple dorsal lateral-line nerve transections the proximal stump fibers usually grew across the wound zone in a single line to the distal stump. After the cutting of large-sized gaps regenerating fibers frequently failed to cross the extensive repair zone the distal stumps were left permanently as aneural lines with neurilemma sheath cells. After the cutting of medium-sized gaps, regenerating fibers formed plexuses of varying degrees of complexity as they grew across the repair zone.

3. Plexus patterns included the following fibers along several paths from the proximal stump to the distal stump of the same side or of the opposite side or of both sides fibers that joined fibers of the opposite side to form a common trunk which then gave rise to branches that reached either one or both distal stumps fibers that joined spinal nerves fibers that crossed to the opposite proximal stump and grew in reverse direction aberrant fibers that failed to reach either distal stump and spinal fibers that entered lateral-line distal stumps.

4 Branching of the cut lateral-line nerve at the proximal edge of the repair zone was brought about by nerve sprout behavior in laying down the pioneer paths. Reassembly of branches and their guidance to distal nerve stumps was brought about by the activities of sheath cells which moved out in tandem lines from the distal stumps into the repair zone thus meeting the advancing nerve sprouts from the proximal stumps.

5 There was a marked tendency for regenerating lateral-line fibers to enter a lateral-line distal stump in preference to a spinal nerve distal stump.

6. There was a marked tendency for aberrant lateral-line fibers to arrive at and innervate displaced lateral-line organs in the repair zone no such tendency was exhibited by regenerating spinal nerve branches nearby

7 Regenerating lateral-line fibers that successfully reinnervated lateral-line organs acquired and maintained sheaths of myelin those that failed to reinnervate organs sometimes acquired thin myelin sheaths transiently but were unable to maintain them.

8 Clusters of sense organs in or near repair zones sometimes became provided with an oversupply of innervating fibers. The sense organs in such clusters increased in number Conversely there was a decrease in number of sense organs in clusters provided with an undersupply of innervating fibers.

9 Additional nerve transections were made in many experimental animals to determine to what extent complex regenerative plexus patterns would be reproduced by a second or third set of regenerating fibers. In general, the chief nerve pathways were completely or nearly completely duplicated. Aberrant and subsidiary pathways were duplicated in some cases but not in others. The paths of fibers lacking functional end connections were most likely to be eliminated.

10 Cross connections were established in some tadpoles between the dorsal lateral line nerves of right and left sides. In these, each disal stump contained fibers from both proximal stumps. Following further transections of each proximal stump in turn, the source of innervating fibers for the two distal stumps was shifted successively from one side to the other several times.

11 A reversed type of reinnervation was induced in some cases; in these regenerating fibers grew from one distal stump across a terminal loop and up the distal stump of the opposite side in a proximal direction thus innervating the associated clusters of lateral-line sense organs in reverse order

12. It was possible also for stray regenerating fibers of the dorsal lateral-line nerve to join the mid-body lateral-line nerve and to innervate organs associated with this nerve. Likewise, it was possible for stray regenerating fibers of the mid-body lateral-line nerve to enter a dorsal lateral-line stump and innervate organs associated with it. Thus the various lateral-line nerve fibers were non-specific as to the location and order of the organs innervated

13. These results emphasize that there exists a special affinity between the nerves and sense organs of the lateral-line. They demonstrate also that there is a definite trophic interrelationship Each influences the other inducing adjustments which result in a suitable nerve-organ balance. The nature of this reciprocal trophic influence and the mechanism(s) by which it is exerted are unknown.

LITERATURE CITED

Duncan D and W H. Jarvis 1943 Observations on repeated regeneration of the facial nerve in cats. J Comp. Neur 79 315–327

Edds, M. V Jr 1950 Collateral regeneration of residual motor axons in partially denervated muscles. J Exp. Zool., 113 517–552.

——— 1953 Collateral nerve regeneration. Quart. Rev Biol., 28 260–276.

Hoffman H. 1950 Local re-innervation in partially denerv ted muscle histo-physiological study Aust. J Exp. Biol. Med. Sci 28 383–397

Murray M. R., and A. P Stout 1942 Characteristics of human Schwann cells in vitro. Anat. Rec 84 275–293.

Simpson, S A and J Z. Young 1945 Regenertion of fiber diameter after cross-unions of visceral and somatic nerves. J Anat. Lond 79 48–65.

Speidel, C. C 1932 Studies of living nerves. I. The movements of individual sheath cells and nerve sprouts correlated with the process of myelin-sheath formation in amphibian larvae. J Exp. Zool., 61 279–331

——— 1933 Studies of living nerves. II. Activities of ameboid growth cones, sheath cells, and myelin segments, as revealed by prolonged observation of individual nerve fibers in frog tadpoles. Am. J Anat., 52: 1–79.

——— 1946a Prolonged histories of vagus nerve regeneration patterns, sterile distal stumps, and sheath cell outgrowths. Anat. Rec., 94 490.

——— 1946b Cinephotomicrographs of tadpole cells in vivo, with special reference to experiments on the nerves and special sense organs of the lateral-line. Anat. Rec., 94: 531.

——— 1947 Living cells in action. Science in Progress, 5th ser Ed. by G. A. Baitsell, Yale University Press, New Haven Chap. IX, 280–314

——— 1947b Reinnervation phenomena as revealed by prolonged observations of vagus nerve stumps and associated sense organs. Anat. Rec., 97 371–372.

——— 1947c Correlated studies of sense organs and nerves of the lateral-line in living frog tadpoles. I. Regeneration of denervated organs. J Comp. Neur 87 29–56.

——— 1948 Correlated studies of sense organs and nerves of the lateral-line in living frog tadpoles. II. The trophic influence of specific nerve supply as revealed by prolonged observations of denervated and reinnervated organs. Am. J Anat., 82: 277–320.

——— 1949 Correlated studies of sense organs and nerves of the lateral-line in living frog tadpoles. III. Experiments on the orange granules and sense hairs of denervated and innervated organs. J Morph., 85 113–140.

——— 1950 Adjustments of peripheral nerve fibers. Genetic Neurology Ed. by P Weiss, University of Chicago Press, Chicago, 66–77

——— 1953 Some adjustments of the nerves and sense organs of the lateral-line after multiple vagus nerve transections. Anat. Rec., 117 616.

——— 1954 Histories of experimentally-induced nerve plexuses involving sensory vagus and spinal fibers. Anat. Rec., 118 410–411.

——— 1963 In vivo studies of myelinated nerve fibers. Internat. Review of Cytology Ed. by G. H. Bourne and J F Danielli, Academic Press, New York, 16 (in press)

Sperry R. W 1948 Orderly patterning of synaptic associations in regeneration of intracentral fiber tracts mediating visuomotor coordination. Anat. Rec., 102 63–76.

——— 1951 Mechanisms of neural maturation Handbook of Experimental Psychology Ed. by Stevens, John Wiley & Sons, New York, Chap. 7 236–280.

Weddell, G., L. Guttman and E. Guttman 1941 The local extension of nerve fibers into denervated areas of skin. J Neur Psychiat., 4 206–225.

Weiss P M V Edds and M. Cavanaugh 1945 The effect of terminal connections on the caliber of nerve fibers. Anat. Rec., 92: 215–233.

Young J Z. 1950 The determination of the specific characteristics of nerve fibers. Genetic Neurology Ed. by P Weiss, University of Chicago Press Chicago, 92–104.

Radioautographic Observations on Variations in Desoxyribonucleic Acid Synthesis in Rat Placenta with Increasing Gestational Age[1]

WILLIAM P JOLLIE
Department of Anatomy Tulane University School of Medicine
New Orleans Louisiana

The chorioallantoic placenta of the rat attains full size at 16 days of gestation and consists of a labyrinth and a junctional zone. The latter is defined as the region, trophoblastic in origin, which lies adjacent to the decidua basalis and into which fetal capillaries do not penetrate (Bridgman, 48) Histologically the junctional zone consists of at least three distinct trophoblastic elements all of which are believed to be derived from the chorionic ectoplacental cone of the implanting blastocyst (1) trophospongial cells (2) glycogen cells, and (3) trophoblast giant-cells. In addition, the trabeculae of the labyrinth are surfaced with trophoblastic elements which also are believed to be derived from ectoplacental cone. Labyrinthine trophoblast has been shown to be both cellular (rather than syncytial, as was previously supposed) and of constant persistence throughout the course of pregnancy thereby making the rat placenta hemochorial (Dempsey and Wislocki, '53 Wislocki and Dempsey '55) rather than hemoendothelial, as was previously believed (Mossman '37)

Although the labyrinth is generally credited with constituting the placental barrier across which materno-embryonic exchanges take place (viz between maternal blood sinuses in the interstices of the trabeculae and allantoic capillaries in the trabecular cores) there is increasing evidence to suggest that, particularly during earlier stages of pregnancy the junctional zone acts as an alternate route of exchange (Amoroso '55 Dempsey '59) In both regions chorionic trophoblast constitutes an integral part of the barrier

In rodents another site of materno-fetal exchange, one whose importance is not secondary to the chorioallantois is the vascularized splanchnopleure of the yolk sac. Indeed, anatomically developmentally and functionally this constitutes a separate placenta (Everett '35) With rupture of Reichert's membrane at 16 days of pregnancy parietal yolk sac consisting of abembryonal trophectoderm and endoderm together with the remnants of the decidua capsularis retract and the visceral yolk sac is thereby exposed to the uterine lumen. This last named membrane consists of endodermal villi containing a vitelline circulation and presents as a potential transfer route (viz. between uterine lumen and vitelline capillaries) a third "barrier" which contains no trophoblastic elements.

It has long been known that maternofetal exchanges are selective. In addition on the basis of physiological determinations, it appears that for most substances transfer is accomplished either by active transport alone (Hagerman and Villee '60) or by both active transport and facilitated diffusion (Widdas '61) Studies on placental transport are complicated by the facts that: (1) both selectivity of transportable materials and rates of transport appear to vary with gestational age (Brambell '50; Feaster Hansard, Outler and Davis '56 Leissring and Anderson, '61) and (2) with certain exceptions little is known about the actual site of transfer for particular substances, i.e. across which of the barriers described above (Wislocki Dean and Dempsey 46)

In the case of junctional zone elements a progressive reorganization of structure at an electron microscopic level with in-

[1] Supported by a grant from the U. S. Public Health Service ([illegible]). A preliminary report of this investigation was presented at the 75th Annual Meeting of the American Association of Anatomists (Anat. Rec., [illegible], 1963).

11 A reversed type of reinnervation was induced in some cases in these, regenerating fibers grew from one distal stump across a terminal loop and up the distal stump of the opposite side in a proximal direction thus innervating the associated clusters of lateral-line sense organs in reverse order

12. It was possible also for stray regenerating fibers of the dorsal lateral-line nerve to join the mid-body lateral-line nerve and to innervate organs associated with this nerve. Likewise, it was possible for stray regenerating fibers of the mid-body lateral-line nerve to enter a dorsal lateral-line stump and innervate organs associated with it. Thus, the various lateral-line nerve fibers were non-specific as to the location and order of the organs innervated.

13 These results emphasize that there exists a special affinity between the nerves and sense organs of the lateral-line. They demonstrate also that there is a definite trophic interrelationship. Each influences *the other inducing adjustments which* result in a suitable nerve-organ balance. The nature of this reciprocal trophic influence and the mechanism(s) by which it is exerted are unknown

LITERATURE CITED

Duncan, D and W H. Jarvis 1943 Observations on repeated regeneration of the facial nerve in cats. J Comp. Neur 79 315–327

Edds, M. V J 1950 Collateral regeneration of residual motor axons in partially denervated muscles. J Exp. Zool., *113:* 517–552.

——— 1953 Collateral nerve regeneration. Quart. Rev Biol 28 260–276

Hoffman, H. 1950 Local re-innervation in partially denervated muscle histo-physiological study Aust J Exp Biol. Med. Sci., *28* 383–397

Murray M. R. and A. P Stout 1942 Characteristics of human Schwann cells *in vitro*. Anat. Rec *84* 275–293.

Simpson, S. A and J Z. Young 1945 Regeneration of fiber diameter after cross-unions of visceral and somatic nerves. J Anat. Lond 79 48–65.

Speidel, C. C. 1932 Studies of living nerves. I. The movements of individual sheath cells and nerve sprouts correlated with the process of myelin-sheath formation in amphibian larvae. J Exp. Zool., *61* 279–331

——— 1933 Studies of living nerves. II. Activities of ameboid growth cones, sheath cells, and myelin segments, as revealed by prolonged observation of individual nerve fibers in frog tadpoles. Am. J Anat., 52. 1–79

——— 1946a Prolonged histories of vagus nerve regeneration patterns, sterile distal stumps, and sheath cell *outgrowths*. Anat. Rec., *94:* 490.

——— 1946b Cinephotomicrographs of tadpole cells *in vivo* with special reference to experiments on the nerves and special sense organs of the lateral-line. Anat. Rec., *94* 531.

——— 1947 Living cells in action. Science in Progress, 5th ser Ed. by G. A. Baitsell, Yale University Press, New Haven, Chap. IX, 280–314

——— 1947b Reinnervation phenomena as revealed by prolonged observations of vagus nerve stumps and associated sense organs. Anat. Rec., *97* 371–372.

——— 1947c Correlated studies of sense organs and nerves of the lateral-line in living frog tadpoles. I. Regeneration of denervated organs. J Comp. Neur 87 29–56.

——— 1948 Correlated studies of sense organs and nerves of the lateral-line in living frog tadpoles. II. The trophic influence of specific nerve supply as revealed by prolonged observations of denervated and reinnervated organs. Am. J Anat., *82:* 277–320.

——— 1949 Correlated studies of sense organs and nerves of the lateral-line in living frog tadpoles. III. Experiments on the orange granules and sense hairs of denervated and innervated organs. J. Morph., *85:* 113–140.

——— 1950 Adjustments of peripheral nerve fibers. *Genetic Neurology* Ed. by P Weiss, University of Chicago Press, Chicago, 66–77

——— 1953 Some adjustments of the nerves and sense organs of the lateral-line after multiple vagus nerve transections. Anat. Rec., *117* 616.

——— 1954 Histories of experimentally-induced nerve plexuses involving sensory vagus and spinal fibers. Anat. Rec., *118* 410–411

——— 1963 *In vivo* studies of myelinated nerve fibers. Internat. *Review* of Cytology Ed. by G. H. Bourne and J F Danielli, Academic Press, New York, 16 (in press)

Sperry R. W 1948 Orderly patterning of synaptic associations in regeneration of intracentral fiber tracts mediating visuomotor coordination. Anat. Rec., *102:* 63–76.

——— 1951 Mechanisms of neural maturation Handbook *of* Experimental Psychology Ed. by Stevens, John Wiley & Sons, New York, Chap 7 236–280.

Weddell, G., L. Guttman and E. Guttman 1941 The local extension of nerve fibers into denervated areas of skin. J Neur Psychiat., *4* 206–225.

Weiss, P., M V Edds and M. Cavanaugh 1945 The effect of terminal connections on the caliber of nerve fibers. Anat. Rec., 92: 215–233.

Young J Z. 1950 The determination of the specific characteristics of nerve fibers. Genetic Neurology Ed. by P Weiss, University of Chicago Press, Chicago, 9?–104.

graphic processing, the sections were stained through the gel emulsion with Harris hematoxylin and triple eosin.

On each slide, the regions studied for silver deposition (evidence of radioactivity) were: the junctional zone (each of its three elements) the labyrinth, and the yolk sac.

RESULTS

Of the two groups of rats those in the first group (each of which was injected with tritiated thymidine eight hours before autopsy) showed silver reduction over radioactive nuclei to a degree optimal for photomicrography in pregnancy stages from 16 to 22 days, but showed very little reduction in 12 and 14-day pregnancies and none in eight to ten-day sites. For this reason a second group was tested in which each animal was injected with a similar dosage two hours before autopsy In this group radioactivity of nuclei in 12- and 14-day placentas was visualized, but nuclei of eight and ten-day stages remained unlabeled.

The optimal length of time for exposure of the emulsified slides to radioactivity varied widely with the group (*vide supra*) and with the stage of pregnancy In general, earlier stages (in group 2) required six weeks of exposure for good resolution, [illegible]ther stages (in group 1) were optimally exposed at eight weeks except for 22-day placentas which showed best resolution of silver deposition after exposure time of four weeks.

Radioactivity in the junctional zone

[illegible] in the implanting blastocyst (day 8 post [illegible]) nuclei of none of the trophoblast [illegible] types in either group exhibited reduced [illegible] grains (i.e., evidence of radioactivity) even after eight weeks of exposure. [illegible] lack of labeling occurred despite la[illegible]g of uterine cells (e g. decidua and [illegible]metrium) and despite abundant mito[illegible] which were evident in the ectoplacental [illegible] (fig. 1) In the ten-day embryo the [illegible] situation was evident although mito[illegible] were distinguishable in the ectopla[illegible]l cone neither cell type of the cone— the peripherally placed [illegible]rt-cells [illegible]ndary trophoblast giant-cells) and the more deeply situated (trophospongial?) cells — exhibited labeling over its nucleus

Between 10 and 12 days the cone becomes more broadly based and against the inner layer of this base (viz. the future fetal surface of the placenta) the distal end of the allantoic diverticulum becomes apposed. With the allantois is associated an umbilical circulation, evident in the 12-day placenta as a loose cellular reticulum at the center of the fetal surface (the base of the cone) which contains embryonic blood cells (i.e., nucleated erythrocytes) (fig. 2) This reticulum is the primordium of the labyrinth the remainder of the cone, which, at this stage, is the larger part, is now designated junctional zone and consists of giant-cells and trophospongium. In slides of tissues in group 2, nuclei of these latter two types of trophoblast were seen to be randomly labeled after exposure times of six weeks, both at 12 days and at 14 days of pregnancy (fig. 3)

At 16 days glycogen cells were distinguishable within the junctional zone (fig. 4) but showed no evidence of radioactivity None of the nuclei of trophoblast giant-cells were labeled; and the labeling of trophospongial cell nuclei had declined markedly At 18 days no nuclei of giant cells or glycogen cells showed silver reduction; and the great majority of trophospongial nuclei also were unlabeled The only radioactivity observed in the three specimens examined was in one placenta where a very few cells were labeled (fig. 5) These were in a tight cluster (a single clone"?) directly subjacent to the labyrinth.

In later placentas all three junctional zone elements failed to show evidence of DNA synthesis.

Radioactivity in the labyrinth

As described above a labyrinthine anlage first appears at 12 days. All cells in it were unlabeled at this day Although through the fourteenth and sixteenth days, the labyrinth increases progressively in size — both in absolute size and in size relative to the subjacent junctional zone— the labyrinth failed to show silver reduction at any of these stages. All cells in the

[illegible]

[illegible] lavage typical of estrus were caged with breeding males at 11:00 A.M. Lavages were taken of these females again at 4:00 P.M. and those showing sperm were assumed to have bred at 2:30 P.M.

The day of breeding being counted as day 0, pregnant females in two groups were autopsied on days 8, 10, 12, 14, 16, 18, 20 and 22. In the first group, eight hours before autopsy each female was injected intraperitoneally with 50 microcuries of tritiated thymidine[1] in 0.2[illegible] ml. [illegible] saline. Three animals were so injected for each of the days listed. Second group females were [illegible] injected [illegible] autopsy [illegible] and 14 days of pregnancy [illegible] animals [illegible] between [illegible] and [illegible] microcuries of [illegible] per gram body weight, either at [illegible] or at eight hours [illegible]

[illegible] animals were anesthetized [illegible] intraperitoneal injection of [illegible] [illegible] from the [illegible]

[illegible]

graphic processing, the sections were stained through the gel emulsion with Harris hematoxylin and triple eosin.

On each slide the regions studied for silver deposition (evidence of radioactivity) were the junctional zone (each of its three elements) the labyrinth and the yolk sac.

RESULTS

Of the two groups of rats those in the first group (each of which was injected with tritiated thymidine eight hours before autopsy) showed silver reduction over radioactive nuclei to a degree optimal for photomicrography in pregnancy stages from 16 to 22 days but showed very little reduction in 12 and 14-day pregnancies and none in eight to ten-day sites. For this reason a second group was tested in which each animal was injected with a similar dosage two hours before autopsy In this group radioactivity of nuclei in 12 and 14-day placentas was visualized, but nuclei of eight and ten-day stages remained unlabeled.

The optimal length of time for exposure of the emulsified slides to radioactivity varied widely with the group (*vide supra*) and with the stage of pregnancy In general, earlier stages (in group 2) required six weeks of exposure for good resolution; later stages (in group 1) were optimally exposed at eight weeks except for 22-day placentas which showed best resolution of silver deposition after exposure time of four weeks.

Radioactivity in the junctional zone

In the implanting blastocyst (day 8 post coitum) nuclei of none of the trophoblast cell types in either group exhibited reduced silver grains (i.e., evidence of radioactivity), even after eight weeks of exposure This lack of labeling occurred despite labeling of uterine cells (e g decidua and myometrium) and despite abundant mitoses which were evident in the ectoplacental cone (fig. 1) In the ten-day embryo the same situation was evident although mitoses were distinguishable in the ectoplacental cone neither cell type of the cone— viz., the peripherally placed gi ?t-cells (secondary trophoblast giant-cells) and the more deeply situated (trophospongial?) cells — exhibited labeling over its nucleus

Between 10 and 12 days the cone becomes more broadly based; and against the inner layer of this base (viz., the future fetal surface of the placenta) the distal end of the allantoic diverticulum becomes apposed. With the allantois is associated an umbilical circulation, evident in the 12-day placenta as a loose cellular reticulum at the center of the fetal surface (the base of the cone) which contains embryonic blood cells (i.e., nucleated erythrocytes) (fig. 2) This reticulum is the primordium of the labyrinth the remainder of the cone, which, at this stage, is the larger part, is now designated junctional zone and consists of giant-cells and trophospongium. In slides of tissues in group 2, nuclei of these latter two types of trophoblast were seen to be randomly labeled after exposure times of six weeks both at 12 days and at 14 days of pregnancy (fig. 3)

At 16 days glycogen cells were distinguishable within the junctional zone (fig 4) but showed no evidence of radioactivity None of the nuclei of trophoblast giant-cells were labeled and the labeling of trophospongial cell nuclei had declined markedly At 18 days no nuclei of giant cells or glycogen cells showed silver reduction and the great majority of trophospongial nuclei also were unlabeled. The only radioactivity observed in the three specimens examined was in one placenta where a very few cells were labeled (fig. 5) These were in a tight cluster (a single clone"?) directly subjacent to the labyrinth.

In later placentas, all three junctional zone elements failed to show evidence of DNA synthesis.

Radioactivity in the labyrinth

As described above a labyrinthine anlage first appears at 12 days. All cells in it were unlabeled at this day Although through the fourteenth and sixteenth the labyrinth increases size — both in absolute size and relative to the subjacent the labyrinth failed to show tion at of these stages.

creasing gestational age has been de scribed (Jollie, '62a) Furthermore, per sistence of these elements has been shown to be directly influenced by maternal ovarian hormones both *in situ* (Jollie '62b) and when transplanted to extrauterine sites (Jollie '60) It is not known, how ever whether the ultrastructural changes which have been observed in these hormonally fixed" cells reflect functional changes in selectivity and transfer rates. Nor indeed is it known whether the observed changes in structure of a given trophoblastic element during the course of pregnancy result from individual cellular aging, or from progressive differentiation in a given mitotic lineage of cells.

It is hoped that a determination of mitotic activity in placental elements at increasing gestational ages, then will serve as a basis for studying placental aging" and consequently will help elucidate the mechanics of placental function.

The purpose of the present investigation is to determine variations in synthesis of DNA in the nuclei of various elements of the rat placenta. The method employed for such determination is radioautography fol ing injection of pregnant animals with thymidine. This radioactive iso- has been shown to become incorpo- ted into nuclei during DNA synthesis presumably at the time of chromosomal replication (Doniach and Pelc '50 Taylor Woods and Hughes '57) If this is so, one can assume that nuclei which produce radioautographs on a photoemulsion following the injection are nuclei which have synthesized DNA in preparation for mitosis. The possibility also exists — indeed in the case of trophoblast giant-cells seems most likely — that DNA synthesis and consequently uptake of tritiated thymidine also occurs preparatory to nuclear hypertrophy (polyploidy?) where no mitosis follows.

EXPERIMENTAL PROCEDURES

A highly inbred strain (Charles River Breeding colony) of Sprague-Dawley rats ranging in weight from 200 to 250 gm were used in this investigation Pregnancies were timed within ∓ two and one-half hours by the following method. Vaginal lavages were taken of cycling females daily at 9 00 A.M. Animals which exhibited a lavage typical of estrus were caged with breeding males at 11 00 A.M. Lavages were taken of these females again at 4 00 P.M. and those showing sperm were assumed to have bred at 2 30 P.M.

The day of breeding being counted as day 0 pregnant females in two groups were autopsied on days 8 10 12, 14 16, 18 20 and 22. In the first group eight hours before autopsy each female was injected intraperitoneally with 50 microcuries of tritiated thymidine[1] in 0.20 ml normal saline Three animals were so injected for each of the days listed. Second group females were similarly injected two hours before autopsy at 8 10 12 and 14 days of pregnancy two animals per day In all, then, rats received between 0.20 and 0.25 microcuries of the isotope per gram body weight, either at two or at eight hours preceding autopsy

At autopsy animals were anesthetized with an intraperitoneal injection of 0.30 ml nembutal and tissues from the living animal were fixed in Bouin's picric-acid formol. Eight and ten day implantation sites were fixed entire for 24 hours sites 12 days and older were bisected after the first hour of the 24 hour fixation period. Tissues were dehydrated in a graded ethanol series, cleared in toluol and embedded in paraffin (tissue-mat")

Eight and ten-day specimens were cut serially at 7 µ in a plane perpendicular to the long axis of the uterus sections of older gestation sites were taken at 5 µ against the bisected surface of the site i.e in a plane both perpendicular to the fetal surface and through the center of the placenta. Mounted sections were deparaffinized in toluol, rinsed in ethyl ether and air dried. Next in a darkroom the slides were dipped in liquified photoemulsion, air-dried and sealed with dessicant (anhydrous calcium chloride) in five light tight boxes The boxes were stored in a refrigerator each box containing one slide from each gestation site. The contents of each box subsequently were developed in Kodak D-19 developer after exposure times of one week, two weeks four weeks six weeks and eig t weeks Following photo-

Purch sed from Schwarz Bioresearch, Inc., Orangeburg, N. specific activity 1.9 c/mm.
Ilford Nuclear Research Emulsion, purchased from Ilford, Ltd Ilford, Essex, England.

The basement membrane on the stromal surface, best shown by uranyl acetate staining, was ill-defined in lead-stained preparations. The most abundant cytoplasmic components were the myofilaments which formed a dense background to the mitochondria, RNP particles, smooth and rough endoplasmic reticulum. No special study has been made of the myofilaments, however to determine how close the similarity with ordinary smooth muscle myofilaments may be. In transverse sections (plate 3 fig. 7) the finely punctate appearance of these filaments was sometimes very clear but, whether due to inconsistencies of staining or variation in thickness of section, this was not uniformly so. The processes of the cells, especially near the stromal border appeared as numerous islands of variable shape, and generally it was quite impossible to relate these components to individual cells. Plate 3 figure 7 however shows portions of two nuclei and central areas of sarcoplasm from which processes are clearly arising While we have no clear three dimensional picture of these cells it is of interest to find out whether they interlock not only by intermingling of processes but perhaps by other special devices so that on contraction all cells may pull on the surrounding tissues in a radial direction. It is becoming increasingly clear that smooth muscle fibers commonly form intrusions by the insertion of a slender process from one fiber into a pocket on an adjacent fiber (Richardson, '62; Merrillees Burnstock and Holman, '63) Whether these structures serve as a purely mechanical link within the tissue or have other functions, remains unknown. In the dilator the processes not only interlocked with their surface membranes separated by a distance of ~200 Å, which is about the same interval occuring at the intrusions of ordinary smooth muscle, but also there were special contact zones or junctional complexes where the nature of the cell membranes was specialized.

Farquhar and Palade ('63) in an excellent review of junctional complexes in epithelia, have proposed a new terminology to clarify an already rather confused subject. In the present material the desmosome as defined by Farquhar and Palade was rare but the zonula occludens (tight junction) and the zonula adherens (intermediate junction) occurred profusely between all the cells of the posterior epithelium on their lateral surfaces between the posterior epithelium and the myoepithelium, and between the processes of the dilator cells. Examples of these are shown in plates 3 and 4. Without attempting to describe these junctions in detail, which would form a complete study in themselves the following points related to the contractile behavior of the myoepithelium must be emphasized. The muscle processes adhered to each other sometimes over quite extensive band-like areas by a fascia occludens (plate 3 figs. 6 7; plate 4 fig. 10) in which the opposing membranes were fused and the intercellular space obliterated. Such a relationship has already been described by Taxi ('61b) in intestinal smooth muscle and by Dewey and Barr ('62) who called it a nexus. The same structure has also been found among the smooth muscle fibers of the sphincter pupillae (plate 5 fig. 13) Sometimes occurring independently but commonly in association with the fascia occludens, were regions of opposing membranes separated by an interval (~200 Å) and in which the cell membranes were dense with a broad zone of dense material in the subjacent cytoplasm. These were taken to be examples of the fascia adherens type of junction. Where the processes formed intrusions rather than simply interdigitating, there were either no specializations of the cell membranes, as mentioned above for other types of muscle or the related structures were sealed together by a true zonula occludens (plate 4, fig. 11) The example in plate 5 figure 12 suggests that if the intrusions could be followed in serial sections, perhaps all of them might be found to terminate in a zonula occludens. A question which cannot be settled, however concerns whether all junctions exist between separate cells, or whether in some cases the processes of the same cell adhere to each other in this intimate manner. That separate cells are stuck together by a fascia occludens is shown in plate 3 figure 7

The nerves examined at various levels in the iris superficial to the intrinsic mus-

to define the individual fiber-cells in a perfectly satisfactory manner in the dilator though I have often teased out portions of the outer part of the iris." According to van Alphen ('63) who has studied sections of monkey iris fixed *in situ* by freezing during different degrees of miosis and mydriasis all the components of the stroma and epithelial layers undergo very remarkable size and shape changes. He found the posterior epithelial cells increased four times in height as the pupil changed from extreme miosis to extreme mydriasis. There was considerable distortion of the nerves and even of isolated cells such as melanocytes. It is not surprising therefore to find that the epithelial cells as well as the muscle cells are bound together by special junctional complexes. Tousimis and Fine ('61) however appear to minimize the importance of firm cellular contacts and regard the posterior epithelium as quite loosely adherent to the underlying muscle and stroma. They give an illustration of what appears to be a zonula adherens between epithelial cells but do not mention such junctions in the text, nor do they seem to have found any [illegible] in the myoepithelium. From the [illegible]ssion which followed presentation of [illegible] paper some doubt was expressed about the identification of desmosomes and their importance as attachment bodies in the iris epithelium. Actually zones of attachment have proved to be so numerous in the situations already described that there can be little doubt that they form an important component maintaining the integrity of the tissues through considerable three dimensional changes. They may also function in controlling the permeation of aqueous fluid between the epithelial cells. As regards the muscle cells it is possible that some of the contact zones between the myoepithelial processes may serve for conduction of excitation from one cell to another. How muscle cells, which are not all supplied with separate nerve endings contract in unison is one of the pressing problems of smooth muscle physiology. All the morphologist can do is to point out special relationships such as the intrusion of a process from one muscle fiber into a pocket in an adjacent fiber and that specialized areas of surface contact do exist and are quite common. It remains for the biophysicist to say whether any of these specializations meet the requirements for transmission. Burnstock and Holman ('63) dismiss the intrusions as being too limited in area of contact to serve as sites of transmission but they do not give adequate theoretical data to support their conclusions.

The double autonomic innervation of the iris and its central and peripheral connections which are discussed in detail by Lowenstein and Lowenfeld ('62) in relation to the various types of pupillary reflexes and abnormal reactions due to disease, are too well known to be described here except that mention must be made of the possibility that, in addition to sensory fibers and motor fibers to the dilator sphincter and blood vessels there may be adrenergic inhibitor fibers supplying the sphincter. Guyton ('40) has stated that "anatomical evidence does not appear to exclude the possibility of these muscles (sphincter and ciliary) also having some sympathetic innervation. Thus the sphincter may have excitatory cholinergic nerves and also inhibitory adrenergic nerves. This concept is based partly upon the work of Joseph ('21) who claimed to have cut the dilator away from the sphincter in the intact animal whereupon stimulation of the cervical sympathetic caused relaxation of the sphincter. From detailed knowledge, however of the interrelationships of dilator and sphincter previously mentioned, it would seem to be virtually impossible to isolate these two muscles. Lowenstein and Lowenfeld ('62) regard inhibition of the sphincter as being due to inhibitory activity within the oculomotor nucleus.

Of the many papers devoted to the investigation by light microscopy of nerve-muscle relationships within the iris, mention should be made of the work of Boeke ('33) who described a very rich innervation of the sphincter in the monkey following silver impregnations. The axons showed ring-like formations in series and appeared to terminate in a ring closely resembling some silver-stained synapses in the C.N.S. Some of the "rings" appeared actually to be intra-cellular in location. There is little doubt that Boeke was deal

ing with beaded nonmyelinated axons and that he was able to demonstrate the ultimate anatomical end-points of some of the branches of these fibers. Similar endings in the ciliary muscle have been very clearly illustrated in photomicrographs by Génis-Gálvez ('57) The most recent ac count of the innervation of the albino rabbit eye is given by Beatie and Stilwell ('61) *Their low magnification photomicrographs* from methylene blue prepa rations give an excellent idea of the richness of the autonomic innervation. The method *par excellence* for demonstrating networks of beaded adrenergic nerves in thick preparations and in sections is that of Falck ('62) and his colleagues (Falck, Hillarp Thieme and Torp '62) who have shown that the nerves in freeze-dried preparations, treated with formaldehyde gas at 80 C are highly fluorescent owing to the formation of condensation products from catechol amines and 5-hydroxytrypt amine. While this method may indeed make a greater contribution than electronmicroscopy towards solving many of the problems of autonomic innervation, it cannot deal effectively with the fine structural relationships between individual axons and effector cells. In a short account of the innervation of the rat dilator pupillae Falck ('62) *demonstrates the extraordinary* richness and complexity of the autonomic ground plexus and states that sin gle fibers can be seen leaving the bundles of beaded fibers. Occasionally a single fiber runs a short distance with or without branching, and then seems to terminate. However as the axons begin to pass as we know between the processes of the dilator cells ultimately to become completely surrounded by them, one wonders whether the fluorescence may not be masked by the dense sarcoplasm of the myoepithelium, remembering, of course that he is describing total mounts of the iris and not thin sections.

Following the publication of an impor tant paper by Burnstock and Holman ('61) who postulated from electrophysiological observations that the longitudi nal smooth muscle coat of the guinea-pig vas deferens must have a very rich innervation, because junctional potentials could be recorded from every muscle cell following stimulation of the hypogastric nerve, electronmicroscopical investigation of nerve-muscle relationships in the vas deferens was undertaken (Richardson '62) The present author chose by chance to work on the rat vas deferens and found that the naked axons lying between the muscle fibers appeared to terminate in *beaded enlargements which* were packed with granular and agranular vesicles. It was concluded that true nerve endings in both anatomical and physiological senses had been demonstrated and that, as they were very numerous in the small samples examined, it might be inferred that every muscle fiber had an ending. Meanwhile Merrillees, Burnstock and Holman ('63) had been examining the longitudinal muscle coat of the guinea-pig vas deferens confining their attention strictly to the region from which junctional potentials had been recorded. They also made quantitative measurement of the relative numbers of muscle fibers and axons in transverse sections. Their results were quite different from those the present author had obtained in the rat. They favored the hypoth esis outlined in the introduction of the present paper namely that close contacts which they found to be rare in the guinea pig are of no special significance, and that axons release transmitter into the tissue spaces at varying distances from the muscle membranes. At this stage it is pointless for the present author to argue whether or not he is in error in thinking that enlargements of naked axons which lie in grooves on the surface of the muscle fibers are nerve endings. Prolonged examination of serial sections will be necessary to decide whether these structures are actual anatomical end-points, and some other approach will be required to determine whether or not all beads on an axon discharge transmitter simultaneously What is important at present is the possibility that the vas deferens may have a unsuspected mixture of adrenergic cholinergic innervations and that th portions of these two kinds of vary in different species. Merri stock and Holman ('63)

axons in the guinea-pig vas deferens contained a uniform population of agranular vesicles 300–600 Å in diameter with an occasional larger vesicle showing higher internal density which was considered to be a type 1 vesicle according to the Grillo and Palay ('62) classification. The "endings" in the guinea-pig were clearly quite different from those in the rat in lacking the large numbers of granular vesicles. The present author has confirmed that the majority if not all, of the axons in the superficial regions of the guinea-pig longitudinal muscle coat lack granulated vesicles but on examination of the internal circular muscle it was found that the nerves were virtually identical with those previously described in the rat. The guinea-pig clearly has two kinds of "endings" in its smooth muscle. This is probably the case in the rat although "endings" without granular vesicles (Richardson, '62 see plate 4 fig. 14) seem to be very rare.

Evidence for the association of granular vesicles (at least of types 2 and 3) with the presence of catecholamines would appear to be very strong. A summary of this evidence is given by Wolfe et al. ('62a b) ... demonstrated in the rat pineal that tritiated norepinephrine, injected intravenously could be localized by autoradiography combined with electronmicroscopy in the terminal and preterminal parts of the sympathetic axons which contained granular vesicles. A similar localization was found by Wolfe and Potter ('63) in nerves of the rat heart. Moreover Potter and Axelrod ('62) have shown that tritiated norepinephrine is present in highest concentration in a "microsomal" fraction of homogenized rat heart, rather than in the clear supernatant. This would be consistent with localization in a small vesicular component.

It is suggested therefore that the nerves in the guinea-pig vas deferens described by Merrillees, Burnstock and Holman ('63) are not adrenergic but cholinergic in function because they lack the granular vesicles (types 2 and 3). This would make them structurally identical with the "endings" now found in the sphincter pupillae which are known to be cholinergic, and with "endings" described by Thaemert ('63) and others in the smooth muscle of the gastro-intestinal tract and by Ishikawa ('63) in human ciliary muscle. The vas deferens in both the guinea-pig and the rat, however is known to contain an unusually high concentration of norepinephrine which would presuppose not only a rich innervation but also that adrenergic nerves would predominate. It is interesting to note in figure 11 of the paper by Falck ('62) that the apparent numbers of strongly fluorescing nerves in a transverse section of the guinea-pig vas deferens vary from a sparse distribution at the periphery of the longitudinal coat to a very dense accumulation within the deeper circular coat. This difference may of course be due to the fact that the nerve fibers are cut transversely and appear as dots in the longitudinal muscle whereas they are cut longitudinally in the circular coat. Re-examination of this tissue by fluorescence microscopy is clearly needed. Another suggestion that the vas deferens is not innervated purely by adrenergic fibers comes from the recent work of Jacobowitz and Koelle ('63) who have combined staining for cholinesterase with the fluorescence method for catecholamines. Although there may be some objection to the modification of the Falck ('62) technique which these authors found necessary to avoid inactivation of the cholinesterase, it seems relevant to the present discussion that, while the vasa deferentia of the guinea-pig and cat were found to be similar in their content of adrenergic nerve fibers the population of AChE-stained fibers was dense in the former and sparse in the latter species. It is also important, if their technique can be validated, that they found individual nerve bundles to contain a mixture of adrenergic and cholinergic axons within the same Schwann sheath. This would be the case in the rat (Richardson, '62 plate 2, fig. 5) if one accepted the labeling which the two types of vesicles appear to provide.

One further characteristic of autonomic nerves concerns the large type 1 vesicles. Are these vesicles indicative of adrenergic inhibitory axons or of cholinergic axons? It would seem to be a point of some sig-

nificance that these special vesicles occur in the axons described by Merrillees Burnstock and Holman ('63) in axons of the rabbit sphincter muscle and indeed, according to Coupland ('62) in the preganglionic terminals supplying adrenal medullary cells. They are not characteristic of the adrenergic terminals of the rabbit dilator muscle, nor of the rat vas deferens Knowing so little about the origin of vesicles and their dynamic behavior in the axon, however it is premature to speculate. A much more important finding at this stage would be to determine the significance of the large numbers of agranular vesicles in the adrenergic axons.

SUMMARY

Recent work on the autonomic innervation of smooth muscle and on synaptic formations in the central and peripheral nervous systems, has revealed the existence of at least two structurally distinct types of nerve endings. One type contains numerous small, agranular vesicles ~200–500 A in diameter often called synaptic vesicles, together with an occasional large vesicle about 800–1 000 A in diameter which has a central core of variable size and density The other type also contains agranular vesicles, but mixed with a large number of granular vesicles of about the same size, in which there is a central very dense core or granule. It is highly probable from biochemical and other evidence that this second type of ending is indicative of adrenergic nerves.

The innervation of the sphincter and dilator muscles of the albino rabbit eye has been studied by electronmicroscopy to find out whether there was a structural difference between the intramuscular nerves and nerve endings of these two muscles. The sphincter which is very richly innervated showed nerves and nerve endings of the first type and these are concluded to be typical of cholinergic innervation. The dilator had nerves and nerve endings of the second type Detailed study of the myoepithelial cells of the dilator muscle revealed the presence of numerous junctional complexes between their processes which appear to bind them in a firm union.

LITERATURE CITED

Beatle, J C., and D. L. Stilwell 19?1 Innervation of the eye. Anat. Rec., 141 4–62.

Boeke J 1933 Innervationsstudien III. Die Nervenversorgung des M. ciliaris und des M. sphincter iridis bei Säugern und Vögeln. Ztschr. mik. Anat. Forsch., 33 233–275.

Burnstock, G., and M. E. Holman 19?1 The transmission of excitation from autonomic nerve to smooth muscle. J. Physiol., 1 ? 115–133

——— 1963 Smooth muscle autonomic transmission. Ann. Rev Physiol., 25 61–8?.

Coupland, R. E. 1962 Nerve endings on chromaffin cells in the rat adrenal medulla. Nature 194 310–312.

De Robertis, E., and A. Pellegrino de Iraldi 19?1 Plurivesicular secretory processes and nerve endings in the pineal gland of the rat. J Biophys. Biochem. Cytol., 10 361–372.

Dewey M. M., and L. Barr 1962 Intercellular connection between smooth muscle cells the nexus. Science, 137 670–672.

Duke-Elder S., and K. C. Wybar 1961 System of Opthalmology vol. 2, The Iris 167–1?3. C. V Mosby Co., St. Louis, Mo.

Esterhuizen, A. C., and J D Lever 1961 Pancreatic islet cells in the normal and $CoCl_2$ treated guinea-pig. A fine structural study J Endocrinol., 23 243–253.

Falck, B. 1962 Observations on the possibilities of the cellular localization of monoamines by fluorescence method. Acta Physiol. Scand., 56, suppl. 197 1–25.

Farquhar M. G., and G E. Palade 1963 Junctional complexes in various epithelia. J Cell Biol., 17 375–412.

Génis-Gálvez, J M. 1957 Innervation of the ciliary muscle. Anat. Rec., 127 219–236

Grillo, M., and S. L. Palay 1963 Granule-containing vesicles in the autonomic nervous system. Electron Microscopy ed. S. S. Breese Jr vol. 2, U–1, Academic Press, N Y

Grynfeltt, E. 1898 Sur le développement du muscle dilateur de la pupille, chez le lapin. C. R. Acad. Sci., 127 966–968.

——— 1899 Le muscle dilateur de la pupille chez les mammifères. Ann. Oculist, Paris, 121 331–350.

Guyton, J S. 1940 Pharmacodynamics of the intraocular muscles. Arch. Ophthal., 24 ?–580,

Hager H., and W L. Tafuri 1959 Elektronoptischer Nachweis sog. neurosekretorischer Elementargranula in marklosen Nervenfasern des Plexus myentericus (Auerbach) des Meerschweinchens. Naturwiss., 49 332–333.

Ishikawa, T 1962 Fine structure of the human ciliary muscle. Invest Ophthal., 1

Jacobowitz, D and G. B. Koelle 1963 ...stration of both acetylcholinesterase ...cholamines in same nerve ...cologist, 5 270

Joseph, D. R. 1921 The inl... the cervical sympathetic ...ter muscle of the iris. Am. 270–280.

Krapp, J 1962 Elektronenmikroskopische Untersuchungen über die Innervation von Iris und Corpus ciliare der Hauskatze unter besonderer Berücksichtigung der Muskulatur. Zeit. mik. Anat. Forsch., 68 418–447
Langworthy O R., and L. Ortega 1943 The iris. Innervation of the iris of the albino rabbit as related to its function. Medicine, 22: 287–361
Lever J D., and A. C. Esterhuizen 1961 Fine structure of the arteriolar nerves in the guinea pig pancreas. Nature, 192: 566–567
Lister J 1853 Observations on the contractile tissue of the iris. Quart. J Mic. Sci., 1 8–17
Lowenstein, O. and I. E. Lowenfeld 1962 The pupil. Chap. 9 vol. 3 231–267 In The Eye, ed. H. Davson, Academic Press, N Y
Luft, J N 1961 Improvements in epoxy resin embedding methods. J Biophysic. Biochem. Cytol., 9: 409–414.
Macri, F and J G. Brown 1961 The constrictive action of acetazolamide on the iris arteries of the cat. Archiv Ophthal., 66 570–577
McEwen, L. M. 1956 The effect on the isolated rabbit heart of vagal stimulation and its modification by cocaine, hexamethonium and ouabain. J Physiol., 131 678–689
Mayor H. D., J C. Hampton and B Rosario 1961 A simple method for removing the resin from epoxy-embedded tissue. J Biophysic. Biochem. Cytol., 9 909–910.
Merrillees, N C. R., G. Burnstock and M. E. Holman 1963 Correlation of fine structure and physiology of the innervation of smooth muscle in the guinea-pig vas deferens. J Cell Biol., 19 529–550.
Palay S. L., S. M. McGee-Russell, S. Gordon and M. A. Grillo 1962 Fixation of neural tissues for electronmicroscopy by perfusion with solutions of osmium tetroxide. J Cell Biol., 12: 385–410.
Pallie, W., and D C. Pease 1958 Prefixation use of Hyaluronidase to improve in situ preservation for electron microscopy Ultrastruct. Res., 2: 1–7
Potter L. T and J Axelrod 1962 Intracellular localization of catecholamines in tissues of the rat. Nature, 194 581–582.
Reynolds, E. S. 1963 The use of lead citrate at high pH as an electron-opaque stain in electron microscopy J Cell Biol., 17 208–212.
Richardson, K. C. 1962 The fine structure of autonomic nerve endings in smooth muscle of the rat vas deferens. J Anat., Lond., 96 427–442.
Taxi, J 1961a Étude de l'ultrastructure des zones synaptiques dans les ganglions sympathetiques de la Grenouille. C. R. Acad. Sci., 252: 174–176.
——— 1961b Sur l'innervation des fibres musculaires lisses de l'intestin de Souris. C. R. Acad. Sci., 252 331–333
Thaemert, J C. 1963 The ultrastructure and disposition of vesiculated nerve processes in smooth muscle. J Cell Biol., 16: 361–377
Tormey J McD. 1963 Fine structure of the ciliary epithelium of the rabbit, with particular reference to "infolded membranes, "vesicles, and the effects of Diamox. J Cell Biol., 17 641–659
Tousimis, A. J and B. S. Fine 1959 Ultrastructure of the iris an electron microscopic study Am. J. Ophthal., 48 397–418.
——— 1961 Electron microscopy of the pigment epithelium of the iris. In The Structure of the Eye ed. G. K. Smelser 441–463, Academic Press, N Y
van Alphen, G. W H. M. 1963 The structural changes in miosis and mydriasis of the monkey eye. Arch. Ophthal., 69 802–814.
Wolfe D E., L. T Potter K. C. Richardson and J Axelrod 1962 Localizing tritiated norepinephrine in sympathetic axons by electron microscopic autoradiography Science 138 440–442.
Wolfe, D. E., J Axelrod, L. T Potter and K. C. Richardson 1962 Localization of norepinephrine in adrenergic axons by light — and electron-microscopic autoradiography In Electronmicroscopy ed. S S. Breese J vol. 2, U–I, Academic Press, N Y
Wolfe, D. E., and L. T Potter 1963 Localization of norepinephrine in the atrial myocardium. Anat. Rec., 145: 301

PLATES

with a brief comparison with the thymic lymphocyte of corresponding nuclear diameter Moreover the reticular cells will be briefly described in order to distinguish them from the plasmocytes.

Resting cells

(A) *Reticular cells* The cytoplasm of these cells is pale and thus almost invisible (figs. 12, 27) A few reticular cells, however are seen in which a slight and sometimes patchy basophilia makes it possible to see the cytoplasm. This absence of a well outlined and strongly basophilic cytoplasm permits us to readily distinguish this cell from a plasmocyte. The nucleus varies in size (up to 11 μ in diameter) is pale and has very fine chromatin dots and threads which stain slightly reddish One or two small acidophilic nucleoli are present.

(B) *Large plasmocytes* Cells with nuclei measuring 5 9 μ, or more in diameter are defined as large plasmocytes (fig. 4 L) Their nuclei are round to oval with a colorless sap containing pale blue chromatin structures. Many chromatin dots as fine as those seen in reticular cells as well as a few larger ones are associated with the nuclear membrane The one (figs. 4 8 11 12;L) to four nucleoli (fig. 33;L) vary in size and shape (being round, oval, stellate or elongated) and contain a slightly acidophilic core and a basophilic coat. The nucleus is usually eccentric and occupies 30 to 60% of the cellular volume (table 2, fifth column) A Golgi zone (about 2 μ in diameter) lies adjacent to the nucleus between the nucleus and the bulk of cytoplasm Commonly this zone appears to be located partly within a nuclear invagination and in contact with a nucleolus. The sharply delineated cytoplasm often has the form of an irregular polygon (fig. 4 L) and exhibits a purplish basophilia with several small and nearly colorless vacuoles (fig. 8) Russel's bodies are not seen.

A single and very large nucleolus appears more commonly in large plasmocytes than in large lymphocytes. Otherwise the nuclei of these two cell types are similar except that the few largest plasmocyte nuclei are slightly larger (about 8.9 μ) than the largest thymic lymphocyte nuclei (8 6 μ) Also the cytoplasm of the large plasmocytes differs from that of large lymphocytes by its prominent and pale Golgi zone and by its more purplish basophilia.

(C) *Medium plasmocytes* Cells having nuclei measuring between 5 9 and 4 6 μ in diameter are classified as medium plasmocytes (figs. 4 5;M) The amount of nuclear sap is less in medium than in large plasmocytes so that nuclei of the former appear darker than those of the latter This nuclear sap shows a purple color and, in this respect, differs from the nearly colorless sap of the large plasmocytes. Fine chromatin dots are less frequent in medium than in large plasmocytes. Instead coarser and darker chromatin masses are often seen. The one (fig. 4) to four nucleoli are smaller more regular in shape and darker blue than the nucleoli of large plasmocytes. Again the eccentric nucleus is adjacent to the Golgi zone The cytoplasm is similar to that of large plasmocytes, except for occasional reddish Russel's bodies, colorless crystals or numerous small colorless vacuoles (fig. 9 M).

While the medium have smaller nuclei than the large plasmocytes they have practically as much cytoplasm (table 2, second line and some of the cells forming third line) so that their nuclei fill less of the cellular volume (about 15 to 30%) than those of large plasmocytes.

The nucleolar apparatus also appears to occur more frequently as a single and larger structure in the medium plasmocytes than in medium lymphocytes but otherwise nuclei of both cell types are similar However medium plasmocytes can be readily differentiated from medium lymphocytes by their much greater amount of purplish cytoplasm and by their prominent Golgi zone.

(D) *Small plasmocytes* Cells with nuclei measuring 4 6 μ or less in diameter are defined as small plasmocytes (figs. 4, 5;S) The nuclear form varies, round to oval nuclei being common The chromatin structures and nuclear sap stain still darker than in medium plasmocytes Only coarse masses of chromatin an average of eight, are associated with the nuclear membrane Generally a single oval to round nucleolus is located in the center of the nucleus and it measures up to 1.5 μ (fig. 5 S); less frequently there are two (fig. 23 S) or

even three nucleoli but these are smaller. The chromatin network consists merely of a few fine threads connecting the chromatin masses to the nucleolus. Again the eccentric nucleus has a pale Golgi zone beside it. Cytoplasm is similar to that in larger plasmocytes, except that, much more frequently here, it is filled with small vacuoles which then have a crescent shape and are lying one against the other (fig. 12:8). As described by Beads ('54) in such a case, the basophilic cytoplasm is restricted to filiform bridges between the vacuoles. The appearance of these vacuoles varies being colorless in some cells and reddish in others. The small have as much cytoplasm as the larger plasmocytes; so that their small nuclei account for only 10 to 15% of their cellular volume (table 2, fourth line and part of cells forming third line).

While the nuclei of small plasmocytes are indistinguishable from those of small lymphocytes, the cells are readily distinguished from the latter for they exhibit a much larger amount of cytoplasm with a prominent Golgi zone.

(E) *Generalities.* Under this heading will be described three occasional features of the cells of the plasmocytic series.

(1) *Cytoplasmic inclusions.* Russel's bodies (figs. 10, 11, 32) and crystals are present in some medium, and, more frequently in some small plasmocytes (table 2, last two lines). *Twenty-seven out of the* 32 rats showed small plasmocytes with Russel's bodies (per rat, the numbers of these cells vary between 1 and 11 out of 3,000 plasmocytes). Generally the Russel's bodies are larger (up to about 4 µ) than the cytoplasmic vacuoles, described above, and stain reddish, but occasionally are colorless. Some plasmocytes exhibit a single or few large Russel's bodies and others contain numerous ones of various sizes (fig. 32 S'). At times, these bodies fill so much of the cytoplasm as to create nuclear distortion. Long and colorless crystals occur either singly or in large numbers within a plasmocyte. In the last case, crystals are parallel to each other and distort the nucleus which appears flattened against them. The gross cytoplasmic volume of plasmocytes with inclusions is twice that of other plasmocytes (table 2, two last columns). Hence in these a single nucleus would account for only 9 to 10% of cellular volume. Many of these cells appear binucleated. On the basis that all are binucleated, the two nuclei would account for 18 and 21% of the cellular volumes (table 2, percentage in brackets). These latter ratios are closer to those obtained for correspondingly sized nucleated plasmocytes without inclusion. This might suggest that, at least, most of these cells are actually binucleated.

(2) *Nuclear buds and vacuoles.* The nuclei of plasmocytes show frequently a phenomenon that we did not previously observe in thymic lymphocytes. A nuclear bud (up to 2 µ in diameter) is commonly seen and (figs. 7, 35 arrows) often connected to the nucleus by a thin thread of chromatin (up to 1 µ in length). At times spherules similar in appearance to nuclear buds lie apparently free in the cytoplasm near the nucleus (figs. 14, 24 arrows). These buds and spherules contain a pale core and a dark coat which stains with the same basophilic intensity as the nucleus. Usually these structures are surrounded by a rather pale rim of cytoplasm and are situated on the nuclear side adjacent to the bulk of cytoplasm. Not uncommonly a nuclear bud appears to be within the Golgi zone (fig. 7 upper arrow). In addition to these nuclear buds, occasional pale nuclear vacuoles are seen (figs. 10, 13 arrows); and some observations suggest their elimination in the cytoplasm (fig. 6 arrow).

(3) *Cellular outlines.* The cellular outline of some plasmocytes is irregular and gives rise to cytoplasmic buds of various sizes and shapes (fig. 8:L). Some of these buds seem to be connected to the cell by a fine thread, others appear to have no such connection. Moreover, cytoplasmic fragments can be observed in the vicinity of even regularly delineated plasmocytes. These fragments seem to be free within the extracellular spaces (fig. 10 long arrow). The frequency of such irregularities in cytoplasmic outlines varies with various node areas and also from node to node. Elongation of cytoplasm and or of nucleus were also observed suggesting that some plasmocytes are undergoing an active ameboid motion (fig. 8:L). However diapede-

TABLE 3

Mean muscle fiber weight and mean number of muscle nuclei per muscle fiber

	Suckling	Prepuberal	Young adult
Biceps brachii			
Weight (μg)	2.2	10.0	22.4
Nuclei number	658	973	1201
Extensor carpi r.l.			
Weight (μg)	2.1	11.6	29.0
Nuclei number	474	1432	2122
Gastrocnemius			
Weight (μg)	2.7	17.5	63.1
Nuclei number	1016	1686	3610
Tibialis anterior			
Weight (μg)	2.1	13.4	45.2
Nuclei number	779	1134	2002

regions of any particular muscle belly When the counts were compared in suckling and young adult rats there was either no difference or a slight decrease with age. Hence, no new muscle fibers are formed in the period of growth studied.

Fraction of muscle tissue occupied by muscle fibers endomysium and perimysium (fig. 1) While muscle fibers constituted most of the muscle bellies at all ages, their relative amount varied with age In suckling rats, the muscle fibers constituted only 70–77% of the total weight, at the prepuberal stage the proportion of muscle fibers was 86–88% and at the young adult stage 82–85% of the total weight. The difference between suckling and prepuberal stages was significant for all muscles however that between prepuberal and adult stages was significant only in the muscles of the forelimb ($0.01 > p > 0.001$) The change in the relative weight of muscle fibers was accompanied by inverse changes in the relative weight of endomysium and perimysium (fig. 1).

Fraction of the total number of nuclei present within muscle fibers (fig. 2) At all stages the muscle fiber nuclei constituted approximately 65% the endomysial cell nuclei 25% and the perimysial cell nuclei 10% of all those present. The only salient variation in the percentage of muscle fiber nuclei was a decrease with age in tibialis anterior

CALCULATED RESULTS

Absolute weight of muscle fibers endomysium and perimysium (fig. 3 left). The absolute weight of each of the three component parts of the muscle belly increased with age, more so in the muscles of the hindlimb than forelimb Within each muscle, the increase was more prominent for the fibers than for perimysium and endomysium, at least between the suckling and prepuberal stages.

Absolute numbers of nuclei (fig. 3 right). A significant increase in the absolute number of muscle fiber nuclei and of endomysial and perimysial nuclei occurred with age Like the DNA content, the number of muscle fiber nuclei approximately doubled in biceps brachii, tripled in tibialis anterior and quadrupled in gastrocnemius and extensor carpi radialis longus between the suckling and young adult stages.

The corresponding increase in number of nuclei in the endomysium and perimysium was approximately five-fold (except for biceps brachii where the increase was *but two-fold in the endomysium*)

Mean muscle fiber weight and number of nuclei per muscle fiber The fibers of all four muscle bellies had approximately the same weight in the suckling animals (2.1–2.7 μg table 3). The weight increased with age considerably especially in the

Fig. 3 On the left side the absolute weights of muscle fibers ( ) endomysium (——) and perimysium (– – –) in four muscles of suckling, prepuberal and young adult rats. On the right side the absolute nuclei number in muscle fibers ( ) endomysium (——) and perimysium (– – –) in four muscles of suckling prepuberal and young adult rats.

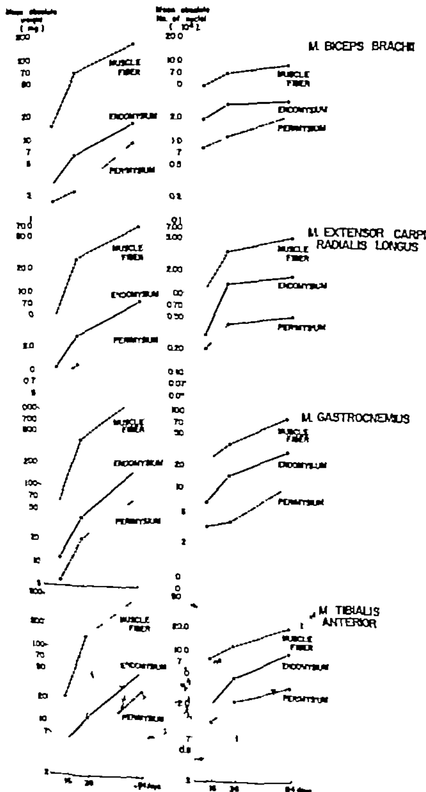

M. BICEPS BRACHII
MUSCLE FIBER
ENDOMYSIUM
PERIMYSIUM
M. EXTENSOR CARPI RADIALIS LONGUS
M. GASTROCNEMIUS
M. TIBIALIS ANTERIOR
days

Figure 3

and Hanok, '51) at least long enough for a layer of normally mineralized postinjection dentin to be formed (Storey '61)

The hypomineralized components of the responses

In the presence of these differences among the more aggregated components the similarities between the fluoride and strontium induced hypomineralized components are striking. The normal, abrupt increase in aggregation which occurs at the dentin-predentin junction was inhibited or reversed by both fluoride and strontium. This change was reflected in all of the staining reactions as well as in the lower content of S^{35}-sulfate in the hypomineralized components than in predentin or dentin. The decreased density in the hypomineralized component after fluoride has also been demonstrated in the interference microscope (Yaeger '63)

The identity of the hypomineralized components in the radiographs and the lightly stained components is demonstrated in several ways. The hypomineralized components demonstrated by radiography were spatially identical to the less aggregated components demonstrated by staining and autoradiography Furthermore the histochemical changes developed at the same time as the radiographic changes in both the fluoride and strontium responses. Finally both histochemical and radiographic changes in the strontium injected animals developed one day later than those in the fluoride injected animals.

This inhibition or reversal of aggregation confirms in general the earlier interpretations of staining reactions made by Schour and Smith ('34) and Irving and Weinmann ('48) These authors interpreted their material as indicating an arrest of maturation of predentin during the development of the responses to fluoride and strontium. Our own previous interpretation of the hypomineralized component as a layer of less aggregated matrix is also confirmed. We however were less cautious than the earlier workers and our hypothesis concerning the inhibition of predentin sulfation must be abandoned. Since predentin normally contains as much sulfate as dentin, sulfation must be reversed, rather than inhibited, to account for the decrease in sulfate in the hypomineralized components.

Mechanisms of action of fluoride and strontium

It is evident that both strontium and fluoride inhibit mineralization at least in part because of their common influence on the state of aggregation of dentin matrix. We have attributed the absence of a hypermineralized component in the strontium response to the different actions of strontium and fluoride on crystal seeding and growth. The ability of strontium to inhibit apatite seeding and crystal growth may also contribute to the development of a hypomineralized component, and a similar action of fluoride has been demonstrated (Sobel and Goldenberg, '51) However Osmanski and Yaeger ('64) have emphasized that since both the hypermineralized and hypomineralized components are developing simultaneously after fluoride it is unlikely that fluoride inhibits crystal growth or seeding during this period.

Fluoride on the other hand, inhibits a substantial number of enzymes (Frajola, '59) several of which may be directly or indirectly involved in protein or polysaccharide synthesis or in mineral metabolism. In this case, no direct evidence is available to indicate that strontium inhibits any appropriate enzyme systems and a number of studies of strontium rickets have not established its etiology (Storey '61) Explanation of the mechanism of action of strontium and fluoride in producing the responses in dentin is therefore limited by the chemical uncertainty of the histologic observations and awaits accumulation of biochemical evidence particularly concerning the toxicology of stable strontium.

SUMMARY

Fifty-day old male rats were injected subcutaneously with sodium fluoride (5 mg/100 g) or strontium chloride (125 mg/100 g) and killed at intervals of up to seven days following injection. Some animals were also injected with tetracycline at the same time as the fluoride or strontium injections. Other animals were in-

beled with S^{35}-sulfate (5 μc/g) during the experimental period. Ground sections of maxillary incisors were radiographed or photographed in ultraviolet light. Demineralized sections were stained with hematoxylin and eosin, alcian blue, dialyzed iron-ferrocyanide or the periodic acid-Schiff method, or autoradiographs prepared.

Hypomineralized components were apparent at one day after the injection of fluoride and two days after the injection of strontium. Histochemically detectable changes developed simultaneously with the radiographic changes. The tetracycline injections labeled the external edge of the hypomineralized components indicating that hypomineralization occurred at least partly in the predentin present at the time of injection. The hypomineralized components stained lighter than normal dentin with all of the staining methods used, and contained less S^{35}-sulfate than normal predentin and dentin. Intensely stained components both external and internal to the hypomineralized components were either normally mineralized or hypermineralized. These observations were interpreted as indicating that strontium and fluoride inhibit or reverse the matrix aggregation normally occurring at the dentin-predentin junction, thus inhibiting mineralization.

LITERATURE CITED

Bélanger, L. F 1954 Autoradiographic visualization of the entry and transit of S^{35} in cartilage, bone, and dentine of young rats and the effect of hyaluronidase in vitro Can. J Biochem. and Physiol., 32: 161–169

Bélanger L. F and B. B. Migicovsky 1961 A comparison between different mucopolysaccharide stains as applied to chick epiphyseal cartilage. J Histochem 9 73–78.

Bloom, W and D W Fawcett 1962 A Textbook of Histology W B. Saunders Company Philadelphia, fig. 22–5.

Bowes, J H., R. G. Elliott and J A. Moss 1953 Some differences in the composition of collagen and extracted collagen and their relation to fiber formation and dispersion. In The Nature and Structure of Collagen. Ed. by J. T Randall, Academic Press, New York, pp. 199–207

Dziewiatkowski, D. D., N DiFerrante, F Bronner and G. Okinaka 1957 Turnover of S^{35}-sulfate in epiphyses and diaphyses of suckling rats. J. Exper. Med., 106: 509–524

Frajola, W J 1959 Fluoride and enzyme inhibition. In Fluorine and Dental Health. Ed. by J C. Muhler and M. K. Hine, Indiana University Press, Bloomington, pp. 60–69.

Gersh, I. 1960 Ground substance and calcification. In: Bone as a Tissue. Ed. by K. Rodahl, J. T Nicholson and E. M. Brown, Jr The Blakiston Division, McGraw-Hill Book Company Inc., New York, pp. 128–143

Gersh, I., and H. R. Catchpole 1960 The nature of ground substance of connective tissue. Perspectives in Biol. and Med., 3 282–319.

Glimcher M. J 1959 Molecular biology of mineralized tissues with particular reference to bone. Rev Mod. Phys., 31 359–393.

——— 1960 Specificity of the molecular structure of organic matrices in mineralization. In Calcification in Biological Systems. Ed. by R. F Sognnaes. American Association for the Advancement of Science (Publication No. 64) Washington, pp. 421–487

Hale C. W 1946 Histochemical demonstration of acid polysaccharides in animal tissues Nature, 157 802.

Heller-Steinberg, M. 1951 Ground substance bone salts, and cellular activity in bone formation and destruction. Am. J Anat., 89 347–380.

Hjertquist, S. O 1960 Biophysical and histochemical studies on tooth germs from normal and rachitic dogs. Acta Path. et Microbiol. Scand., 50: 163–176.

Irving, J T 1943 The action of sodium fluoride on the dentin and predentin of the incisor teeth of rats consuming diets containing calcium and phosphorous in various ratios. J Dent. Res., 22: 447–456.

——— 1944 "Fluoride-like" action of various substances on the teeth. Nature, 154 149–150

Irving, J T and J P Weinmann 1948 Experimental studies in calcification. VI. Response of dentin of the rat incisor to injections of strontium. J Dent. Res 27 669–680.

Irving, J T., J P Weinmann, I. Schour and W R. Tweedy 1949 Experimental studies in calcification. VII. Dentinal changes in the incisor of the nephrectomized rat. J Dent. Res., 28 2–7

Jackson D S. 1953 Chondroitin sulfuric acid as factor in the stability of tendon. Biochem. J 54: 638–641.

Kulonen, E., M. B Mathews and A. Dorfman 1953 Studies in pro-collagen. I. Solubility Proc. Soc. Exper. Biol. and Med., 84 424–428.

Lagergren, C., and D Carlström 1957 Crystallographic studies of calcium and strontium hydroxyapatites. Acta Chem. Scand., 11 545–550.

Leblond, C. P R. E. Glegg and E. Eidinger 1957 Presence of carbohydrates with free 1 2 glycol groups in sites stained by the periodic acid-Schiff technique. J Histochem., 5 445–458.

Martin, G. R., E. Schiffmann, H. A. Bladen and M. U Nylen 1963 Chemical and morphological studies on the in vitro calcification of aorta. J Cell Biol., 16: 243–252.

Massler M. M and M. Serfaty 1960 Effects of different cutting procedures on dentin apposition in rat incisors. J Dent. Res., 39: 619–628.

Milch, R. A., D. P Rall and J E. Tobie 1958 Fluorescence of tetracycline antibiotics in bone. J. Bone and Joint Surg., 40A: 897–910.

Mowry W 1956 Alcian blue technics for the histochemical study of acidic carbohydrates. J Histochem., 4 407

It cannot be said what role they play in the synthesis of yolk bodies but it seems to be significant that their phospholipids are depleted as the ylok bodies grow In mam mals two types of yolk bodies namely compound yolk bodies and lipid droplets originate *de novo* in the cytoplasm by the activity of the yolk nucleus lipid bodies and mitochondria. The latter cell components do not grow directly into yolk bodies as was claimed by earlier workers. The compound yolk bodies, which consist of carbohydrate protein complex, correspond with the inclusion or vitelline elements de scribed by electron microscopists. The lipid droplets composed of phospholipids, are identical with the lipid droplets of electron microscopy Similar type of yolk bodies which are most highly developed and are of complex histochemical nature also appear *de novo* in the cytoplasm, under the influence of various formed cell components, in the oogenesis of birds reptiles and fishes In these species, most of the formed cell components completely disappear from view during yolk synthesis

SUMMARY

The so-called yolk nucleus of young oocytes of mammals differentiates close to e nucleus It is a homogeneous spherical ass having some vacuoles Histochem cal tests show that it consists of proteins lipoproteins and RNA. The lipid bodies, which are in the form of granules and rods and which consist of phospholipids de velop in association with the yolk nucleus. Both the lipid bodies and the yolk nucleus constitute the so-called "Golgi complex" of electron microscopy The yolk nucleus disintegrates before the yolk bodies are formed meanwhile the lipid bodies grow into complex elements which correspond to the multivesicular bodies of electron microscopy The histochemical nature of the mitochondria, endopalmic reticulum or ergastoplasm, chromatoid bodies and yolk is also described.

LITERATURE CITED

Anderson, E and H W Beams 1960 Cytological observations on the fine structure of the guinea pig ovary with special reference to the oogonium, primary oocyte and associated follicle cells. J Ultrastruct. Res 3 433–446.

Baker J R. 1948 The histochemical recognition of lipine. Quart. J Micr Sci., 87 441–470.

——— 1956 Improvements in the Sudan black technique. *Quart. J Micr. Sci.*, 97 621–623.

Blanchette, E. J 1961 A study of the fine structure of the rabbit primary oocyte. J Ultrastruct. Res., 5 349–363.

Blandau, R. J 1961 Biology of eggs and implantation. Sex and Internal Secretion (edited by W C. Young) The Williams and Wilkins Company Baltimore; third ed. 797–882.

Bradbury S. 1956 Human saliva as a convenient source of ribonuclease. Quart. J. Micr. Sci., 97 323–327

Guraya, S S. 1957 Histochemical studies of lipids in oocytes. I. Lipids in the oogenesis of *Columba livia*. Quart. J Micr Sci., 98 407 423.

——— 1958 Histochemical studies of lipids in oocytes. II. Lipids in the oogenesis of *Heteropneustes fossilis* Ruppell. Res. Bull. Panjab Univ 156 245–253.

——— 1959a Histochemical studies of lipids in oocytes. III. Lipids in the oocytes of the rabbit and the hare. Res. Bull. Panjab Univ 10: 81–97

——— 1959b Histochemical studies of lipids in oocytes. IV Lipids in the oogenesis of *Gallus domesticus*, *Streptopelia senegalensis* and *Streptopelia decaocto*. Res. Bull. Panjab Univ 10 119–130.

——— 1959c Histochemical studies of lipids in oocytes. V Lipids in the oogenesis of *Calotes versicolor* and *Uromastix hardwickii*. Res. Bull. Panjab Univ 10 233–246.

——— 1959d Histochemical studies of lipids in oocytes. VI. Lipids in the oogenesis of snakes, *Lycodon a. aulicus* and *Boiga trigonata*. Res. Bull. Panjab Univ 10 291–303.

——— 1959e Histochemical studies of lipids in oocytes. VII. Lipids in the oogenesis of the fresh water turtle, *Lissemys p punctata*. Res. Bull. Panjab Univ 10 305–313.

——— 1959f Lipids in the oogenesis of five species of reptiles. Science and Culture 24 390–391

——— 1960 Histochemical studies of lipids in oocytes. VIII. Lipids in the oocytes of the goat. Res. Bull. Panjab Univ 11 173–181.

——— 1961a Histochemical studies of lip in oocytes. IX. Lipids in the oocytes of t and the kraft. La cellule 61 209–21

——— 1961b Lipids in the hum Quart. J Micr Sci 381–385.

——— 1962 The s and so-called yolk n Quart. J Micr

——— 1963a. yolk nucleus in Anat. Rec., 146:

——— 1963b yolk nucleus in 60 659–666.

Hashimoto, M., T T Shimoyama Electron mic ture of the r J Jap. Obs.

——— 1960b Electron microscopic studies on the fine structure of the rabbit ovarian follicles (Report II) J Jap. Obs. Gyn. Soc., 7 268–278.

Jordan, B. M., and J R. Baker 1955 A simple pyronin/methyl green technique Quart. J Micr. Sci., 96: 177 179.

Munson, J P 1912 A comparative study of the structure and origin of the yolk nucleus. Arch. Zellforsch., 8: 663–716.

Odor D L. 1960 Electron microscopic studies on ovarian oocytes and unfertilized tubal ova in the rat. J Biophys. Biochem. Cytol., 7 567–574

Pearse, A. G. E. 1960 Histochemistry J and A. Churchill LTD., London. Appendix, 8 822–830.

Sotelo, J R., and K. R. Porter 1959 An electron microscope study of the rat ovum. J Biophys. Biochem. Cytol., 5: 327–342.

Yamada, E., T Muta, A. Motomura and H. Koga 1957 The fine structure of the oocyte in the mouse ovary studied with electron microscope. The Kurume Med. J 4: 148–171.

It cannot be said what role they play in the synthesis of yolk bodies, but it seems to be significant that their phospholipids are depleted as the ylok bodies grow In mammals two types of yolk bodies, namely compound yolk bodies and lipid droplets, originate *de novo* in the cytoplasm by the activity of the yolk nucleus, lipid bodies and mitochondria The latter cell components do not grow directly into yolk bodies as was claimed by earlier workers. The compound yolk bodies which consist of carbohydrate-protein complex, correspond *with the inclusion or vitelline elements* described by electron microscopists. The lipid droplets composed of phospholipids are identical with the lipid droplets of electron microscopy Similar type of yolk bodies *which are most highly developed and are* of complex histochemical nature also appear *de novo* in the cytoplasm, under the influence of various formed cell components in the oogenesis of birds, reptiles and fishes In these species, most of the formed cell components completely disappear from view during yolk synthesis.

SUMMARY

The so-called yolk nucleus of young *oocytes of mammals differentiates close to* e nucleus It is a homogeneous spherical ass having some vacuoles. Histochem cal tests show that it consists of proteins, lipoproteins and RNA. The lipid bodies which are in the form of granules and rods and which consist of phospholipids, develop in association with the yolk nucleus. Both the lipid bodies and the yolk nucleus constitute the so-called "Golgi complex of electron microscopy The yolk nucleus disintegrates before the yolk bodies are formed meanwhile the lipid bodies grow into complex elements which correspond to the multivesicular bodies of electron microscopy The histochemical nature of the mitochondria, "endopalsmic reticulum" or ergastoplasm," chromatoid bodies and yolk is also described.

LITERATURE CITED

Anderson, E. and H. W Beams 1960 Cytological observ tions on the fine structure of the guinea pig ovary with special reference to the oogonium, primary oocyte and associated follicle cells. J Ultrastruct. Res 3 432–446.

Baker, J R. 1946 The histochemical recognition of lipine. Quart. J Micr. Sci., 87 441–470.

——— 1956 Improvements in the Sudan black technique. Quart. J Micr. Sci., 97 621–623.

Blanchette, E. J 1961 A study of the fine structure of the rabbit primary oocyte. J Ultrastruct. Res., 5 349–363.

Blandau, R. J 1961 Biology of eggs and implantation. Sex and Internal Secretion (edited by W C. Young) The Williams and Wilkins *Company Baltimore; third ed.* 797–882.

Bradbury S. 1956 Human saliva as conve nient source of ribonuclease. Quart. J Micr Sci., 97 323–327

Guraya, S. S. 1957 Histochemical studies of lipids in oocytes. I. Lipids in the oogenesis of *Columba livia*. Quart. J Micr Sci., 98: 407–423.

——— 1958 Histochemical studies of lipids in oocytes. II. Lipids in the oogenesis of *Hemidactylus flaviviridis* Ruppell. Res. Bull. Panjab Univ 155 245–263.

——— 1959 Histochemical studies of lipids in oocytes. III. Lipids in the oocytes of the rabbit and the hare. Res. Bull. Panjab Univ 10: 81–97

——— 1959b Histochemical studies of lipids in oocytes. IV Lipids in the oogenesis of *Gallus domesticus Streptopelia senegalensis* and *Streptopelia decaocto*. Res. Bull. Panjab Univ 10: 119–130.

——— 1959c Histochemical studies of lipids in oocytes. V Lipids in the oogenesis of *Calotes versicolor* and *Uromastix hardwickii*. Res. Bull. Panjab Univ., 10 233–245.

——— 1959d Histochemical studies of lipids in oocytes. VI. Lipids in the oogenesis of snakes, *Lycodon a. aulicus and Boiga trigonata*. Res. Bull. Panjab Univ 10: 291–303.

——— 1959e Histochemical studies of lipids in oocytes. VII. Lipids in the oogenesis of the fresh water turtle, *Lissemys p. punctata*. Res. Bull. Panjab Univ 10: 305–313.

——— 1959f Lipids in the oogenesis of five species of reptiles. *Science and Culture*, 24 390–391

——— 1960 Histochemical studies of lipids in oocytes. VIII. Lipids in the oocytes of the goat. Res. Bull. Panjab Univ 11 173–181

——— 1961a Histochemical studies of lipids in oocytes. IX. Lipids in the oocytes of the cobra and the krait. *La cellule 61* 209–318.

——— 1961b Lipids in the human oocyte. Quart. J Micr Sci., 102: 381–385.

——— 1962 The structure and function of the so-called yolk nucleus in the oogenesis of birds. Quart. J Micr Sci., 103 411–416.

——— 1963a, Histochemical studies on the yolk nucleus in the oogenesis of *Indian reptiles*. Anat. Rec., 146 17–21

——— 1963b Histochemical studies on the yolk nucleus in fish oogenesis. Z. Zellforsch., 60: 659–666.

Hashimoto, M., T Kawasaki, Y Mori, A. Komori, T Shimoyama, M. Kosaka and K. Akashi 1960a Electron *microscopic studies on the fine* structure of the rabbit *ovarian follicles (Report 1)*. J Jap Obs. Gyn. Soci., 7 228–235.

—— 1960b Electron microscopic studies on the fine structure of the rabbit ovarian follicles (Report II). J Jap. Obst. Gyn. Soc., 7 268–[illegible]

[illegible], R. M and J R. Baker 1953 A simple pyronin/methyl green technique. Quart. J Micr. Sci., 94 177–178.

Munson, J P 1912 A comparative study of the structure and origin of the yolk nucleus. Arch. Zellforsch. 8: 663–716.

Odor, D. L. 1960 Electron microscopic studies on ovarian oocytes and unfertilized tubal ova in the rat. J Biophys. Biochem. Cytol., 7 567–574

Pearse, A. G. E. 1960 Histochemistry J and A. Churchill LTD London. Appendix, 8 823–830

Sotelo, J R., and K. R. Porter 1959 An electron microscope study of the rat ovum. J Biophys. Biochem. Cytol., 5 327–342.

Yamada, E., T Muta, A. Motomura and H. Koga 1957 The fine structure of the oocyte in the mouse ovary studied with electron microscope. The Kurume Medl. J., 4 148–171

It cannot be said what role they play in the synthesis of yolk bodies, but it seems to be significant that their phospholipids are depleted as the ylok bodies grow In mammals two types of yolk bodies namely compound yolk bodies and lipid droplets originate *de novo* in the cytoplasm by the activity of the yolk nucleus lipid bodies and mitochondria. The latter cell components do not grow directly into yolk bodies as was claimed by earlier workers. The compound yolk bodies which consist of carbohydrate protein complex, correspond with the inclusion or vitelline elements described by electron microscopists. The lipid droplets, composed of phospholipids are identical with the lipid droplets of electron microscopy Similar type of yolk bodies which are most highly developed and are of complex histochemical nature also appear *de novo* in the cytoplasm, under the influence of various formed cell components in the oogenesis of birds, reptiles and fishes In these species, most of the formed cell components completely disappear from view during yolk synthesis.

SUMMARY

The so-called yolk nucleus of young oocytes of mammals differentiates close to the nucleus. It is a homogeneous spherical body having some vacuoles. Histochemical tests show that it consists of proteins lipoproteins and RNA. The lipid bodies, which are in the form of granules and rods and which consist of phospholipids develop in association with the yolk nucleus. Both the lipid bodies and the yolk nucleus constitute the so-called "Golgi complex" of electron microscopy The yolk nucleus disintegrates before the yolk bodies are formed meanwhile the lipid bodies grow into complex elements which correspond to the multivesicular bodies of electron microscopy The histochemical nature of the mitochondria, endopalsmic reticulum" or ergastoplasm," chromatoid bodies and yolk is also described.

LITERATURE CITED

Anderson, E and H. W Beams 1960 Cytological observations on the fine structure of the guinea pig ovary with special reference to the oogonium, primary oocyte and associated follicle cells. J Ultrastruct. Res., 3 432–446.

Baker J R. 1946 The histochemical recognition of lipine. Quart. J Micr. Sci., 87 441–470.

——— 1956 Improvements in the Sudan black technique. Quart. J Micr. Sci., 97 621–623.

Blanchette, E. J 1961 A study of the fine structure of the rabbit primary oocyte. J Ultrastruct. Res., 5: 349–363.

Blandau, R. J 1961 Biology of eggs and implantation. Sex and Internal Secretion (edited by W C. Young) The Williams and Wilkins Company Baltimore; third ed. 797–882.

Bradbury S. 1956 Human saliva as a convenient source of ribonuclease. Quart. J Micr. Sci., 97 323–327

Guraya, S. S. 1957 Histochemical studies of lipids in oocytes. I. Lipids in the oogenesis of Columba livia. Quart. J Micr. Sci., 98 407–423.

——— 1958 Histochemical studies of lipids in oocytes. II. Lipids in the oogenesis of Hemidactylus flaviviridis Ruppell Res. Bull. Panjab Univ 156: 245–253.

——— 1959a Histochemical studies of lipids in oocytes. III. Lipids in the oocytes of the rabbit and the hare. Res. Bull. Panjab Univ 10: 81–97

——— 1959b Histochemical studies of lipids in oocytes. IV Lipids in the oogenesis of Gallus domesticus Streptopelia senegalensis and Streptopelia decaocto. Res. Bull. Panjab Univ 10 119–130.

——— 1959c Histochemical studies of lipids in oocytes. V Lipids in the oogenesis of Calotes versicolor and Uromastix hardwickii. Res. Bull. Panjab Univ 10. 233–245.

——— 1959d Histochemical studies of lipids in oocytes. VI. Lipids in the oogenesis of snakes, Lycodon a. aulicus and Boiga trigonata. Res. Bull. Panjab Univ 10 291–303.

——— 1959e Histochemical studies of lipids in oocytes. VII. Lipids in the oogenesis of the fresh water turtle Lissemys p punctata. Res. Bull. Panjab Univ 10: 305–313.

——— 1959f Lipids in the oogenesis of five species of reptiles. Science and Culture, 24 390–391.

——— 1960 Histochemical studies of lipids in oocytes. VIII. Lipids in the oocytes of the goat Res. Bull. Panjab Univ 11 175–181

——— 1961a Histochemical studies of lipids in oocytes. IX. Lipids in the oocytes of the cobra and the krait. La cellule, 61 209–218.

——— 1961b Lipids in the human oocyte Quart. J Micr. Sci., 102: 381–385.

——— 1962 The structure and function of the so-called yolk nucleus in the oogenesis of birds. Quart. J Micr Sci., 103 411–418.

——— 1963a. Histochemical studies on the yolk nucleus in the oogenesis of Indian reptiles. Anat. Rec 146: 17–21.

——— 1963b Histochemical studies on the yolk nucleus in fish oogenesis. Z. Zellforsch 60. 659–666.

Hashimoto, M., T Kawasaki, Y Mori, A. Komori, T Shimoyama, M Kosaka and K. Akashi 1960 Electron microscopic studies on the fine structure of the rabbit ovarian follicles (Report 1). J Jap Obs. Gyn. Soc., 7 229–235.

ment and about the internal and external medullary laminae. Most of these fibers appears to end in the neuropil. Quantitatively nigropallidal fibers are less numerous than subthalamopallidal fibers.

Only a relatively small number of unquestioned nigrostriatal fibers were seen in this material. Virtually all of these fibers were seen along the medial margin of the putamen. This finding substantiates that of previous authors (Ranson and Ranson 42 Kimmel, 42 Mettler 43; Rosegay 44) who used the Marchi method. It was expected that the use of silver impregnation techniques might reveal nigrostriatal fibers that could not be detected by the Marchi method and provide confirmatory evidence consistent with that based upon cell loss following large lesions of the striatum (Ferraro '25 '28; Mettler 43). A considerable number of pseudodegenerated fibers were seen in some parts of the striatum. Comparisons of these fibers with unequivocally degenerated fibers in other parts of the same section convinced us that almost all of these fibers in the striatum were normal. This still leaves the loss of cells in the substantia nigra following striatal lesions unexplained.

Although relatively few nigrostriatal fibers were demonstrated in this study nigrostriatal fibers have been described as entering the striatum via the so-called comb-bundle. It is of interest in this connection that Johnson and Clemente ('59) found degeneration in the comb system following lesions of the globus pallidus and putamen. Photographs published by Szabo ('62) suggest that strionigral fibers may form the principal fibers passing in this formation. Nigropallidal fibers traverse the internal capsule in a comb-like fashion, but do not appear to constitute the "comb-bundle.

Thalamic degeneration observed in association with lesions of the substantia nigra in this study appeared to be caused by concomitant interruption of other fiber systems rather than destruction of parts of the substantia nigra. Degeneration seen in the ventral anterior nucleus of the thalamus was due to interruption of pallidofugal fibers in the inferior thalamic peduncle or in parts of the internal capsule. No degeneration in this part of the thalamus was seen when lesions were produced by electrodes introduced in the lateromedial axis of the substantia nigra. Concomitant destruction of parts of the medial lemniscus caused abundant degeneration in the ventral posterior lateral and medial nuclei regardless of the stereotaxic approach used. Although Glees and Wall (46) concluded that nigral efferent fibers projected to the centromedian nucleus of the thalamus no preterminal degeneration in this nucleus was seen in the present study. It is our opinion that the lesions produced by these authors were not sufficiently discrete to be reliable.

One of the most interesting findings in this study was the absence of nigral efferent fibers passing to the subthalamic nucleus. This point was established in cases in which lesions were produced by electrodes introduced in a coronal plane corresponding closely to the lateromedial axis of the substantia nigra. Relatively few observers have commented upon fiber connections between these adjacent nuclear masses. Glees and Wall (46) remarked that fibers from the substantia nigra converged upon the ventral surface of the subthalamic nucleus and that some fibers terminated in the nucleus. Rioussy and Mosinger ('34) described essentially reciprocal connections between these nuclei, while other authors mention only subthalamonigral fibers (Woodburne Crosby and McCotter, '46 Whittier and Mettler 49).

Nigrotegmental fibers have been described by numerous authors (Mingazzini, 1889 Spitzer and Karplus '07 Foix and Nicolesco '25 Roussy and Mosinger '34 Shaner '36; Papez, 42; Mettler, 43) but opinions differ concerning the nuclei of termination. According to Papez (42) cell clusters in the compact part of the substantia nigra give rise to well myelinated fibers coursing dorsally and caudally in the midbrain tegmentum. These bundles of fibers traverse the medial lemniscus and are described as terminating in the "tegmental nucleus and in the parabigeminal body." Certain fibers from the rostral part of the nigra were described as passing caudally ventral to the red nucleus prior to projecting dorsally into the tegmentum. In embryonic material Shaner ('36) traced nigral fibers into the lateral midbrain tegmentum, but was unable to follow

5

described (Grünstein '11; Wilson '14; Foix and Nicolesco, '25; Johnson and Clemente, '59). Even though Johnson and Clemente ('59) reported pallidonigral fibers which could be traced into the pars reticularis of the lateral part of the substantia nigra, this evidence is questionable since the lesion involved medial portions of the putamen. In experimental studies by other authors (Ranson and Ranson '41, '42; Verhaart '50) no pallidonigral fibers were found. According to Nauta and Mehler ('61) lesions in the lateral part of the globus pallidus produce some fiber degeneration in the substantia nigra, but they expressed the opinion that such degeneration might be due to concomitant involvement of putaminonigral fibers of passage.

Descriptions of subthalamonigral fibers have been based upon study of normal (Woodburne, Crosby and McCotter '46) and Marchi stained material (Morgan '27b; Whittier and Mettler '49; Carpenter, Whittier and Mettler '50a). Subthalamonigral fibers would appear difficult to establish even though lesions may be limited to the subthalamic nucleus because involvement of capsular fibers produces degeneration of corticonigral fibers which tend to obscure findings. Precise evaluation of this pathway would seem to require the application of silver staining methods.

The principal nigral efferent fibers described in the literature include: (1) nigrostriatal fibers, (2) nigropallidal fibers, (3) nigrotegmental fibers, and (4) nigrotectal fibers. Of the various nigral efferent fibers nigrostriatal fibers sometimes are considered to form the largest group (Crosby and Lauer '59). These fibers are described as ascending to the striatum in the so-called comb bundle (Edinger '08) that is, by interdigitating with fibers in the peduncular part of the internal capsule. The most conclusive evidence of nigrostriatal fibers is based upon retrograde cell changes and cell disappearance following large cerebral lesions. Von Monakow (1895) demonstrated that cerebral lesions including portions of the striatum produced extensive cellular degeneration in the substantia nigra, an observation confirmed by others (Holmes '01; Dresel and Rothman, '25; Morrison, '29). Ferraro ('25, '28) and Mettler ('43) demonstrated that cell changes in the ipsilateral substantia nigra resulted from lesions of the striatum and were not related to ablations of cerebral cortex. According to Ferraro ('28) the disappearance of cells in the substantia nigra is proportional to the extent of injury to the neostriatum. This author reported that removal of both the neo- and paleostriatum was followed by almost total disappearance of the substantia nigra. In this discussion Ferraro mentions a small nucleus in the cat located medially between the oculomotor nerve and the medial part of the substantia nigra which he refers to as the "nucleus linearis suboculomotorius. This cell group, considered as a part of the substantia nigra, disappeared only after lesions involving both the cerebral cortex and the striatum. The homologue of this nucleus apparently has not been described in man (Olszewski and Baxter '54).

Attempts to trace myelinated fibers from the substantia nigra to the striatum in Marchi preparations have been disappointing (Ranson and Ranson '42; Kimmel, '42; Mettler '43; Rosegay '44) though several observers have felt that some nigral efferent fibers passed to the striatum. These authors, however, were able to demonstrate nigropallidal fibers. According to Ranson and Ranson ('42) lesions involving the substantia nigra in the monkey produced ascending fiber degeneration distributed largely to the medial segment of the globus pallidus, though some fibers passed into the lateral segment. Kimmel ('42) found that degenerated fibers from the nigra in the cat entered the globus pallidus and the entopeduncular nucleus. Mettler ('43) concluded that the great majority of fibers from the compact part of the nigra are distributed to the globus pallidus. The observations of Fox and Schmitz ('44) demonstrated that lesions involving the globus pallidus and entopeduncular nucleus caused disappearance of cells in the ipsilateral substantia nigra.

The current study confirms the existence of nigropallidal fibers. These fibers appear to arise largely from the pars compacta, ascend to the prerubral region and enter the globus pallidus by traversing the fibers of the internal capsule. Within the globus pallidus nigral efferent fibers are distributed to the apical part of the medial seg-

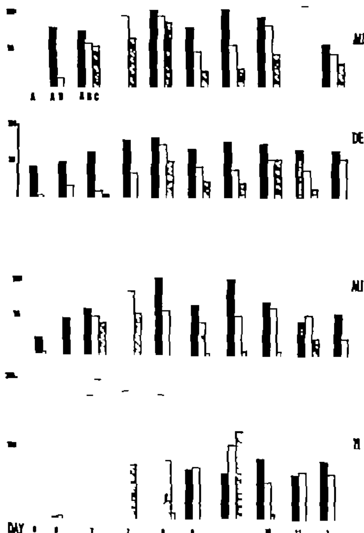


Fig. 13 Total counts of radioactive nuclei distributed in the zones of the periodontal ligament. A zone — solid black; B zone — unshaded; C zone — diagonal lines.

DISCUSSION

Proliferation in relation to periodontal ligament formation and eruption

Essential for an interpretation to the findings is the recognition of two distinct mitotic behavior patterns in components of the periodontal ligament (figs 6 7 and 8). On one hand, there is a rather consistent pattern of mitosis in the apical area with its twin peaks in numbers of radioactive cells in the pulp and a second pair of peaks in the circumapical periodontal ligament (fig. 5). This persistent concentration of mitotic cells in the apical area during root formation suggests the presence here of a *constant* stimulus for proliferation. On the other hand, in the abapical system of the periodontal ligament, there is an irregular pattern of mitosis which suggests an *intermittent* stimulus for proliferation. Although the abapical system consists of the horizontal portion (H) located at the crests of the interradicu-

Fig. 10 Peak counts of radioactive nuclei in apical periodontal ligament vs. age in days.

Fig. 11 Total counts of radioactive nuclei in the horizontal periodontal ligament vs. age in days.

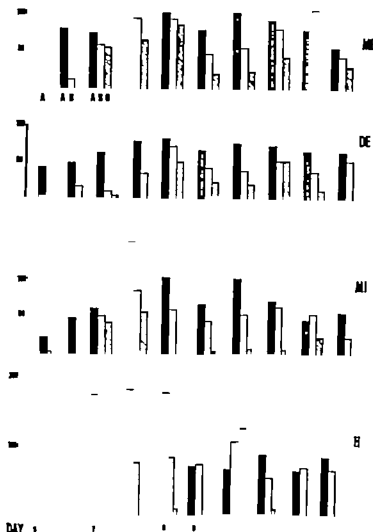


Fig. 12 Total counts of radioactive nuclei distributed in the zones of the periodontal ligament. A zone — solid black B zone — unshaded; C zone — diagonal lines.

DISCUSSION

Proliferation in relation to periodontal ligament formation and eruption

Essential for an interpretation to the findings is the recognition of two distinct mitotic behavior patterns in components of the periodontal ligament (figs. 6 7 and 8) On one hand, there is a rather consistent pattern of mitosis in the apical area with its twin peaks in numbers of radioactive cells in the pulp and a second pair of peaks in the circumapical periodontal ligament (fig. 5) This persistent concentration of mitotic cells in the apical area during root formation suggests the presence here of a *constant* stimulus for proliferation. On the other hand, in the abapical system of the periodontal ligament, there is an irregular pattern of mitosis which suggests an *intermittent* stimulus for proliferation. Although the abapical system consists of the horizontal group (H) located at the crests of the interradicular

the lack of mitoses in the cells visualized here Mitotic figures (fig. 4) can be observed elsewhere in areas of active cell proliferation although the identity of the cells which are dividing is uncertain.

Primitive reticular cells (PR, fig. 5) which may be either elongated and irregular or more rounded in configuration, are especially characterized by a paucity of formed elements within the cytoplasm. In addition to scattered 75 Å–150 Å cytoplasmic particles (probably ribonucleoprotein) these cells typically reveal only a few mitochondria, parallel membranes and vesicles. The large ovoid nuclei contain homogeneous chromatin surrounded by a double nuclear membrane with nuclear pores.

A rounded configuration and an apparent lack of cytoplasmic differentiation, as seen in primitive reticular cells are features also found in lymphocytes. In figure 6 a medium-sized lymphocyte exhibits cytoplasm with a diffuse distribution of clumps or rosettes of RNP particles among which are scattered a few ovoid mitochondria with cristae some ergastoplasmic sacs and a few vesicles. The notched nucleus contains fine homogeneous chromatin circumscribed by a double nuclear membrane with nuclear pores. Small lymphocytes present a similar appearance except that they have a smaller nucleus less cytoplasm, and a reduced concentration of particles within the cytoplasm.

Some free cells which are sporadically observed and are difficult to identify reveal cytoplasm which contains short tubules of endoplasmic reticulum a moderate number of vesicles and a diffuse distribution of RNP particles (fig. 7) From the appearance of the cytoplasm, these cells seem to be proplasmacytes (Bessis and Thiéry '61) or immature secretory cells representing an early stage in the differentiation of plasma cells. Even though the ovoid nucleus suggests that cells such as the one in figure 7 are similar to primitive reticular cells, this cell also resembles the lymphocyte cell line.

Medulla Like the cortex, the inner region or medulla of the parenchyma consists of cells very tightly packed together In marked contrast to the cortex, which consists mainly of cells with little ergastoplasm, the medulla commonly has a large percentage of cells with abundant ergastoplasm (fig. 8)

Most of these cells are plasma cells (PC figs. 8–10) The nuclei are eccentrically located, ovoid or rather irregular in configuration, and contain chromatin which is often clumped and which is circumscribed by a double nuclear membrane with nuclear pores. The cytoplasm reveals ergastoplasm which varies considerably in appearance depending upon the extent to which membranes of endoplasmic reticulum are separated by contents of the cisternae. A series of stages in dilatation of cisternae exists in figure 8a, b c, d, figures 9 and 10 immediately adjacent cells may differ widely in this respect. The contents of cisternae usually are of low to moderate density with a flocculent appearance but sometimes highly dense finely granular material is found (fig. 11) which may represent Russell bodies (Wellensiek, '57; Thiéry '58) Other cytoplasmic components found in these cells are ovoid or elongated mitochondria scattered about the endoplasmic reticulum, and perinuclear Golgi areas.

Further attention to the Golgi areas indicates that some plasma cells have multiple stacks of Golgi membranes (arrows, fig 10) Also paired Golgi membranes appear to form tubes or flattened sacs which are oriented in several directions in some cells (figs. 12 13) These Golgi membranes circumscribe material with a wide range of density (fig. 12) Vesicles or granules of different sizes and densities also exist inside Golgi areas (v figs. 12–14) The contents of these vesicles and granules bear a close resemblance to material circumscribed by nearby Golgi membranes (figs. 12, 13)

Other cells in the medulla are reticular cells which are found in strands of the reticulum coursing through the parenchyma Of particular interest is the appearance of the cytoplasm in these cells. Some reticular cells (labeled PR in figs. 8 16 17) contain sparse ergastoplasm while other cells (labeled RC in figs. 8 15) contain abundant ergastoplasm suggesting a secretory role. Indeed the cytoplasm of some reticular cells resembles the cytoplasm of plasma cells. One cannot always

be certain about the identity of a given cell with prominent ergastoplasm as a reticular cell or a plasma cell. Most cells which directly adjoin the extracellular core of the reticulum are reticular cells, but this criterion does not always hold because plasma cells infrequently contact the extracellular core through separations between reticular cells (arrows fig 17) Therefore, in some instances identification of certain cells as reticular cells or plasma cells may rest upon the configuration of the plasma membrane and nucleus recognizing that intermediate forms between these cells appear

Phagocytes Reticular cells which are phagocytic occur in both the cortex (Ph, fig 2) and medulla (Ph fig 9) The cytoplasmic appearance of phagocytes is exceedingly variable, depending upon the material ingested.

Phagocytes with ingested red blood cells present a very complex array of cytoplasmic inclusions (fig. 18) Ingested red cells become irregular in configuration and are disrupted, with vesicles (v) appearing inside the red cell remnants (RBC) These vesicles contain homogeneous material of low density with a series of small (50–100 A) black particles at the periphery of each vesicle. Adjacent to ingested red blood cell remnants are clumps of coarse moderately dense material (x) and parallel rows of granular membranes (pm) Surrounding the aggregation of red blood cell remnants, clumped particles and parallel membranes is a limiting membrane (arrows) which forms a very large vesicle separating the phagocytized material from the remainder of the cytoplasm of the phagocyte. Near this large vesicle is a series of smaller satellite vesicle (s) which contain clumped material of high density interspersed with a substance of low density These features are exemplified in the legend accompanying figure 18

Other components of the cytoplasm of the phagocyte in figure 18 are some ovoid mitochondria, scattered ergastoplasmic sacs and clumps of Palade s particles.

Phagocytes also ingest other cells such as lymphocytes plasma cells and polymorphonuclear neutrophiles (fig 19) A question arises about deciding whether a given cell such as a polymorphonuclear neutrophile is actually within the cytoplasm of a phagocyte or is extracytoplasmic and merely indents the cytoplasm of the phagocyte. Two observations may aid in the decision. First, there is often only a single plasma membrane (cm) separating the cytoplasm of the ingested cell (IC, fig. 19) from the cytoplasm of the phagocyte (Ph) rather than two parallel plasma membranes as in the case of two cells lying side by side. (Compare two encircled areas in fig 19) Second, the ingested cell usually differs from the appearance accepted as normal for that type of cell, suggesting a state of degeneration. For example, in figure 19 the plasma membrane (cm) of the ingested cell may be disrupted (arrow) Also the cytoplasm of the ingested cell looks disorganized. Discrete cytoplasmic components are no longer readily identified. Lobes of the nucleus of the ingested cell (Npn) are discernible, but their margins are ragged and frayed.

Other phagocytic material also occurs in the cytoplasm of reticular cells. Miscellaneous vesicles which are thought to be digestive vesicles or vacuoles are frequently observed In figure 20 is a vesicle 1 µ × 1 7 µ in size with a double membrane (arrows) surrounding dense flocculent material. Near this vesicle is a smaller vesicle (v) of finely granular dense material surrounded by a single membrane. In addition a multitude of tiny vesicles is scattered diffusely through the cytoplasm of the same cells. Another type of unidentified material is shown in figure 21 This material consists of several complex inclusions which contain very dense ovoid bodies (OB) surrounded by a substance of moderate density Scattered within these complex inclusions and also throughout the cytoplasm of the phagocyte are numerous 30 A–60 A black particles. Further magnification of one of these complex inclusions (fig. 22) reveals a group of dense ovoid bodies about 0.2–0 6 µ in largest diameter and a membrane which not only courses around the periphery of this inclusion but also passes between the ovoid bodies. Around each ovoid body are clumps of material (x) which resemble the contents of the ovoid bodies Again there are small dense particles (p) within the complex inclusion, these particles range from 30 A–60 A in size Still another example

the lack of mitoses in the cells visualized here. Mitotic figures (fig. 4) can be observed elsewhere in areas of active cell proliferation, although the identity of the cells which are dividing is uncertain.

Primitive reticular cells (PR, fig. 5) which may be either elongated and irregular or more rounded in configuration, are especially characterized by a paucity of formed elements within the cytoplasm. In addition to scattered 75 A–150 A cytoplasmic particles (probably ribonucleoprotein) these cells typically reveal only a few mitochondria, parallel membranes and vesicles The large ovoid nuclei contain homogeneous chromatin surrounded by a double nuclear membrane with nuclear pores.

A rounded configuration and an apparent lack of cytoplasmic differentiation, as seen in primitive reticular cells are features also found in lymphocytes. In figure 6 a medium-sized lymphocyte exhibits cytoplasm with a diffuse distribution of clumps or rosettes of RNP particles among which are scattered a few ovoid mitochondria with cristae, some ergastoplasmic sacs and a few vesicles. The notched nucleus contains fine homogeneous chromatin circumscribed by a double nuclear membrane with n pores. Small lymphocytes present a similar appearance except that they have a smaller nucleus less cytoplasm and a reduced concentration of particles within the cytoplasm.

Some free cells which are sporadically observed and are difficult to identify reveal cytoplasm which contains short tubules of endoplasmic reticulum, a moderate number of vesicles and a diffuse distribution of RNP particles (fig. 7) From the appearance of the cytoplasm these cells seem to be proplasmacytes (Bessis and Thiéry '61) or immature secretory cells representing an early stage in the differentiation of plasma cells. Even though the ovoid nucleus suggests that cells such as the one in figure 7 are similar to primitive reticular cells, this cell also resembles the lymphocyte cell line.

Medulla. Like the cortex, the inner region or medulla of the parenchyma consists of cells very tightly packed together In marked contrast to the cortex which consists mainly of cells with little ergastoplasm, the medulla commonly has a large percentage of cells with abundant ergastoplasm (fig. 8)

Most of these cells are plasma cells (PC, figs. 8–10) The nuclei are eccentrically located ovoid or rather irregular in configuration and contain chromatin which is often clumped and which is circumscribed by a double nuclear membrane with nuclear pores. The cytoplasm reveals ergastoplasm which varies considerably in appearance depending upon the extent to which membranes of endoplasmic reticulum are separated by contents of the cisternae. A series of stages in dilatation of cisternae exists in figure 8a b c, d, figures 9 and 10 immediately adjacent cells may differ widely in this respect. The contents of cisternae usually are of low to moderate density with a flocculent appearance, but sometimes highly dense finely granular material is found (fig 11) which may represent Russell bodies (Wellensiek, '57; Thiéry '58) Other cytoplasmic components found in these cells are ovoid or elongated mitochondria scattered about the endoplasmic reticulum and perinuclear Golgi areas.

Further attention to the Golgi areas indicates that some plasma cells have multiple stacks of Golgi membranes (arrows fig 10) Also paired Golgi membranes appear to form tubes or flattened sacs which are oriented in several directions in some cells (figs. 12, 13) These Golgi membranes circumscribe material with a wide range of density (fig 12) Vesicles or granules of different sizes and densities also exist inside Golgi areas (v figs. 12–14) The contents of these vesicles and granules bear a close resemblance to material circumscribed by nearby Golgi membranes (figs. 12, 13)

Other cells in the medulla are reticular cells which are found in strands of the reticulum coursing through the parenchyma. Of particular interest is the appearance of the cytoplasm in these cells. Some reticular cells (labeled PR in figs. 8 16 17) contain sparse ergastoplasm, while other cells (labeled RC in figs. 8 15) contain abundant ergastoplasm, suggesting a secretory role Indeed, the cytoplasm of some reticular cells resembles the cytoplasm of plasma cells. One cannot always

be certain about the identity of a given cell with prominent ergastoplasm as a reticular cell or a plasma cell. Most cells which directly adjoin the extracellular core of the reticulum are reticular cells but this criterion does not always hold because plasma cells infrequently contact the extracellular core through separations between reticular cells (arrows fig. 17) Therefore, in some instances identification of certain cells as reticular cells or plasma cells may rest upon the configuration of the plasma membrane and nucleus recognizing that intermediate forms between these cells appear

Phagocytes. Reticular cells which are phagocytic occur in both the cortex (Ph fig. 2) and medulla (Ph fig 9) The cytoplasmic appearance of phagocytes is exceedingly variable, depending upon the material ingested.

Phagocytes with ingested red blood cells present a very complex array of cytoplasmic inclusions (fig. 18) Ingested red cells become irregular in configuration and are disrupted, with vesicles (v) appearing inside the red cell remnants (RBC) These vesicles contain homogeneous material of low density with a series of small (50–100 Å) black particles at the periphery of each vesicle. Adjacent to ingested red blood cell remnants are clumps of coarse moderately dense material (x) and parallel rows of granular membranes (pm) Surrounding the aggregation of red blood cell remnants clumped particles and parallel membranes is a limiting membrane (arrows) which forms a very large vesicle separating the phagocytized material from the remainder of the cytoplasm of the phagocyte Near this large vesicle is a series of smaller satellite vesicle (s) which contain clumped material of high density interspersed with a substance of low density These features are exemplified in the legend accompanying figure 18.

Other components of the cytoplasm of the phagocyte in figure 18 are some ovoid mitochondria scattered ergastoplasmic sacs, and clumps of Palade s particles.

Phagocytes also ingest other cells such as lymphocytes, plasma cells and polymorphonuclear neutrophiles (fig. 19) A question arises about deciding whether a given cell such as a polymorphonuclear neutrophile is actually within the cytoplasm of a phagocyte or is extracytoplasmic and merely indents the cytoplasm of the phagocyte Two observations may aid in the decision. First, there is often only a single plasma membrane (cm) separating the cytoplasm of the ingested cell (IC fig 19) from the cytoplasm of the phagocyte (Ph) rather than two parallel plasma membranes as in the case of two cells lying side by side. (Compare two encircled areas in fig. 19) Second the ingested cell usually differs from the appearance accepted as normal for that type of cell, suggesting a state of degeneration. For example in figure 19 the plasma membrane (cm) of the ingested cell may be disrupted (arrow) Also the cytoplasm of the ingested cell looks disorganized. Discrete cytoplasmic components are no longer readily identified. Lobes of the nucleus of the ingested cell (Npn) are discernible but their margins are ragged and frayed.

Other phagocytic material also occurs in the cytoplasm of reticular cells. Miscellaneous vesicles, which are thought to be digestive vesicles or vacuoles, are frequently observed. In figure 20 is a vesicle 1 μ × 1 7 μ in size with a double membrane (arrows) surrounding dense flocculent material. Near this vesicle is a smaller vesicle (v) of finely granular dense material surrounded by a single membrane. In addition, a multitude of tiny vesicles is scattered diffusely through the cytoplasm of the same cells. Another type of unidentified material is shown in figure 21 This material consists of several complex inclusions which contain very dense ovoid bodies (OB) surrounded by a substance of moderate density Scattered within these complex inclusions and also throughout the cytoplasm of the phagocyte are numerous 30 Å–60 Å black particles. Further magnification of one of these complex inclusions (fig. 22) reveals a group of dense ovoid bodies about 0.2–0 6 μ in largest diameter and a membrane which not only courses around the periphery of this inclusion but also passes between the ovoid bodies. Around each ovoid body are clumps of material (x) which resemble the contents of the ovoid bodies. Again there are small dense particles (p) w[illegible] complex inclusion; these [illegible] 30 Å–60 Å in size. [illegible]

of unidentified material observed in reticular cells are myeloid figures formed by small whorls of membranes (figs. 22, 23) The myeloid figure shown in figure 23 is 0.5 μ × 0.22 μ in size, and each membrane is about 30 A thick.

DISCUSSION

Electron microscopic appearances of lymphocytes and plasma cells have been shown in other publications (Bessis, '58; Wellensiek '57 Amano '58a, Low and Freeman '58 Thiéry '59 and other workers cited below) Previous descriptions are confirmed in most respects by this study

Further attention to possible pathways of cellular differentiation in lymph nodes is warranted in view of recent electron microscopic evidence. Most electron microscopists who have published on this subject agree that lymphocytes plasma cells and macrophages stem from undifferentiated cells which contain few formed cytoplasmic inclusions.

According to Amano ('58a, b) and coworkers, lymphocytes stem from young reticular cells or "lymphatic reticular cells" through transitional stages called "lymphogonia, while plasma cells arise from adventitial cells (not reticular cells) around blood vessels. Braunsteiner and Pakesch ('55) believe that plasma cells stem from cells resembling undifferentiated "lymphoid reticular cells.

/ Bernhard and Granboulan ('59) and Granboulan ('60) hold that lymphocytes and plasma cells both originate from free reticular cells. Again, lymphocytes plasma cells, and also macrophages are said to arise from primitive cells resembling large lymphocytes of Maximow (Sorenson, '60) and from non-differentiated reticular cells (Han '61)

Also lymphocytopoiesis in lymphoepithelial follicles of the bursa of Fabricius has been studied with the electron microscope by Ackerman ('62) His interpretation was that lymphocytes have a dual origin — from endodermal epithelial cells and from mesenchymal cells.

It is recognized that one cannot be certain of developmental pathways in cell lines when a technique of comparing static cytologic images is employed. Yet variations in cytoplasmic appearance as observed with the electron microscope can be classified in such a way that it seems reasonable to postulate three transitional pathways or patterns of cell differentiation in lymph nodes, beginning at the level of primitive reticular cells.

Under this concept, primitive reticular cells would represent multipotent mesenchymal or embryonal cells. Their chief cytoplasmic characteristic is a diffuse array of tiny particles, which are thought to be ribosomes in conjunction with a paucity of other cytoplasmic inclusions.

Large lymphocytes or lymphoblasts could evolve from primitive reticular cells by one pattern of differentiation in which the primitive reticular cells become rounded and larger with an increase in the concentration of ribosomes. Further evolution to small lymphocytes would then include a reduction in volume of the nucleus and cytoplasm and a reduction in the concentration of ribosomes. Correspondingly little change in the actual electron microscopic appearance of the cytoplasm is seen in this pattern

By a second pattern of differentiation from primitive reticular cells many reticular cells reveal more abundant ergastoplasm, more prominent Golgi areas and a moderate increase in the number of mitochondria. Some reticular cells which accumulate ergastoplasm are believed to be freed from the reticulum, becoming plasma cells which produce antibodies or gamma globulins (Reiss et al., '50 Coons et al. 55 Ortega and Mellors, '57 Coons '59 and others) and possibly mucoproteins and glycoproteins (Pearse, 49 White '54 Zlotnick et al. '59) Other reticular cells rich in ergastoplasm remain fixed as part of the reticulum and produce a variety of substances as yet unidentified. Such reticular cells are the most logical source of some proteins and polysaccharides which appear in the extracellular component of the reticulum (reticular interstitium — Moe '63) That is to say some cells of the reticulum which are rich in ergastoplasm probably produce collagen precursors (Han, '61) mucopolysaccharides which are found with collagen (Engström and Finean, '58) and glycoproteins. In agreement with Han ('61) these reticular cells bear a close resemblance to fibroblasts in which abundant

ergastoplasm is associated with the production of collagenous fibrils (Ross and Benditt, '61)

By a third pattern of differentiation from primitive reticular cells, a transition to phagocytic reticular cells is suggested. In the cytoplasm one sees increased vesiculation, scant to moderate ergastoplasm and an increased number of mitochondria. While the principal feature of these cells consists of miscellaneous cytoplasmic vesicles and digestive vacuoles, the presence of moderately abundant ergastoplasm in some of these cells might reflect the production of enzymes required for digestive processes, or this ergastoplasm could indicate that reticular cells which are phagocytic might also have secretory capabilities.

The above three patterns of differentiation are diagrammed in figure 1 In the first pattern, primitive reticular cells seem to remain relatively undifferentiated in becoming large lymphocytes. In the second pattern, primitive reticular cells appear to become secretory cells which evolve into plasma cells or which remain as reticular cells. In the third pattern, primitive reticular cells become phagocytic. The techniques used here preclude a definitive statement as to the direction in which a sequence of cytologic differentiation proceeds or whether dedifferentiation occurs or whether some features of cellular differentiation are reversible. Cytologic observations in the three patterns of differentiation reported here seem to be in general agreement with the descriptions reported by most of the electron microscopists mentioned above. Even though the stem cells may not have been labeled identically in those publications, the salient characteristics of the stem cells are quite similar On the basis of evidence from this present study the stem cells or primitive reticular cells are believed either to become free of the reticulum and then to differentiate into lymphocytes or plasma cells or to remain fixed in the reticulum as resting cells, or to differentiate along a secretory or phagocytic pathway while remaining fixed. Some of the latter cells would then be freed at a later stage of differentiation to appear as plasma cells or as free phagocytes.

This study supports work with the light microscope by Reed ('02) and Downey and Weidenreich ('12) on heteroplastic formation of lymphocytes from reticular cells, an idea which was mentioned earlier by Billroth (1858) and others. Maximow ('32) reported that large lymphocytes can develop from undifferentiated reticular cells although he held that most large lymphocytes are formed from medium-sized lymphocytes. Leblond and Sainte-Marie ('60) described a model of cell formation in the thymus, based on counts of resting and dividing cells In this model, reticular cells are a source of large lymphocytes, which later become smaller and smaller lymphocytes. Leblond's model of lymphocyte formation in the thymus was supported for lymph nodes by Everett et al. ('60) with data obtained by labeling cells with tritiated thymidine. Other investigators also accept the concept that lymphocytes stem from reticular cells in lymph nodes (Sundberg, 47 '55 Rebuck et al., '58) and in the spleen (Campbell and Good, '50) Trowell ('58) holds that lymphocytes arise from phagocytic reticular cells, which are not the same as primitive reticular cells.

This present study also supports the light microscopic studies of Fagraeus ('48) on the formation of plasma cells from cells of the reticuloendothelial system. She stated that plasma cells develop from reticuloendothelial cells during the course of a process in which cells belonging to the reticuloendothelial system form antibodies The observations of Kolouch et al. ('47) led to similar conclusions. According to Ehrich et al. ('49) there is little doubt that undifferentiated mesenchymal cells give rise to immature plasma cells if properly stimulated. Among other workers favoring an origin of plasma cells from reticular cells are Marshall and White ('50) and Moeschlin et al. ('51)

Yet there is a substantial body of information obtained by various light microscopic techniques which indicates a lymphocytic origin of plasma cells (Bloom '28 Fichtelius '60 Holub and Riha '60 Roberts '60) A recent report by Gowans et al ('62) offers strong evidence that small lymphocytes can evolve into large pyroninophilic cells during the course of antibody formation. A model of plasma cell formation in medullary cords of lymph nodes was proposed by Leblond and

The Accessory Nerve and its Relation to the Upper Spinal Nerves[1]

ANTHONY A. PEARSON, RONALD W. SAUTER AND
GERALD R. HERRIN
Department of Anatomy, University of Oregon Medical School, Portland, Oregon

This is one of a series of papers on the structure and development of the cranial and spinal nerves. These observations were made on serial sections of human embryos and fetuses cut in different planes and stained with various neurological methods. These include the protargol method of Bodian ('36) and the silver gelatin method of Pearson and O'Neill ('46).

The human embryos and fetuses used in this study are in the collections in the Department of Anatomy of the University of Oregon Medical School and the Department of Embryology of the Carnegie Institution of Washington at Baltimore. Our studies at the Carnegie Institution were through the courtesy of the Director Dr J D Ebert, and Dr Mary E. Rawles, and Dr Elizabeth Ramsey.

In accordance with the Nomina Anatomica as revised by the Seventh International Congress of Anatomists of 1963 the terms nervus accessorius (accessory nerve) and musculus sternocleidomastoideus (sternocleidomastoid muscle) will be used. Figure 3 is a reproduction of figure 7 from Pearson, Sauter and Bass ('63).

OBSERVATIONS

This study is primarily concerned with the course of the accessory nerve and its relation to the upper cervical nerves. Since the hypoglossal nerve in mammals represents phylogenetically a fusion of several of the most rostral spinal nerves in lower forms a consideration of this nerve [illegible] also be included.

A small, spindle shaped ganglion (fig. [illegible]) was found in relation to the hypoglossal nerve on each side of a 47 mm human [illegible] (no. 101). The peripheral root of each ganglion joined the caudal roots [illegible] the hypoglossal nerve on each side and the conjoined bundles passed through the hypoglossal canal. This ganglion lies ventral to the trunk of the spinal accessory nerve and is located just dorsal to the hypoglossal canal. It more closely resembles a dorsal root ganglion of a typical spinal nerve than it does the accessory ganglia along the trunk of the accessory nerve. This is the only human embryo in our collection and in those which we studied at the Carnegie Institution which possessed a ganglion of this type connected to the hypoglossal nerve.

The first cervical nerves were studied on both sides in 25 human embryos and fetuses making a total of 50 first cervical nerves. The presence or absence of dorsal root ganglia were noted. When a ganglion was present it was recorded as being small, medium sized or large. These ganglia ranged in size from a small cluster of cells to a mass approximating the size of the dorsal root ganglion of the second cervical nerve. The former were classified as small while the latter were considered to be large. When the ganglia appeared to be about one-half to one third of the size of the second cervical dorsal root ganglia they were classified as medium sized. Clusters of [illegible] first cervical nerve [illegible] in the gross adult [illegible] probably not be [illegible] examination. The [illegible] cells [illegible] occurred in more [illegible] group [illegible] along the course of [illegible] dorsal ro[illegible] 2). Those located within [illegible] in [illegible] or the [illegible]

[1] This [illegible] Health [illegible] Institute [illegible] 00180-19 [illegible] Health and [illegible] [illegible] sample [illegible] by Public [illegible] from [illegible] and [illegible]

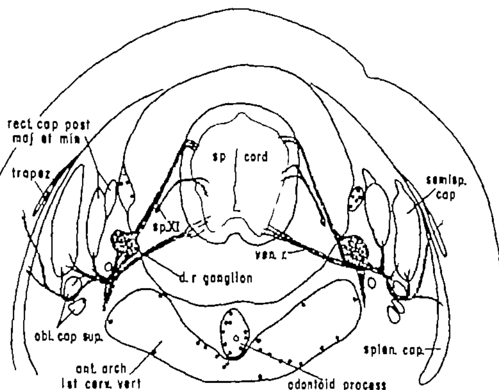


Fig. 3 A composite drawing of cross sections of the spinal cord of 18 mm human (no. 67) at the level of the first cervical nerves. A typical outer dorsal root ganglion is present both sides. Slides 22–24 Bodian method. × 20.

shaped mass (fig. 4) These and other data are summarized in the table in figure 5

Accessory ganglia are present along the course of the accessory nerve as it passes cephalad through the upper part of the vertebral canal and the cranial cavity toward the jugular foramen (figs 6 and 7) The ganglia extend caudally along the accessory nerve into the levels of the upper cervical nerves. In some embryos these ganglia were present down the levels of the dorsal roots of cervical nerve. Mature ganglion shown in the course of the of the accessory nerve of a 34 baby (fig. 6a) A large is often present at the 1st cervical nerve (fig 6) ganglia extend along the to become continuous (jugular) ganglion of Rootlets resembling

of dorsal roots extend from the ganglia and enter the medulla.

The spinal trunk of the accessory n and the more caudal accessory ganglia often in close relation to the dorsal and ganglia of the upper cervical (see table fig 5) In 11 cases the accessory nerve ran through the of C 1 In three cases the accessory glia of the th cranial nerve fused the ganglia the first cervical nerve. three cases the central processes of dorsal of C 1 mingled w or trunk the fibers of the nerve. In 16 the of the dorsal C 1 ganglia on the of the ve In the root could ed of sory l root n access

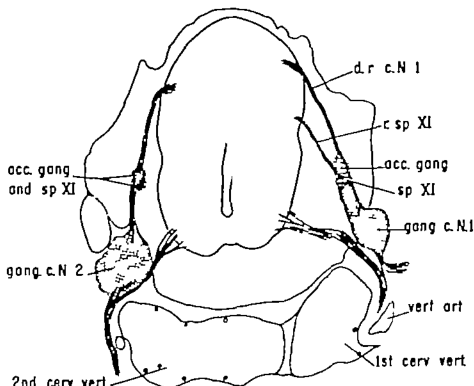


Fig. 4 Oblique section through the upper end of the spinal cord of 34 mm human embryo (no. 246). The right side of the section was little higher than the left. The ganglion of C1 has an inner and outer part which are fused. The left side of the picture is at the level of the second cervical nerve. Slide 10–1 Bodian method. × 28.

In one embryo (no. 65) where the dorsal root ganglia of C 1 were absent bilaterally fibers from the accessory ganglia of the spinal trunk of XI ran caudally to join the ventral roots of the first cervical nerves and to course peripherally with these fibers (fig. 9) In 15 cases the first cervical nerves were distinct and separate from the accessory nerve with no intermingling of fibers (fig 10 right side)

Sections of young human embryos (figs. 2 and 11) show the course of the rootlets of the accessory ganglia as they enter the caudal end of the medulla oblongata. Some of these fibers could be traced directly into the caudal end of the fasciculus solitarius. In older embryos and fetuses similar fiber bundles could be traced into the fasciculus solitarius and further dorsally into the posterior funiculus (figs 12 and 13)

In cross sections of the upper end of the spinal cord near its junction with the lower end of the medulla in a 34 day old baby a large bundle was observed entering the lateral wall (fig 14) This bundle swept medially just ventral to the substantia gelatinosa and then dorsally into the posterior funiculus where it joined the fibers of fasciculus cuneatus. This bundle is thought to be a component of the accessory nerve or an aberrant bundle of the dorsal root of the first cervical nerve which has ascended with the accessory nerve to enter the upper end of the spinal cord. This bundle on entering the cord ascended about 1.5 mm. No bundles of this type were observed on the other side.

The cells of the spinal nucleus of the accessory nerve are typical motor neurons and are located in the upper five or six segments of the spinal cord. In the upper cervical levels i.e. at levels above the brachial plexus this nucleus is located in the lateral part of the ventral horn (figs. 12, 13–15) From these neurons fibers

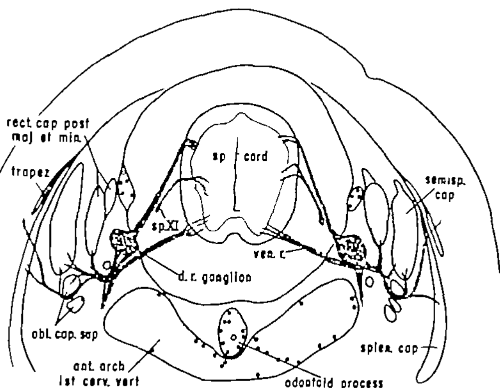


Fig. 3 A composite drawing of cross sections of the spinal cord of 28 mm human embryo (no. 67) at the level of the first cervical nerves. A typical outer dorsal root ganglion is present on both sides. Slides 22–24, Bodian method. × 20.

shaped mass (fig. 4) These and other data are summarized in the table in figure 5

Accessory ganglia are present along the course of the accessory nerve as it passes cephalad through the upper part of the vertebral canal and the cranial cavity toward the jugular foramen (figs 6 and 7) The ganglia extend caudally along the accessory nerve into the levels of the upper cervical nerves. In some embryos these ganglia were present down through the levels of the dorsal roots of the upper cervical nerve Mature ganglion cells are shown in the course of the spinal trunk of the accessory nerve of a 34 day old human baby (fig. 8a) A large accessory ganglion is often present at the level of the first cervical nerve (fig. 6) Rostrally these ganglia extend along the accessory nerve *to become continuous with the superior* (jugular) ganglion of the vagus nerve. Rootlets resembling the central processes of dorsal roots extend from the accessory ganglia and enter the medulla.

The spinal trunk of the accessory nerve and the more caudal accessory ganglia are often in close relation to the dorsal roots and ganglia of the upper cervical nerves (see table fig 5) In 11 cases the spinal accessory nerve ran through the ganglion of C 1 In three cases the accessory ganglia of the XIth cranial nerve fused wi the ganglia of the first cervical nerve. three cases the central processes of the dorsal root ganglion of C 1 mingled wit or appeared to join the fibers of the spina trunk of the accessory nerve. In 16 case the central processes of the dorsal roots o C 1 entered accessory ganglia on the trunl of the accessory nerve. In some the dorsa root fibers of C 1 could be traced rostrall along the course of the accessory nerv (fig. 7 x) In others the dorsal root fiber were lost among the cells of the accessor ganglia (figs. 6 and 7)

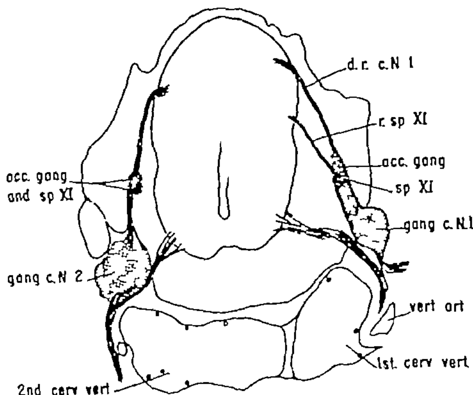


Fig. 4 Oblique section through the upper end of the spinal cord of a 24 mm human embryo (no. 246) The right side of the section was little higher than the left. The ganglion of C1 has an inner and outer part which are fused. The left side of the picture is at the level of the second cervical nerve. Slide 10–1, Bodian method. X 28.

In one embryo (no. 65) where the dorsal root ganglia of C 1 were absent bilaterally fibers from the accessory ganglia of the spinal trunk of XI ran caudally to join the ventral roots of the first cervical nerves and to course peripherally with these fibers (fig. 9) In 15 cases the first cervical nerves were distinct and separate from the accessory nerve with no intermingling of fibers (fig. 10 right side)

Sections of young human embryos (figs. 2 and 11) show the course of the rootlets of the accessory ganglia as they enter the caudal end of the medulla oblongata. Some of these fibers could be traced directly into the caudal end of the fasciculus solitarius. In older embryos and fetuses similar fiber bundles could be traced into the fasciculus solitarius and further dorsally into the posterior funiculus (figs. 12 and 13)

In cross sections of the upper end of the spinal cord near its junction with the lower end of the medulla in a 34 day old baby a large bundle was observed entering the lateral wall (fig. 14) This bundle swept medially just ventral to the substantia gelatinosa and then dorsally into the posterior funiculus where it joined the fibers of fasciculus cuneatus. This bundle is thought to be a component of the accessory nerve or an aberrant bundle of the dorsal root of the first cervical nerve which has ascended with the accessory nerve to enter the upper end of the spinal cord. This bundle on entering the cord ascended about 1.5 mm. No bundles of this type were observed on the other side.

The cells of the spinal nucleus of the accessory nerve are typical motor neurons and are located in the upper five or six segments of the spinal cord. In the upper cervical levels i.e. at levels above the brachial plexus, this nucleus is located in the lateral part of the ventral horn (figs. 12, 13, 15) From these neurons fibers

articular surface had none. The uppermost cells in the zone of proliferation in the epiphyseal plate contained clearly outlined patches of glycogen but the deeper cells had none. Some of the hypertrophied and degenerated cells of the epiphyseal plate stained diffusely for glycogen whereas others did not stain at all.

Electron microscopy

Articular cartilage In both ages of rats, the cells of the articular cartilage (figs. 7 and 8) were round or slightly flattened with their longitudinal axes parallel to the surface Short projections extended from the irregular surface of the cell into the matrix. Ergastoplasm was extensive and consisted of occasionally dilated cisternae parallel to the nuclear surface. Mitochondria were small and nearly round. Some cells had small patches of pale homogeneous material corresponding to the small flecks of PAS-positive material seen in the light microscope. Rare small lipid vacuoles were present. The Golgi apparatus consisted of flattened vesicles (figs. 7 and 8) The matrix of the articular cartilage appeared to be identical to that of hyaline tracheal cartilage Areas of pale matrix, the articular cartilage of the infant (15 gm) rats, however were larger and more common than in either the articular cartilage of the 40-gm rats or in tracheal cartilages

Epiphyseal center of ossification. In the 15-gm rats the central portion of the epiphysis destined to become the epiphyseal center of ossification, was occupied by cells distinctly different from those of the articular cartilage. The ergastoplasm was more extensive and more dilated. The intraergastoplasmic substance often was dense while the cytoplasmic ground substance between the closely packed cisternae was pale. In addition, areas of pale homogeneous material (glycogen) were consistently present. The epiphyseal center of ossification was more definite at 40 gm but still completely cartilaginous. There was an area of transition between the articular cartilage and the outer zone of the epiphyseal center of ossification and in this area the cells were indistinguishable from those occupying the central portions of the epiphysis of the infant rats (fig 9)

Well within the *outer zone* of the epiphyseal center of ossification of the 40-gm rats, the cells were large and either single or arranged in isogenous couplets and triplets. There were two main types of cells in this zone. Glycogen almost filled the cytoplasm of the commoner type of cell (fig. 10) in which it occupied a more or less central zone almost free of cytoplasmic organelles other than lipid vacuoles. The ergastoplasm and other organelles were confined to a thin rim just beneath the plasma membrane and often at one side of the cell formed a bulge or peninsula extending into the pale flocculent glycogen. In some cells the nucleus was at the tip of the peninsula or perhaps within it; but in others due to the plane of section it seemed to be isolated deep within the glycogen. Only rarely (fig. 11) were organelles distributed throughout the glycogen The eragstoplasm was extensive and prominent because of the sharp contrast between the dense intracisternal substance and pale ground substance. Mitochondria were few and small as in other chondrocytes Small irregular shrunken lipid vacuoles were scattered within the glycogen. Nuclei were bizarrely shaped with a dense chromatin. An eccentrically located round nucleolus was usual suggesting that its true shape in three-dimensions was that of a cylindroid.

In addition to the type of cell just described, there were a few strikingly different cells (figs. 11 and 12) These cells were electron dense a combined effect of a dense cytoplasmic ground substance and a closely packed ergastoplasm formed of vesicles and short double-membraned strands rather than the large cisternae of other chondrocytes. Pale zones of glycogen stood out sharply often in close association with moderate sized lipid vacuoles. These cells typically were paired with a cell of the previously described more common type in an isogenous couplet. The matrix was for the most part identical with other cartilaginous matrix except in th area between cells of a recently divide couplet (fig. 11) or more rarely surround ing an isolated cell. In these regions th

matrix was pale seemingly because of a relative paucity of fibrils.

The cells in the inner zone of the epiphyseal center of ossification in 40-gm rats were represented by remnants of degenerated cells within large lacunae that were separated by narrow bands of matrix. The cells or cell remnants, could be grouped into three types. The most common type of cell (fig. 13) occurred in almost all parts of the epiphyseal center of ossification. It had a bizarre nucleus which was intact even though the rest of the cell was disrupted. Its chromatin was evenly dense. The poorly preserved ergastoplasmic cisternae appeared as dispersed strands of double membranes. The plasma membrane was discontinuous but it and its spiny projection were readily identified. Cytoplasmic ground substance varied from a pale amorphous material to an apparently empty space. It was the emptiness of the cytoplasm and the discontinuity of the cell membrane which gave the appearance of disruption.

In those portions which border on the outer part of the inner zone were cells (fig. 14) whose cytoplasm was made up almost entirely of glycogen throughout which there were round unlined apparently empty spaces. These cells correspond in distribution to the foamy glycogen-filled cells seen in the light microscope. Their bizarre nuclei were similar to those of other chondrocytes in the inner zone. The plasma membrane again was discontinuous usually at the places where the unlined empty spaces touch the edge of the cell.

In that portion of the inner zone nearest the epiphyseal plate a third type of cell (figs 15 and 17) occurred. In the light microscope these cells were small, dense stringy masses in otherwise empty lacunae. In electron micrographs they were extremely dense bizarrely-shaped strands of protoplasm interspersed within the fibrillar matrix filling the lacunae. Only occasionally was there any internal structure within the protoplasmic strands (fig. 12) Mineral deposits were evident in the matrix of the central portion of the inner zone In the slightly calcified areas, there were round clusters of crystals interspersed in a dense amorphous substance (fig. 16) These clusters coalesced to form solidly calcified zones separated from the pale intercellular spaces by an even rim of uncalcified dark matrix (fig 15)

Zone of proliferation. The cells of this zone were electron dense with numerous spiny processes (fig. 18) Their cytoplasm was composed of closely packed ergastoplasm represented either by long arrays parallel to the longitudinal axis of the cell (fig. 19) or less often by small round and oval sacs (fig 20) Small distinctive vacuoles with a moderately dense center surrounded by a pale rim rare in tracheal and epiphyseal cartilage were numerous in these chondrocytes (fig 18). These usually were concentrated centrally at one end of the eccentric nucleus. The outline of the nucleus was indistinct and difficult to identify with certainty

As correlated with the periodic acid Schiff reaction, the cells nearest the epiphysis had patches of glycogen (fig 20) Lipid vacuoles were rare but when present in these superficial cells were close to the glycogen (fig. 20)

The matrix immediately surrounding each cell in the zone of proliferation was pale with few fibrils and resembled the light matrix of the outer zone of the epiphyseal center of ossification Two cells might be within one area of pale matrix and occasionally thin spiny processes formed cytoplasmic bridges between them. The remainder of the matrix had more fibrils and an overall greater density In this darker matrix, the fibrils between the columns were oriented parallel to the columns whereas the fibrils between the cells in the same column were oriented parallel to the longitudinal axes of the cells.

Zones of hypertrophy and degeneration of the epiphyseal plate This zone was formed by the last 2 to 5 cells in each column. The superficial cells nearest the proliferating cells were larger than the proliferating cells above them but otherwise similar Some of the deeper cells were irregularly shaped with many spiny protoplasmic processes in varying degrees of disruption and identical to the first type of degenerating cell described in the inner zone of the epiphyseal center of ossification. Other cells (figs. 21 and 22) different. They too, had thorny mic extensions even longer and

merous than those of other cartilage cells The nucleus was irregular and dense. Pale zones of glycogen were scattered through an otherwise dense cytoplasm that contained only rare mitochondria interspersed among closely packed membranes of the ergastoplasm. Numerous small characteristic vacuoles like those seen in the zone of proliferation were also present (fig. 22) The intercellular space was analogous to that in the epiphseal center of ossification and contained similar zones of calcification.

Ear

Light microscopy The auricular cartilage of the 15-gm rat was not yet fully developed. It consisted of polyhedral cells with large nuclei and scant cytoplasm separated by a sparse matrix. Staining with Verhöeff elastica revealed a dense network of elastic fibers in the matrix. The auricular cartilage of the 40-gm rat was strikingly different from that of the infant rat. The cells were larger and each contained a big central lipid vacuole and abundant glycogen. The cross sectional width of the cartilage was increased due both to the enlargement of cells and to increased amounts of matrix, but the number of cells from one side to the other remained the same

Electron microscopy The electron microscopic structure of chondrocytes in the ear of the infant rat is evident in figure 23 Two nuclei occasionally were present within a single cell. The Golgi apparatus was perinuclear and formed by stacks of flattened double membranes with associated small vesicles. The cytoplasm also contained short strands of ergastoplasm and mitochondria.

The intercellular matrix was scant and contained only a few fine fibrils. At this time the elastica consisted of irregular clumps and strands of dense homogeneous material occasionally touching the cell (figs. 23 and 24) No definitive ultrastructural features were identified in elastica, although there were occasional suggestions of a longitudinal fibrillar substructure or periodic transverse banding

The most striking feature of chondrocytes in elastic cartilage of young 40-gm rats (fig. 25) was large central lipid filled cytoplasmic vacuole. Its electron dense central portion was surrounded by an apparently empty zone probably due to shrinkage of the lipid. Some cells had two vacuoles and in a few they were mutiple. The rim of cytoplasm around the lipid droplet consisted almost entirely of glycogen interspersed with denser amorphous aggregates (fig 26) Recognizable cytoplasmic organelles were rare. The plane of section frequently missed the nucleus even though some cells had multiple nuclei. The extracellular matrix was increased in comparison to that of infant rats and the elastica was further removed from the cell surface but otherwise the extracellular material was similar in appearance.

DISCUSSION

The outstanding feature of cartilage is its unique matrix — a firm gel composed mainly of mucopolysaccharides containing a network of collagen fibrils (Ham '61; Maximow and Bloom, '57) The matrix of some cartilages when viewed in the electron microscope is of a uniform appearance from the plasma membrane of one chondrocyte to that of its neighbor Such is the case for the articular and tracheal cartilages (figs 2, 3 4 5 6 and 7) of this study and of the articular cartilage of the murine phalanges studied by Takuma ('60) Except for the elastica, the intercellular space of ear cartilage is also identical everywhere (figs. 23 24 and 25) (Sheldon and Robinson '58) In other cartilages however there are zones of pale matrix interposed between the dark matrix and the chondrocytes (Robinson and Cameron, '56 Scott and Pease '56 Cameron and Robinson '58 Zelander '59 Takuma, '60; Kreese and Knoop '61a, '61b) The paleness of these areas is related to the fineness as well as to the paucity of their fibrils.

There is evidence that in at least some cartilages fineness of the fibrils and the resultant paleness of the matrix is due to the immaturity of the matrix Zelander ('59) found that the fine fibrils near the cell gradually become broader over a zone 2 to 4 μ wide blending imperceptibly into the dark matrix with broad fibrils Others (Takuma '60 Godman and Porter '60) have similarly noted that the fibrils im-

mediately surrounding the chondrocytes were fine, the broader ones being midway between the cells. These observations suggest that the fine fibrils are early collagen fibrils which grow with age as still younger matrix is laid down between them and the chondrocytes. Topographical evidence lends further support to this idea. Pale matrix is found not only surrounding isolated chondrocytes, but also between the cells of a recently divided isogenous couplet (fig. 11) (Godman and Porter '60) Furthermore, pale matrix is particularly prevalent in areas where matrix production is rapid, such as in the zone of proliferation of the epiphyseal plate (figs. 18 and 20) (Scott and Pease '56 Cameron and Robinson, '58; During, '58 Takuma, '60) and the fibrils are broad in older topographical areas such as in the portion of the epiphysis nearest the epiphyseal plate (Godman and Porter '60) This concept also is supported by studies of developing cartilages. Martin ('53 '54) found that the cartilage matrix of the embryonic fowl contained only fine fibrils the broader ones making their appearance later in embryonic life and eventually predominating in the adult. Randall et al. ('52) likewise described only fine fibrils in the cartilage matrix of fowl embryos, whereas in the adult they found broad fibrils as well. The fibrils which Hay ('58) observed in newly formed cartilage of the regenerating limb of *Amblystoma* larvae also were delicate, as were those Takuma ('60) demonstrated in the articular cartilage of young (1–4 days) mice

In addition to the wide areas of pale matrix with fine fibrils, a narrow empty rim may surround some chondrocytes (Zelander '59; Godman and Porter '60 Knese and Knoop, '61a) Zelander ('59) suggests that these rims may be collections of newly formed mucopolysaccharides in which fibrils have not yet been deposited, corresponding to the capsule in light microscopy which because of its strong metachromasia, is thought to consist mainly of chondroitin sulphate (Ham, '61) The inconstancy with which these rims were observed in both the tracheal and articular cartilages of this study and the variability with which different investigators have found them suggest that to some extent at least artifact may play a role in producing these empty-looking rims.

Some cartilages contain a network of elastica in the matrix between the cells. Although its exact nature is unknown elastica is identified readily by its affinity for specific stains and high refractility The elastica of ear cartilage (figs. 23 24 and 25) (Sheldon and Robinson, '58) is dense, homogeneous, and resembles that of other tissues (Karrer '58) A fibrillar substructure of elastic fibers in ear cartilage is evident in some sections, much as in other elastic fibers (Rhodin and Dalhamn, '55 Karrer '58 Charles '61)

In all areas studied, the mineral of calcified cartilage is present as spherical clusters in lightly calcified areas coalescing into a solid calcified spicule in more heavily calcified zones. The crystals that form the clusters are randomly arranged, though some preference for radial arrangement has been noted, especially at the magins of the cluster (Robinson and Cameron '56, '57 Durning '58 Takuma, '60) The crystals are approximately 500 A long and 50 A wide in sectioned material (Scott and Pease '56 Robinson and Cameron '56 '57 Durning, '58 Takuma, '60)

Biochemical events occurring during calcification of cartilage have not yet been elucidated. The crystal size correlates well with the size of hydroxyapatite crystals formed *in vitro* (Watson and Robinson '53) but electron microscopic evidence suggests that something more than simple precipitation takes place. The calcified area is well demarcated from the uncalcified matrix in a remarkably even line (fig. 15) and Takuma ('60) has demonstrated a dense border between calcified and uncalcified matrix that is present even after decalcification of sections. A dense amorphous substance is also present within the mineral clusters (fig 16) as has been seen in decalcified sections (Takuma, '60) and considered to correspond to the cloud around early crystals found by Robinson and Cameron ('57) The process of calcification differs morphologically in cartilage and in bone. In cartilage the crystals are in clusters and bear no apparent relationship to collagen fibrils (Robinson and Cameron, '56) whereas in bone crystals are laid down in a definite relationship to the

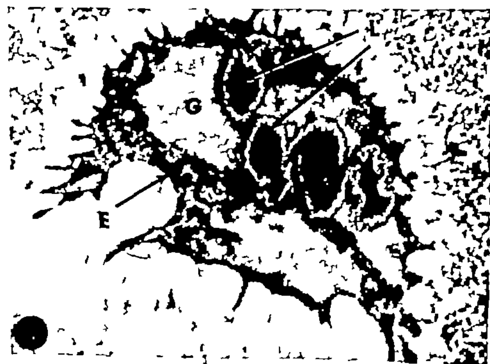
PLATE 5

EXPLANATION OF FIGURES

~ ~ure in the outer zone of the epiphyseal center of ossifi- ~ ~ ~gm rat. × 3,500 On the left is a cell in which the ~ cisternae (E) are widely distributed throughout the ~ that fills all part of the cell The nucleus (N) is ~ ~ contains dense nucleol A small part of two other ~ ~ is seen on the right They re separated by pale ~ few fibrillar component A narrow empty rim surrounds ~ ~cytes and I best seen t the rrow

~ detail of one of the hondrocytes f figure 10 × 10,000 ~ ~graph demonstrates that the erg steplasm (E) of these ~ in the outer zone of the epiph seal center of ossification ~ up of small vesicles with dense gran lar component Lipid ~ (L) are in lose relation with the are of glycogen concen- ~ G)




L
G
E

animals and in organotypic cultures can be assessed.

The authors wish to emphasize the practical significance of the hamster flank organs for investigation of hormone/cancer relationships, e.g. they afford a unique opportunity for direct daily visualization, palpation and ready intermittent sampling by biopsy of an endocrine target organ which also happens to be amenable to the induction of cancer by treatment with exogenous sex hormones. This ready accessibility and ease of surgical manipulation combined with hormone specificity should attract the attention of more investigators.

MATERIALS AND METHODS

It was desirable to include in this study a description of flank organ melanization therefore only the golden form of the Syrian hamster was used. Stock breeders were from our own colony and from several commercial sources in California. Two to six month old females were selected for breeding, handled extensively to assure tameness and housed individually in nesting cages amply provided with dry alfalfa. Both males and females were fed on a diet of Wayne mouse breeder pellets and water *ad libitum*, wheat germ carrots and greens were given twice weekly the diet of gravid females was supplemented with chocolate flavored powered milk.

As hamster breeders well know matings are much easier to obtain during the night. Timed mating is best secured by observing the precise time of copulation. To obviate the necessity for a night breeding schedule, a small breeding room was blacked-out and equipped with a timer which permitted the room to be illuminated during the night and darkened during the day. Ventilation was provided for by the installation of baffled vents and a small air circulation unit. Room temperature was maintained at approximately 75 F.

In order to assure an accurate reckoning of gestation time all breeding was conducted under visual inspection. Breeding pairs were placed in an empty cage since bedding and feed tended to distract them. If copulation failed to take place within 15 minutes it was assumed that the female was not in the receptive phase of the estrous cycle and both animals were returned to their cages. If copulation was observed the pair was permitted to remain together for an additional quarter hour and the pregnancy measured from the time of copulation.

Fetuses were obtained by hysterectomy. Fetuses older than nine days were dissected free of the uterus and investing membranes in a saline medium; removal of nine day embryos required use of a dissecting microscope.

Several representative embryos for each time interval studied were fixed in Bouin's solution, paraffin imbedded and serially sectioned at 7–10 μ. In addition, developing flank organs and adjacent skin were dissected free for microtechnical processing. Unless otherwise specified all sections were stained by the Mallory-azan method. For studies of the flank organ alone it is best to remove it from the fetus, when possible. If the organ is to be used in any studies *in vitro* it is imperative that it be cleanly removed. Removal and subsequent handling of the organ from fetuses less than 12 days of age is relatively difficult and requires considerable experience.

OBSERVATIONS

Prior to parturition (16 days) it is impossible to detect grossly the flank organs *in situ*. In the newborn, however if the costovertebral surfaces are examined under a dissecting microscope using incident light, the organs appear as tiny glistening roughly circular glabrous spots. With practice it is possible to accurately remove areas of skin containing the developing organs from fetuses as young as 12 days. Developing glands in fetuses younger than that can best be studied in serial sections of the whole costovertebral area.

With experience it is possible to detect the incipient gland in the late nine or early ten day embryos. Prior to this time there is nothing in the prospective gland-forming region to distinguish it from developing skin elsewhere.

Ten day embryos

Between the ninth and tenth days of gestation the simple squamous epithelium constituting the epidermal component of the forming flank organs thickens progres-

sively to simple cuboidal epithelium overlying a bed of condensed mesenchyme in which non-cellular fibrous material has not been observed (fig. 3) Between this cuboidal layer and the underlying condensation a faint but distinct basement membrane is visible. This membrane can also be detected under adjacent epidermis but is relatively thin and delicate. In our routine flank organ preparations vascularity seems to be no greater than in forming skin elsewhere at this period.

Although the mammary primordia (milk lines) and flank organ primordia appear at approximately the same time (tenth day) the former are decidely the more active especially their ectodermal components. This precocity continues throughout the neonatal period.

Eleven day embryos

By the eleventh day the entire epidermis has become bilamminar and is approximately 2 to 3 times thicker in the region of the flank organ than elsewhere. Cells in the basal layer tend to bulge irregularly into the underlying tissue although there is no evidence that any basement membrane penetration occurs (fig. 5)

Although the developing gland is only about 10% increased in surface area over the previous day it is much better defined and can be located microscopically without difficulty This is made possible for the most part, by a progressive, saucer-like condensation in the underlying mesenchyme (fig. 4) and by what appears to be a much higher blood supply than is found in the general skin. Within this mesenchymal plate are appreciable quantities of aniline blue-staining fibrillar matter which we presume to be collagen. At this stage exceedingly few or no formed fibers are observed in the surrounding skin.

As can be seen in figure 4 the developing milk line superficially resembles the flank organ however under slightly higher magnification it is at once apparent that whereas the main mass of the flank organ is mesenchymal that of the milk line is epidermal (fig. 7)

Twelve day embroys

Between the eleventh and twelfth days of gestation the developing flank organ (fig. 6) is easily recognizable histologically more so in fact, than during several subsequent days. The reason for this is that differentiation in the organ is advanced over that in adjacent areas of skin particularly the dermal contribution to the forming gland which is densely cellular and relatively heavily vascularized and which contains a few discrete bundles of connec tissue fibers. This condensation forms a shallow cup which extends nearly to the layer of differentiating panniculus carnosus fibers which appear for the first time at this stage (fig. 6) In adjacent regions the dermis is relatively thin, indefinite and contains only a diffuse scattering of delicate fibers.

The epidermal component has increased in thickness by about 33% through its thicker central region. The general epidermis at 12 days has a rather definite cuboidal basal layer and usually one layer of squamous surface cells the basal layer of the flank organ epidermis is columnar and is overlain by two or three layers of squamous cells. In the flank organ the epidermis is separated from the dermal portion by a conspicuously heavier basement membrane than is found anywhere else in the skin with the exception of the developing mammary system (fig. 7) The epidermal rugosites observed in the 11 day old specimens are not as apparent at 12 days and the inner boundary of epidermis presents a relatively smooth surface to the underlying dermis.

Thirteen day embryos

Although when studied in detail it is obvious that the 13 day fetal flank organ has undergone considerable growth and differentiation, it is actually not as clearly delineated from adjoining skin as it was a day earlier. This is due, not to a lesser increment in flank organ growth but to a great burst of activity in the general skin, e.g. establishment of a definite dermal layer profuse formation of large primordial hair follicles (fig 8) and an increase in vascularity especially in the vicinity of forming hairs. An interim sample at twelve and one-half days reveals that hair primordia are well started.

Within the epidermis of general skin a cuboidal germinative layer rests upon a

liquid yet not hot enough to coagulate the serum This requirement was met by combining small amounts of agar and serum mixtures at 41 C drawing the medium into a warm serological pipette and discharging it into the culture flasks.

Specimens for histological and histochemical study were harvested at regular intervals after explantation. These were usually fixed in cold Rossman's fluid for study of glycogen, mucoproteins and mucopolysaccharides by the periodic acid Schiff (PAS) reaction employing diastase controls. Acid mucopolysaccharides were identified by staining with alcian blue (Steedman '50 Spicer '60) Other specimens were fixed for histological study in cold buffered osmium tetroxide at pH 7 4–7 7 for embedding in plastics in Serra's fluid Allen's B-15 or 10% neutral formalin. For histochemical localization of enzymes the material was frozen and sections were cut at 10 μ in a cryostat. The enzymic reactions employed included the Gomori metal-salt procedure for alkaline acid and adenosine triphosphatase activity the nitro-blue tetrazolium method (Nachlas et al '58) for succinic dehydrogenase and the alpha naphthyl acetate — diazo blue B reaction for non-specific esterases These histochemical techniques were applied in the manner described in previous papers (Padykula and Herman, '55 Padykula '58) Lipids were studied in preparations stained with Sudan black B before and after acetone extraction as well as in sections examined under polarized light. For electron microscopy specimens were embedded in Epon, sectioned, stained with lead using Karnovsky's ('61) Method A and examined in RCA microscopes models EMU-3E and F

OBSERVATIONS

I Morphology of the visceral yolk sac in vivo

The visceral yolk sac (fig 1) is a highly vascular membrane consisting of extraembryonic endoderm and mesoderm The endoderm is a simple columnar epithelium composed entirely of absorptive cells that line the yolk sac cavity The mesoderm comprises the mesenchyme surrounding and forming the vitelline vessels, the serosal basement membrane and the mesothelium. The serosal basement membrane separates the mesenchymal layer from the mesothelium a simple squamous epithelium that lines the exocoelom. Near its attachment to the chorioallantoic disc the endodermal surface and the underlying mesenchyme are evaginated to form permanent ridges, or folds that are often erroneously called villi. The remainder of the endodermal surface is smooth

Between the thirteenth day of gestation and term (day 23) the visceral endoderm undergoes successive changes in the appearance and content of its cytoplasm. A phase of lipid storage between days 10 and 15 is succeeded by a period of glycogen storage from days 15 to 21 From 13 days to term, droplets of complex polysaccharide (other than glycogen) are present in the apical cytoplasm a transient decrease in their number occurs around day 18. The activities of certain hydrolytic enzymes (alkaline phosphatase esterase ATPase) are low on day 13 become elevated near days 17–19 and thereafter decline until term Despite the terminal decline in enzymic activities and glycogen content, there is physiological evidence of increased transport of antibodies near term (Brambell '57) This increased activity may be partially consequent to the fifty fold increase in weight of the visceral yolk sac between day 13 and term.

II Morphology of the organ cultures

When placed in culture the visceral yolk sac continues to develop along the general lines followed in vivo Both villous and non villous portions of the membrane develop equally well In the former for example mitotic activity (fig 2) is distributed differentially between epithelium and mesenchyme much as in vivo since the folds heighten and the membrane retains its normal histological appearance (figs 3 5) Fragments explanted on days 13 and 15 generally preserve good morphology for two weeks or some four days beyond term (day 23) Thereafter the ratio of mesenchyme to epithelium increases gradually the fold shorten and the epithelium becomes low A few fragments remain alive after 33 days in vitro or twice the normal period of gestation

(fig. 9); but overgrowth by mesenchyme prevents the organ cultures from surviving much longer

Most explants were made at 13 days of gestation. At that time the visceral endoderm is composed of simple columnar cells having a central nucleus with a cytoplasm rich in lipid and exhibiting perinuclear basophilia. The apical cytoplasm is faintly acidophil in reaction. It is surmounted by a conspicuous microvillous border The endodermal cells maintain this appearance during the first few days of culture (fig. 15) As incubation continues, the cells become taller their nuclei are pushed downward (figs 16 25) and the microvillous border grows more prominent and more irregular in shape (figs. 26–28) Although the apical border reaches its greatest development *in vivo* between days 13 and 15 (Wislocki and Padykula, '53) the microvilli *in vitro* continue to maintain their height beyond "term (fig. 23) Moreover when cultures are made of near term membranes (days 21 and 22) the normally short brush border regains its height within a day and the explants continue to survive for several days more. *Patches of stratified squamous cells occur* infrequently in the epithelium of speci mens maintained until "term (fig. 17) Still older cultures contain occasional multinucleate epithelial cells.

The cytoplasm of the mesodermal cells is basophil; as the cultures are continued these cells become increasingly separated by the the deposition of fine reticular fibers and later by collagen (fig. 4) After a fortnight *in vitro* mesoderm begins to dominate the cultures. The serosal basement membrane becomes thickened and *folded into a mass of connective tissue* increasingly characterized by irregularity of contour a fibrous texture, and acidophilia. Eventually necrotic areas and macrophages appear within the cultures.

III *Functional activities in vitro*

The cultured yolk sac membrane stores glycogen and lipid in all its tissues as does its counterpart *in vivo*, but principally in the epithelium. In addition, the visceral endoderm engages in phagocytosis and may secrete its products into the ambient medium.

Storage of glycogen. Explants made on days 12–13 begin to store glycogen near day 15 This is in accord with the behavior of the membrane *in vivo* where glycogen storage commences around day 14 reaches a peak at days 18–19 and diminishes before birth (Padykula and Richardson, '63) A similar cycle of storage and depletion occurs *in vitro* (figs. 6–9) but glycogen accumulates more slowly than *in vivo* The peak is reached between days 20–25 (fig. 8); the decline sets in slowly thereafter Glycogen levels in the cultures thus fall as *in vivo* but they begin to diminish at a time when mesenchymal overgrowth *is already under way* Glycogen-depleted membranes explanted near term (days 21 and 22) deposit glycogen in their cells (figs. 19 20) All postnatal" membranes, regardless of their time of explantation, contain small amounts of glycogen as long as their morphological appearance remains good (fig 9) Epithelial glycogen is primarily basal in the cell (figs. 7 25) although during peak storage it is also apical (fig. 8); this corresponds to the cytological distribution observed *in vivo*

Storage of lipids The lipids present in the visceral yolk sac at explantation are largely infranuclear acetone-soluble droplets which stain with Sudan dyes exhibit Maltese cross aeolotropy (Lison '60) are strongly fluorescent, and give a positive Schultz test for cholesterol (Wislocki and Padykula, '61) *In vivo* these lipids are abundant in the visceral endoderm from days 9–17 During cultivation *in vitro* the yolk sac retains these lipids longer; they are present in sizeable but variable quan tities in the visceral endoderm of 13- or 15-day explants until days 23–26 (figs *13 14 25) and then decline to a lower* level. As time passes the lipid droplets tend to become distributed more evenly through the cytoplasm than at explantation. At first the epithelium contains al most all of the lipid but in older cultures the mesoderm accumulates appreciable amounts. In addition droplets, some of anisotropic lipid appear at the margins of healthy cultures during incubation (fig 18)

Absorption of materials The visceral endoderm has a notable capacity for absorption of large *molecules and colloidal*

liquid yet not hot enough to coagulate the serum. This requirement was met by combining small amounts of agar and serum mixtures at 41 C drawing the medium into a warm serological pipette, and discharging it into the culture flasks.

Specimens for histological and histochemical study were harvested at regular intervals after explantation. These were usually fixed in cold Rossman s fluid for study of glycogen mucoproteins and mucopolysaccharides by the periodic acid-Schiff (PAS) reaction employing diastase controls. Acid mucopolysaccharides were identified by staining with alcian blue (Steedman '50 Spicer '60) Other specimens were fixed for histological study in cold buffered osmium tetroxide at pH 7 4–7 7 for embedding in plastics In Serra s fluid Allen s B-15 or 10% neutral formalin. For histochemical localization of enzymes the material was frozen, and sections were cut at 10 μ in a cryostat. The enzymic reactions employed included the Gomori metal-salt procedure for alkaline acid and adenosine triphosphatase activity the nitro-blue tetrazolium method (Nachlas et al '58) for succinic dehydrogenase and the alpha naphthyl acetate — diazo blue B reaction for non-specific esterases. These histochemical techniques were applied in the manner described in previous papers (Padykula and Herman, '55 Padykula '58) Lipids were studied in preparations stained with Sudan black B before and after acetone extraction as well as in sections examined under polarized light For electron microscopy specimens were embedded in Epon, sectioned stained with lead using Karnovsky s ('61) Method A, and examined in RCA microscopes models EMU 3E and F

OBSERVATIONS

I Morphology of the visceral yolk sac in vivo

The visceral yolk sac (fig 1) is a highly vascular membrane consisting of extraembryonic endoderm and mesoderm. The endoderm is a simple columnar epithelium composed entirely of absorptive cells that line the yolk sac cavity The mesoderm comprises the mesenchyme surrounding and forming the vitelline vessels the serosal basement membrane and the mesothelium. The serosal basement membrane separates the mesenchymal layer from the mesothelium a simple squamous epithelium that lines the exocoelom. Near its attachment to the chorioallantoic disc, the endodermal surface and the underlying mesenchyme are evaginated to form permanent ridges or folds that are often erroneously called villi. The remainder of the endodermal surface is smooth

Between the thirteenth day of gestation and term (day 23) the visceral endoderm undergoes successive changes in the appearance and content of its cytoplasm. A phase of lipid storage between days 10 and 15 is succeeded by a period of glycogen storage from days 15 to 21 From 13 days to term droplets of complex polysaccharide (other than glycogen) are present in the apical cytoplasm a transient decrease in their number occurs around day 18 The activities of certain hydrolytic enzymes (alkaline phosphatase, esterase ATPase) are low on day 13 become elevated near days 17–19 and thereafter decline until term. Despite the terminal decline in enzymic activities and glycogen content, there is physiological evidence of increased transport of antibodies near term (Brambell '57) This increased activity may be partially consequent to the fifty fold increase in weight of the visceral yolk sac between day 13 and term.

II Morphology of the organ cultures

When placed in culture the visceral yolk sac continues to develop along the general lines followed in vivo Both villous and non-villous portions of the membrane develop equally well In the former for example mitotic activity (fig 2) is distributed differentially between epithelium and mesenchyme much as in vivo since the folds heighten and the membrane retains its normal histological appearance (figs. 3 5) Fragments explanted on days 13 and 15 generally preserve good morphology for two weeks or some four days beyond term" (day 23) Thereafter the ratio of mesenchyme to epithelium increases gradually; the folds shorten and the epithelium becomes low A few fragments remain alive after 33 days in vitro or twice the normal period of gestation

ing this period. There is, however some evidence of decreased absorptive capacity by individual cells of the visceral endoderm from studies of *in vitro* uptake of vitamin B_{12}-intrinsic factor complex (Padykula and Wilson, '60) In the yolk sac the known terminal regressive changes are: a fall in the height of epithelial brush border, a decline in the storage of glycogen and lipid, decreases in certain enzymic activities, and rare occurrence of pycnosis in nuclei of the epithelium. Under conditions of organ culture the enzymic levels remain elevated at an age corresponding to term *in vivo* furthermore, when near term membranes are cultured the brush border increases in height, and glycogen storage begins anew This evidence when added to that of the membrane's long survival *in vitro* allows one to see that these terminal morphological and physiological changes in the yolk sac are imposed on the membrane and do not result from its inherent senility Furthermore, when parturition has been delayed either naturally or experimentally with the aid of hormones, placental membranes of rabbits (Snyder '34) cattle (Holm mentioned by Villee, '60) and man (Clifford, '57) have survived for some time beyond the date of parturition normal for the species.

After a long period *in vitro* the organ cultures of the yolk sac exhibit what may be a true manifestation of aging over growth of the membrane by connective tissue. This leads to loss of the membrane's histological integrity the formation of foci of necrosis and the appearance of macrophages. These effects, common enough in any "exhausted" culture may of course, be the result of some nutritional deficiency Perhaps with substitution of another medium, survival could be extended, but eventually the same histological changes would foreshadow the death of the cultures. Just such changes in company with a decline in the number of functional units (Shock, '60) are among the most verifiable manifestations of aging as it occurs in most organs of the Metazoa (Korenchevsky '61). Essentially the observations made on old cultures of yolk sac correspond to Metchnikoff's descriptions of the events of aging ('03 '08) It is certainly not clear whether aging first becomes manifest in the noble parenchymal elements in the view of Metchnikoff or in the connective tissue, in the view of Bogomolets (quoted in Nikitin, '61) In other organs morphological and physiological aspects of aging have been described at both sites (Andrew '51 Cowdry '52; Bourne '60 Gross '61; Strehler '62) As in aging organisms the parenchymal cells of the cultures undergo some morphological regression the connective tissue elements not only continue to flourish but they are stimulated to produce heavy deposits of extracellular fibers and ground substance (fig. 4) *In vivo* the basement membrane of the visceral endoderm thickens between day 13 and term; this could progressively alter the barrier between endoderm and circulating fetal blood (Wislocki and Padykula, '53) *In vitro* more sizeable depositions of extra cellular materials by fibroblasts increasingly separate cells of the endoderm and mesoderm from functional interactions. Such interactions are known to be essential to organogenesis (Grobstein, '54) and may as well be necessary for maintenance of specific morphological and biochemical characteristics (Ebeling and Fischer '22; Sorokin, '61) Metazoan cells in tissue culture, where unorganized growth is favored have demonstrated the potential immortality of their lineage (Carrel, '12 Ebeling, '22) Explants to organ culture where organized growth is fostered, eventually display morphological changes shared by aging organisms, and die Hence age associated phenomena are more apparent in systems having organized growth. It is worth keeping in mind that, thus far the largest age decrements that have been observed in cellular functions are no greater than 15% in contrast to decrements of 40–60% in total organ performances (Shock, '60) Aging, a long-continued process, may progress rapidly when interactions between cells of the parenchyma and connective tissue become difficult.

Lipid and glycogen storage The following circumstantial evidence suggests that the large store of cholesterol-containing lipid in the visceral endoderm represents material absorbed from the yolk sac cavity Various substances experimentally introduced *in vivo* enter the absorptive

cells by pinocytosis, become enclosed within cytoplasmic membranes and may also penetrate the nucleus (Luse '57; Luse Davies and Smith '59 Luse Davies, and Clark, '59) When a colloidal substance such as trypan blue is introduced, either *in vitro* or *in vivo* the absorptive cells phagocytose the material readily The foreign substance is segregated in the supranuclear region and evidently is not transported across the cell. On the other hand protein such as antibodies, are transmitted across the visceral endoderm to the fetal circulation. The evidence admittedly somewhat tenuous, that between days 10 and 15 the absorptive cells *in vivo* are engaged in the transportation of large amounts of anisotropic lipid is based on the distribution of the droplets in the supranuclear cytoplasm (Wislocki and Padykula, '61) Such droplets are found enclosed by cytoplasmic membranes. At the peak of storage they also occur in the nucleus (fig. 25) These localizations coincide with the intracellular positions of artificially introduced colloidal substances and thus suggest that the cholesterol-rich lipid has been absorbed. It should be mentioned that much infranuclear lipid lies free in the cytoplasmic matrix. Although this lipid appears to be identical cytochemically to that above the nucleus its *actual relationship to the membrane* enclosed droplets is not known.

In our investigation most explants were made on day 13 a time of maximal storage of lipid. The intracellular persistence of this lipid *in vitro* for a period much longer than normal suggests either interference in normal transport activity or possibly in metabolic handling by the cell. The accumulation of lipid in the mesoderm of older cultures may also be related to an interruption of the normal pathway of absorption. On the other hand the appearance of anisotropic droplets at the surface of healthy cultures (fig. 18) suggests a secretory phenomenon but it is not known whether it has any *in vivo* counterpart.

The possible significance of glycogen in the differentiating visceral endoderm has been considered in detail in a previous publication (Padykula and Richardson '63) The mimicking of the *in vivo* glycogen cycle in organ culture indicates that glycogen has an intrinsically determined role in the differentiation and in the functional activities of this membrane. The dependence of fetal tissues on glycogen as an energy source is well known and it is significant that an isolated fetal organ will reproduce a pattern of glycogen storage so accurately This is strikingly illustrated in organ cultures of developing mammalian lungs which duplicate a characteristic histological pattern of glycogen distribution seen *in vivo* (Sorokin, '61) Developing lungs concentrate glycogen in the terminal buds where mitoses are most frequent; as differentiation into more proximal segments occurs the glycogen disappears. Thus, with yolk sacs or lungs the explanted segment carries a *timetable* of differentiation that provides for metabolic accompaniment to the various morphological and functional events.

Experimental systems for investigations of the mammalian yolk sac Grafts of rat yolk sac have shown remarkable potentialities when transplanted to the mother's omentum (Payne and Payne '61) These yolk sac fragments, transplanted on days 14–15 and permitted to grow for 1–3 months, gave origin to a variety of tissues smooth muscle cartilage bone, and to mucus-secreting and epidermoid cysts. Payne and Payne ('61) suggest that the yolk sac at this time possesses the potentiality for developing into intestine. Although these studies should be strengthened by a systematic analysis of early changes in the yolk sac grafts they provide us with an interesting glimpse of the differentiative potential of this extraembryonic endodermal-mesodermal complex.

The system of organ culture not only lends itself to the study of differentiation functional activities also can be analyzed under various environmental conditions Popp ('58) demonstrated high metabolic rates and active synthesis of nutrients in cultures of visceral yolk sac of mice explanted during the second half of gestation. Under conditions of culture employed in our study a strong interaction was observed between endodermal cells and the culture medium The heightened brush border with highly pleomorphic microvilli signifies a cell surface that was

responding constantly to its environment. Conceivably alteration of the culture medium would affect this phagocytic or pinocytotic response.

The earliest hematopoiesis of the fetus could also be approached experimentally with organ culture. Although most of our explants were made after the cessation of blood cell formation in the yolk sac, some of the younger specimens showed islands of differentiating blood cells. Membranes explanted at 10–12 days would include hematopoietic tissue that could be maintained *in vitro*

SUMMARY

Differentiation of the visceral wall (visceral splanchnopleure) of the yolk sac placenta of the albino rat is approximated in organ culture Furthermore explanted membranes survive *in vitro* considerably beyond their normal life span.

A cycle of glycogen storage and depletion by the endodermal cells occurs *in vitro* and closely resembles that observed *in vivo*. This metabolic recapitulation *in vitro* indicates that the glycogen cycle is primarily an intrinsic function. On the other hand, glycogen-depleted membranes explanted at term are capable of reaccumulating glycogen, suggesting that extrinsic factors modify this pattern. Certain enzymic activities appear intensify and persist for as long as the membranes remain healthy Explantation of lipid-rich membranes at 13 days interferes with the normal handling of this storage material.

A major cytological deviation from normal differentiation occurs at the free surface of the endodermal cells *In vivo* the microvilli are longest and most luxuriant at days 13–15; thereafter they become less conspicuous. *In vitro* the microvilli are at all times highly developed; under these conditions the endodermal cells are actively phagocytic. They ingest components of the culture medium that react with PAS and alcian blue. Such material is concentrated in the supranuclear cytoplasm of the endoderm. If trypan blue is added it is ingested and stored in the same region.

The significance of these findings is discussed in relation to the events of aging and to functional activities of the yolk sac. Some suggestions are made for use of such organ cultures in other biological studies. In conclusion regressive changes in the yolk sac at term are not primarily the result of senility but are imposed by modification of the milieu.

ACKNOWLEDGMENTS

Technical assistance to the progress of this study was contributed by Mrs. Mary O Moore and by Misses Harriet A. Mc Kelvey Eileen Hall, and Ann G Campbell their skill and cooperation are greatly appreciated. Mr. Leo Talbert prepared many of the light micrographs and gave valuable advice on the photography of the others. The project was begun while the senior author was a member of the Department of Pathology in this school.

LITERATURE CITED

Anderson, J W 1959 The placenta barrier to gamma-globulins in the rat. Am. J Anat. 104: 403–430.

Andrew W 1951 Age changes in the skin of Wistar Institute rats with particular reference to the epidermis. Am. J Anat 89: 283–320

Baker, S. P N W Shock and A. H. Norris 1962 Influence of age and obesity in women on basal oxygen consumption expressed in terms of total body water and intracellular water In Biological Aspects of Aging. Ed. N W Shock. Columbia University Press, New York. 84–91

Bourne, G. H. 1960 General aspects of aging in cells from physiological point of view In The Biology of Aging. Ed. B H. Strehler American Institute of Biological Sciences, Washington, 133–146.

Brambell, F W R. 1957 The development of fetal immunity Macy Foundation Conferences on Gestation, 4 143–201.

Brambell, F W R., and R. Halliday 1956 The route by which passive immunity is transmitted from mother to foetus in the rat. Proc. Roy Soc., London, ser. B., 145 170–185.

Brambell, F W R., and W A. Hemmings 1960 The transmission of antibodies from mother to fetus. In The Placenta and Fetal Membranes. Ed. C. A. Villee. Williams and Wilkins Company Baltimore, 71–84.

Bridgman, J 1948 A morphological study of the development of the placenta of the rat. I. An outline of the development of the placenta of the white rat. J. Morph., 83: 61–85.

Bulmer D., and A. D. Dickson 1960 Observations on carbohydrate materials in the rat placenta. J Anat., 94 46–58.

Carrel, A. 1912 On the permanent life of tissues outside of the organism. J Exp. Med., 15 516–528.

Clifford, S. H. 1957 Postmaturity In Advances in Pediatrics. Ed. S. Z. Levine. Year Book Publ., Chicago, 9 13–63.

Cowdry E. V 1952 Ageing of individual cells In Cowdry's Problems of Ageing. Biological and Medical Aspects, 3rd ed. Ed. A. I. Lansing. Williams and Wilkins Company Baltimore 50–88.

Ebeling, A. H. 1922 A ten year old strain of fibroblasts. J Exp. Med., 35: 755–760.

Ebeling, A. H., and A. Fischer 1922 Mixed cultures of pure strains of fibroblasts and epithelial cells. J Exp. Med., 36 285–290.

Everett, J W 1935 Morphological and physiological studies of the placenta of the albino rat. J Exp Zool., 70 243–285

Farber E., E. A. Hines, H. Montgomery and W McK. Craig 1947 The arterioles of the skin in essential hypertension. J Invest. Dermat., 9 285–297

Flexner L. B., and A. Gellhorn 1942 The comparative physiology of placental transfer. Am. J Obstet. Gynec., 43: 965–974.

Flexner L. B D. B. Cowie, L. M. Hellman, W S. Wilde and G. J Vosburgh 1948 The permeability of the human placenta to sodium in normal and abnormal pregnancies and the supply of sodium to the human fetus as determined with radioactive sodium. Am. J Obstet. Gynec., 55 469–480.

Fryer, J H. 1962 Studies of body composition in men aged 60 and over. In Biological Aspects of Aging. Ed. N. W Shock. Columbia University Press, New York, 59–78.

Grobstein, C 1955 Tissue interaction in the morphogenesis of mouse embryonic rudiments in vitro. In Aspects of Synthesis and Order in Growth. Ed. D. Rudnick. Princeton University Press, Princeton, New Jersey 233–256.

Gross, J 1961 Ageing of connective tissue; the extracellular components. In Structural Aspects of Ageing. Ed. G. H. Bourne Hafner Publishing Company New York, 177–195.

Gross, L., E. Z. Epstein and M. A. Kugel 1934 Histology of the coronary arteries and their branches in the human heart. Am. J Path., 10 253–274

Hertig, A. H. 1946 Involution of tissues in fetal life review J Gerontol., 1 96–117

Karnovsky M. J 1961 Simple methods for staining with lead" at high pH in electron microscopy J Biophys. Biochem. Cytol., 11 729–732.

Korenchevsky V 1961 Physiological and Pathological Ageing. Hafner Publishing Company New York.

Lison, L. 1960 Histochimie et Cytochimie Animale, Principes et Methodes, 3rd ed. Gauthier-Villars, Paris, 491–494

Luse S. A. 1957 The morphological manifestations of uptake of materials by the yolk sac of the pregnant rabbit. Macy Foundation Conference on Gestation, 4 115–142.

Luse, S. A., J D vies and S. L. Clark, Jr 1959 Electron microscopy of nuclear inclusions. Am. J Path., 35 688.

Luse S. A., J Davies and M. Smith 1959 Electron microscopy of experimental inclusions in cytoplasm and nuclei of yolk sac cells. Fed. Proc., 18 491

Mayersbach, H. 1958 Zur Frage des Proteinüberganges von der Mutter zum Foeten. I. Befunde an Ratten am Ende der Schwangerschaft. Ztschr Zellforsch. mikroskop. Anat., 48 479–504

McKay, D. G., A. T Hertig, E. C Adams and M. V Richardson 1958 Histochemical observations on the human placenta. Obstet. Gynec., 12: 1–36.

Metchnikoff E. E. 1903 The Nature of Man; Studies in Optimistic Philosophy English translation. Ed. P C. Mitchell, G. P Putnam's Sons, New York.

——— 1908 The Prolongation of Life; Optimistic Studies. English translation. Ed. P C. Mitchell. G. P Putnam's Sons, New York.

Nachlas M. M., K.-C. Tsou, E. DeSouza, C. Cheng and A. M. Seligman 1957 Cytochemical demonstration of succinic dehydrogenase by the use of a new p-nitrophenyl substituted ditetrazole. J Histochem. Cytochem., 5: 420–436.

Nikitin, V N 1961 Russian Studies on Age-Associated Physiology Biochemistry and Morphology National Inst. Health, Bethesda Maryland.

Padykula, H. A. 1958 A histochemical and quantitative study of enzymes of the rat's placenta. J Anat., 92: 118–129.

Padykula, H. A., and E. Herman 1955 Factors affecting the activity of adenosine triphosphatase and other phosphatases as measured by histochemical techniques. J Histochem. Cytochem., 3 161–169.

Padykula, H. A., and T H. Wilson 1960 Differentiation of bsorptive capacity in the visceral yolk sac of the rat. Anat. Rec 136 254.

Padykula, H. A., and D. Richardson 1963 A correlated histochemical and biochemical study of glycogen storage in the rat placenta. Am. J. Anat., 112 215–242.

Payne, J M., and S. Payne 1961 Placental grafts in rats. J Embryol. Exp. Morph., 9 106–116.

Popp, R. A. 1958 Comparative metabolism of blastocysts, extraembryonic membranes, and uterine endometrium of the mouse J Exp. Zool., 138 1–23.

Pritchard, J J 1947 The distribution of alkaline phosphatase in the pregnant uterus of the rat. J Anat., 81 352–364.

Ring, J R. 1960 Histological and histochemical age changes in oral subepithelial connective tissue. In Aging Some Social and Biological Aspects. Ed. N W Shock. Amer Assoc Adv Science, Washington, 393–404.

Shock, N W 1960 Some of the facts of aging. In Aging Some Social and Biological Aspects. Ed. N W Shock. Amer Assoc. Adv Science Washington 241 260.

Snyder F F 1934 The prolongation of pregnancy and complications of parturition in the rabbit following induction of ovulation near term. Bull. Johns Hopkins Hosp., 54 1 23.

Sorokin, S 1961 A study of development in organ cultures of mammalian lungs. Develop Biol., 3 60–83.

Sorokin, S., and H. A. Padykula 1960 Differentiation of visceral yolk sac in vitro. Anat. Rec., 136: 348.

Spicer, S. S. 1960 A correlative study of the histochemical properties of rodent acid mucopolysaccharides. J. Histochem. Cytochem., 8: 18–34.

Steedman, H. F. 1950 Alcian blue 8GS: a new stain for mucin. Quart. J. Micr. Sci., 91: 447–479.

Strehler, B. H. 1962 Time, Cells and Aging. Academic Press, New York.

Thomsen, K. 1954 Zur Morphologie und Genese der sog. Placentarinfarkte. Arch. Gynäk., 185: 221–247.

Villee, C. A. 1953 The metabolism of the human placenta in vitro. J. Biol. Chem., 205: 113–123.

——— 1960 Discussion. In: The Placenta and Fetal Membranes. Ed. C. A. Villee. Williams and Wilkins Company, Baltimore, 233–234.

Wislocki, G. B. 1956 Morphological aspects of ageing in the placenta. Ciba Foundation Coll. Ageing, 2: 105–114.

Wislocki, G. B., and E. W. Dempsey 1955 Electron microscopy of the placenta of the rat. Anat. Rec., 123: 33–64.

Wislocki, G. B., and H. A. Padykula 1953 Reichert's membrane and the yolk sac of the rat investigated by histochemical means. Am. J. Anat., 92: 117–152.

——— 1961 Histochemistry and electron microscopy of the placenta. Chap. 15. In: Sex and Internal Secretions, 3rd ed., Ed. W. C. Young. Williams and Wilkins Company, Baltimore.

PLATE 1

EXPLANATION OF FIGURES

Except for figure 1 all illustrations are of *organ cultures* of the visceral yolk sac.

1 Cross-section of the rat uterus through the placental site on day 13. The visceral yolk sac encloses the fetus and is attached to the placental disc. Note that the portion of the visceral yolk sac near its attachment to the disc is ridged ("villous) The membrane t this stage was the usual starting material for the organ cultures. Only a portion of the fetus is shown, and the amnion is not evident. 7 ×

2 Mitotic activity is conspicuous in the visceral endoderm during the first days of culturing. Explanted on day 13, *in vitro* two days. Iron hematoxylin. 360 ×

3 After seven days *in vitro* this specimen displays normal folding of the membrane and an orderly arrangement of the columnar endodermal cells. Within the folds the fetal blood vessels are dilated, and proliferation of connective tissue is not excessive. Explanted on day 13. Iron hematoxylin. 360 ×.

4 Appearance of an aging" organ culture. Beneath the epithelium the connective tissue has thickened by deposition of collagenous fibers. Mesenchymal overgrowth is regularly present in cultures maintained several days past term; occasionally it becomes manifest somewhat earlier as illustrated here. The nutrient medium (lower right) is darkly stained. Explanted on day 13, *in vitro* eight days. Embedded in Epon. Toluidine blue. 235 ×

5 For the most part, good morphological preservation is evident after seven days *in vitro*; however some excess connective tissue is seen in one quadrant (upper left) In this particular specimen piece of fetal heart muscle (h) became attached to one side. Explanted on day 13. Iron hematoxylin. 35 ×

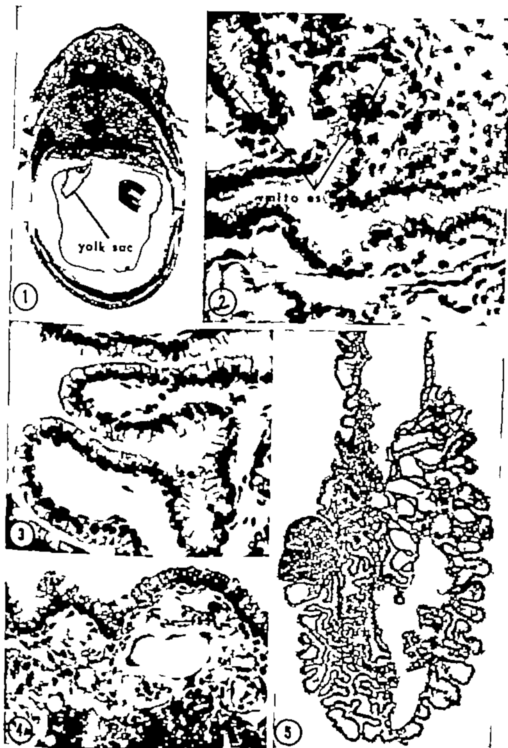

yolk sac
1
2
3
4
5

PLATE 5

EXPLANATION OF FIGURE

25 An electron micrograph of an endodermal cell after six days *in vitro*. The apical cytoplasm is crowned by brush border of microvilli. Above the nucleu lie large esicles containing bsorbed material (abs vesicle) that gives a positive reaction for neutral and acid mucopolysaccharides. Well-developed mitochondria are distributed throughout the cytoplasm, but the large Golgi apparatus and the endoplasmic reticulum are most developed in perinuclear regions. Lipid is found in large droplets typically below the nucleus; at times it occurs as well in the nucleus. Glycogen (inset) is concentrated below the nucleus (N). The epithelial cell are linked together by terminal bars (tb) and small desmosomal attachments (arrows) along their lateral margins. Explanted on day 13. 7,000 ×


obs v cicl
obs vesicl
Golgi
N
glycog
Golgi
25

Studies of Rat Kidney and Liver Growth Using Total Nuclear Counts

BARNETT ZUMOFF AND MORTON R. PACHTER
Department of Pathology State University of New York, Downstate Medical Center Brooklyn, New York

Organ growth in young animals proceeds by multiplication of discrete units the cell nuclei. There has been considerable interest in the use of total nuclear counts as a criterion of organ growth and regeneration, but studies of the normal course of organ growth in terms of total nuclear count have not been reported. In part, this is because the use of stained histological sections for counts as reported by Brues, Drury and Brues ('36) Kosterlitz ('44) and Bucher and Glinos ('50) is time consuming and impractical for any large volume of work. A method of performing nuclear counts on organ homogenates was described by Pearce and Gerard ('42) but is laborious and in the writers experience, not very reproducible The observation by Mirsky and Ris ('47) that a low pH in the suspending medium will protect nuclei from powerful shearing forces provides the background for development of the method to be described according to Mirsky ('49) the method produces suspensions of nuclei in which no free chromosomes can be detected.

The present paper reports the results of application of this method to a study of the growth of rat liver and kidney in terms of total nuclear count. It was found that, normally the curves for increase in nuclear count, except in female rat liver exhibited a plateau which began at the onset of puberty in the midportion of the active growth period This plateau was not seen in curves for organ weight increase. Because of these findings studies of nuclear count increase in the organs of castrated and of castrated hormone-treated animals were undertaken in an effort to clarify the mechanisms involved A study was also made of the influence of castration and hormone supplementation on the course of kidney hypertrophy after unilateral nephrectomy

METHOD

Livers were prepared by rinsing in tap water patting dry and trimming all ligaments and connective tissue Kidneys were gently pressed free of blood and decapsulated the capsules, together with the major blood vessels ureters, and renal pelvis, were then amputated at the hilus. The organ was placed in the chamber of a Waring Blendor with enough 0 01 N hydrochloric acid to yield a final concentration of nuclei in the homogenate of about 5 000 per cu mm This amount varied from 100 to 400 ml for a rat liver or two rat kidneys depending on the size of the animal. The quantity of liquid used for the homogenization was just under the desired final volume after homogenization was complete, the suspension was made up to exact volume in a graduated cylinder The Blendor was run for two minutes. The timing did not need to be exact; any time interval from 45 seconds to 12 minutes was satisfactory (fig 1) but two minutes was used throughout for the sake of uniformity After the Blendor was turned off, 5 to 10 drops of capryl alcohol were added to the suspension to break up the foam and the homogenate was made up to final volume with 0 01 N hydrochloric acid. After thorough shaking for a few minutes samples were withdrawn with a capillary pipette and run onto the stage of a standard hemocytometer No staining was necessary; the nuclei stood out since the homogenate was free of debris (fig 2) A count was made of the total number of nuclei in the five standard red-cell counting boxes

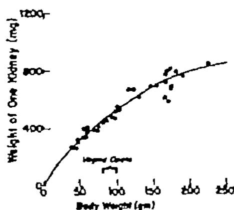
Present address: Division of Neoplastic Medicine, Montefiore Hospital, New York, N. Y

Findings

Organ weights The curves of organ weights vs. body weight for animals of Series A (figs. 3 4 5 6) were nearly identical to those of Series B (figs. 7 8 9 10) and quite similar to those described in the literature by Donaldson ('24) and Freudenberger and Hashimoto ('37)

Total nuclear count

(a) *Kidney* The growth curves in animals of both series showed a rather sharp plateau in the mid-portion of the active growth period In Series A, this plateau extended from body weight 60 gm to body



F gure 3

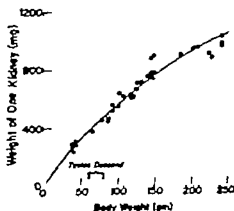


Figure 4

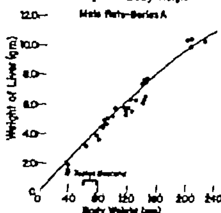


Figure 5

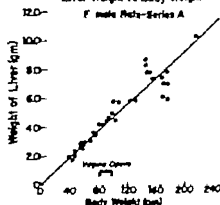


Figure 6

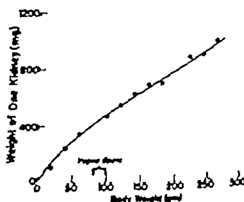


Figure 7

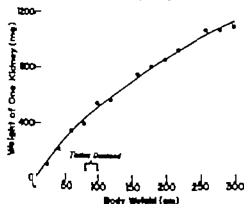


Figure 8

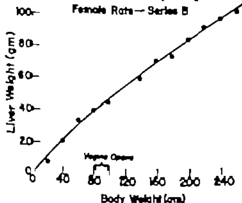


Figure 9

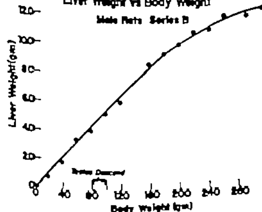


Figure 10

weight 140 gm for males (fig. 11) and from body weight 70 gm to body weight for females (fig 12) In Series B the plateau extended from body weight 80 gm to body weight 200 gm for both sexes (figs. 13 and 14) The plateau began at puberty in all four groups and ended at an age which had no obvious physiological significance

(b) *Liver* Females of both Series showed growth curves which were quite similar in shape to the organ weight curves, and in which there was no evidence of a growth plateau (figs. 15 16) Males of Series B showed a growth curve which included a sharp plateau from body weight 100 gm to body weight 200 gm (fig. 17) whereas males of Series A showed a growth curve which did not include a plateau (fig 18) This was the only qualitative growth

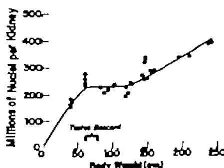


Figure 11

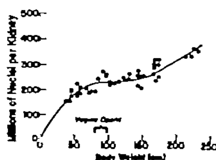


Figure 12

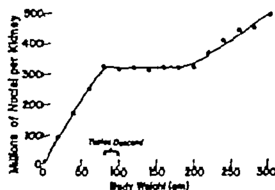


Figure 13

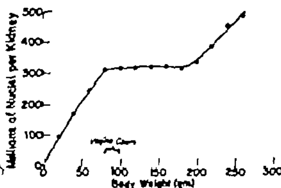


Figure 14

difference observed between the Series A and Series B rats Table 1 which summarizes the total nuclear counts of livers for normal male rats of Series A and Series B at different body weights shows that the nuclear counts of the livers of Series A rats of all body weights from 40 to 160 gm were significantly lower than those of Series B rats the difference decreasing as the animals got larger The possible bearing of these differences in total nuclear count on the occurrence or non-occurrence of a plateau in the nuclear count growth curve will be discussed later in the paper It should be noted that where the plateau did occur namely in males of Series B it began at puberty

PART II — EXPERIMENTAL MODIFICATIONS OF GROWTH

All the studies in this portion of the work were carried out on animals of Series B Since the growth plateau began at puberty it was suspected that the sex hormones might be responsible for the phenomenon. Furthermore, although the age at the end of the plateau had no obvious physiological significance it was postulated that a de-

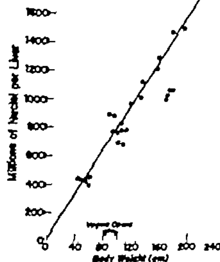


Figure 15

TABLE 1

Comparison of the total nuclear counts in the livers of normal male rats of series A and series B at various ages

Body weight	Millions of nuclei per liver	
	Series A	Series B
grams		
40	310	856
60	460	1139
80	615	1281
100	760	1323
120	915	1328
140	1070	1333
160	1220	1333
180	1370	1319
200	1520	1325
220	1675	1325

Average values estimated from the curve drawn through the scatter points there was so great scatter of weights as well individual values for total nuclear count that exact arithmetical averages would be somewhat meaningless. (This was not true for Series B rats, in which the scatter was very small, and exact average figures are given in the table.)

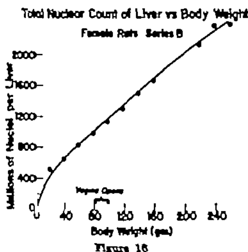


Figure 16

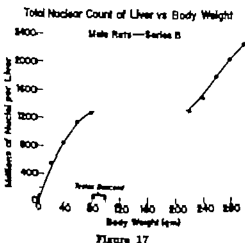


Figure 17

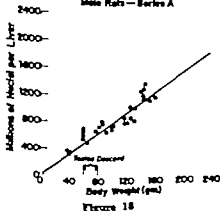


Figure 18

crease of hormone secretion might be occurring at this time or perhaps a decrease of organ susceptibility to the hormones effects. These postulates were tested as follows: a large number of male and female rats were gonadectomized at about 40 gm body weight, and then divided into two approximately equal groups Group I animals were followed up to body weight 300 gm without hormone replacement therapy — sets of four animals were sacrificed at body weight intervals of 20 gm, and kidney weights and total nuclear counts were determined. Group II animals began parenteral sex hormone therapy on the day after operation, males received a calculated replacement dose of 50 μg of testosterone propionate daily as described by Miescher Wettstein, and Tschopp ('36) females received a calculated replacement of 0 02 μg of estradiol benzoate daily as described by Miescher Scholz and Tschopp ('38) — sets of four animals were sacrificed at body weight intervals of 20 gm, up to body weight 120 gm. Those animals which survived to the latter weight were then transferred to a hormone dosage regimen consisting of ten times the previous "replacement dose, to see whether the natural plateau could be artificially prolonged

Findings

Organ weight. The kidney and liver weights of Group I and Group II rats did not differ greatly from one another or from those of normal rats. There were small differences which were not consistent as to direction in the various age groups.

Total nuclear counts For both sexes, in the case of kidney and for males only in the case of liver castrated animals (Group I) showed growth curves which no longer manifested the plateau phenomenon observed in normal animals. Hormone-treated castrates (Group II) showed plateaus which began at the same age as those of normal animals but which failed to terminate at the expected time persisting instead throughout the entire life-period covered by these studies, i.e. up to 240 gm body weight. Figure 19 depicts a comparison of the kidney nuclear counts for males: normals, untreated castrates

and hormone-treated castrates Figure 20 *depicts corresponding data for females* The differences between normals and untreated castrates were statistically significant in all animals weighing 80 gm or more ($P < 0.05$ in the 80 gm group and increasingly smaller in older animals). The treated castrates were statistically indistinguishable from normals in the body weight range 80–200 gm In 220 gm and 240 gm animals the treated castrates had significantly lower nuclear counts than the normals ($P < 0.05$)

Figure 21 depicts a comparison of the *liver nuclear counts for males normal* untreated castrates and hormone-treated castrates. *The differences between normals and untreated castrates were statistically significant in all animals between* 120–280 gm body weight ($P < 0.01$) The 300 gm animals showed no significant difference between the two groups (i.e. the curves converged again in old rats) The treated castrates were statistically indistinguishable from normals in the body weight range 60–220 gm In 240 gm 260 gm and 280 gm animals the treated castrates had significantly lower nuclear counts than the normals ($P < 0.01$) Castrated females of both Groups presented liver growth curves which did not differ significantly from one *another or from the curve of normal females*

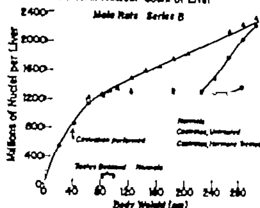


Figure 21

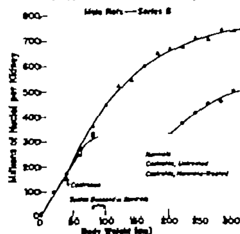


Figure 19

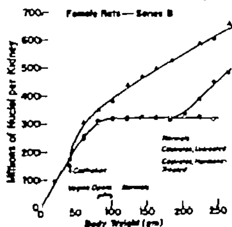


Figure 20

Total nuclear counts in castrates treated with "replacement doses of hormones of the opposite sex ("crossed-hormone therapy"). To determine whether the hormonal effects previously observed were specific for the isosexual hormone the following study was carried out: *16 males* and 16 females were gonadectomized at body weight 40 gm and were given replacement doses of the sex hormones of the opposite sex, beginning on the day after operation. Eight males were sacrificed at body weight 140 gm and the other eight at body weight 180 gm. Eight females were sacrificed at body weight 120 gm and the other eight at body weight 140 gm. Organ weights and total nuclear counts were compared with those of normal animals and with those of castrated

animals receiving isosexual hormone replacement therapy. The results are summarized in tables 2 and 3. It was found that, for kidney replacement therapy with either isosexual or contrasexual hormone produced an equal restoration to normal of the weight and nuclear counts of castrated animals. In the case of liver treatment of female castrates with male sex hormone produced a growth curve like that of nor

TABLE 2

Comparison of the effects on kidney growth of "crossed-hormone" therapy and isosexual hormone therapy

	140 gram rats		180 gram rats	
	Weight of one kidney	Millions of nuclei per kidney	Weight of one kidney	Millions of nuclei per kidney
	mg		*mg*	
	Males			
Castrates, no treatment	568	543	780	650
Castrates, iso-hormone treated	686	321	829	318
Castrates, treated with "crossed hormone"	623	320	846	315
Normal males	626	318	811	324
	120 gram rats		140 gram rats	
	Females			
Castrates, no treatment	641	434	720	464
Castrates, iso-hormone treated	551	320	602	318
Castrates treated with "crossed-hormones"	617	312	624	312
Normal females	538	318	610	321

Five animals in each weight group.
Eight animals in each weight group.

TABLE 3

Comparison of the effects on liver growth of "cross-hormone" therapy and isosexual hormone therapy

	140 gram rats		180 gram rats	
	Weight of the liver	Millions of nuclei per liver	Weight of the liver	Millions of nuclei per liver
	gm		*gm*	
	Males			
Castrate males, no treatment	6.654	1596	9.121	1769
Castrate males, treated with "crossed-hormone"	7.132	1469	8.267	1819
Normal females	6.103	1603	7.485	1970
Castrate males, treated with iso-hormone	6.683	1320	8.606	1326
Normal males	6.850	1333	9.259	1319
	90 gram rats		140 gram rats	
	Females			
Castrate females, no treatment	6.519	1252	7.293	1506
Castrate females, iso-hormone treated	5.618	1299	5.622	1500
Normal females	6.897	1307	6.103	1503
Castrate females, treated with "crossed-hormones"	6.179	1326	7.281	1247
Normal males	6.050	1329	6.850	1333

Five animals in each weight group.
Eight animals in each weight group.
Four animals in each weight group.

mal males and treatment of male castrates with female sex hormone produced a growth curve like that of normal females or more accurately did not affect the growth curve of the male castrates which was practically identical to that of normal females to begin with. It was evident that treatment of castrates of either sex with the male sex hormone induced liver growth typical of normal males. Thus, the normal sex difference in liver growth appeared to be related to the presence of androgen in the male and estrogen in the female rather than to any sex difference in receptivity of the liver cells to hormonal stimuli.

Total nuclear counts in castrates treated early with intensive sex hormone therapy Since intensive sex hormone therapy (ten times the "replacement dose) was able to produce an artificial prolongation of the growth plateau of the nuclear count curve, an attempt was made to induce a premature onset of this pleatu by giving intensive hormone dosage from the very first, immediately following castration. Sixteen males and 16 females gonadectomized at body weight 40 gm, were begun immediately on intensive hormone doses 500 μg daily of testosterone propionate for males and 0 2 μg daily of estradiol benzoate for females. Half of the animals were sacrificed at body weight 120 gm, and the remaining half at body weight 180 gm Organ weights and total nuclear counts were determined and compared with those of normal animals and those of castrates receiving replacement hormone doses (i.e. 1/10 of the intensive doses) Results are summarized in tables 4 and 5 The results for female liver were omitted since castration produced no changes. It was found that the animals which received intensive hormone dosage had values for kidney and liver weight and nuclear count quite similar to those of the other two groups. This suggested that the growth curves up to the age at the time of sacrifice had probably been similar- in other words, a premature onset of the growth plateau had not been produced.

Total nuclear counts in adrenalectomized animals To test the possibility that a non-specific effect of operation might have produced the results observed in castrated animals, a group of adrenalectomized animals were studied. This operation afforded an especially severe test of the effects of operation, since in addition to the trauma involved, the adrenals normally produce a variety of physiologically active substances, among them small quantities of both male and female sex hormones. Eight males and eight females were bilaterally adrenalectomized at body weight 40 gm and maintained thereafter by substitution of isotonic saline for their drinking water No hor

TABLE 4

Comparison of kidney growth in normals castrates treated with normal replacement doses of isosexual hormone and castrates treated with intensive doses of isosexual hormone

	120 gram animals		180 gram animals	
	Weight of one kidney	Millions of nuclei per kidney	Weight of one kidney	Millions of nuclei per kidney
	mg		mg	
Males				
Normal males	575	322	811	324
Castrates, treated with replacement doses	584	324	829	318
Castrates, treated with intensive doses	596	301	893	304
Females				
Normal females	538	318	691	315
Castrates, treated with replacement doses	551	320	773	316
Castrates, treated with intensive doses	540	297	735	[illegible]

Five animals in each weight group.
Eight animals in each weight group.
These animals had received replacement doses up to 120 grams body weight, and subsequently had received intensive doses (see text). It seems safe to assume that no great change occurred between body weight 120 grams and body weight 180 grams because of the change in dose, since both weights are on the plateau period.

monal replacement therapy was given. All 16 animals were sacrificed at body 180 gm. Kidney and liver weights and total nuclear counts were compared with those of normal animals (table 6) No significant differences were found between the normal and adrenalectomized animals.

PART III — KIDNEY HYPERTROPHY AFTER UNILATERAL NEPHRECTOMY

All the studies in this portion of the work were carried out on animals of Series B A number of animals were subjected to unilateral nephrectomy at approximately 160 gm body weight (i.e. 70–75 days of age) The operations were performed under ether anesthesia using conventional techniques and customary sterile precautions. For technical reasons the left kidney was removed in each case. A preliminary study revealed that there was no significant difference ($P > 0.3$) between the weights or total nuclear counts of the two kidneys (table 7) Following nephrectomy the animals were subdivided into four groups Group 1 — controls (no further treatment or manipulation); Groups II, III and IV — castrated at the same time

TABLE 5

Comparison of liver growth in normals, castrates treated with normal replacement doses of isosexual hormone and castrates treated with intensive doses of isosexual hormone

	130 gram animals		180 gram animals	
	Weight of the liver	Millions of nuclei per liver	Weight of the liver	Millions of nuclei per liver
	gm		gm	
Normal males	6.050	1329	9.359	1319
Male castrates, treated with replacement doses	6.340	1319	8.808	1328
Male castrates, treated with intensive doses	6.315	1274	8.198	1257

Five animals in each weight group.
Eight animals in each weight group.
These animals had received replacement doses up to 130 grams body weight and subsequently had received intensive doses (see text). It seems safe to assume that no great change occurred between body weight 130 grams and body weight 180 grams because of the change in dose, since both weights are in the plateau period.

TABLE 6

Comparison of organ growth in normal and adrenalectomized rats

	Male rats (180 gm)		Female rats (180 gm)	
	Weight of one kidney	Millions of nuclei per kidney	Weight of one kidney	Millions of nuclei per kidney
	mg		mg	
	Kidney			
Normal animals	811	324	691	315
Adrenalectomized animals	879	316	763	319

	Male rats (180 gm)		Female rats (180 gm)	
	Weight of the liver	Millions of nuclei per liver	Weight of the liver	Millions of nuclei per liver
	gm		gm	
	Liver			
Normal animals	9.359	1319	7.483	1970
Adrenalectomized animals	8.846	1261	7.551	1962

Five animals in each weight group.
Eight animals in each weight group.

nephrectomies were performed; Group II was then maintained without hormone therapy Group III was given daily replacement doses of isosexual sex hormone (50 μg daily of testosterone propionate and 0.02 μg daily of estradiol benzoate); and Group IV was given daily "intensive doses" of isosexual sex hormone (i.e. ten times the "replacement dose") Kidneys removed at nephrectomy were weighed and the total nuclear counts determined The animals were permitted to survive for 16 days and were then sacrificed. The remaining kidney was weighed, and the total nuclear count determined. Addis (47) had shown that 16 days was a period adequate for nearly complete compensatory hypertrophy as judged by organ weight.

Findings

Table 8 shows that control nephrectomized animals exhibited a marked increase in kidney weight, and no increase in nuclear count in these animals compensatory "hypertrophy" was due completely to true hypertrophy In untreated castrates the increase in organ weight was essentially the same and there was a moderate but significant ($P < 0.05$) increase in total nuclear count, in these animals hyperplasia accounted for a significant proportion of the compensatory "hypertrophy Supplementation of the castrates with "replacement doses of isosexual hormones completely prevented any hyperplastic response The results with "intensive doses of sex hormone were indistinguishable from those with replacement doses. Thus the effect of isosexual hormone on kidney hyperplasia in both males and females was purely inhibitory During the period of life when the kidney was fully receptive to hormonal inhibition of nuclear multiplication namely the plateau period normal compensatory "hypertrophy" after unilateral nephrectomy consisted purely of hypertrophy without significant hyperplasia Presumably at life stages before and after the plateau period when inhibition of nuclear multiplication was not effectively present, hyperplasia as well as true hypertrophy might occur during compensatory "hypertrophy The present report contains no data which bear directly on the latter point.

DISCUSSION

The data revealed a phenomenon which had not been described previously The normal growth of the kidney in male and female rats and of the liver in male rats (but not females) as expressed by nuclear counts, was attended by a virtual cessation of cellular multiplication in the mid-portion of the active growth period, although the weight of these organs increased in the well known progressive manner Castration abolished this phenomenon. In the case of kidney treatment of castrates with male or female sex hormone restored it; in the case of liver only male hormone had this effect. The experiments performed suggested that nuclear multiplication ceased when sex-hormone activity began, and resumed when it waned. The waning might be due to one or a combination of several factors: an absolute decrease in the amount of available hormone a relative

TABLE 7

Animal no.	Body weight	Kidney weight		Millions of nuclei per kidney	
		Right	Left	Righ	Left
	gm	mg	mg		
21	113	443	466	200	250
22	115	440	414	265	200
23	108	452	452	220	325
24	112	490	490	320	265
25	107	417	414	235	345
26	123	461	478	240	300
27	117	448	461	245	250
28	112	387	396	240	225
29	119	484	480	275	345
Average	113	447	449	249	269

The mean values for the nuclear counts of the right and left kidneys do not differ significantly (T 1 07 $P > 0.5$).

TABLE 8

Compensatory kidney "hypertrophy" in rats; comparison of the various experimental groups described in the text

	Weight of one kidney	Millions of nuclei per kidney
	mg	
Males		
At operation (unilateral nephrectomy)	700	315
At sacrifice		
Controls	1343	321
Castrates, untreated	1284	408
Castrates treated with replacement doses of isosexual hormones	1485	311
Castrates treated with intensive doses of isosexual hormones	1286	299
Females		
At operation (unilateral nephrectomy)	650	315
At sacrifice		
Controls	1039	388
Castrates, untreated	992	621
Castrates treated with replacement doses of isosexual hormones	1142	434
Castrates treated with intensive doses of isosexual hormones	919	393

Each group consisted of four or five animals.

decrease in the amount of available hormone as a result of increased organ mass or a decreased responsiveness of the target organs to hormonal stimuli. The present study did not permit a definite choice between these possibilities

There are several possible explanations for the difference in growth behavior of liver and kidney:

1 Female liver tissue was refractory to inhibition by either male or female sex hormone. This possibility was eliminated by the demonstration that treatment of female castrates with androgen produced a plateau phenomenon.

2 The presence of estrogenic hormone in females prevented androgen inhibition of nuclear multiplication. This possibility was not directly tested since no series was run with uncastrated females given androgen; however it seemed unlikely in view of the fact that estrogenic and androgenic hormones were equally effective inhibitors of nuclear proliferation in the rat kidney

3 Nuclear multiplication in liver was inhibitable by androgenic hormones but not by estrogenic hormones. This, of course is merely a restatement of the experimental findings rather than an explanation, the ultimate explanation is probably to be found at a cellular metabolic level involving the interaction of sex hormones with nucleoprotein and energy metabolism.

The results of the experiments in which intensive doses of replacement hormone were given from the first, following castration, were of theoretical interest. It was impossible to produce any significant inhibitory effect on nuclear proliferation in either kidney or liver before the time at which it was normally scheduled to occur nor to effect any significant reduction of the magnitude of nuclear count that was normally observed during the plateau period. This suggested that the organ had to be receptive to the inhibitory stimulus regardless of the magnitude of the latter or else no inhibition occurred. Probably related to this was the fact that male rats of Series A failed to show any nuclear count plateau at all. As was pointed out in the Findings the total nuclear counts of the livers in males of Series A were uniformly lower than those of males in Series B for reasons which were entirely obscure. Thus the ratio of cytoplasm to nuclei in rats of any given age was far higher in rats of Series A than in rats of Series B At the age when the growth plateau normally began (i.e. body weight 100 gm) the ratio of liver weight to nuclear count in male rats of Series B was 4 0 (mg per million nuclei); the same ratio in male rats of Series A was 6.9 Interestingly the ratio in Series B male rats at 200 gm body weight was 7.5 thus the ratio in male rats of Series A

which were at an age when the plateau was expected to begin, was the same as the ratio in male rats of Series B at the time the plateau was expected to end This may well explain the failure of a plateau to appear in rats of Series A: If as we postulated, a relative decrease of available sex hormone resulting from increased cytoplasm/cell number ratio could cause a waning of the inhibition of nuclear proliferation it would be only reasonable that the presence of an unduly high cytoplasm/cell ratio at the critical age (i.e. puberty) could prevent the plateau from appearing altogether These findings had attractive implications with respect to the problem of carcinogenesis: it had frequently been postulated that carcinogenesis entails a process of becoming refractory to a normal inhibitory stimulus. The present results demonstrated concrete examples of variation in local receptivity to a stimulus inhibitory to cell proliferation. Investigation of the reason why livers and kidneys of Series B rats between 40 and 100 gm body weight did not respond to inhibition while those of older rats did, and why the liver nuclear count curves of Series A males differed so strikingly from those of Series B might yield interesting clues to the analogous problem in carcinogenesis.

The results from the series of adrenalectomized animals showed that neither operative procedures nor non-specific hormonal effects were the cause of the observed phenomena, suggesting that the effect of androgen and estrogen on nuclear proliferation was specific.

The effect of androgenic and estrogenic hormones on renal hyperplasia in these animals was uniformly an inhibitory one. This was in agreement with the findings concerning the sex hormone effects during normal kidney growth. The data showed that by suitable manipulation of the experimental conditions, compensatory kidney "hypertrophy" after unilateral nephrectomy could be made to result in a predominantly hyperplastic kidney or a predominantly hypertrophic kidney Exploration of the inevitable differences in physiological function between these two types of kidneys might be very interesting especially with respect to the question of which is more advantageous to the animal.

SUMMARY

1 Study of the growth of rat kidney and liver in terms of total nuclear count revealed a previously undescribed phenomenon: during that period of a rat's life represented by the increase of body weight from 80 gm to 200 gm, there was, in the kidney of both sexes and the liver of males only a cessation of nuclear multiplication despite a continuing increase in organ weight. The cessation of nuclear multiplication began at the onset of puberty and ended at an age which had no obvious physiological significance. In female rats the growth of the liver in terms of both weight and total nuclear count was steady and progressive throughout life.

2. Androgenic and estrogenic hormones exerted inhibitory effects on nuclear multiplication in rat kidney and were apparently responsible for the natural cessation of nuclear multiplication (plateau) that occurred during normal kidney growth, since castration abolished the plateau and administration of sex hormones to castrates restored it. This inhibitory effect appeared to depend partly on tissue receptivity since it could not be artificially induced earlier in life than it normally appeared.

3. Androgenic hormones were capable of inhibiting nuclear multiplication in liver whereas estrogenic hormones were not. This inhibition depended importantly on tissue receptivity in two respects:

(a) It could not be produced earlier in life than it was normally scheduled to appear

(b) If the ratio of liver mass to liver cell number was above a certain figure (not yet clearly defined) the normal physiological doses of androgen would not inhibit nuclear multiplication (though larger doses might have been capable of doing so)

4 During the period of the animal's life when there was normally a cessation of nuclear multiplication in the kidney compensatory renal "hypertrophy" after unilateral nephrectomy probably consisted entirely of true hypertrophy with no hyperplastic component. Castration simultaneous with the unilateral nephrectomy resulted in a marked hyperplastic response in addition to true hypertrophy Treatment of the castrated animals with isosexual sex

hormones prevented this hyperplastic component from appearing.

LITERATURE CITED

Addis, T 1948 Glomerular Nephritis, Diagnosis and Treatment. Macmillan and Co., New York.

Brues, A. M., D R. Drury and M. C. Brues 1936 A quantitative study of cell growth in regenerating liver. Arch. Path., 22: 658–673.

Bucher, N L. R., and A. D. Glinos 1950 The effect of age on regeneration of rat liver Cancer Research, 10: 324–333.

Donaldson, H. H. 1924 The Rat. Wistar Institute of Anatomy and Biology Philadelphia.

Freudenberger, C. B., and F. I. Hashimoto 1937 A summary of data for the effects of ovariectomy on body growth and organ weights of the young albino rat. Amer Jour Anat., 62: 93–119

Kosterlitz, H. W 1944 Effect of dietary protein on liver cytoplasm. Nature, *154* 207–209.

Miescher K., A. Wettstein and E. Tschopp 1936 The activation of the male sex hormones. Biochem. Jour., 30 1970–1976.

Miescher K., C. Scholz and E. Tschopp 1938 The activation of female sex hormones. Biochem. Jour., 32: 1273–1280

Mirsky A. E. 1949 Personal communication.

Mirsky A. E., and H. J Ris 1947 Isolated chromosomes. Jour. Gen. Physiol., *31* 1–6.

Norris, J J J Blanchard and C. Povolny 1942 Regeneration of rat liver at different ages. Arch. Path., 34: 208–217

Pearce, J and R. W Gerard 1942 The respiration of Neurones. Amer. Jour. Physiol., *136* 49–65.

Histochemical Studies on the Interstitial Gland in the Rabbit Ovary

SARDUL S. GURAYA AND GILBERT S. GREENWALD
Department of Obstetrics and Gynecology University of Kansas Medical Center Kansas City Kansas

By employing polarization microscopy and histochemical methods, Claesson and Hillarp (47) identified cholesterol in the the birefringent granules of the interstitial gland of the rabbit ovary They described these granules as the "sterol granulae" and postulated that they were the precursor of the active estrogenic hormone. Claesson et al ('48) using biochemical techniques for lipids, have shown cholesterol (stored chiefly as cholesterol esters), phospholipids, acetal phospholipids and residual fatty acids as the main lipid constituents of the interstitial gland of the rabbit ovary According to these workers gonadotropic stimulation, probably mobilizes all the cholesterol stored as precursor and coincidently the content of phospholipid greatly increases This stimulation also causes a marked decrease in the residual fatty acid content. The detailed histochemical nature of the so-called sterol granulae was not studied by Claesson and his collaborators. Their studies were mainly directed towards finding cholesterol and its esters. The present histochemical studies were therefore, undertaken to determine the composition and changes of the sterol granules in the interstitial gland of rabbit ovaries removed at various times after gonadotropic stimulation. An additional objective of the present investigation was to throw light on the origin of the interstitial gland cells about which there is considerable controversy in the literature (see references in Brambell, '56)

MATERIAL AND METHODS

New Zealand giant white rabbits which were sexually mature, have been used. The animals were divided into three groups. The ovaries in the first group were from estrous rabbits and were used to study the histochemical nature of the lipids in the interstitial gland. In the second group, the ovaries were removed at different times (2 to 11 hours) after the intravenous administration of 100 i.u. human chorionic gonadotropin (HCG) These ovaries were used to investigate the mobilization of the lipids from the interstitial gland. Ovulation occurred approximately 10 to 11 hours after the injection of HCG In the third group 1 to 3 day postovulatory ovaries were included to examine the distribution and replenishment of lipids in the interstitial gland. Ovulation was also induced in this group by HCG administration. The recovery of eggs from the oviduct as well as the presence of corpora lutea were the criteria for ovulation.

The fixatives used for the histochemical studies of lipids included formaldehyde-calcium with and without postchroming (Baker 44 46 '56) formaldehyde-saline with and without postchroming (Baker 49) and 10% neutral formalin (Lillie '54) After fixation and subsequent post chroming, material was embedded in gelatine after Baker (46 49) The frozen gelatine sections were cut at 10 μ. The sections were washed briefly in water and stained by the following histochemical techniques for lipids Sudan black B in 70% ethanol (after Baker 44) and in propylene glycol after Chiffelle and Putt, '51 (cited in Pearse '60) for coloring lipids in general Nile blue sulfate technique for neutral and acidic lipids (after Cain, 47 48) Sudan III and IV method for neutral fats after Kay and Whitehead, 44 (cited in Pearse) the gelatine — Sudan III and

Population Council post-doctoral Fellow
Contribution from the Research Professorship in Human Reproduction. The research was supported, in part, by Grant [illegible] from the National Institutes of Health, United States Public Health

Sudan IV method after Govan 44 (cited in Pearse) for neutral lipids the Fettrot method (as described by Pearse) for neutral fats acid haematein technique followed by pyridine extraction control (after Baker 46) for phospholipids; Schultz method (as described by Gomori, '52) for cholesterol and its esters and performic acid-and peracetic acid Schiff techniques followed by controls (after Pearse, '60; Lillie '54) for lipids containing unsaturated bonds. Small pieces of fresh material were also treated with cold acetone and ethanol for 24 to 48 hours with three changes of each of the solvents. After extractions with these solvents the material in each case was treated with formaldehyde-calcium and dichromate-calcium to fix the lipids that resisted the action of acetone and ethanol; the frozen gelatine sections were prepared as usual. Sections were treated with various histochemical methods described above to determine the selective solubility of different lipids in cold acetone and ethanol. For investigating substances other than lipids some of the material was fixed in Carnoy Zenker and Bouin, embedded in paraffin and sectioned at 10 μ. For the study of RNA in the material fixed in Zenker and Carnoy the methyl green/pyronin techniques (after Jordan and Baker '55 Kurnick, '55 (cited in Pearse) followed by control sections treated with trichloracetic acid after Schneider 45 (cited in Pearse) or hydrochloric acid after Dempsey et al. '50 (cited in Pearse) were used Toluidine blue method (as described by Pearse) was also employed in the study of RNA with the above controls. The periodic acid-Schiff technique after Hotchkiss, 48 (cited in Pearse) was used for the demonstration of carbohydrates in the material fixed in Carnoy Zenker Bouin and weak Bouin (after Baker 46) with pyridine extraction.

OBSERVATIONS

In the rabbit ovary the interstitial glandular tissue is extensively developed and occupies all of the ovary except for the extreme cortical portions which constitute the tunica albuginea and which contain small follicles. The connective tissue is poorly developed and divides the glandular tissue into lobules of various sizes (fig. 1)

1 Lipids in the estrous ovary In estrous ovaries fixed in formaldehyde-calcium formaldehyde-saline and 10% neutral formalin and colored in Sudan black B the interstitial glandular tissue is loaded with sudanophilic lipid droplets of various sizes (figs. 1 2). The glandular tissue near the tunica albuginea is comparatively richer in such droplets than the medullary regions. The sudanophilic lipid droplets stain blue-black with acid haematein (fig. 3) followed by a negative reaction in pyridine extracted material (fig. 4) This indicates that they contain phospholipids. They stained deep pink with 1% Nile blue indicating the presence of neutral lipids. In 0 02% Nile blue, they become purple indicating some acidic lipids (phospholipids) Their deep orange-red color with Sudan III and Sudan IV and deep pinkish red with the Fettrot method also reveal neutral fats (triglycerides). The intensity of coloring with the red Sudan coloring reagents and with the Fettrot technique depends upon the amount of triglycerides present in these lipid droplets. Thus, the color varies between orange-red and red, revealing different concentrations of triglycerides in individual lipid droplets. The large droplets seem to contain more triglycerides than the small ones.

When the Schultz test is applied to gelatine sections of material fixed in formaldehyde-calcium or formaldehyde-saline or 10% neutral formalin, the sudanophilic lipid droplets of the glandular tissue appear as blue-green bodies of various sizes. The color of these bodies fades after some time. This positive reaction further reveals the presence of cholesterol and its esters in the lipid droplets of the interstitial glandular tissue. Their Schultz positive reaction does not appear in material extracted with acetone showing the solubility of cholesterol and its esters in acetone After acetone extractions, some phospholipids consisting of small lipid droplets continue to persist as revealed by their positive reactions in Sudan black B and acid haematein and their blue stain in Nile blue. The large lipid droplets are completely dissolved in acetone.

After extraction in ethanol, the material of the lipid droplets is completely removed as shown by their negative reaction in the

various techniques used. Similarly after pyridine extractions, they are completely dissolved as revealed by their absence in Sudan black B preparations. These solubility tests indicate the complete lipid nature of the lipid droplets of the interstitial gland.

The sudanophilic lipid droplets give a red-purple color with performic acid — and peracetic acid-Schiff methods, followed by a negative reaction in control sections treated with bromine water as recommended by Lillie ('54). Their positive reaction also does not appear in material treated with performic acid and peracetic acid reagents containing no hydrogen peroxide (Lillie '54). These reactions indicate that the lipids of the sudanophilic droplets are comparatively unsaturated.

None of the methods used for the study of nucleic acids and carbohydrates in paraffin sections stain the sudanophilic droplets which do not resist paraffin embedding after fixation in Carnoy, Zenker and Bouin. The cytoplasm of the interstitial gland cells is basophilic and stains with methyl green/pyronin and toluidine blue techniques, followed by a negative reaction in material treated with acids used for the extractions of RNA. This shows that the cytoplasm contains some RNA.

2. *Changes in lipids of the estrous ovaries after HCG administration. a. Preovulatory changes.* The animals in this group were sacrificed 2 to 11 hours after the injection of HCG. The interstitial gland in the ovaries of rabbits killed 2 to 5 hours after gonadotropic stimulation still contains appreciable amounts of sudanophilic droplets (figs. 7–10). However the mobilization of sudanophilic droplets from the cells has been initiated as evidence by their aggregation along the blood vessels of the medullary region of the ovary. The lipid droplets, however, do not enter the lumen. In the animals sacrificed after six hours there is a conspicuous reduction in the amount of sudanophilic droplets. The lipid droplets that remain in the interstitial gland continue to show positive reactions for phospholipids, triglycerides and cholesterol and its esters. By 8 hours after HCG injection, there is a further reduction in the amount of sudanophilic droplets (fig. 11). The lipid droplets which are still present, react positively for phospholipids and triglycerides. However the Schultz positive reaction is very weak at this stage and is seen only in the lipid droplets of certain outer regions of the ovaries which are still rich in them. At this stage the aggregations of lipid droplets along the blood vessels are very conspicuous (fig. 12). In rabbits killed 11 hours after gonadotropic stimulation there is more or less complete depletion of lipid droplets from the cells of the interstitial gland (figs. 13, 14). However some sparse lipid droplets are still present. These remaining lipid bodies react positively for phospholipids (figs. 15, 16) and triglycerides but not for cholesterol and its esters as revealed by their completely negative Schultz reaction. This indicates that 11 hours after HCG injection, there is nearly a complete mobilization of the lipid droplets composed of phospholipids, triglycerides and cholesterol and its esters from the interstitial gland. But cholesterol and its esters completely disappear from the interstitial gland of ovaries, in which there are newly ruptured follicles. The lipid droplets that aggregated along the blood vessels during their mobilization from the interstitial gland have disappeared *in situ*.

b. Postovulatory changes. The animals in this group were killed 1 to 3 days after ovulation was induced by HCG. In ovaries of rabbits, killed one day after ovulation, lipid droplets are present (fig. 17) which react positively for phospholipids and triglycerides but negatively for cholesterol and its esters. These newly formed lipid droplets arise in the same lobules of interstitial glandular tissue which were depleted of their lipid droplets during the preovulatory period by HCG. Three days after ovulation, the lipid droplets in the cells of the interstitial gland are, more or less, replenished (fig. 18). The appearance of such ovaries treated with various techniques for lipids is similar to that of the estrous ovaries. The lipid droplets react positively for phospholipids, triglycerides and cholesterol and its esters. With the Schultz test, the corpora lutea of the postovulatory ovaries used give a negative reaction indicating the absence of cholesterol and its esters in them.

3 Formation of interstitial gland. The differentiation of the interstitial gland has been studied in the ovaries treated with various histochemical techniques for lipids. For this part of the study the appearance of sudanophilic lipid droplets described in the interstitial gland is of considerable value in determining the source of the interstitial gland cells.

In the present material, two types of atresia of the follicles can be distinguished. One type of atresia is accompanied by a degeneration and dissolution of follicles In the second type of atresia, which is responsible for the formation of interstitial gland the various elements of the follicle become luteinized, depending on the stage of follicle development at the time of luteinization. Both types of atresia which affect the small, medium and large follicles seem to occur at all stages of the sexual cycle The interstitial gland originates from atretic oogonia, granulosa of preantrum atretic follicles and the theca interna and granulosa of atretic Graafian follicles in the adult rabbit ovary

In the ovaries of adult rabbits some atretic oogonia are transformed into interstitial gland cells by the formation of lipid droplets in their cytoplasm. For some time, the atretic oocytes continue to be visible in the tunica albuginea among the other young oocytes (figs. 1 3 5–8); gradually they are incorporated into the main interstitial glandular tissue Similarly the granulosa cells of some preantrum atretic follicles are seen to store lipid droplets in their cytoplasm (figs. 6 8). Initially lipid droplets are sparse and they react positively for phospholipids and triglycerides. At a later stage (figs. 5 7) when their amount is considerably increased they also react positively for cholesterol and its esters. After this transformation into interstitial gland such preantrum follicles, loaded with lipid droplets, form conspicuous areas in the ovaries. The ova of such follicles slowly regress and disappear whereas the zonae pellucidae persist for a long time Such newly formed areas of interstitial gland, located near the tunica albuginea, contain comparatively more lipid droplets, than the old ones lying towards the medullary region of the ovary A major part of the interstitial gland seems to be formed from this luteinization of the granulosa cells of preatrum follicles. In atretic Graafian follicles the theca interna along with the outer cells of membrana granulosa are transformed to interstitial gland as evidenced by the appearance of sudanophilic lipid droplets (fig. 1 7) These lipid droplets which consist of phospholipids and triglycerides to start with and of phospholipids, triglycerides and cholesterol and its esters later on, are not present in normal follicles.

DISCUSSION

Various histochemical techniques used in the present investigation demonstrate the considerable development and dramatic changes in the interstitial gland of the rabbit ovary In estrous ovaries, the interstitial gland is filled with sudanophilic lipid droplets of various sizes which consist of phospholipids triglycerides and cholesterol and its esters which are comparatively unsaturated. The large lipid droplets dissolve completely in acetone because of the presence of triglycerides and cholesterol and its esters along with phospholipids. Similarly the lipid bodies consisting of phospholipids and triglycerides dissolve completely in acetone as observed by Guraya ('57 '59a) in the oogenesis of birds. Cain ('50) has also stated that a small amount of triglycerides will cause phospholipids to dissolve completely in acetone Such a possibility has also been suggested by Lovern ('57) Here the problem arises why the small lipid droplets which also contain phospholipids triglycerides and cholesterol and its esters do not lose their phospholipids in acetone It is possible that the amount of neutral lipids in the droplets is so small that they are dissolved in acetone without affecting the presence of phospholipids. Such a possibility has also been suggested by Guraya during histochemical studies on lipids in the oogenesis of birds. These solubility tests indicate that the amount of different lipids (phospholipids triglycerides and cholesterol and its esters) varies in the lipid droplets of the interstitial gland The present observations suggest that the solubility tests for the selective extractions of different lipids are not reliable unless they are followed by histochemical staining techniques

The lipid droplets of the present investigations are identical with the sterol granulae identified in the rabbit ovary by Claesson and Hillarp (47). Claesson ('54a) using Sudan black B also described the sterol granulae of his previous investigations as lipid granules. With polarization optical and histochemical methods they (Claesson and Hillarp) demonstrated cholesterol or some related sterol in the granules. In a further study Claesson et al (48) employing biochemical techniques for lipids, recovered cholesterol phospholipids, acetal phospholipids and residual fatty acids from the rabbit ovary. According to these workers, the source of these different lipids is exclusively the interstitial gland since they removed the larger Graafian follicles before carrying out the biochemical analysis. The present observations have clearly revealed the histochemical nature of their so-called sterol granulae or "lipid granules *in situ*. It cannot be determined whether the fatty acids described by Claesson et al are derived from the triglycerides seen in abundance by the present histochemical methods.

After treatment with HCG the lipid droplets, which consist of phospholipids triglycerides, and cholesterol and its esters are depleted from the interstitial gland. From 10 to 11 hours after the injection of HCG when the large follicles have ruptured, sparsely scattered lipid droplets are still seen in some portions of the interstitial gland, adjacent to the tunica albuginea. These remaining lipid droplets do not contain cholesterol and its esters. Similarly the mobilization or depletion of sterol granulae (lipid droplets of the present investigations) has been studied by Claesson and Hillarp (47). By using biochemical techniques Claesson and his co-workers (Claesson Diczfalusy Hillarp and Högberg, 48; Claesson Hillarp and Hogberg, '53 Claesson '54b) stated that the applied gonadotropic stimulation probably mobilizes all the cholesterol stored as precursor and coincidently the amount of phospholipids greatly increases. But the present observations indicate that the phospholipids and triglycerides of lipid droplets in the interstitial gland also show a parallel reduction in their amount. The increase in the amount of phospholipi[illegible] biochemically by Claesson and h[illegible] orators is possibly due to the ap[illegible] of more lipoproteins in the ovary [illegible] gonadotropic stimulation. The mas[illegible] phospholipids of these lipoproteins cou[illegible] not be demonstrated with the histochemical techniques employed. With the techniques employed in the present paper it is difficult to say what role the lipid droplets play during ovulation but it is significant that they disappear from the interstitial gland. Claesson and his co-workers (references in Claesson '54a) have repeatedly stated that sterol granules act as precursors in the formation of estrogenic hormones. However Claesson presents no evidence for the formation of estrogenic hormones from the sterol granulae in any of his papers.

By employing physicochemical methods, Hilliard et al. ('63) have recently concluded that the interstitial tissue in the preovulatory rabbit ovary is the principal site of progestin synthesis. The rise in the progestin content of ovarian vein effluent after coitus or injection of HCG has been attributed to increased synthesis rather than the discharge of stored hormone. From the present studies on the lipid changes in the preovulatory as well as postovulatory ovaries it appears that the stored cholesterol and its esters in lipid droplets possibly are the precursor for the synthesis of progesterone and 20 hydroxy pregn-4-en-3-one reported by Hilliard et al. In the current study the significance of the association of cholesterol and its esters with other lipids such as phospholipids and triglycerides could not be determined. The experiments of Hammond and Marshall ('25) demonstrated that pregnancy was interrupted in the rabbit after extirpation of the corpora lutea. This suggests that the interstitial tissue by itself is unable to release sufficient hormones to maintain pregnancy. At the present time no function can be assigned to the preovulatory surge in release of lipids from the interstitial gland cells.

During the present histochemical studies on the rabbit ovaries two types of atresia i e degenerative atresia and (2) luteinized atresia, have been identified. Knigge and Leathem ('56) using histochemical tech-

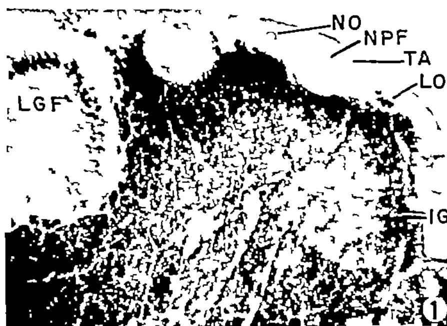
PLATE 1

EXPLANATION OF FIGURES

Figures 1 and 2 are microphotographs from gel tine sections of estrous ovaries fixed in formaldehyde-calcium, post-chromed in dichromate-calcium and colored with Sudan black B

1. *The interstitial gland (IG) which is loaded with lipid droplets, is* arranged in the form of lobules and is well organized. The tunica albuginea (TA) which contains normal oogonia (NO) normal pre-antrum follicles (NPF) and some luteinized oogonia (LO) forms narrow zone above the interstitial gland (IG) in the microphotograph. On the left side of the microphotograph are the theca and granulosa cells of luteinizing Graafian follicle (LGF) × 66

2. *Higher power view of the interstitial gland.* × 275


NO
NPF
TA
LO
LGF
IG
1

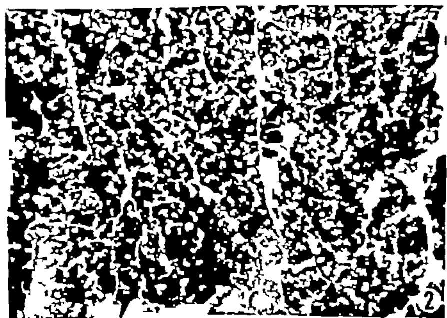

2

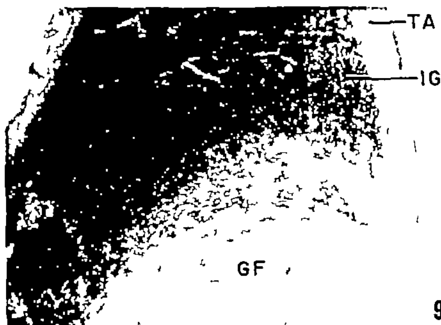
PLATE 1

EXPLANATION OF FIGURES

Figures 1 and 2 are microphotographs from gelatine sections of estrous ovaries fixed in formaldehyde-calcium, post-chromed in dichromate-calcium and colored with Sudan black B.

1 The interstitial gland (IG) which is loaded with lipid droplets, is arranged in the form of lobules and is well organized. The tunica albuginea (TA) which contains normal oogonia (NO) normal pre-antrum follicles (NPF) and some luteinized oogonia (LO) forms narrow zone above the interstitial gland (IG) in the microphotograph. On the left side of the microphotograph are the thec and granulosa cells of a luteinizing Graafian follicle (LGF) 66

2 Higher power view of the interstitial gland. × 275.


TA
IG
GF
9

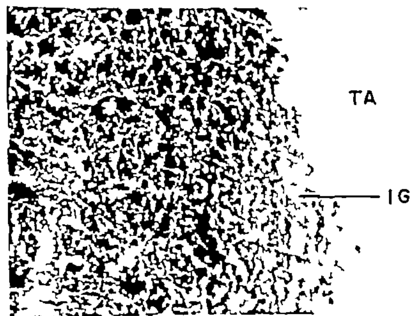

TA
IG
10

PLATE 7

EXPLANATION OF FIGURES

Figures 13 and 14 are microphotographs from gelatine sections of ovaries prepared as in figures 1 and 2. Ovaries were removed ten hours and 40 minutes after the injection of 100 I.U. HCG.

13 At ten hours and 40 minutes after gonadotropic stimulation there is, more or less, complete depletion of lipid droplets from the interstitial gland. However some sparsely scattered lipid droplets are still present. The left upper corner of the microphotograph shows the spot from where the follicle has ruptured. Some luteinized oogonia as well as normal oogonia are present in the tunica albuginea (TA). × 60.

14 Higher power view of the interstitial gland (IG) and tunica albuginea (TA) showing sparsely scattered lipid droplets which are left behind in the interstitial gland at ten hours and 40 minutes after gonadotropic stimulation. × 275.


TA
IG
13


TA
IG
14

PLATE 9

EXPLANATION OF FIGURES

Figures 17 and 18 are the microphotographs from postovulatory ovaries prepared as in figures 1 and 2. Ovulation was induced after the administration of 100 i.u. HCG.

17 One d y after ovulation, some new lipid droplets are formed in the same interstitial gland (IG) that was depleted of its lipid droplets during ovulation. The corpus luteum (CL) also contain some lipid droplets. × 66.

18 Three days after ovulation, showing the replenishment of lipid droplets in the interstitial gland (IG) As compared with the interstitial gland, the corpus luteum (CL) contains ery little amount of lipid bodies. × 66.


TA
IG
17


CL
TA
IG
18

observed the cells, and Tomes (1859) first described the function of the cells that Kölliker (1873) named and established as osteoclasts. When Wolff (1869 1884 1891 1892) and Meyer (1867) pointed out the relation of the form of a bone to its function it became clear that these bone cells were the engineers of the constantly changing architecture of bone.

Ollier (1858 1867 1889) and Macewen (1887 '07 12a, '12b) began the "battle of the periosteum and the less spectacular discussions of the endosteum. Ollier regarded the periosteum as the source of cells that could produce new bone and fatty marrow as capable of the production of bone tissue. Macewen, on the other hand felt that only bone itself was capable of producing more bone. Both recognized the epiphyseal growth plate as capable of producing a great deal of bone very rapidly

Much of the disagreement concerning the osteogenetic properties of periosteum stemmed from the fact that the periosteum was assumed to be the same at all times and under all circumstances. The periosteum was the structure that could be dissected from the surface of the bone and was defined in terms of its gross structure, usually without attention to the microscopic details. It was not realized that in a young animal what was lifted off as periosteum was by no means the same as what was lifted from an adult bone. Manipulations of pieces of this variable periosteal material under different circumstances and in animals of different ages was presumed to supply proof of what particular cells could do. Presumptions of cell behavior and cell activity from such data are of course unwarranted without serial microscopic studies. Although microscopic slides were prepared, they were interpreted without the realization that a cell does not remain the same throughout its life cycle. The spindle-shaped cells of the fibrous layer of the periosteum may become the plump osteoblastic cells of the inner layer as the bone grows in diameter or is activated for repair of a fracture (Pritchard '56)

Accurate information concerning the developmental stages and timing of bone growth in the chick embryo was supplied by Johnson (1883) while the cellular details were elaborated by Fell ('25) Comparable studies of the chick after hatching were carried out by Wolbach and Hegsted ('52) as a control for other work. Recent measurements of the rate at which the epiphyseal growth plate transforms into bone were reported by Sissons ('53) for rabbits and by Eeg Larsen (56) for rats. The first observations of the rate at which individual osteoblasts produce bone and osteoclasts destroy bone were made by Sandison ('28) and Kirby-Smith ('33) who used rabbit ear chambers To fully understand the cartilage cell physiology that precedes endochondral bone formation, it is necessary to measure the size of the cell at each stage of its development and to know how much matrix is associated with each cell at each stage The first such studies relating individual cartilage cells to their matrix were reported by Saaf ('50) in studies of articular cartilage

Changes of the growth cartilage are duplicated by the articular cartilage in producing endochondral bone if there is an epiphysis. Articular cartilage also contributes materials to synovial fluid The first to recognize this dual behavior of articular cartilage was Ogston (1875–76 1878) who pointed out that articular cartilage grows continuously giving rise on its bony surface to new bone although at a much slower rate than the epiphyseal growth cartilage and that it continuously sheds the surface layers into the joint space In many long bones of the chick a single cartilaginous end piece serves as both the articular cartilage and growth cartilage yet they can be distinguished by their histologic detail. Since it is easy to obtain accurately dated specimens of every stage of chick development, detailed studies were undertaken of the rates of growth of the humerus and of the tibia.

MATERIALS AND METHODS

The study was carried out on a strain of chicken produced by crossing a New Hampshire male with a Barred Rock female This strain has the advantage of being easily sexed at hatching, since all males have a white spot on the top of the

head, while the females are completely black.

Individual and serial measurements of total body weight and of length and diameter of long bones were made on 680 chicks of various ages from three days of incubation to 60 weeks after hatching

Growth-rate measurements for the prehatch stages were obtained by sacrificing 180 fertile eggs, ten each day from the third to the twenty-first day of incubation. The yolk sacs were clamped, cut, and weighed. Embryos were dissected free weighed, and x-rayed. Long bones were dissected, measured directly and x-rayed

Growth-rate measurements for the post hatching stages were obtained from 420 chicks. For statistical growth curves ten males and ten females were sacrificed daily from hatching through the first 21 days. An additional five males and five females were x-rayed daily to determine growth curves for each of the ten individual birds during the same 21-day period

Growth rates after 21 days were obtained by serial individual x-ray measurements on 30 additional birds taken at weekly intervals from three through 16 weeks at two-week intervals from 16 through 24 weeks and at monthly intervals from 24 to 60 weeks

Five male and five female one-day-old chicks each had a pin placed in the mid shaft of one humerus for measurement of differential growth in length at the two ends.

Thirty chicks were injected intraperitoneally with 5 ml of a saturated solution of alizarin red S in 5% glucose and sacrificed serially at daily intervals to determine the amount of growth at each end of the tibia by measuring the amount of bone added beyond the alizarin line. This was further checked by direct measurements to each end from the medullary opening of the nutrient canal

Measurements for determination of rates of growth were made directly from dissected bones from their x rays and from x rays of the live chicks

Measurements were made directly from x rays of length and midshaft diameter by using a Boley gauge that could be read to 0 1 mm. From the x-ray the total length and the length of the calcified shaft could be measured separately

X-rays of live chicks were taken by placing them in a spread-eagle position on their backs and tying them down to a piece of wall board with their limbs straight and in contact with the board. An 8 × 10" Kodak Blue Brand Medical film in a cardboard cassette was placed between the chick and the wall board The chicks relaxed when securely tied so that excel lent films could be made. As a result measurements comparable to those of dissected bones were possible on the humerus ulna, tibia, fibula, and metatarsal bones, and serial determination of bone length and diameter on individual birds could be made.

OBSERVATIONS

Figure 1 shows the rate of growth of the chickens by weight, figure 2 the rate of growth in length of long bones and figure 3 the comparable rate of growth in diameter of the midshaft of these bones

Particular attention was directed to the stages of growth during the first three weeks. Figure 4 is a composite curve based upon the summation of measurement of 40 chicks, sacrificed at the rate of five each day for eight days. There was a uniform and regular skew in the curve between the fifth and sixth days for each of the bones measured. Measurements from serial daily x-rays of individual chicks plotted in figures 5 and 6 demonstrated no skew To clarify this discrepancy every individual measurement for each humerus was plotted in figure 7 and the weights were similarly plotted in figure 8 (composite curve) and figure 9 (individual weights) It was clear that weight and bone growth curves for various chicks were almost identical during the first five days and that after the sixth day a wider range of variation developed between individual chicks. This was not related to sex because separate curves for males and females gave the same results

---

These chicks and eggs were obtained through the generosity of Dr Robert Little, U. S. Department of Agriculture Experimental Station, Beltsville, Maryland. The diet consisted of [illegible] produced and supplied by the Wilkins-Rogers Milling Co W ashington, D.C.

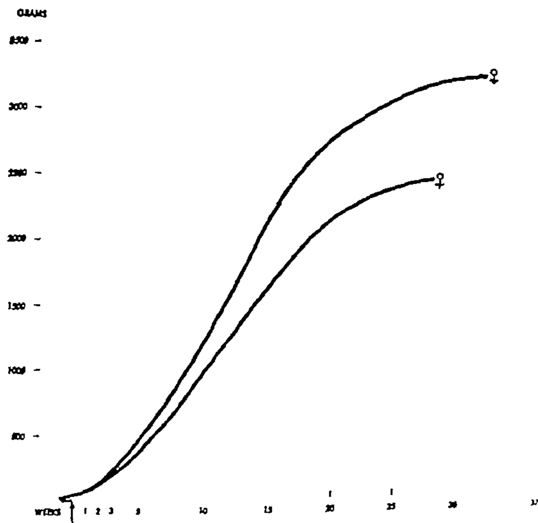


Fig. 1 Growth of chicks by weight

Most long bones of these birds showed no secondary centers of ossification. Exceptions however were the proximal end of the metatarsus and the proximal and distal ends of the tibia. In figure 10 are tracings of x-rays of the humerus tibia, and metatarsus. These show the appearance and growth of secondary centers of ossification. In the tibia a pair of secondary centers appear at the distal end at one week and the two became fused into a single center by ten weeks. The growth plate closed at 14 weeks. At the proximal end of the tibia a secondary center of ossification appeared at five weeks and the growth plate closed at 18 weeks. The humerus on the other hand had no secondary ossification centers. The secondary ossification center at the proximal end of the metatarsus was discernible a day or so after hatching, and the growth plate closed at 16 weeks.

The rate at which each individual growth plate adds to the length of the diaphysis of the humerus tibia and metatarsus is shown in figure 11 In figure 12 growth of the radius at the midshaft of the bone and of the medullary cavity is charted.

DISCUSSION

When the curves of figures 1 and 2 were compared with the similar curves of Latimer's ('27) white Leghorn chickens it became apparent that the New Hampshire Barred Rock cross used in this study

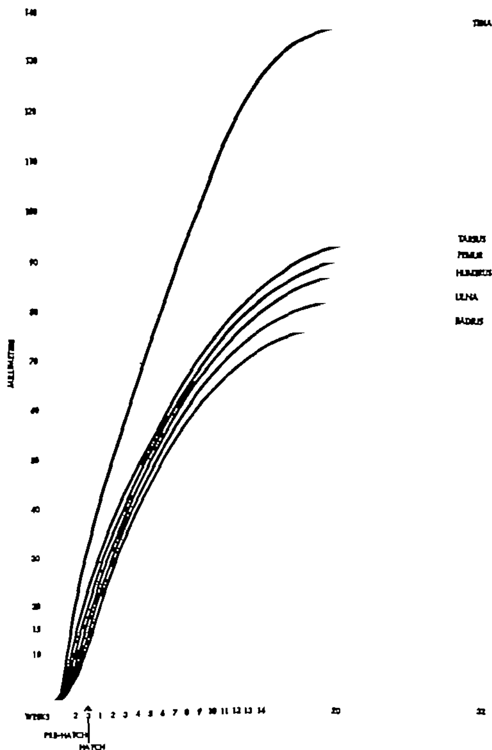


Fig. 2 Growth in length of long bones.

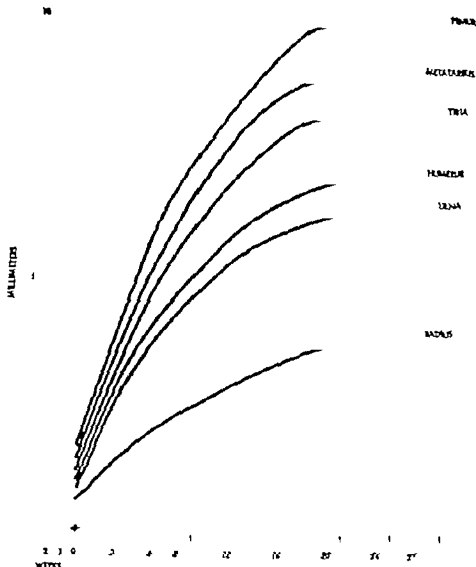


Fig. 3 Growth in diameter of midshaft.

was a somewhat shorter heavier and more rapidly maturing bird. Both males and females of this study averaged 500 gm heavier than those of Latimer and they matured with plateauing of the curves four to five weeks earlier at 15 to 18 weeks. The two strains are compared in table 1 Both strains showed the most rapid rate of growth in length of long bones during the first three weeks and attained a steady constant rate between three and four weeks.

It is generally believ have no secondary centers bony epiphysis in any of despite the fact that P ported "a true epiphy of the tibiotarsus tae Latimer de visible on extern and gave a tabl of ossification of the humerus and tarsometat

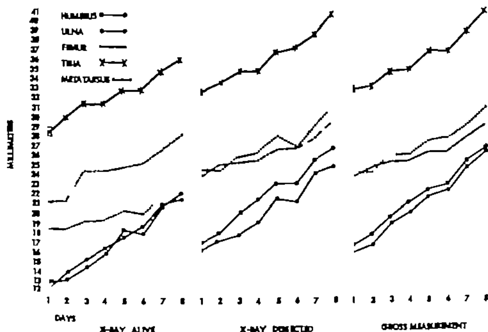


Fig. 4 Average bone growth — five chickens per day

TABLE 1

Rate of growth in length on bones between 3 and 14 weeks

	White Leghorn (Latimer)	New Hampshire-Barred Rock cross
Humerus	4.7 mm/week	5 mm/week
Femur	5.6 mm/week	5 mm/week
Tibia	8.6 mm/week	8 mm/week
Metatarsal		5 mm/week
Termination of growth	20 weeks	16 weeks
Final weight — male	2600 gm	3500 gm

ment that there was no distal epiphysis in the metatarsal and that the two epiphyses at the lower end of the tibia fused to form a single epiphysis. Fell's ('25) discussion of avian epiphyses was somewhat equivocal. While acknowledging Parsons report, she added that some believe the independently ossifying structures at the lower end of the tibiotarsus and upper end of the tarsometatarsus are fused tarsal elements not true epiphyses. She stated that in most avian long bones the epiphysis was small remains cartilaginous and could be distinguished only in histologic preparations and adds that with the exceptions mentioned above the epiphysis did not ossify independently of the diaphysis. It appeared to be her view that since the cartilage end pieces differentiate a well-defined "belt of cartilage having the histologic structures of the "intermediate cartilage that persists between the primary and secondary ossification centers of the mammal, this structure should be called an epiphysis.

Confusion seems to stem from the phylogenetic interpretation of chick embryology and from extension of the terms for the mammalian secondary centers of ossification to those chicken bones that do not have such centers. This confusion could be avoided if the term epiphysis (as in BNA nomenclature) is restricted to the secondary centers of ossification at the ends of long bones, while the histologically characteristic "belt of cartilage responsible for growth in length of a long bone is referred to as the growth plate. As Fell indicated growth plates were present at the ends of all the long bones but as Parsons indicated, there were no true epiphyses on the ends of most avian bones. Furthermore whatever the phylogenetic

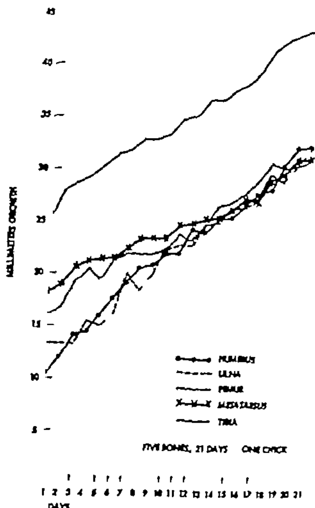


Fig. 6 Growth of individual bones from serial x-ray

interpretation may be a single cartilage model that develops an ossified diaphysis with a secondary center of ossification in the cartilaginous end of the model, separated from diaphysis by a growth plate becomes an epiphysis.

The serial x rays of this present study clearly demonstrated (as shown in the x-ray tracing of fig. 10) the appearance of a secondary center of ossification in the upper end of the metatarsal (tarsometatarsal) and upper and lower ends of the tibia (tibiotarsal) bones and only these bones separated from the diaphysis by a growth plate (histologically verified) which subsequently closed as the epiphysis became fused with the diaphysis between 14 and 18 weeks

Table 2, showing the embryonic stages of bone formation in the chick, was constructed from the summary of the literature presented by Romanoff and Romanoff ('60) Chondrogenesis began in various bone anlagen between 5.5 and 8.5 days of incubation. It took 2.0 to 5 5 days to complete chondrogenesis with the earlier anlagen progressing more slowly so that all cartilage models were complete at about the same time. Erosion of the model began centrally at ten days and extended through the middle third by 15 days and the marrow cavity occupied two-thirds of the shaft by 18 days. Erosion lagged so that at hatching a rather large cone of uncalcified cartilage still filled the metaphysis at each end. The same sequence of events was

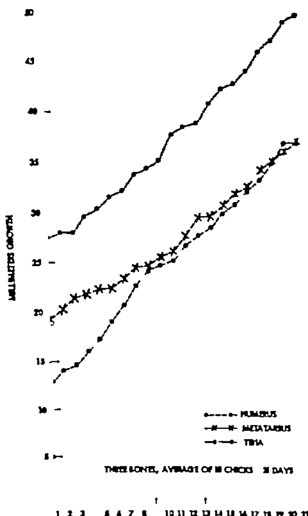


Fig. 6 Growth in length from serial x-rays.

observed in the present study so that the ends of the long bones at hatching were filled with a long cone of uncalcified car tilage This persisted until the fifth day after hatching when resorption without prior calcification became active By the twenty first day after hatching the cone was gone and the growth plate became comparable to that of the mammal. Despite this characteristically avian behavior a well-organized histologic growth plate was present at the base of the cone by the sixteenth embryonic day separating the articular cartilage from the metaphyseal cartilage cone

The behavior of the metaphyseal cone of cartilage, as described by Parsons manifested by incomplete cellular hypertrophy failure of calcification, persistence, and delayed resorption, could be correlated in time with the behavior of the yolk sac, as seen in figure 13. Measurements of the yolk sac weights of these chicks correspond generally with those in the summary of the literature given by Romanoff and Romanoff. It is noteworthy that active resorption of the cartilage cone began at the time of the final disappearance of the yolk at about six days. The first five to six days after hatching also constituted a

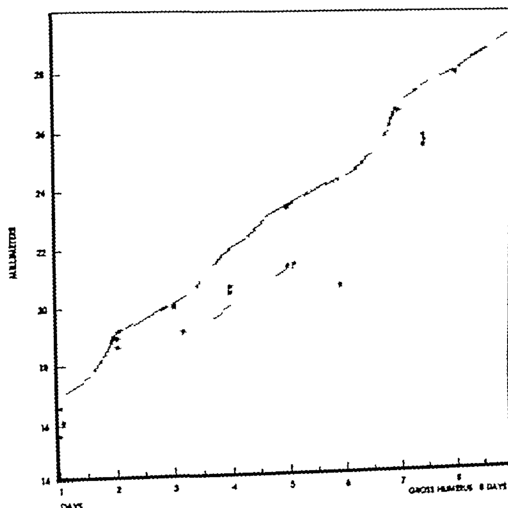


Fig. 7 Individual length of humeri.

period when the chicken was relatively undisturbed by temporary lack of food and water (as in shipping). During this period growth rates were virtually uniform, with scant individual variation. Furthermore, no endocrine changes have been reported during this period by Romanoff and Romanoff. Since the cartilage cone was present from the beginning of medullary cavity formation until the yolk sac disappeared, this temporary nonmammalian behavior of the cartilage may be imposed by the special very high sterol and phospholipid metabolism of yolk nutrition.

The skew in the statistical summation of growth rates for bones seen at five to six days in figure 4 also seemed to be related to the end of yolk sac metabolism and suggested release from yolk control. Furthermore, as seen in figures 5 and 6, the skew was not found in serial studies of the bones of individual birds. Since the growth rate scattergram for individual bones (fig. 7) began to spread out after the skew, it was interpreted as due to the appearance of individual variations resulting from the cross of the two breeds. The similar skew of the statistical curve for growth in weight with a similar spread in the scattergram of weights after the eighth day supported this interpretation. As the down began to be replaced by feathers, individual feather patterns and weight variations became apparent, as might be

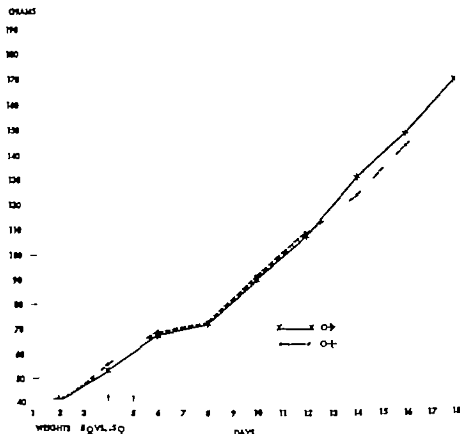


Fig. 8 Composite weight curve — first three weeks.

TABLE 2
Histogenesis of long bones

Days of incubation	Length of limb bud	Embryonic stage of bone formation
4.5	0 06–0.1	Axial proliferation with interzones.
5–6	0 06–0.1	Condensation to skeletal anlage (length = 3 × width) Chondrification.
6–7	0.15–0.2	Cartilage cell hypertrophy begins. Perichondrium develops.
7–8	0.2 –0.25	Osteoid sheath calcifies.
8–9	0.25–0.3	Slanted lamella added to surface of bone cylinder Clefts appear in interzones to become joint spaces.
9–10	0.5 –0 8	Cartilage erosion begins in midshaft.
12		Bone cylinder extends to bulbous ends.
14	1 5	
16		Cartilage cells become organized into zones and growth plate.
20		
21		Chick hatches.

Constructed from summary of the literature presented by Romanoff and Romanoff

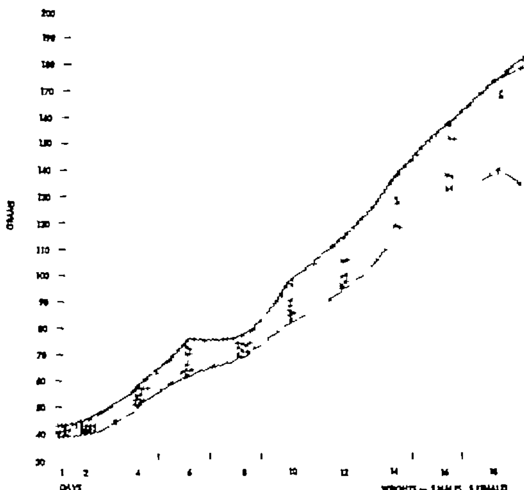


Fig. 9 Individual weight.

expected from the fact that the Barred Rock averages a full pound heavier than the New Hampshire Red when mature. These observations suggest that when nutrition is dependent on the yolk, it is uniform but after the yolk is gone, individual variations in the efficiency of digestion absorption and assimilation appear

The primary purpose of this study was to determine the rates at which bones grow in length and diameter for a subsequent correlation with the histology and calculation of the rates of performance of cartilage cells in the growth plate and of bone-forming cells in the periosteum. The rates of growth in length achieved by the growth plates are found in figure 11 These show the rate of growth at either end of the humerus, tibia and metatarsal bones The summation of each pair of curves with addition of the diaphyseal length at hatching and of the cartilaginous or bony epiphysis at each end will reproduce the curves for total bone length in figure 2. Table 3 was developed from these curves by reading the millimeters of added length attained during various time periods.

Since the average growth plate is 1 mm thick, the number of days or hours required for cartilage to develop from the beginning of proliferation through calcification to degeneration may be calculated. For rapidly growing ends like the upper tibia and upper metatarsal growth plates the life span or turnover rate is from two to three days. Comparable figures for small

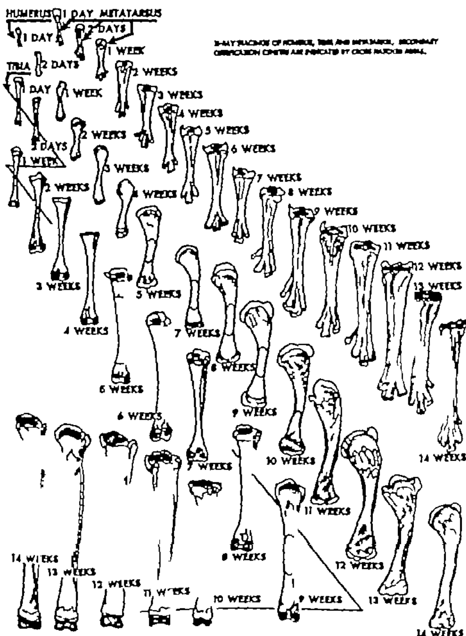


Fig. 10 Growth of individual bones from serial x-rays.

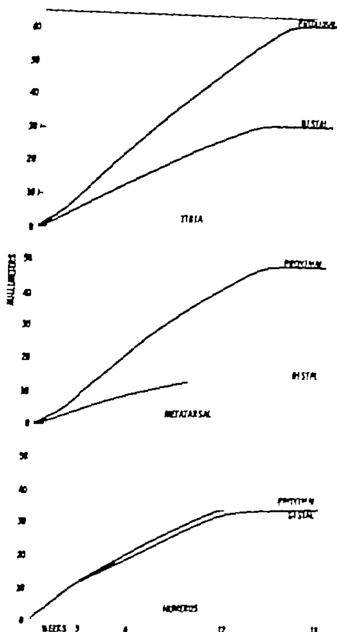


Fig. 11 Rate of growth of individual "Growth Plates.

intermediate-sized mammals are shown in table 4 From a direct inspection of the curve it was clear that growth plates associated with a bony epiphysis grew both faster and for a longer time than those without an epiphysis. This suggested that an increased rate of growth leads to changes in the center of this cartilage mass that engender the development of an epiphysis.

Similar data on the life span and turnover rates of the cortex may be calculated from the curves of growth in radius of the cortex. Uniform circumferential growth was assured without remodeling Both the outer diameter and the thickness of the

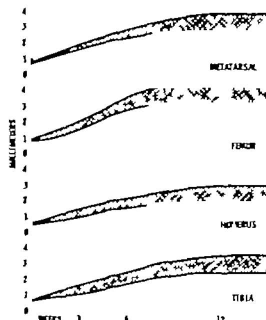


Fig. 12 Growth in radius of midshaft cortical bone and marrow cavity Thickness of cortex.

cortex were charted By measuring the number of days between the same internal and external diameter of the cortex, the life span of the piece of cortex was determined as given in table 5 During rapid growth the life span of the cortex ranged from one-half to three weeks. Once growth in diameter ceases the life span would be that of the animal, unless remodeling of the cortex occurred.

SUMMARY AND CONCLUSIONS

1 Studies were made of the growth of long bones of 680 New Hampshire male — Barred Rock female strain of chickens from three days of incubation to 60 weeks after hatching

2. The avian intramedullary metaphyseal cone of cartilage persisted until six days after hatching and then gradually receded between seven and 21 days.

3 During the first week, the growth of chicks and their long bones were virtually uniform; after this individual variations appeared.

TABLE 3

Incremental rate of growth of growth plates

Plate	Time period (week)	mm/Week	Turnover rate Days	Turnover rate Hours
Proximal metatarsal	0–2	2.5	2.8	67
	2–8	4	1.75	42
	8–12	3	2.3	56
	12–14	2.5	2.8	67
Distal metatarsal	0–6	1.5	4.6	112
	6–10	1	7	168
Proximal and distal humerus	0–3	4	1.75	42
	3–5	2.5	2.8	67
	5–10	2.4	2.9	70
	10–12	2	3.5	84
Proximal tibia	0–1	3	2.3	56
	1–2	4	1.75	42
	2–8	4	1.75	38
	8–14	4	2.3	42
	14–16	2	3.5	84
Distal tibia	0–2	2	3.5	84
	2–8	2.7	2.7	63
	8–12	2.2	3.2	63
	12–14	1.5	4.6	112

Growth plate thickness averages 1 mm.

$\frac{7 \text{ days} \times \text{plate thickness}}{\text{mm growth/week}}$ = duration of plate in days (i.e., turnover rate)

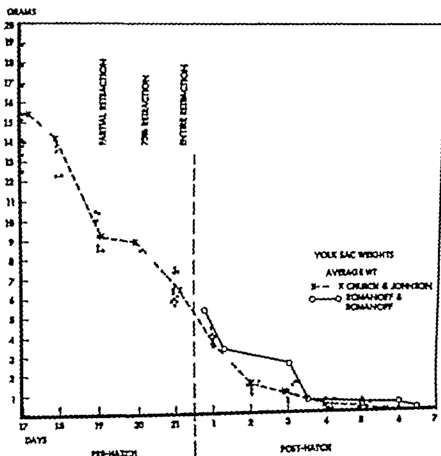


Fig. 13 Rate of absorption of yolk sac.

TABLE 4

Rate of turnover of epiphyseal growth plate

Author	Specie	Growth plate measured	mm/Day	mm/Week
Dubreuil, '13	rabbit	upper tibia	0.4	2.8
Leblond, '30	rat	upper tibia	0.15	1.05
		upper humerus	0.10	0.7
Payton, '32	pig	several @ 80 days	0.2 –0.5	1.4 –3.5
		several @ 150 days	0.05–0.18	0.35–1.26
Bisgard and Bisgard, '35	goat	lower ulna @ 32 days	0.36	2.52
		lower ulna @ 180 days	0.1	0.7
Sissons '53	rabbit, rat	lower femur @ 9 weeks	0.31–0.4	2.17
		lower femur @ 50 days	0.18	2.16
Eeg Larsen, '56	rat	upper tibia @ 1–4 weeks	0.3 –0.4	2.0 2.8
		lower tibia @ 1–4 weeks	0.23	1.6

TABLE 5

Mid shaft cortex duration — in weeks

Bone	Weeks when internal and external diameter are equal		Life span
Tibia	1	3	2
	3	6	3
	5½	10	4½
	6	30+	30
Humerus	0	0.8	0.8
	1.2	3	1.8
	3	6	3
	5	10	5
	6	30+	30+
Femur	0	1	1
	1	2.2	1.2
	3	4.5	1.5
	4	5.5	1.5
	5	7	2
	6	30+	30
Metatarsal	0	0.4	0.4
	1	1.5	0.5
	2	2.7	0.7
	3	4.2	1.2
	4	6	2.0
	5	7	2.0
	6	30+	30+

4 Resorption of intramedullary cartilage cones and individual variations in growth appeared after resorption of the yolk was completed at six days.

5 A growth plate appeared at the base of the intramedullary cartilage cone at each end of long bones at the sixteenth day of hatching and persisted until the end of growth at 30 weeks after hatching.

6. True bony epiphyses; i.e. secondary centers of ossification, developed in the proximal end of the tarsometatarsal bone and the proximal and distal ends of the tibiotarsal bones. They appeared soon after hatching and fused with the diaphysis between 14 and 18 weeks of age

7 Bony epiphyses developed in those bone ends that exhibited the most rapid rates of growth in length.

8. The life span of the growth plate of long bones with and without epiphyses was calculated it ranged between 1 75 and seven days

9 The life span of the cortex of the midshaft of the diaphysis was calculated and found to range between 0 5 and five days during rapid growth.

LITERATURE CITED

Belchier, J 1736a An account of the bones of animals being changed to red color by aliment only Phil. Trans. (London) 39 287 288.

——— 1736b A further account of the bones of animals being made red by aliment only Phil. Trans. (London) 39 299–300.

Bisgard, J D., and M. E. Bisgard 1935 Longitudinal growth of long bones. Arch. Surg. Chicago, 31 568–578.

Dubreuil, G. 1913 La croissance des os des Mammifères, III. Laccroissement interstitial n existe pas dans les os longs. C. R. Soc. Biol. Paris, 74 935–937

Duhamel, H. L. 1742 Sur le Developpement et la Crue des Os des Animaux Hist. et Mem. Acad. Roy Sciences (Paris) 2: 354–370.

Eeg-Larsen, N 1956 An experimental study on growth and glycolysis in the epiphyseal cartilage of rats. Acta Physiol. Scand., 38 1 77

Fell, H. B. 1925 The histogenesis of cartilage and bone in the long bones of the embryonic fowl. J Morph. and Physiol., 40: 417–459.

Gegenbauer C. 1864 Uber die Bildung des Knockengewebes. Jena Zeit f Med. and N t. Leipzig. Verlagom Wilhelm Engelmann. Vol. 1 pp. 343–369

——— 1867 Ibid. Vol. 3, p. 206.

Goodsir J and H. D. S. Goodsir 1845 Anatomical and Pathological Observations. MacPhail, Edinburgh.

Hales, S. 1727 Statistical Essays. London. Vol. I

Haller A. 1758 Deux Memoires sur la formation des Os. Lausanne, Switzerland.

——— 1763 De Partium Corporis Humani. Lausanne, Switzerland. I 75–241

——— 1767 De Ossium Formation. Chap. 32, Vol. 2, pp. 460–600.

Hunter J 1772 Quoted by Edward Howe, Transactions of Society for Improvement of Medicine and Chirurgery Knowledge Vol. II, London 1858, pp 277–288.

Johnson, A. 1883 On the development of the pelvic girdle and skeleton of the hind limb of the chick. Quart. J Micr. Sci., 23 399–411.

Kirby-Smith, H. T 1933 Bone growth studies—a miniature bone fracture observed microscopically in a transparent chamber introduced in the rabbit's ear. Am. J Anat., 53: 377–402.

Kolliker A. 1859 Handbuch der Gewebelehre der Menschen W Englemann, Leipzig, 3rd ed.

——— 1873 Die Normale Resorption des Knochengwebes und Ihre Bedeutung für die Entstehung der Typischen Knockenformen. Vogel, Leipzig.

Latimer, H. B 1927 Postnatal growth of the chicken skeleton. Am. J Anat., 40: 1–57

LeBlond, C. P G. W Wilkinson, L. F Belanger and J Robichon 1950 Radio-autographic visualization of bone formation in the rat. Am. J Anat., 86 289–341

Macewen, W 1877 The osteogenic factors in the development and repair of bone. Ann. Surg., 6 289–306.

——— 1907 The role of the various elements in the development and regeneration of bone. Proc. Roy Soc. London, 79. 397–396.

——— 1912a Discussion on development and growth of bone, normal and abnormal. British Med. J 2: 766–768.

——— 1912b The Growth of Bone. Observations on Osteogenesis. James Maclehose and Sons, Glasgow

Meyer H 1867 Die Architectur der Spongiosa. Reighart and DuBois (Eds.) Raymond's Arch. Anat. Physiol. und Wissenschaftliche Medicin.

Ogston, A. 1875–78 On articular cartilage. J Anat. Physiol., 10 49–74.

——— 1878 On the growth and maintenance of the articular ends of adult bones. J Anat. Physiol., 12 503–517

Ollier L. 1858 De la Production Artificielle des os au Moyen de la Transplantation du periosteo t des greffes osseuses. Comp. Rend. Soc. de Biol., 5 145–165.

——— 1867 Traité expérimental et clinique de la régénération des os et de la production artificielle due theu os seux, Vol. 1. Masson et fils, Paris.

——— 1880 De la Greff Osseuse Chez L'homme. Arch. de Physiol. Norm. et Path., I (series 5) 166–180.

Parsons, F G. 1904 Observations on traction epiphyses. J Anat. & Phys., 39 248–258.

Payton C. G. 1933 The growth in length f the long bones in the madder fed pig. J Anat., 66 414–425.

Pritchard, J J 1956 The osteoblast. In Biochemistry and Physiology of Bone G. H Bourne ed. Academic Press, New York, Chap. VIII.

Robins, C. H. 1849 Sur deux novelles especes delements anatomiques Compt. rend. et Mem. de la Societe de Biologie, Paris.

——— 1850 Tom. I, p. 149 Tableaux d' anatomie, Paris.

——— 1864 Journal de l'Anat. et de la Physiol. Bd. I, pp. 88–109

Romanoff, A. L., and A. N Romanoff 1960 The Avian Embryo. The MacMillan Co., New York

Saaf J 1950 Effects of exercise on adult articular cartilage. Acta Orthoped. Scand Supplement 7 pp. 7–84

Sandison, J 1928 Observ tions on the growth of blood vessels as seen in the transparent chamber introduced into the rabbit ear Am J Anat., 41 475–496.

Simons, H. 1953 Experimental determination of rate of longitudinal bone growth. J An t 87 228–236.

Tomes, J. 1850 Philosophical Tra sactions of Royal Society London.

Tomes, J and C. DeMorgan 1853 Philosophical Transactions, Royal Society London.

Wolbach, S. B and D. M. Hegsted 1952 Endochondral bone growth in the chick. A.M.A Arch. Path., 54 1–12.

Wolff, J 1869 Uber die Bedeutung der Architecture der spongiösen Substanz für die Frage vom Knochenwachstum. Centralbl. f d. med Wissench., 54: 849–851

——— 1884 Das Gesetz der Transformation der innern Architectur der Knocken bei pathologischen Veränderungen der äusseren Knockenform. Ber 0 d. Verhandl. d. deutsch Gesellsch. f Chir Lepiz., 21–23.

——— 1891 Ueber die Theorie des Knocken schwundes durch ver mehrten Druch und der Knochenanbildung durch Druckenlastung Arch. Klin. Chir., 42: 302 321

——— 1892 Das Gesetz der Transformation der Knochen. A Hirschwald Berlin

Morphological Changes Accompanying Fetal Resorption in the Golden Hamster

M. S. MILLAN STANLEY AND A. L. SODERWALL
Biology Department University of Oregon

The resorption of tissues is a common biological phenomenon. It may occur in living tissues as during the loss of the tail in the metamorphosing anuran, and is a typical method of disposal of dead but still attached tissues. The process probably differs greatly in these quite different situations. Fetal resorption is generally characterized by the disintegration of the decidua, placenta and fetus within the uterus, followed by the absorption of the products through the uterine wall. In many cases a portion of these substances is discharged through the cervix. Thus this process grades imperceptibly with abortion. This was discussed by Brambell ('48) who stated:

> "Both processes occur in most, if not all, mammals, but whereas abortion is the commoner in monotocous species, reabsorption is the rule in polytocous forms. Since abortion involves the abrupt termination of pregnancy whereas reabsorption does not, it being quite frequent for neighboring embryos to one which is dead to continue to develop and survive to term, the latter should be of survival value to mammals which produce several young at birth.

Fetal resorption has been reported to occur in many mammals, including the opossum rat mouse guinea pig Chinese hamster golden hamster wild rabbit cat, dog and man. Resorption of fetuses may be triggered by almost any conceivable means of severely damaging or killing the young including lethal mutations faulty maternal nutrition hormonal dysfunction antimetabolites, and quick freezing of the mother. The diversity of conditions known to induce fetal resorptions suggests that resorption is a common method of disposal of non-viable embryos irrespective of the cause of death. Although there have been many instances of resorption of term fetuses, resorption apparently occurs more commonly during the first two-thirds of gestation while pregnancies nearer term are more often terminated by abortion.

There are but few accounts of the fetal and maternal changes that accompany resorption. Morphological changes have been described in the rabbit by Henderson ('54) and in the mouse and the Chinese hamster by Fortuyn ('20 and '29). Corey ('33) has described resorptive changes in the near-term rat fetus killed by separation from the maternal blood supply.

Our interest in this problem was originally aroused by the occurrence of spontaneous resorptions in the senile hamsters in the local colony (Soderwall and Turbyfill, '57). It is hoped that morphological changes occurring during fetal resorption due to a known factor maternal ovariectomy may later be compared with those accompanying the spontaneous resorptions in the aged animals.

MATERIALS AND METHODS

The animals used in this study were from a colony of golden hamsters, *Mesocricetus auratus* Waterhouse that has been maintained by the Biology Department of the University of Oregon since 45. The females used were between three and ten months of age. The upper limit was necessitated by the high incidence of spontaneous resorptions among older animals. The males were selected for activity apparent vigor and copulatory behavior. Their age was not considered directly.

The females were bred between the hours of 9 and 11 P.M. Daily weight records were kept and the animals were tested for estrus response every night by placing them with a male for a few minutes. Any animal showing estrus response or any

Now at the Department of Biology Westminster College Salt Lake City Utah.

Hales S. 1727 Statistical Essays. London. Vol. 1

Haller A. 1758 Deux Memoires sur la formation des Os. Lausanne, Switzerland.

——— 1763 De Partium Corporis Humani. Lausanne, Switzerland. 1 75–241.

——— 1767 De Ossium Formation. Chap 32, Vol. 2, pp. 460–600.

Hunter J 1772 Quoted by Edward Howe Transactions of Society for Improvement of Medicine and Chirurgery Knowledge, Vol. II, London 1856, pp. 277–286.

Johnson, A. 1883 On the development of the pelvic girdle and skeleton of the hind limb of the chick. Quart. J. Micr. Sci., 23 399–411

Kirby-Smith H. T 1933 Bone growth studies—a miniature bone fracture observed microscopically in a transparent chamber introduced in the rabbit's ear. Am. J Anat., 53 377–402.

Kölliker A. 1859 Handbuch der Gewebelehre der Menschen W Englemann, Leipzig, 3rd ed.

——— 1873 Die Normale Resorption des Knochengewebes und Ihre Bedeutung für die Entstehung der Typischen Knochenformen. Vogel, Leipzig.

Latimer H. B. 1927 Postnatal growth of the chicken skeleton. Am. J. Anat., 40: 1–57

LeBlond, C. P C. W Wilkinson, L. F Belanger and J Robichon 1950 Radio-autographic visualization of bone formation in the rat. Am. J Anat., 86 289–341

Macewen, W 1877 The osteogenic factors in the development and repair of bone Ann. Surg., 6 289–306.

——— 1907 The role of the various elements in the development and regeneration of bone Proc. Roy Soc. London, 79 397–396.

——— 1912a Discussion on development and growth of bone, normal and abnormal. British Med. J 2 766–768.

——— 1912b The Growth of Bone. Observations on Osteogenesis. James Maclehose and Sons, Glasgow

Meyer H. 1867 Die Architectur der Spongiosa. Reighart and DuBois (Eds.). Raymond's Arch. Anat. Physiol. und Wissenschaftliche Medicin.

Ogston, A. 1875–76 On articular cartilage. J Anat. Physiol 10 49–74

——— 1878 On the growth and maintenance of the articular ends of adult bones. J Anat. Physiol., 12 503–517

Ollier L. 1858 De la Production Artificielle des os au Moyen de la Transplantation du perioste et des greffes osseuses. Comp. Rend. Soc. de Biol., 5 145–165.

——— 1867 Traité expérimental et clinique de la régénération des os et de la production artificielle des tissu os seux, Vol. 1 Masson et fils, Paris.

——— 1889 De la Greffe Osseuse Chez L'homme. Arch. de Physiol. Norm. et Path., 1 (series 5); 166–180.

Parsons F G. 1904 Observations on traction epiphyses. J Anat. & Phys., 39 248–258.

Payton, C. G. 1932 The growth in length of the long bones in the madder fed pig. J Anat., 66: 414–425.

Pritchard, J. J 1956 The osteoblast. In Biochemistry and Physiology of Bone. G. H Bourne ed. Academic Press, New York, Chap VIII.

Robins, C. H. 1849 Sur deux novelles especes delements anatomiques Compt. rend. et Mem de la Societe de Biologie, Paris.

——— 1850 Tom. I, p. 149. Tableaux d' anat omie, Paris.

——— 1864 Journal de l'Anat. et de l Physiol. Bd. I, pp. 88–109.

Romanoff, A. L., and A. N Romanoff 1960 The Avian Embryo. The MacMillan Co., New York

Saaf J 1950 Effects of exercise on adult articular cartilage. Acta Orthoped. Scand Supplement 7 pp. 7–84.

Sandison, J 1928 Observations on the growth of blood vessels as seen in the transparent chamber introduced into the rabbit' ear Am J. Anat., 41 475–496.

Simons, H. 1953 Experimental determination of rate of longitudinal bone growth. J Anat 87 228–236.

Tomes, J 1859 Philosophical Transactions of Royal Society London.

Tomes, J and C. DeMorgan 1853 Philosophical Transactions, Royal Society London.

Wolbach, S. B., and D. M. Hegsted 1953 Endochondral bone growth in the chick. A.M.A Arch. Path., 54 1 12.

Wolff, J 1869 Über die Bedeutung der Architecture der spongiösen Substanz für die Frage vom Knochenwachstum. Centralbl. f. d. med Wissench., 54 849–851

——— 1884 Das Gesetz der Transform tion der innern Architectur der Knocken bei pathologischen Veränderungen der äusseren Knochenform. Ber ü. d. Verhandl. d. deutsch Gesellsch. f. Chir., Leipz., 21–28.

——— 1891 Ueber die Theorie des Knochenschwundes durch ver mehrten Druch und der Knochenanbildung durch Druckentlastung Arch. Klin. Chir 42 302–324

——— 1892 Das Gesetz der Transformation der Knochen A Hirschwald Berlin

certain whether the better-preserved embryos succumbed more recently than the more resorbed ones, or if these observations result from differences in the rate of resorption.

A. The embryonic phase of resorption

Each implantation site that was classified as having been in the embryonic phase of resorption contained an embryo in which the differentiation into distinct tissues remained recognizable. In all cases the embryonic tissues evidenced some initial degenerative cytological changes. These changes were diffuse, there being no recognizable locus of autolysis.

In the least affected embryos, such as those in which the umbilical cord still maintained its normal placental relationship the cytological changes were barely detectable. These changes were confined to slight differences in nuclear texture and chromaticity These were most easily seen in the neural ectoderm. When degeneration was further advanced, particularly in the more highly differentiated embryos that had not been subjected to maternal ovariectomy until the tenth day of gestation, cytoplasmic changes were evident. This was particularly true in the undifferentiated mesenchyme where the cytoplasm was markedly reduced in volume and somewhat more dense.

Even in the best preserved embryos there was a general relaxation of the characteristic gross form. This was accompanied by a disorganization of the tissues which was particularly evident in the central nervous system (fig. 1)

Finally the embryo was reduced to an amorphous group of loose cells. This appeared to occur by the progressive loss of contact between formerly contiguous cells. As this process continued, it was accompanied by increasing pycnosis of the nuclear material. The nuclei of the cells of the exterior surfaces were often completely disintegrated. Erosion of the embryonic form, if evident, was always limited to these external surfaces. Leukocytic infiltration was also limited to the periphery

The amnion was maintained during the initial stage of the resorptive process although it often appeared to have been broken. The nuclei exhibited a moderate degree of pycnosis and the cytoplasm was shrunken and showed increased density The amniotic cavity was usually free from evidences of hemorrhage or intrusion of other heavily proteinaceous fluids.

The proximal vitelline sac was also intact during early resorption. In one case it exhibited nearly normal morphology including an extensive vascular supply with many apparently normal fetal red blood cells. However in the implantation sites where resorption was further advanced, the mesodermal components showed slight to marked degrees of degeneration. The characteristic convoluted outline was lost and the component tissues tended to separate. In the further resorbed implantations the mesodermal components were often missing and the nuclei of the endodermal components became pycnotic and the cytoplasm increased in density Gradually the structure was reduced to broken fragments of degenerating endoderm with an occasional bit of adhering mesodermal tissue. The exocoelomic cavity and the decidual cavity (vitelline cavity) contained varying quantities of a relatively homogeneous fluid that was apparently precipitated at fixation. This substance presented a staining reaction similar to that of hemoglobin. In a few instances maternal erythrocytes were observed. In some of the more advanced resorptive stages hemosiderin granules were apparent within this material.

During normal gestation a new uterine cavity begins to extend on the ninth day from the interembryonic spaces toward the mid implantational areas. This results in the gradual separation of the decidua capsularis from the muscularis by the very rapid proliferation of the newly re-formed endometrial stroma. This area is closely packed with small, young stromal nuclei which demonstrate a marked, though relatively uniform affinity for hematoxylin Gradually these lines of new nuclei separate along their longitudinal axes after first forming a core of cuboidal cells that then become the epithelial lining of the new uterine cavity In this study all tissue representing the initial stages of resorption were from animals sacrificed during the ninth to eleventh days of gestation when

the new uterine cavity normally forms. It is not possible to state conclusively whether this process was accelerated by the concurrent resorptive changes. However on the mesometrial aspect of the decidua basalis, degeneration and leukocytosis marked the area of the incipient new uterine cavity. These were not observed in the control tissues. Near the interembryonic areas the new uterine cavities were extremely irregular in shape, extending as slit-like or groove-like indentations often separating sheets of stromal tissue. In these areas new uterine glands were occasionally observed. In the embryonic areas the new stroma often formed sheath-like extensions into the new uterine cavity. These stromal sheaths like the rest of the new uterine cavity were lined with a simple, non-vacuolated epithelium that ranged from cuboidal to columnar in shape. Very often that part of the lining applied to the decidua capsularis was atropic or missing. This probably resulted from necrotic changes in the decidua capsularis proper.

Degenerative changes within the labyrinth were distinct and showed a consistent pattern. These changes are shown in figure 4. The allantoic vessels were filled with fetal erythroblasts. The fetal syncytium was reduced to a coarse firm membrane frequently containing hemosiderin granules. Cellular detail was usually obliterated. The surrounding lacunae contained the laked remains of maternal erythrocytes. As resorption progressed the pycnosis and the hematoxylin affinity of the fetal blood cell nuclei became very pronounced. Figure 3 presents the relationships in the normal pregnant female.

The area of most marked degeneration centered in the trophospongium. A cavernous lesion was found in the region normally occupied by the secondary giant cells (for this and other terminology relating to the normal hamster placenta see Orsini '54). This lesion extended into the decidua basalis and included most of the trophospongium. The few scattered cells within the lesion and those on the periphery exhibited advanced degenerative changes. A much smaller region of necrosis known as the junctional zone is normally present in this region as the result of giant cell activity. The maternal arterial spaces were obliterated. Evidence of masses of degenerated blood was found as regions of dense hemosiderin granule deposits. This vast discontinuity of tissue allowed the labyrinth to sag. It was often found displaced toward one end of the implantation region while the embryo and membranes were lodged toward the other end.

The edge of the decidua basalis bordering this lesion was also fragmented. The adjacent areas demonstrated a marked degree of chromatolysis. The decidual tissue was less affected toward the mesometrium. Often the upper half of the decidual tissue resembled in color and vacuolarity the glycogen-laden portions of the control tissues. However some nuclear pycnosis was usually present. Intact maternal erythrocytes were occasionally found in the lumina of the decidual blood vessels however the walls of these vessels were usually somewhat degenerate and leucocytic infiltration was often prominent. In one instance tertiary giant cells containing phagocytized material were found in the lumen of a sheathed artery. The decidual cells near the region of the incipient new uterine lumen were necrotic often exhibiting fragmented nuclei.

The primary giant cells of the reticulum exhibited but slight increases in nuclear density. Lysed maternal blood cells and hemosiderin granules were abundant. The remainder of the primary giant cell tissue was markedly distended with maternal blood (fig. 3). In some instances unlysed cells could be discerned and the leukocytes were always prominent. Although the endothelium was not readily distinguishable it is assumed that this blood was contained within sinus-like capillary beds. The accumulation of erythrocytes resulted from the relaxation of the capillary bed. Similar though less marked vascularity is present in the control tissue. The nuclear chromatin of these primary giant cells often differed little from the normal pattern. The cytoplasm could in some instances be discerned owing to the segregation of the erythrocytes into packets. Hemosiderin granules were often found outlining the cytoplasmic extensions.

The decidua capsularis showed degenerative changes marked by nuclear pycnosis and cytoplasmic vacuolization. Laterally it was supported by stromal proliferation but centrally this support was missing. This thin band of tissue was further eroded by the primary giant cells. As in the normal uterus an area of marked decidual destruction lay between these two tissues.

B Bag of cells phase of resorption

The most characteristic feature of the *bag of cells* phase of resorption (fig 5) was the prominent sac of giant cell tissue that enclosed the embryonic remains. The giant cell tissue at this phase was usually smaller in cross-section than that of the corresponding normal uterus but possessed a considerably thickened wall. No attempt was made to compute the volume of this tissue. In some cases the giant cell layer rather than decreasing its perimeters, had folded into convolutions and had thus attained a size that could be accommodated within the reduced uterine lumen. This tissue sac was generally broader toward the mesometrium, where the primary giant cells constitute a ring of tissue, known as the reticulum, around the edges of the decidua basalis. The secondary giant cells that are normally present in the central area between the trophospongium and the decidua basalis were not found. On its anti-mesometrial aspect, the giant cell tissue sac was often drawn to a point and frequently ruptured. In the more advanced resorptive sites the antimesometrial portions of the sac were collapsed against the labyrinth or the decidua basalis.

The contents of the giant cell tissue sac sometimes included broken remnants of the endodermal layer of the proximal vitelline sac. The embryonic remains consisted of loose cells with pycnotic nuclei and occasional wisps of cytoplasm. Tissue differentiation was completely obliterated. In one instance a few giant cell nuclei were found mixed with the embryonic remains. In the lesser resorbed sites hemosiderin granules were a prominent feature of the embryonic remains. Occasionally the labyrinth was found displaced into the giant cell sac The pattern that has been described was the usual one however distortion, apparently due to uterine movement, was often evident.

The decidua capsularis was sometimes eroded sufficiently to leave the giant cell tissue exposed to the new uterine lumen. This lumen had, in most instances extended the full circumference of the uterine cavity pinching the decidua basalis free from the muscularis. In these cases the new epithelium was extended to cover the denuded muscularis. In some sites the extent of the new uterine lumen was limited and the decidua capsularis remained relatively thick.

In one resorption site the decidua basalis remained attached in one lateral region and showed only minimal degenerative changes. The epithelization of the new uterine lumen had covered the antimesometrial aspect of the decidua basalis on the side where it remained attached to the uterine wall. There was no evidence of underlying decidual or stromal resurgence.

Stromal rugae and cones were found to extend into the new uterine cavity from various positions on the wall.

The suppurative process was quite marked in some instances. Leukocytes were found to have infiltrated into almost all degenerating tissues into areas of exposed muscularis and also into the newly proliferated stroma.

The labyrinth usually remained distinguishable, although the degeneration described earlier had progressed resulting in a tissue that appeared literally to have "fallen apart. The trophospongium was often unrecognizable. In a few places bits of decidua basalis retained continuity with the uterine wall and provided a marked contrast with the atrophy and pycnosis of the mesometrial portion of the decidua The more central and antimesometrial areas were chromatolytic and cellular detail had been obliterated.

C. Clot phase of resorption

In each case the clot was composed of a central area which was identified as the old decidua basalis. Outlines of vascul r and other histological structure remained in the least degenerate specimens There were no demonstrable cytological details

and no affinity for hematoxylin. This situation prevailed in the center of the clot and to varying degrees toward the periphery. Around this decidual mass there was a layer of cellular debris, thought to be the remains of the embryonic and placental tissues. Leukocytes were present at the periphery of the clot. Figure 6 shows a typical clot.

There was no longer any visible orientation of the uterine contents in relation to the mesometrial-antimesometrial axis. Since there was no connection with the uterine wall and since the clot was roughly spheroid, it is possible that it may have been rotated by uterine contractions.

Evidence of strong uterine contractions was found in the areas of the lumen denuded of the new epithelial lining. This lining appeared occasionally as cords or balls of relatively healthy tissue among the cellular debris that formed the outer layer of the clot (fig. 7).

Rugae, sheaths and other projections of endometrial tissue into the uterine cavity were greatly increased in size. There was a resulting wide variation in cavity shape between the different sites. The clots demonstrated molding corresponding to the shapes of the lumina. The stroma often approached 1 mm in depth and was differentiated into basal and compact regions. The development of the uterine glands was marked. The basal portion of the endometrial stroma and the connective tissue layer between the stroma and the muscularis was heavily laden with blood vessels. Fine vessels appeared in the compact stroma. Stromal sheaths in the inter-embryonic areas contained invaginating cores of muscular tissue. The stroma supported luxuriant columnar epithelium in which mitotic figures were abundant. These mitotic figures were often confined to the luminal extreme of the cells, while the interphase nuclei were always found in the basal region. In one instance vacuoles were noted near the free edge of the cells.

DISCUSSION

From this study it was hoped that morphological evidence of the key tissue affected by maternal ovariectomy producing resorptions could be obtained. Two striking observations were made. The first is that an extensive lesion occurs in the trophospongium. It is possible that this lesion is responsible for the death of the embryo. Obliteration of the maternal arterial spaces and the masses of lysed blood suggest that a failure of the placental circulation could have led to the death of the embryo. On the other hand, a separation of the placenta is normal at parturition and may represent a response to dead embryonic tissues. The second observation, that degenerative changes occur with great rapidity in the embryonic tissues, may suggest that the primary defect lies in the embryo.

The speed with which resorption occurs in the golden hamster is matched only by the rapidity of its organogenesis and the shortness of its gestation. In many instances the embryo and the membranes were reduced to cellular detritis in 48 hours. This contrasts with the five days required to reach a similar stage for rabbit implantations (Henderson, '54) and ten days for the disintegration of the near-term rat fetus (Corey, '33). The disorganization of the form of the tissues of the central nervous system has also been mentioned by Fortuyn ('29) and Henderson ('54). In both instances evidence indicated that the initial degenerative changes centered in the placenta. Fortuyn concluded that the unusual folding of the neural tissues resulted from the abnormal growth pattern in an altered environment before the death of the tissues. This appears more likely than does macerative disorganization due to the action of the uterine musculature. The external tissues of the embryo were not sufficiently disturbed to have been subjected to such violent action.

The persistence of the decidua during fetal resorption seems to be quite common. Meyer ('19) stated:

> One reason for prolonged preservation of the decidua no doubt lies in the fact that it, as a whole, or at least in part, retains vitality because it remains quite undisturbed in its vascular relations.

Henderson ('54) noted that although the decidua was the first tissue to show necrosis, it was the last to disintegrate

Although there are probably many factors at work in fetal resorption observations during this study suggest the importance of cytolysis and uterine contractions.

Henderson ('54) observed that during resorption, the antimesometrial epithelium and submucosa of the rabbit uterus was eroded. This is of particular interest since this tissue is not disturbed during parturition in this species. Kerr ('47) found that the uterine epithelium of the mouse died wherever it was in contact with necrotic cells. In the present study it was noted that denudation of the endometrial stroma was followed immediately by re-epithelization, except where necrotic tissues or fluids lay in contact with the uterine wall. In some instances, the new epithelium was found loose and degenerating. These observations indicate that cytolytic enzymes are present in necrotic, resorbing tissues.

Corey ('33) dealing with near-term rat fetuses, found evidence that lytic enzymes originated in the viscera, particularly the liver and the gastro-intestinal tract. This possibility had been suggested by Long and Parkes in '24. However dissolution of the tissues seemed to have proceeded uniformly in the young embryos observed in the present study No locus of autolysis could be found. It is likely that lytic enzymes are present in all necrotic tissues, but are found in great concentration in the digestive tract of well-differentiated organisms.

Changes in muscle tone after ovariectomy in the rat have been discussed by Frazer ('55) Typically he observed the contraction of the transverse muscles and the relaxation of the longitudinal muscles. Since the cessation of pregnancy is usually marked by the expulsion of the uterine contents some uterine contraction would not be unexpected in the uterus of the oöphorectomized female. Although no attempt was made here to evaluate the muscle tone or motility of the experimental uteri, histological examination of the uterine contents during the *clot phase* offered ample evidence that these had been subjected to squeezing and kneading At the less affected loci the embryo and the labyrinth were usually displaced toward the interembryonic areas. In the later resorptions the epithelial lining of the new uterine lumen was often torn from the stroma and mixed with cellular debris. Uniformity of thickness of the detrital layer of the clot, along with certain deformations suggest that it had been subjected to rolling and molding against the stromal sheaths. This hypothesis of the role of uterine action is supported by many accounts of embryonic maceration such as that given by Corey ('33)

SUMMARY

The morphology and histology of fetal resorption in the golden hamster is described. The changes occurring during this process are divided into three phases.

During the *embryonic phase* specific tissue characteristics remain evident. Disintegration proceeds uniformly and is accompanied by pycnosis of the nuclear material and increased cytoplasmic density Extravasated maternal blood engorges the exocoelom the vitelline (decidual) cavity and the primary giant cell tissue. A cavernous lesion replaces a major portion of the trophospongium and associated tissues.

The *bag of cells phase* is marked by the reduction of the embryo and membranes to an amorphous mass of cells contained within a distinctive layer of giant cell tissue.

The *clot phase* is typified by a uterine lumen containing the chromatolysed detached decidua basalis surrounded by a loose layer of cellular detritus infiltrated by leukocytes. The shape of the clot and the presence in the clot of bits of apparently healthy endometrium suggest that uterine contractions play a major role in the disintegrative process. Resorption occurs so rapidly in this species that the clot phase may be attained within 24 hours.

LITERATURE CITED

Brambell, F W Rogers 1948 Prenatal mortality in mammals, IX. The removal of dead embryos. Biological Rev 23, 399–402

Corey E. L. 1933 The maceration and resorption of fetuses in the rat. Anat. Rec 56. 195–200

Fortuyn, A. B. Droogleever 1920 The involution of the placenta in the mouse after the death of the embryo. Arch. Biol., 30, 323–335

——— 1929 Prenatal death in the striped hamster Arch. Biol., 39 583–605.

Fraser, J. F. C. 1955 The mechanism of foetal loss after pregnant rats are spayed. J. Physiol., 130: 253–256.

Henderson, Megan 1954 Foetal regression in rabbits: experimental studies in histolysis and phagocytosis. Proc. Roy. Soc. B., 142: 88–112.

Kerr, T. 1947 On the effects of colchicine treatment of mouse embryos. Proc. Zool. Soc. Lond., 116: 551–564.

Long, C. N. H., and A. S. Parkes 1924 On the nature of foetal re-absorption. Biochem. J., 18: 800–805.

Meyer, Arthur William 1919 Uterine, tubal and ovarian lysis and resorption of conceptuses. Biol. Bull., 36: 283–306.

Orsini, Margaret Ward 1954 The trophoblastic giant cells and endovascular cells associated with pregnancy in the hamster Cricetus auratus. Am. J. Anat., 94: 273–331.

Soderwall, A. L., and C. L. Turbyfill 1957 Fetal resorption in senescent female golden hamsters, Mesocricetus auratus Waterhouse. Ore. Acad. Sci. (unpublished data)

PLATE 1

EXPLANATION OF FIGURES

1 Portion of a transverse section of a resorbing embryo removed on the tenth day of gestation. The mother was ovariectomized 24 hours previously. Note the abnormally convoluted neural ectoderm (A). The amnion (B) is relatively unchanged. The mesodermal components of the proximal vitelline sac (C) show greater change than does the endodermal portion. The amnionic cavity (D) is conspicuously free of precipitated fluids when compared with the vitelline or decidual cavity (G) and the exocoelomic cavity (F) (69 ×).

2 Transverse section through normal placenta t the tenth day of gestation (69 ×).

C, Proximal vitelline sac
E, Giant cell
G, Decidual or vitelline cavity
J, Allantoic vessel
H, Trophospongium
I, Labyrinth
K, Maternal blood space

3 A highly magnified (960 ×) view of the primary giant cell tissue of a resorbing implantation site. Note the maternal erythrocytes that distend the tissue. It is assumed that these lie in sinus-like capillary beds. The suggestion that they might represent hemorrhage into the giant cell tissue has not been disproven.

L, Giant cell nucleus
M, Giant cell cytoplasm
N, Maternal erythrocytes

4 View of portion of a transverse section of the placenta of a resorbing embryo. The mother was ovariectomized on the ninth day of gestation and sacrificed 24 hours later. The proximal vitelline sac (C) is no longer distended, but ags into the uterine cavity. Both the decidual (G) and the exocoelomic (F) cavities contain precipitated fluids. The trophospongium (H) is nearly consumed by degenerative lesion (47 ×).


A
B
C
D
GL
1
G
N
L
3
G
P

Axial tissue may be stained a medium gray *by increasing impregnation of sections* beyond the optimum for epithelial tissue (fig. 10) *Numerous small* deeply stained granules appear in the cytoplasm of the cells of the proximal *convoluted tubules* (fig 1) Nerve fibers are occasionally stained in extraglomerular regions reticulin collagen fibers and basement membranes are unstained in all parts (fig. 1) Erythrocytes are unstained (fig. 4)

Form and distribution of glomerular epithelial cells

Where epithelial cells are shown most extensively as in tangential sections through the periphery of lobules (fig. 3) the cell body appears sharply demarcated from *branching processes* The nucleus is ovoid and set centrally within a narrow cytoplasmic investment but may appear eccentrically placed in cell bodies which include portion of a process in the plane of section (fig 10)

The inner surfaces of the cells conform to the curvature of the basement membrane of the capillary to which they are applied (fig 5) the interface being most clearly demarcated in thin sections When epithelial and endothelial cells are included in a cross section of a capillary the *epithelial cell body frequently* occurs on the outer surface (considered in relation to the lobule embracing the capillary) and the endothelial cell nucleus on the opposite inner wall (fig. 5) This arrangement is reflected by the appearances of longitudinal sections of outer (fig 3) and inner (fig 4) capillary walls.

Except in the basal regions of the glomeruli epithelial cell bodies are concentrated near or upon the surfaces of lobules. *This is most clearly shown by* thicker sections owing to the inclusion of a relatively *larger number of* cell bodies (figs 7–10) but is sometimes obscured by the irregularity of lobule surfaces and the occurrence of cell bodies in minor crevices (figs 8 13) The superficial distribution of epithelial cell bodies helps to delineate the lobules and the inter lobular spaces (fig 7) formed at the level of the primary branches of the afferent arteriole as well as giving greater *distinctness to axial tissues* (figs 4 7 10) These relationships are brought out by sections of the lobule at successively deeper levels. Sections through the outer surfaces of the peripheral capillaries (fig. 8) show epithelial cell bodies on these outer walls and the most superficial of their ramifying processes Deeper sections cut so as to exclude axial tissue (fig 9) contain an abundance of epithelial cell bodies and reveal the complexity of *their branching processes* Sections through the central region of the lobule (fig 10) show a concentration of axial tissue emphasized by a peripheral arrangement of capillaries and epithelial cell processes

Axial tissue

Axial tissue is in general distributed towards the central regions of lobules ften with an apparent longitudinal orientation (figs 2 4 *and* 7) *at some points it bord* the capsular chamber often through int r lobular clefts (fig 12) *Most often it* shown in direct contact with *one or more* adjacent capillary lumens (figs 2 10 and 13) or is separated from these by m jor epithelial cell processes frequently both conditions occur in the same cross-section (fig 10) There is thus no simple relation between *the axial tissue* and the capillaries around it and its central position does not *imply that it forms a central core* or stalk for all adjacent capillaries. Counterstained preparations show that ovoid nuclei are most numerous in axial region (figs 2 5 6) some clearly belonging to endothelial cell bodies The cytoplasm f the axial cells is barely distung ishable fr m non argentophil *intercellular m te l which i* continuou with basement mem ane of *outer capillary walls In h il impreg* nated sections a faintly st i e granular *material* occurs around u l ules Th outline of the cells det i i th way i irregular with process xte ding int the intercellular substanc d to the lumen of the adjacent capill ri All ob servations suggest that the d tinctive *fea tures* of axial regions *accent d* in thick sections *could be produc d* the localiza tion of endothelial tis ue upon the axial surfaces of capillary wall Variations are attributable to the effect of section planes upon convoluted refl cted and probably branching capillaries

Epithelial cell processes on outer and axial capillary walls

All glomerular epithelial cells show free extensions of the cell bodies. These processes are of variable length and branch profusely (figs 3 9) Many deeply stained rods or filaments cut lengthwise or in cross section have no visible connection with cell bodies (fig. 6) Intermediate forms, serial sections and constant relations to capillary walls and axial tissues indicate that these are all fragments of epithelial cell processes. No capillary whether occurring superficially or deeply in the lobules is without accompanying epithelial cell processes

Processes of fine or medium caliber may originate abruptly from cell bodies and extend over adjacent capillary walls more or less at right angles to the long axis of the capillaries (figs. 3 5) these are direct annular branches. Cytoplasm is also produced more gradually into thicker processes or dendrites (figs. 3 8 9) which are usually directed lengthwise along the outer capillary walls thus contributing to the peripheral delineation of the lobules (figs 7 9) The dendrites may produce annular branches immediately or after irregular branching When annular branches which surround a considerable portion of the capillary wall penetrate into the axial regions the annular arrangement is lost.

Both dendritic and annular branches of the outer capillary wall are closely applied to the basement membrane (fig. 5) The annular branches are more or less evenly spaced and give a characteristic ladder pattern (figs. 3 8 9) or if a capillary is cut longitudinally parallel rows of processes are seen in cross section (fig. 9) Alternation of annular processes of different caliber may be seen following the interdigitation of branches from the same or adjacent epithelial cells. There is no overlap of branches where the epithelial cells are clustered the formation of processes is restricted or apparently absent on adjacent surfaces (fig. 13)

Epithelial cell processes extend into axial regions close to the clustered cells (figs 2 4 6 13) Contact between axial and epithelial cell processes is often apparent in heavily impregnated sections.

The axial epithelial cell processes originate as extensions of annular branches (fig 2) or may be formed directly from cell bodies (fig. 13) They are often varicose (figs 11–13) in contrast to the smooth annular processes of the outer capillary wall. Instead of an annular arrangement they form a network (fig. 11) with meshes of fairly uniform dimensions attributable to the regular penetration of the processes between the axial cells (figs. 4 6)

DISCUSSION

By this silver procedure the glomerular epithelial cell is shown to be a branching structure forming direct and indirect annular branches which run parallel and equidistant around the wall of the glomerular capillaries at right angles to their long axes

The pedicels observed in electron microscopy probably extend between the annular branches The localization of epithelial cell bodies indicates that lobulation is a normal feature of the glomerular tuft and the opposed relation of epithelial and endothelial cell bodies which is accentuated by the present techniques implies the existence of significant differences of behavior between peripheral and axial capillary walls. Differences in deposition and disposal of ferritin particles in these two regions have been recently reported in the electron microscope studies of Farquhar Wissig and Palade ('61)

Our staining methods are not adapted to provide evidence for a third type of glomerular cell Consequently our observations emphasize the contribution of endothelial cells or cells resembling them to axial tissue. Collagen and reticulin are absent from the region Axial intercellular substance is not distinguished by these silver techniques from basement membrane material and is probably identical with it If this were so the finding that epithelial cell processes penetrate deep into the axial region is further evidence for the endothelial nature of the cells in this region and is to be expected in view of electron microscopic observation of the development of the human glomerulus (Kurtz, '58) which demonstrated close relation between endothelial cells and epithelial cell processes. Basement membrane was first formed in

PLATE 1

EXPLANATION OF FIGURE

All figures are from sil er preparations; figures 2, 5 6, 12, 13 are counterstained with Ehrlich s hem toxylin and picric acid

1 A glomerul with surrounding convoluted tubules Glomerular epithelial cells and processes tain black; their nuclei are un tained The cells of the convoluted tubules contain argentophil cytoplasmic granules. 15 µ × 300

2 Concentrations of axial tissue are denoted by clustered harply tained nuclei; branches of annular epithelial processes (arrow) penetrate between axial cells. 7 µ × 600.

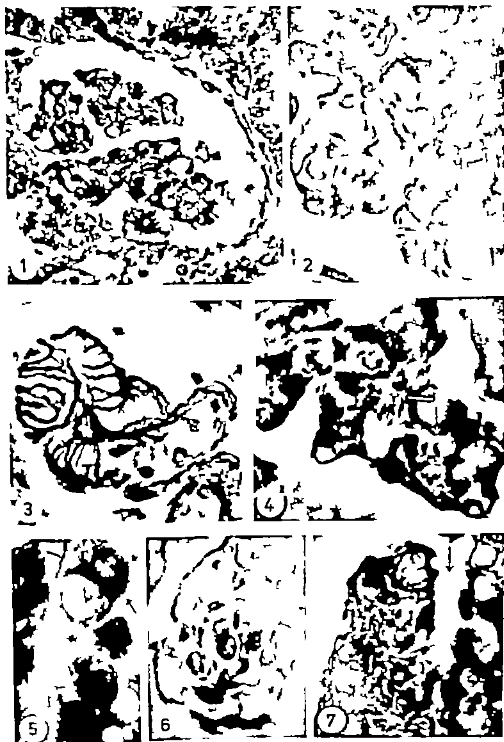
3 The outer surfaces of peripheral capillary loops. A central glomerular ep thelial cell shows an ovoid ucleus, direct nnular processes d dendrites a ladder pattern is formed by indirect annular processes arising from dendrites. 15 µ × 600.

4 The inner surfaces of capillary segments. Axial tissue (arrow) is shown by clustered nuclei (grey) and interspersed varicose epithelial cell processes (black) The outlines of erythrocytes re perceptible in the capillary lumen. 15 µ × 600.

5 A capillary cut in cross-section, is partly surrounded by the direct annular processes of a cell body (rrow) in the plane of section opposite the cell body nucleu (presumably of an endothelial cell) appears very close to the lumen Other uclei of annular ppe rance ppear collectively t distinguish an axial region within the lobule 20 900.

6 Portion of lobule howing the penetration of epithelial cell processes between uclei of the axial tissue cut in trans erse sec ion and urrounded by capillary lumens. 7 µ × 600

7 A interlobular pace (arrow) i delineated by epithelial cell bodies and their processes Branches of the processes penetrat d as nate the axial tissue 15 µ 600.


1
2
3
4
5
6
7

M

N

O

P

T

U

V

W

Y

Z

R

S